

Copyright
by
Yin-Cheng Lin
2007

**The Dissertation Committee for Yin-Cheng Lin Certifies that this is the approved
version of the following dissertation:**

**Characterizing V_s Profiles by the SASW Method and Comparison with
Other Seismic Methods**

Committee:

Kenneth H. Stokoe, II, Supervisor

David W. Fowler

Sung-Ho Joh

Clark R. Wilson

Jorge G. Zornberg

**Characterizing V_s Profiles by the SASW Method and Comparison with
Other Seismic Methods**

by

Yin-Cheng Lin, B.S.; M.S.

Dissertation

Presented to the Faculty of the Graduate School of

The University of Texas at Austin

in Partial Fulfillment

of the Requirements

for the Degree of

Doctor of Philosophy

The University of Texas at Austin

May, 2007

Dedicated

to

My Parents, My Wife and My Son

Acknowledgements

I would like to express my appreciation and respect to my supervising professor Dr. Kenneth H. Stokoe, II for his advice, support, inspiration and encouragement through the course of this study. It has been a great experience to work with Dr. Stokoe. Because of him, I have the chance to be involved in several import projects to achieve this research.

I also would like to thank the remaining members of my dissertation committee, Dr. David W. Fowler, Dr. Sung-Ho Joh, Dr. Clark R. Wilson, and Dr. Jorge G. Zornberg for reviewing this dissertation in such a limited time frame and for their valuable contributions to this work. Thanks also extend to the rest of the geotechnical engineering faculty.

Thanks to Dr. Sung-Ho Joh and Dr. Brent L. Rosenblad for passing me their knowledge and experience of the SASW method. I also want to thank Jeffrey Lee, Hyung-Choon Park, Brady R. Cox, Min Jae Jung, Songcheng Li, Jung Jae Lee, Kwangsoo Park and many others that I unfortunately omitted for their friendship and support.

Thanks also extended to Pacific Earthquake Engineering Research Center (PEER), Pacific Northwest National Laboratory Richland, WA and Bechtel SAIC Company (BSC). Without their support, this research would not have been possible.

I would also like to thank Teresa Tice-Boggs, Alicia Zapata, and Chris Trevino for their administrative support.

Lastly, I want to thank my parents, my wife and my son for their support and understanding.

Characterizing V_S Profiles by the SASW Method and Comparison with Other Seismic Methods

Publication No. _____

Yin-Cheng Lin, Ph.D.

The University of Texas at Austin, 2007

Supervisor: Kenneth H. Stokoe, II

The shear wave velocity (V_S) profile has been used as an important parameter in characterizing geotechnical sites and performing earthquake designs. The Spectral-Analysis-of-Surface-Wave (SASW) method, one of the V_S profiling methods, was developed in the early 1980s. This method is a non-intrusive test which uses Rayleigh waves, one kind of surface wave, to explore the subsurface. The SASW method has been widely used in geotechnical earthquake engineering to profile soil and rock sites. All equipment required to conduct the SASW test is deployed on the ground surface and no boreholes are needed.

In this study, the SASW method was used to measure shear wave velocity profiles in four different geographic regions. These four regions are: (1) Imperial Valley, CA, (2) Taiwan, (3) Hanford, WA and (4) Yucca Mountain, NV. The SASW tests performed at these locations were for different purposes. At the Imperial Valley and Taiwan sites, the SASW tests were carried out at the locations of strong motion recorders (SMR) to obtain

V_S profiles of the top 30 m ($V_{S,30}$). At the Hanford and Yucca Mountain sites, deeper profiling (>300 m) was required to obtain V_S values of the geotechnical structure around or beneath critical facilities associated with the handling, treatment and/or storage of high-level radioactive waste.

The $V_{S,30}$ values determined by the SASW method were used to classify the test sites based on the International Building Code (IBC-2006) provisions. Available downhole and suspension logging measurements at/near the SASW test sites were also used to determine $V_{S,30}$. In addition, deeper V_S profiles determined by the SASW, downhole and suspension logging methods were compared. By doing so, the consistency between the three seismic surveys methods and the reliability of the SASW method were studied. Finally, sensitivity studies of the SASW method were conducted to investigate: (1) the impact on the final V_S profile of changing assumed parameters in the SASW data reduction process, and (2) the capability of the SASW method to detect relatively soft layers sandwiched between stiffer layers.

Table of Contents

List of Tables	xiii
List of Figures.....	xvi
Chapter 1 Introduction.....	1
1.1 Background.....	1
1.2 Objectives of the Research.....	2
1.3 Organization of the Dissertation	4
Chapter2 Overview of the SASW Method.....	6
2.1 Introduction.....	6
2.2 Brief Review of Rayleigh Waves	6
2.2.1 Properties of Rayleigh Waves.....	6
2.2.2 Relationship between Shear and Rayleigh Wave Velocities	10
2.3 Review of the Development of the SASW Method.....	12
2.3.1 Steady-State Rayleigh Wave Method	12
2.3.1.1 Test Setup and Procedures	13
2.3.1.2 Analysis Procedures.....	13
2.3.2 Development of the SASW Method	16
2.4 Overview of the SASW Method.....	18
2.4.1 Field Equipment.....	18
2.4.1.1 Seismic Sources	18
2.4.1.2 Dynamic Signal Analyzer	23
2.4.1.3 Transducers/Receivers/Sensors.....	24
2.4.2 Analysis Tool.....	26
2.4.2.1 Capabilities of WinSASW	26
2.4.3 Test Setups for SASW Measurements.....	29
2.4.4 Procedures to Reduce SASW Data	34
2.4.4.1 Interpret Experimental/Field Dispersion Curves	34
2.4.4.2 Forward Modeling	55

2.5	Summary	63
Chapter 3	Overview of the Database and the Study Methodology	64
3.1	Introduction.....	64
3.2	Overview of the Database in This Study	65
3.2.1	SASW Measurements	65
3.2.2	Other Seismic Measurements	66
3.3	Overview of Other Seismic Techniques	70
3.3.1	Downhole Method	70
3.3.2	Suspension (P-S) Logging Method.....	75
3.4	Site Classification System.....	78
3.5	Clarification of Analysis Methodology	79
3.5.1	Data Distribution and Parameters used in Statistical Study.....	79
3.5.2	Criteria for Comparing V_s Profiles.....	80
3.6	Summary.....	81
Chapter 4	SASW Testing in Imperial Valley, California.....	82
4.1	Background of Test Site.....	82
4.2	Review of SASW Testing Performed in Imperial Valley, CA	82
4.3	Testing Results.....	85
4.3.1	SASW Testing	85
4.3.2	Downhole Testing.....	87
4.3.3	Suspension Logging.....	89
4.4	Statistical Analyses and Comparisons	90
4.4.1	General Comparisons (Apples-to-Oranges Comparisons).....	91
4.4.2	Common Site Comparisons (Green-Apples-to-Red-Apples Comparisons).....	96
4.4.3	Identical-site-and-depth comparisons (Green-Apples-to-Green- Apples Comparisons).....	100
4.4.4	Comparisons of COV Values.....	103
4.4.5	Comparisons of Site Classification.....	104
4.5	Calculation of Representative Field Shear Moduli Values.....	106
4.6	Summary.....	108

Chapter 5	SASW Testing in Taiwan	110
5.1	Background of Test Site.....	110
5.2	Review of SASW Testing Performed in Taiwan.....	111
5.3	Testing Results.....	115
5.3.1	SASW Testing	115
5.3.2	Suspension Logging Tests	119
5.4	Statistical Analyses and Comparisons	120
5.4.1	General Comparisons (Apples-to-Oranges Comparisons).....	122
5.4.2	Common Site Comparisons (Green-Apples-to Red-Apples Comparisons).....	124
5.4.3	Identical-Site-and-Depth Comparisons (Green-Apples-to-Green- Apples Comparisons).....	126
5.4.4	Comparisons of COV.....	128
5.4.5	Comparisons of Site Classifications	129
5.4.6	Comparisons of G_{max}	129
5.5	Summary and Conclusions	132
Chapter 6	SASW Testing at Hanford, WA.....	134
6.1	Background of Test Site.....	134
6.2	Review of SASW Testing Performed at Hanford.....	134
6.3	Test Results.....	138
6.3.1	SASW Testing	138
6.3.2	Downhole Testing.....	141
6.4	Statistical Analyses and Comparisons	143
6.4.1	General Comparisons (Apples-to-Oranges Comparisons).....	144
6.4.2	Common Site Comparisons (Green-Apples-to-Red-Apples Comparisons).....	146
6.4.3	Identical Comparisons (Green-Apples-to-Green-Apples Comparisons).....	147
6.4.4	Statistical Analyses and Comparisons Based on Geologic Information	148
6.4.5	Comparison of Site Classification	157
6.5	Calculation of Field Shear Modulus	158

6.6	Summary	163
Chapter 7	SASW Testing in Yucca Mountain, NV	166
7.1	Background of Test Site.....	166
7.2	Review of SASW Testing Performed at Yucca Mountain, NV.....	169
7.2.1	SASW Testing Performed between 2000 and 2001	171
7.2.2	SASW Testing Performed between 2004 and 2005	175
7.3	Testing Results in Terms of V_S Profiles in Terms of V_S Profiles.....	181
7.3.1	SASW Testing	181
7.3.1.1	SASW Testing Performed in 2000 and 2001.....	182
7.3.1.2	SASW Testing Performed in 2004 and 2005.....	189
7.3.2	Downhole Seismic Testing	208
7.3.2.1	Yucca Mountain Area	208
7.3.2.2	WHB Area	210
7.3.3	P-S Suspension Logging.....	212
7.3.4	Laboratory Testing.....	214
7.3.5	Vertical Seismic Profiling (VSP).....	215
7.3.6	Seismic Tomography Testing	218
7.4	Statistical Analyses and Comparisons	221
7.4.1	Comparisons between Different Profiling Methods in the Same Area.....	221
7.4.1.1	Yucca Mountain Area	221
7.4.1.2	WHB Area	226
7.4.2	Comparisons between Different Test Areas	236
7.4.2.1	Surface SASW Testing Sites	236
7.4.2.2	Mountain and Tunnel Testing Sites	237
7.4.3	Comparisons Based on Geologic Information.....	239
7.5	Summary	241
Chapter 8	Sensitivity Studies.....	243
8.1	Introduction.....	243
8.2	Studies of Assumed Parameters Used in Forward modeling with WinSASW.....	243
8.2.1	Poisson's Ratio.....	244

8.2.2 Unit Weight.....	249
8.2.3 Layer Thickness.....	252
8.3 Studies of the Capability of the SASW Method to Detect Soft Layers at Depth.....	253
8.4 Summary.....	260
Chapter 9 Summary, Conclusions and Recommendations.....	262
9.1 Summary.....	262
9.2 Conclusions.....	263
9.2.1 Tests Performed in Imperial Valley, CA.....	263
9.2.2 Tests Performed in Taiwan.....	265
9.2.3 Tests Performed in Hanford, WA.....	266
9.2.4 Tests Performed at the Yucca Mountain Project, NV.....	267
9.2.5 Sensitivity Study of Assumed Parameters Used in Forward Modeling.....	268
9.2.6 Sensitivity Study of Detecting Relative Soft Layer in the Subsurface.....	268
9.2.7 Summation of the Study.....	269
9.3 Recommendations for Future work.....	270
References.....	271
Vita.....	277

List of Tables

Table 2.1	Setup and Criteria for Filtering Near-Field Data	34
Table 2.2	Profile Parameters Used in Step 1 to Develop the Theoretical Dispersion Curve for the Site at Yucca Mountain	56
Table 2.3	Profile Parameters Used in Step 2 to Develop the Theoretical Dispersion Curve for the Site at Yucca Mountain	57
Table 2.4	Profile Parameters Used in Step 3 to Develop the Theoretical Dispersion Curve for the Site at Yucca Mountain	58
Table 2.5	Profile Parameters Used in Step 4 to Develop the Theoretical Dispersion Curve for the Site at Yucca Mountain	59
Table 2.6	Profile Parameters Used in Final Step to Develop the Theoretical Dispersion Curve for the Site at Yucca Mountain	60
Table 2.7	Comparison of V_S profiles Used to Determine Original and Upper and Lower Boundaries Theoretical Dispersion Curves in Figure 5.58	62
Table 3.1	Information about the SASW V_S Profiles Used in This Study	66
Table 3.2	Site Class Definitions (IBC-2006)	79
Table 4.1	Table of Major Earthquakes happen in Imperial Valley, California (from United States Geological Survey, USGS).....	82
Table 4.2	Information of SASW Test Sites in Imperial Valley, CA	86
Table 4.3	Information of Available Downhole Test Sites in Imperial Valley, CA	88
Table 4.4	Information of Three Suspension Logging Test Sites in Imperial Valley, CA	90
Table 4.5	Average COV Values with Different Comparison Criteria.....	104
Table 4.6	Comparisons of $V_{S,30}$ and Site Class Classification determined by Different Seismic Profiling Techniques.....	106
Table 5.1	Information on the 26 SASW Test Sites in Taiwan.....	116
Table 5.2	Information on the Ten Suspension Logging Sites in Taiwan.....	120
Table 5.3	Comparisons of Site Classifications and $V_{S,30}$ between the SASW and P-S Logging Measurements	130
Table 6.1	Information of SASW Testing at Hanford, WA	139

Table 6.2	Information of Downhole Testing at Hanford, WA.....	142
Table 6.3	Geologic Profile of the Ten SASW Test Sites at Hanford, WA.....	144
Table 6.4	Comparisons of Site Classification and $V_{S,30}$ between SASW and Downhole Measurements.....	158
Table 7.1	Information of the 30 SASW Tests Performed on/near the Top of Yucca Mountain during 2000 and 2001.....	183
Table 7.2	Information of 35 SASW Tests Performed at the WHB Area during 2000 and 2001.....	186
Table 7.3	Information of the Five SASW Tests Performed in the ESF Tunnel in 2001.....	188
Table 7.4	Information about the 25 SASW Tests Performed in the Mountain Area during 2004 and 2005.....	190
Table 7.5	Information of the 18 SASW Tests Performed at the NPF Area during 2004 and 2005.....	197
Table 7.6	Information about the Six SASW Tests Performed at the Aging Pad (AP) Area during 2004 and 2005.....	199
Table 7.7	Information about the 45 SASW Tests Performed in the ESF and ECRB Tunnels during 2004 and 2005.....	202
Table 7.8	Information about the Eight Downhole Tests Performed in the Mountain Area in 2001.....	209
Table 7.9	Information about the 17 Downhole Tests Performed at the WHB Area in 2000.....	211
Table 7.10	Information about the 16 P-S Suspension Logging Tests Performed in the WHB Area in 2000.....	213
Table 7.11	Free-Free Resonant Column Results of Different Tuff Specimens from YMP.....	214
Table 7.12	Table of the Boreholes where the Downhole Tests were Performed and the Nearby SASW Test Locations.....	224
Table 7.13	Common Sites in the WHB area Used to Compare V_S profiles from SASW, Downhole and P-S Logging Measurements.....	230

Table 8.1	Original Profile Parameters Used to Develop the Theoretical Dispersion in Figure 8.1	246
Table 8.2	New Profile Parameters Used to Develop the Theoretical Dispersion Curve in Figure 8.4 for a Constant Value of Poisson's Ratio of 0.20	250
Table 8.3	New Profile Parameters Used to Develop the Theoretical Dispersion Curve in Figure 8.4 for a Constant Value of Poisson's Ratio of 0.40	250
Table 8.4	Maximum Detectable Depth with Respect to Different Thicknesses and Velocity Contrasts of the Soft Layers	257
Table 8.5	Normalized Maximum Detectable Depth with Respect to Different Thicknesses and Velocity Contrasts of the Soft Layer	258

List of Figures

Figure 2.1	Illustration of the Media Particle Motion of Different Wave Types (Modified from Bolt, 1976)	8
Figure 2.2	Dispersion Curves of Plane Rayleigh Wave Traveling in (a) Isotropic, Homogeneous Half Space and (b) Layered System	9
Figure 2.3	Comparisons of Different Waveforms from (a) Normally Dispersive Geotechnical Site and (b) Inversely Dispersive Pavement Site (Not Real Record, for Illustration Only)	9
Figure 2.4	Variation of the Ratio of Rayleigh Wave to Shear Wave Velocity with Poisson's Ratio.....	11
Figure 2.5	Illustration of the Test Setup Used in the Steady-State Rayleigh Wave Method	14
Figure 2.6	Determination of Average Wavelengths of Rayleigh Waves and Associated Rayleigh Wave Velocities (from Richart et al. 1970).....	14
Figure 2.7	Shear Wave Velocity Profile Reduced from Figure 2.6	15
Figure 2.8	A bulldozer Used as a Seismic Source to Perform SASW Test at Waste Handling Building (WHB) at Yucca Mountain, NV	20
Figure 2.9	DynaSource Used as Impact Source at Kung-Chung Elementary School Site (TCU-52) in Taiwan	20
Figure 2.10	Large Drop Weight Used as Impact Source to Perform SASW Test at LA Fire Station #99, Los Angeles, CA.....	21
Figure 2.11	A Traditional Vibroseis Performing the SASW Test at El Centro Array #1 in Imperial Valley, CA.....	21
Figure 2.12	Photographs of the Three Nees@UTexas Mobile Vibrators (from Stokoe et al., 2006)	22
Figure 2.13	Comparison of the Theoretical Output Force Levels in Vertical Shaking of Four Different Vibrators in the Frequency Range of 0.2 to 20 Hz (from Stokoe et al., 2006)	23
Figure 2.14	Photograph of an Agilent 35670A Dynamic Signal Analyzer.....	24

Figure 2.15	Photograph of 1-Hz Geophone on the Yard of the Brawley Airport in Imperial Valley, CA.....	25
Figure 2.16	Photograph of an Accelerometer - Wilcoxon Model 736.....	26
Figure 2.17	Illustration of Difference between Forward Modeling and Inversion Analysis.....	28
Figure 2.18	Initial Generalized Configuration of the SASW Test Used in the Field.....	30
Figure 2.19	Illustration of the Common Receiver Midpoint (CRMP) Geometry Used in Initial SASW Testing with Two Receivers.....	31
Figure 2.20	Illustration of the Common Source (CS) Geometry Used in Initial SASW Testing with Two Receivers	32
Figure 2.21	Illustration of the General Source-Receiver Arrangement Used in the SASW Tests Performed as Part of this Study	33
Figure 2.22	Wrapped Phase Plot Determined in the Field from the Cross Power Spectrum Calculated Using Two Adjacent Receivers (or Any Receiver Pairs)	36
Figure 2.23	Comparison of Wrapped and Unwrapped Phase Plots Determined from the Cross Power Spectrum Evaluated from One Pair of Receivers	37
Figure 2.24	Illustration of Masking Undesired Data in a Wrapped Phase Plot	38
Figure 2.25	Flow Chart of Calculating Wavelengths of Rayleigh Waves and the Corresponding Phase Velocities to Build the Experimental Dispersion Curve.....	38
Figure 2.26	Experimental Dispersion Curves Calculated from Figure 2.23 and All Other Receiver Spacings at the Site.....	40
Figure 2.27	Wrapped Phase Plot Measured by SASW Testing with a 1600-ft Receiver at One Yucca Mountain Site.....	42
Figure 2.28	Experimental Dispersion Curves Determined from Figure 2.27 and All Other Receiver Spacings at One Yucca Mountain Site	42
Figure 2.29	Wrapped Phase Plot Measured by SASW Testing with a 1200-ft Receiver at One Yucca Mountain Site.....	43

Figure 2.30	Experimental Dispersion Curves Determined from Figure 2.29 and All Other Receiver Spacings at One Yucca Mountain Site	43
Figure 2.31	Wrapped Phase Plot Measured by SASW Testing with a 800-ft Receiver at One Yucca Mountain Site	44
Figure 2.32	Experimental Dispersion Curves Determined from Figure 2.31 and All Other Receiver Spacings at One Yucca Mountain Site	44
Figure 2.33	Wrapped Phase Plot Measured by SASW Testing with a 600-ft Receiver at One Yucca Mountain Site (from d_1 : $d_2 = 600$ ft : 1200 ft Setup)	45
Figure 2.34	Experimental Dispersion Curves Determined from Figure 2.33 and All Other Receiver Spacings at One Yucca Mountain Site	45
Figure 2.35	Wrapped Phase Plot Measured by SASW Testing with a 600-ft Receiver at One Yucca Mountain Site (from d_1 : $d_2 = 300$ ft : 600 ft Setup)	46
Figure 2.36	Experimental Dispersion Curves Determined from Figure 2.35 and All Other Receiver Spacings at One Yucca Mountain Site	46
Figure 2.37	Wrapped Phase Plot Measured by SASW Testing with a 300-ft Receiver at One Yucca Mountain Site	47
Figure 2.38	Experimental Dispersion Curves Determined from Figure 2.37 and All Other Receiver Spacings at One Yucca Mountain Site	47
Figure 2.39	Wrapped Phase Plot Measured by SASW Testing with a 150-ft Receiver at One Yucca Mountain Site	48
Figure 2.40	Experimental Dispersion Curves Determined from Figure 2.39 and All Other Receiver Spacings at One Yucca Mountain Site	48
Figure 2.41	Wrapped Phase Plot Measured by SASW Testing with a 75-ft Receiver at One Yucca Mountain Site	49
Figure 2.42	Experimental Dispersion Curves Determined from Figure 2.41 and All Other Receiver Spacings at One Yucca Mountain Site	49
Figure 2.43	Wrapped Phase Plot Measured by SASW Testing with a 40-ft Receiver at One Yucca Mountain Site	50
Figure 2.44	Experimental Dispersion Curves Determined from Figure 2.43 and All Other Receiver Spacings at One Yucca Mountain Site	50

Figure 2.45	Wrapped Phase Plot Measured by SASW Testing with a 20-ft Receiver at One Yucca Mountain Site	51
Figure 2.46	Experimental Dispersion Curves Determined from Figure 2.45 and All Other Receiver Spacings at One Yucca Mountain Site	51
Figure 2.47	Wrapped Phase Plot Measured by SASW Testing with a 10-ft Receiver at One Yucca Mountain Site	52
Figure 2.48	Experimental Dispersion Curves Determined from Figure 2.47 and All Other Receiver Spacings at One Yucca Mountain Site	52
Figure 2.49	Wrapped Phase Plot Measured by SASW Testing with a 10-ft Receiver at One Yucca Mountain Site (from Reverse Direction).....	53
Figure 2.50	Experimental Dispersion Curves Determined from Figure 2.49 and All Other Receiver Spacings at One Yucca Mountain Site	53
Figure 2.51	Wrapped Phase Plot Measured by SASW Testing with a 5-ft Receiver at One Yucca Mountain Site (from Reverse Direction)	54
Figure 2.52	Experimental Dispersion Curves Determined from Figure 2.51 and All Other Receiver Spacings at One Yucca Mountain Site	54
Figure 2.53	Illustration of Forward Modeling – Step 1: (a) Assumed V_S Profile; (b) Comparison of Theoretical Dispersion Curve from Assumed V_S Profile with the Experimental Dispersion Curve.....	56
Figure 2.54	Illustration of Forward Modeling – Step 2: (a) Assumed V_S Profile; (b) Comparison of Theoretical Dispersion Curve from Assumed V_S Profile with the Experimental Dispersion Curve.....	57
Figure 2.55	Illustration of Forward Modeling – Step 3: (a) Assumed V_S Profile; (b) Comparison of Theoretical Dispersion Curve from Assumed V_S Profile with the Experimental Dispersion Curve.....	58
Figure 2.56	Illustration of Forward Modeling – Step 4: (a) Assumed V_S Profile; (b) Comparison of Theoretical Dispersion Curve from Assumed V_S Profile with the Experimental Dispersion Curve.....	59

Figure 2.57	Illustration of Forward Modeling – Final Step: (a) Assumed V_S Profile; (b) Comparison of Theoretical Dispersion Curve from Assumed V_S Profile with the Experimental Dispersion Curve	60
Figure 2.58	Comparisons between V_S Profiles and the Corresponding Theoretical Dispersion Curves That Fit the Average and Upper and Low Boundaries of the Field Dispersion Curve in Figure 5.57	62
Figure 3.1	Distribution of V_S Profiles Measured at Surface Sites with Respect to Survey Technique and Geographic Location.....	68
Figure 3.2	Distribution of V_S Profiles Measured at Surface Sites with Respect to Survey Technique and Profiling Depth.....	69
Figure 3.3	Histogram of Common Test Sites for the Different Survey Techniques.....	69
Figure 3.4	General Configuration of Downhole Testing	71
Figure 3.5	Downhole Travel Time Measurements and Resulting Shear Wave Velocity Profile.....	72
Figure 3.6	Setup of Downhole Testing with Two (or more) Receivers	72
Figure 3.7	Different Downhole Measurements: (a) Direct Measurements, (b) Pseudo-Interval Measurements, and (c) True-Interval Measurements	74
Figure 3.8	Illustration of the Setup of the Suspension Logging Method (from http://www.geovision.com/PDF/M_PS_Logging.PDF)	76
Figure 3.9	An Example of a Single Depth Data of Suspension Logging Test (Modified from http://www.geovision.com/PDF/M_PS_Logging.PDF)	76
Figure 3.10	Example of S- and P-Wave Velocity Profiles from the Suspension Logging Test (from http://www.geovision.com/PDF/M_PS_Logging.PDF)	77
Figure 4.1	Approximate Locations of 30 SASW Testing Sites Superimposed on a Map of Imperial Valley, CA	84
Figure 4.2	Approximate Locations of SASW Testing Sites Superimposed on a Map of Imperial Valley, CA (Continued)	85
Figure 4.3	Individual Profile and Statistical Information of 31 SASW V_S Profiles from Imperial Valley, CA	87

Figure 4.4	Individual Profile and Statistical Information of 23 Downhole V_S profiles (From 21 Sites) from Imperial Valley, CA.....	89
Figure 4.5	Individual Profiles and Statistical Information of Three Suspension Logging V_S Profiles from Imperial Valley, CA.....	90
Figure 4.6	Comparison of the Median and 16 th and 84 th Percentile Boundaries of All Available 31 SASW and 21 Downhole V_S Profiles Measured in Imperial Valley, CA.....	93
Figure 4.7	Comparison of the Median and 16 th and 84 th Percentile Boundaries of V_S Profiles of 28 SASW and 20 Downhole Test Sites not in the Mountain Areas of Imperial Valley, CA	94
Figure 4.8	Comparison of the Median and 16 th and 84 th Percentile Boundaries of V_S Profiles of 23 SASW and 18 Downhole Test Sites in the Central Valley Area of Imperial Valley, CA.....	95
Figure 4.9	Comparison of the Median and 16 th and 84 th Percentile Boundaries of 23 SASW, 19 Downhole and Three P-S Logging V_S Profiles in the Central Valley Areas in Imperial Valley, CA.....	96
Figure 4.10	Comparison of the Median and 16 th and 84 th Percentile Boundaries of Available SASW and Downhole V_S Profiles from 21 Common Sites in Imperial Valley, CA.....	97
Figure 4.11	Comparison of the Median and 16 th and 84 th Percentile Boundaries of Available SASW and Downhole V_S Profiles from 20 Common Sites not in the Mountain Areas in Imperial Valley, CA.....	98
Figure 4.12	Comparison of the Median and 16 th and 84 th Percentile Boundaries of Available SASW and Downhole V_S Profiles from 18 Common Sites in the Central Valley Area of Imperial Valley, CA	99
Figure 4.13	Comparison of the Median and 16 th and 84 th Percentile Boundaries of Available SASW and P-S Logging V_S Profiles from Three Common Sites in Imperial Valley, CA.....	100

Figure 4.14	Comparison of the Median and 16 th and 84 th Percentile Boundaries of Available SASW and P-S Logging V_S Profiles at the Identical Depths from 21 Common Sites in Imperial Valley, CA	101
Figure 4.15	Comparison of the Median and 16 th and 84 th Percentile Boundaries of Available SASW and P-S Logging V_S Profiles at the Identical Depths from 20 Common Sites not in the Mountain Areas of Imperial Valley, CA	102
Figure 4.16	Comparison of the Median and 16 th and 84 th Percentile Boundaries of Available SASW and P-S Logging V_S Profiles at the Identical Depths from 18 Common Sites in Central Valley Area of Imperial Valley, CA....	103
Figure 4.17	Field G_{max} Profiles Calculated from Representative V_S Profile Determined from 23 SASW Test Sites in the Central Valley Area.....	107
Figure 5.1	Schematic diagram showing present plate tectonic configuration of Taiwan (from Ernst et al., 1985).....	110
Figure 5.2	Approximate Locations of SASW Testing Sites Superimposed on a Map of Taiwan	112
Figure 5.3	Approximate Locations of SASW Testing Sites Superimposed on a Map of Taiwan (Continued).....	113
Figure 5.4	Modified Source-Receiver Geometry Used with the Large DynaSource and Larger Receiver Spacings in Taiwan	114
Figure 5.5	Individual Profiles and Statistical Information of the 26 SASW V_S Profiles from Taiwan Test Sites.....	117
Figure 5.6	Illustration of :(a) Low-Velocity Group: Four “D” Sites, and (b) Higher-Velocity Group: 22 “C” Sites Determined by SASW Tests in Taiwan.....	118
Figure 5.7	Comparisons of Statistical Information of “C” and “D” Sites Determined by SASW Tests in Taiwan.....	119
Figure 5.8	Individual Profiles and Statistical Information of the Ten Suspension Logging V_S Profiles from the Taiwan Test Sites.....	121

Figure 5.9	Illustration of : (a) Low-Velocity Group: Two “D” Sites, and (b) Higher-Velocity Group: Eight “C” Sites Determined by P-S Logging Tests in Taiwan.....	122
Figure 5.10	Comparison of the Median and 16 th and 84 th Percentile Boundaries of the 22 SASW and 8 Suspension Logging V _S Profiles from “C” Sites Measured in Taiwan.....	124
Figure 5.11	Comparison of the Median and 16 th and 84 th Percentile Boundaries of the SASW and Suspension Logging V _S Profiles at Ten Common Sites in Taiwan.....	125
Figure 5.12	Comparison of the Median and 16 th and 84 th Percentile Boundaries of the SASW and Suspension Logging V _S Profiles at Eight Common “C” Sites in Taiwan.....	126
Figure 5.13	Comparison of the Median and 16 th and 84 th Percentile Boundaries of the Available SASW and P-S Logging V _S Profiles over Identical Depths from Ten Common Sites in Taiwan.....	127
Figure 5.14	Comparison of the Median and 16 th and 84 th Percentile Boundaries of the Available SASW and P-S Logging V _S Profiles over Identical Depths from Eight Common “C” Sites in Taiwan.....	128
Figure 5.15	Comparison of Gravel Material between SASW, Downhole and Cyclic Triaxial Tests Results.....	131
Figure 6.1	Map of Approximate Locations of SASW Testing Arrays at Hanford, WA.....	135
Figure 6.2	Common-Middle-Receiver Geometry Used in SASW Testing at Hanford Sites.....	136
Figure 6.3	Individual Profiles and Statistical Information of Ten SASW V _S profiles from the Hanford Test Sites.....	140
Figure 6.4	Individual Profiles and Statistical Information of Nine SASW V _S Profiles from the Hanford Test Sites; Each Site has Soil Layers over Basalt.....	141

Figure 6.5	Individual Profiles and Statistical Information of Six Downhole V_S Profiles (from Five Sites) at the Hanford Test Sites	142
Figure 6.6	General Comparison of Individual SASW and Downhole V_S Profiles: (a) with Site H10 and (b) without Site H10 at Hanford, WA	143
Figure 6.7	Comparison of the Median and 16 th and 84 th Percentile Boundaries of All Ten SASW and Five Downhole V_S Profiles Measured at Hanford, WA.....	145
Figure 6.8	Comparison of the Median and 16 th and 84 th Percentile Boundaries of Nine SASW and Five Downhole V_S Profiles Measured at Hanford, WA..	146
Figure 6.9	Comparison of the Median and 16 th and 84 th Percentile Boundaries of SASW and Downhole V_S Profiles Measured at Five Common Sites at Hanford, WA.....	147
Figure 6.10	Comparison of the Median and 16 th and 84 th Percentile Boundaries of SASW and Downhole V_S Profiles over Identical Depths at Five Common Sites at Hanford, WA	148
Figure 6.11	Comparison of the Median and 16 th and 84 th Percentile Boundaries of Nine SASW and Four Downhole V_S Profiles of Hanford Formation (Sand and Gravel Sequences) at Hanford Test Sites	150
Figure 6.12	Comparison of the Median and 16 th and 84 th Percentile Boundaries of the SASW and Downhole V_S Profiles of Hanford Formation (Sand and Gravel Sequences) at Four Common Sites at Hanford	151
Figure 6.13	Comparison of the Median and 16 th and 84 th Percentile Boundaries of the SASW and Downhole V_S Profiles of Hanford Formation (Sand and Gravel Sequences) over Identical Depths at Four Common Sites at Hanford	152
Figure 6.14	Comparison of Median and 16 th and 84 th Percentile Boundaries of Nine SASW and Four Downhole V_S Profiles of Sand Sequence of Hanford Formation at Hanford Test Sites	153

Figure 6.15	Comparison of the Median and 16 th and 84 th Percentile Boundaries of the SASW and Downhole V _S Profiles Sand Sequence of Hanford Formation at Four Common Sites at Hanford.....	154
Figure 6.16	Comparison of the Median and 16 th and 84 th Percentile Boundaries of the SASW and Downhole V _S Profiles of Sand Sequence of Hanford Formation over Identical Depths at Four Common Sites at Hanford	155
Figure 6.17	Statistical Analysis of Ten, Top-Aligned SASW Profiles of Saddle Mountain Basalt at the Hanford Test Sites	156
Figure 6.18	Comparison of the SASW and Downhole Average V _S Regardless of Depth and Thickness of the Five Formations at Hanford Test Sites	157
Figure 6.19	Field Shear Modulus of the Waste Treatment Plant Area Based on Nine SASW V _S Profiles (H1 through H9) Acquired at Hanford, WA	160
Figure 6.20	Field Shear Modulus of the Hanford Formation (Sand and Gravel Sequences) at the Waste Treatment Plant Area Based on Nine SASW V _S Profiles (H1 through H9) Acquired at Hanford, WA	161
Figure 6.21	Field Shear Modulus of the Sand Sequence of the Hanford Formation at the Waste Treatment Plant Area Based on Nine SASW V _S Profiles (H1 through H9) Acquired at Hanford, WA	162
Figure 6.22	Field Shear Modulus of the Saddle Mountain Basalt Based on Ten SASW V _S Profiles Acquired at Hanford, WA.....	163
Figure 7.1	Location of Yucca Mountain, NV (Simmons, 2004).....	167
Figure 7.2	Generalized Lithostratigraphic Column of the Paintbrush Group at Yucca Mountain (Simmons, 2004).....	168
Figure 7.3	Earthquake History within 100 km of Yucca Mountain (Simmons, 2004)	170
Figure 7.4	Approximate Locations of SASW Tests Performed on/near the Top of Yucca Mountain (from Schuhen, 2004).....	172
Figure 7.5	Approximate Locations of SASW Tests Performed at the WHB Area	173
Figure 7.6	Approximate Locations of SASW Tests Performed in the ESF Tunnel (Modified from a Slide of Dr. David Buesch's Presentation at UT-Austin (Buesch, 2005a)).....	174

Figure 7.7	Approximate Locations of the YM Sites above the Proposed Repository Area and the Areas of the NPF and AP Sites.....	177
Figure 7.8	Approximate Locations of the SASW Tests Performed in the ESF and ECRB Tunnels Performed in 2004 (Modified from a Slide of Dr. David Buesch’s Presentation at UT-Austin (Buesch, 2005a))	178
Figure 7.9	Approximate Locations of the SASW Tests Performed in the ESF and ECRB Tunnels Performed in 2005 (Modified from a Slide of Dr. David Buesch’s Presentation at UT-Austin (Buesch, 2005a))	179
Figure 7.10	Individual Profiles and Statistical Analysis of 30 SASW Tests Performed on/near the Top of Yucca Mountain during 2000 and 2001	184
Figure 7.11	Individual Profiles and Statistical Analysis of 35 SASW Tests Performed at the WHB Area during 2000 and 2001.....	187
Figure 7.12	Locations of Faults or Possible Faults at the WHB area (BSC, 2004a)	187
Figure 7.13	Individual Profiles and Statistical Analysis of Five SASW Tests Performed in the ESF Tunnel in 2001	189
Figure 7.14	Individual Profiles and Statistical Analysis of 25 SASW Tests Performed at the Mountain Area during 2004 and 2005	191
Figure 7.15	Individual Profiles and Statistical Analysis of 19 SASW Tests Performed at the Mountain Area during 2004 and 2005; These Sites are above Proposed Repository Area.....	192
Figure 7.16	Individual Profiles and Statistical Analysis of the Nine “Stiffer” SASW V_S Profiles at the Mountain Area that were Measured during 2004 and 2005.....	193
Figure 7.17	Individual Profiles and Statistical Analysis of the Ten “Softer” SASW V_S Profiles at the Mountain Area that were Measured during 2004 and 2005.....	194
Figure 7.18	Individual Profiles and Statistical Analysis of the Six “Neutral” SASW V_S Profiles at the Mountain Area that were Measured during 2004 and 2005.....	194

Figure 7.19	Individual Profiles and Statistical Analysis of the Eight “Stiffer” SASW V_S Profiles that were Measured at the Mountain Area and above the Proposed Repository Area during 2004 and 2005	195
Figure 7.20	Individual Profiles and Statistical Analysis of the Nine “Softer” SASW V_S Profiles that were Measured at the Mountain Area and above the Proposed Repository Area during 2004 and 2005	195
Figure 7.21	Individual Profiles and Statistical Analyses of 18 SASW Tests Performed at NPF Area during 2004 and 2005	198
Figure 7.22	Individual Profiles and Statistical Analyses of 17 SASW Tests Performed at NPF Area without Site NPF 28 and Bottom V_S profiles of Sites NPF 2 and 14 and NPF 3 and 9 during 2004 and 2005	198
Figure 7.23	Individual Profiles and Statistical Analysis of the Six SASW V_S Profiles in the AP Area during 2004 and 2005	200
Figure 7.24	SASW V_S Profiles of (a) Single Sample, (b) Tmbt1, (c) Tпки and (d) Tptpul Tuffs Reduced from ESF and ECRB Tunnels in 2004 and 2005 ...	203
Figure 7.25	Nine SASW V_S Profiles of the Tptpmn Tuff in the ESF and ECRB Tunnels in 2004 and 2005.....	204
Figure 7.26	Fourteen SASW V_S Profiles of the Tptpmn Tuff in the ESF and ECRB Tunnels from 2001 and 2005	205
Figure 7.27	Eight Softer SASW V_S Profiles of the Tptpmn Tuff in the ESF and ECRB Tunnels from 2001 and 2005.....	205
Figure 7.28	Six Stiffer SASW V_S Profiles of the Tptpmn Tuff in the ESF and ECRB Tunnels from 2001 and 2005	206
Figure 7.29	Seventeen SASW V_S Profiles of the Tptpll Tuff in the ESF and ECRB Tunnels in 2004 and 2005.....	207
Figure 7.30	Three SASW V_S Profiles of the Tptpln Tuff in the ECRB Tunnel in 2005.....	207
Figure 7.31	Locations of the Downhole Tests Performed in the Mountain Area in 2001.....	209

Figure 7.32 Individual Profiles and Statistical Analysis of the Eight Downhole Tests Performed in the Mountain Area in 2001	210
Figure 7.33 Individual Profiles and Statistical Analyses of the 17 Downhole Tests Performed at 16 Sites at the WHB Area in 2000	211
Figure 7.34 Individual Profiles and Statistical Analysis of the 16 P-S Suspension Logging Tests Performed at the WHB Area in 2000.....	213
Figure 7.35 Locations of Boreholes where the Vertical Seismic Profiling (VSP) were Performed.....	216
Figure 7.36 Four VSP V_S Profile Performed in Borehole W-2, NRG-6, UZ-16 and G-2 in Yucca Mountain (Re-plotted based on BSC, 2004a)	217
Figure 7.37 Four VSP V_S Profile Performed in Borehole W-2, NRG-6, UZ-16 and G-2 in Yucca Mountain (Re-plotted based on BSC, 2004a)	218
Figure 7.38 P-Wave Velocity Estimates at the Repository Horizon Based on Curved-Ray-Travel-Time Inversion (Gritto et al., 2004)	220
Figure 7.39 Illustrations of: (a) the Seismic Tomography Test Location and (b) the Survey Configuration (Descour et al., 2001).....	222
Figure 7.40 General Comparison between SASW and Downhole Measurements Performed in the Mountain Area during 2000 and 2005	223
Figure 7.41 Comparison between the SASW and Downhole Measurements Performed at Common Borehole Locations in the Mountain Area during 2000 and 2005.....	224
Figure 7.42 Identical-site-and-depth comparison between the SASW and Downhole Measurements Performed at Common Borehole Locations in the Mountain Area during 2000 and 2005	225
Figure 7.43 Comparisons of: (a) 19 SASW V_S Profiles and Four VSP Profiles and (b) Median and 16 th and 84 th Percentile Boundaries of 19 SASW V_S Profiles, the Smoothed VSP Profile, and Base Cases #1 and #2 at the Mountain Area	227
Figure 7.44 General Comparison of SASW and Downhole Measurements at the WHB Area	228

Figure 7.45	General Comparison of SASW and P-S Logging Measurements at the WHB Area	228
Figure 7.46	General Comparison of Downhole and P-S Logging Measurements at the WHB Area.....	229
Figure 7.47	Comparison of SASW and Downhole Measurements at Common Sites in the WHB Area	230
Figure 7.48	Comparison of SASW and P-S Logging Measurements at Common Sites in the WHB Area	231
Figure 7.49	Comparison of Downhole and P-S Logging Measurements in the Common Sites at WHB Area.....	231
Figure 7.50	Identical-site-and-depth comparisons of SASW and Downhole Measurements at Common Sites and the Same Profiling Depths in the WHB Area	233
Figure 7.51	Identical-site-and-depth comparisons of SASW and Downhole Measurements at Common Sites and the Same Profiling Depths in the WHB Area with Borehole Information.....	233
Figure 7.52	Identical-site-and-depth comparisons of SASW and P-S Logging Measurements at Common Sites and the Same Profiling Depths in the WHB Area	234
Figure 7.53	Identical-site-and-depth comparisons of SASW and P-S Logging Measurements at Common Sites and the Same Profiling Depths in the WHB Area with Borehole Information.....	234
Figure 7.54	Identical-site-and-depth comparisons of Downhole and P-S Logging Measurements at Common Sites and the Same Profiling Depths in the WHB Area	235
Figure 7.55	Identical-site-and-depth comparisons of Downhole and P-S Logging Measurements at Common Sites and the Same Profiling Depths in the WHB Area with Borehole Information.....	235
Figure 7.56	Comparisons of SASW Measurements Obtained from Different Areas in the YMP from 2000 to 2005	237

Figure 7.57	Comparisons of: (1) SASW Measurements in the Mountain Area above the Proposed Repository Area, (2) SASW Measurements in the ESF and ECRB Tunnels, (3) Seismic Tomography Surveys Performed by Gritto et al., and (4) Seismic Tomography Surveys Performed by NSA Engineering, Inc.	238
Figure 7.58	Comparisons of the High-and-Low Velocity Groups of the SASW Measurements at Mountain Area above the Proposed Repository Area and V_S Values of the Tptpmn Tuff Measured in the ESF and ECRB Tunnels.....	239
Figure 7.59	Comparisons of V_S Measurements from Different Techniques with Respect to the Alluvium and Different Tuffs	241
Figure 8.1	Original Experimental and Theoretical Dispersion Curves from a SASW Test Site (Site NPF 20 in Yucca Mountain, NV).....	245
Figure 8.2	Original Shear Wave Velocity Profile Determined from the Forward – Model Match Shown in Figure 8.1	245
Figure 8.3	Comparison of Original Experimental and Theoretical Dispersion curves in Figure 8.1, and Two New Theoretical Dispersion Curves of Original V_S Profile with Modified Poisson’s Ratios ($\nu = 0.20$ and $\nu = 0.40$).....	247
Figure 8.4	Comparison of Original Experimental and Theoretical Dispersion curves in Figure 8.1, and Two New Best-Matched Theoretical Dispersion Curves	247
Figure 8.5	Comparison of Original and New Shear Wave Velocity Profiles Determined for the Same Site with Different Assumed Values of Poisson’s Ratios.....	248
Figure 8.6	Comparison of the Original Field and Theoretical Dispersion Curves with Two New Theoretical Dispersion Curves Generated using from Modified Unit Weights and the Original V_S Profile	251
Figure 8.7	V_S Profiles with Various Thickness of Layer #9 (in Table 8.1) and Corresponding Theoretical Dispersion Curves.....	252

Figure 8.8	V_s Profiles with Various Thickness of Layer #8 (in Table 8.1) and Corresponding Theoretical Dispersion Curves	253
Figure 8.9	Illustration of the Methodology to Study the Sensitivity of the SASW Method in Detecting a Soft Layer.....	255
Figure 8.10	Relationships of Maximum Detectable Depth of Soft Layers with Respect to Different Velocity Contrast and Their Thickness	256
Figure 8.11	Normalized Relationships of Maximum Detectable Depth of Soft Layers with Respect to Different Velocity Contrast and the Ratio of Depth to Thickness	257
Figure 8.12	Representative Curve of Normalized Relationships of Maximum Detectable Depth of Soft Layers with Respect to Different Velocity Contrast and the Ratio of Depth to Thickness	258
Figure 8.13	Representative Curve of Normalized Relationships of Maximum Detectable Depth of Soft Layers with Respect to Different Velocity Contrast and the Ratio of Depth to Thickness in Log Scale	259
Figure 8.14	Representative Curves of Normalized Relationships of Maximum Detectable Depth of Soft Layers with Different “Detectable” Criteria with Respect to Different Velocity Contrast and the Ratio of Depth to Thickness in Log Scale	260

Chapter 1 Introduction

1.1 BACKGROUND

Over the past 70 years, many in-situ geophysical techniques have been used to explore the subsurface to help engineers and geologists evaluate the properties of soil deposits and rock formations. Over the past 35 years, several seismic survey techniques have been specially developed for the geotechnical engineers to evaluate in-situ shear wave velocity (V_s) profiles. Nowadays, they are widely adopted in academic research and industrial projects. However, some seismic techniques are more costly compared to others in obtaining in-situ shear wave velocity profile. For instance, seismic methods that require a borehole for testing, such as the downhole and suspension logging methods, are more costly than surface wave methods, such as the spectral-analysis-of-surface-waves (SASW) method. Of course, seismic methods like the crosshole method that require several boreholes are the most expensive. This difference occurs mainly in the expenses and time required to drill the boreholes.

Development of the spectral-analysis-of-surface-waves method in the early 1980s initiated much activity and research in the area of improved surface wave methods for use in geotechnical earthquake engineering. Since the SASW method is non-intrusive, it does not require any boreholes to perform the test. As a result, the SASW method is cost effective compared with borehole seismic methods. In addition, it is easy to perform because all equipment is deployed on the ground surface. The SASW method has also been improved and become more robust since its initial development. Nowadays, the method is widely accepted as a subsurface investigative tool and is employed in a wide variety of geotechnical environments, including pavements, solid waste landfills, and seabeds.

The data studied in this work involves SASW measurements from four different geographic regions. These regions are: (1) Imperial Valley, CA, (2) Taiwan, (3) Hanford, WA, (4) Yucca Mountain, NV. These V_S profiles were determined for different purposes. For instance, SASW tests performed in Imperial Valley, CA and in Taiwan were used for earthquake design purposes because the magnitude and frequency of earthquakes in these two regions are generally higher than the other places. In addition, the potential for liquefaction at these sites were also investigated. The Hanford and Yucca Mountain sites involved the handling and storage of high-level radioactive waste. Facilities are being built at these sites and it is important to characterize and understand the soil and rock supporting the facilities. Profiles of V_S acquired by SASW testing at these locations are also used in earthquake analyses of the facilities. In addition, engineers and seismologists want to compare SASW V_S profiles with the results from other profiling methods to better understand the V_S profiles and make sure that they are not biased and that any uncertainty is properly taken into account. Also, at the Yucca Mountain sites, the SASW V_S profiles were also used to evaluate variability of the alluvial and rock formations.

1.2 OBJECTIVES OF THE RESEARCH

The primary objective of this research is to study the shear wave velocity profiles determined with the SASW test method and to compare these profiles with available V_S profiles obtained from other test methods, such as the downhole and suspension logging methods, performed at the same or near-by test locations. By doing so, the reliability and precision of the SASW technique is investigated. However, as shown in this work, such comparisons can be misleading if not handled properly. The large database used in the work has allowed an in-depth study of these comparisons and how they should be done.

Based on the geologic profiles, the representative shear wave velocities of different soil and rock types can be determined at the test sites. For some sites, resonant column (RC) tests with intact samples were also performed. These laboratory tests were conducted in the Soil Dynamics Laboratory at the University of Texas at Austin (UTA). A second objective is to compare the field SASW and laboratory RC test results with respect to different soil and rock types to study the relationship between field and laboratory V_S .

The homogeneity or inhomogeneity of a test area can be an important issue in many projects and in comparing results from different field methods and in comparing field and laboratory results. For some important facilities, if the geological characteristics at the construction site are highly variable, the difficulty in design and construction of these facilities increases which, in turn, increases the construction cost and time. The coefficient of variation (COV), the ratio of one standard deviation to the corresponding mean value, of the V_S profiles obtained in this study could be an index to help engineers evaluate the variability at a site. Another objective in this research is to study this topic and determine the potential usefulness of the COV.

Nowadays, earthquake engineers used the top 30 m in the V_S profile ($V_{S,30}$) to classify the site. The value of $V_{S,30}$ can be evaluated using the Uniform Building Code (UBC-97), the National Earthquake Hazards Reduction Program (NEHRP-94) procedure or the most current International Building Code (IBC-2006) provisions. The value of $V_{S,30}$ is used to obtain the predicted site response or ground motion for structural design purposes. The reason to use only the top 30 m of the V_S profile is because it is a common depth of many boreholes. In this work, the site classifications determined by different seismic profiling methods are compared at the same sites to study the

consistency or inconsistency between the different methods at shallow depths and site classifications.

Finally, sensitivity studies were conducted in this research to investigate the impact of various parameters used in the SASW data analysis. For this topic, the impact of the change of Poisson's ratio, unit weight, and layer thickness on the final shear wave velocity profile was investigated. Moreover, the capability of the SASW method to detect a soft layer between stiffer layers (or stiffer layer between soft layers) was studied. An analysis software, WinSASW (Joh, 1992), was utilized in these topics.

1.3 ORGANIZATION OF THE DISSERTATION

In Chapter 2, a brief review of surface waves of the Rayleigh type is presented. The SASW method is introduced and a general description of the SASW test method is given. The test equipment, test setup, software and data reduction procedure are discussed. Also, the theoretical background of the SASW method is discussed.

In Chapter 3, an overview of the test data used in the study is presented. These data are from four different geographic regions, three within and one outside the United States. Statistical information describing the data obtained from the SASW, downhole and suspension logging methods are presented. The criteria of site classification by the International Building Code (IBC-2006), which was used in this dissertation, is described. In addition, methodologies of the downhole and suspension logging tests are briefly discussed. Finally, the approach to perform the comparisons between the V_S profiles determined by the different seismic methods is discussed.

Statistical analyses of SASW tests performed in Imperial Valley, CA are presented in Chapter 4. Available V_S profiles from downhole and suspension logging in this area are compared to the SASW profiles in several different aspects, such as site classification and median V_S profiles with 16th and 84th percentile ranges.

The SASW test results performed in Taiwan are presented Chapter 5. Similar comparisons are conducted between the SASW, downhole and suspension V_S profiles as is done in Chapter 4.

In Chapter 6, the SASW test results from Hanford, WA are discussed. In addition to similar comparisons of the V_S profiles from SASW and downhole tests in the Chapters 5 and 6, the ranges of shear wave velocity of different formations are studied based on the geologic profiles.

In Chapter 7, the V_S profiles from the Yucca Mountain test sites are presented. These profiles represent over one half of the SASW V_S profiles used in this dissertation. The number of available V_S profiles from downhole and suspension logging at this site are also dominant compared to the other sites in this study.

The sensitivity study of the SASW method is performed in Chapter 8. The computer program called WinSASW was used to investigate the sensitivity of some crucial parameters used in these studies and the capability of the SASW method to detect the relatively soft layer at depth.

In Chapter 9, summary, conclusions and recommendations are presented.

Chapter2 Overview of the SASW Method

2.1 INTRODUCTION

The SASW method is a seismic technique that uses Rayleigh waves to profile the subsurface. At the start of its development in the early 1980s (Nazarian, 1984), this method was primarily used at pavement sites. Nowadays, this technique is commonly used at geotechnical sites and other places, such as tunnels, solid waste landfills and seabeds. Maybe someday it will be utilized in outer space explorations (on Mars or the moon).

In this chapter, a review of Rayleigh waves is presented and the SASW test method is discussed in general terms. The field test setup and post-field testing analysis procedures are included. To better understand the SASW method, the steady-state Rayleigh wave method, which inspired the development of SASW method, is also described.

2.2 BRIEF REVIEW OF RAYLEIGH WAVES

2.2.1 Properties of Rayleigh Waves

Rayleigh waves (R-wave), a type of surface wave, are named after Lord Rayleigh, the first investigator of Rayleigh waves (1885). Rayleigh waves are a unique waveform which has many special properties different from body waves (compression (P) and shear (S) waves). First, unlike body waves, Rayleigh waves only travel along the free surface of a half space. Second, the near-surface particle motion that R waves is not simply parallel or perpendicular to the direction of wave propagation as for P and S waves, respectively. Instead, the particle motion is a combination of the two body wave motions which forms a retrograde elliptical motion. The particle motions of these

different waves are illustrated in Figure 2.1. Third, based on the study of Miller and Pursey (1955), Rayleigh waves carry about 67% of the energy generated by a uniformly loaded circular source vertically vibrating on the ground surface. Fourth, Rayleigh waves spread out in a two-dimensional cylindrical pattern (radius r) and their amplitude (in an elastic continuum) decreases from the source proportional to $1/\sqrt{r}$. In contrast, the amplitudes of body waves propagating along the ground surface decrease much faster than Rayleigh waves (proportional to $1/r^2$ in a hemispherical pattern). Therefore, Rayleigh waves can more easily be observed than body waves at longer distances from the same source over the same media. Because of these properties, many researchers have used Rayleigh waves to determine the upper crustal structure based on their evident signatures on the seismogram (Aki, 1980). Also, because of the same properties, Rayleigh waves are responsible for causing significant damage during earthquakes.

Rayleigh waves are a type of dispersive waves. When Rayleigh waves propagate along the surface of an isotropic, homogeneous half space, waves with different frequencies (hence different wavelengths) travel at the same velocity. In this case, no dispersion occurs in velocity which is shown in Figure 2.2 (a). In other words, the Rayleigh wave velocity is independent of frequency when it travels in this kind of medium. However, if Rayleigh waves propagate in a layered system, their velocities disperse with respect to different frequencies (wavelengths) which can be observed in Figure 2.2 (b). In general, for a normally dispersive geotechnical site (shear wave velocity increasing with depth), low-frequency (long wavelength) Rayleigh waves travel faster than high-frequency (short wavelength) Rayleigh waves as shown in Figure 2.3 (a). However, for some sites, such as pavement sites which are inversely dispersive, the high frequency Rayleigh waves may arrive earlier than the low-frequency Rayleigh waves (Figure 2.3 (b)). The actual time record may not be as simple/clear as shown in Figures

2.3 (a) and (b) because higher modes or body wave reflections and refractions may be involved.

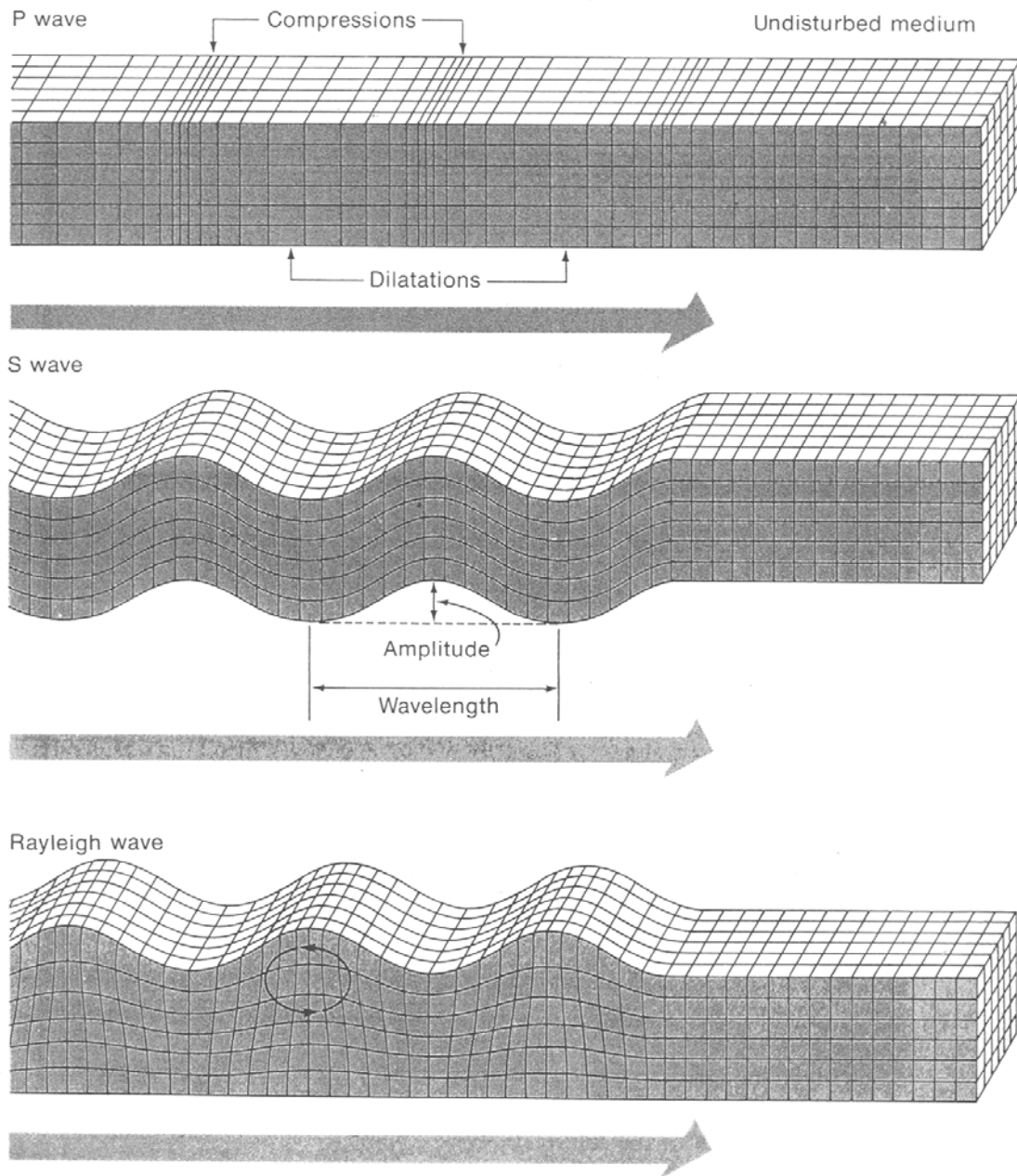


Figure 2.1 Illustration of the Media Particle Motion of Different Wave Types (Modified from Bolt, 1976)

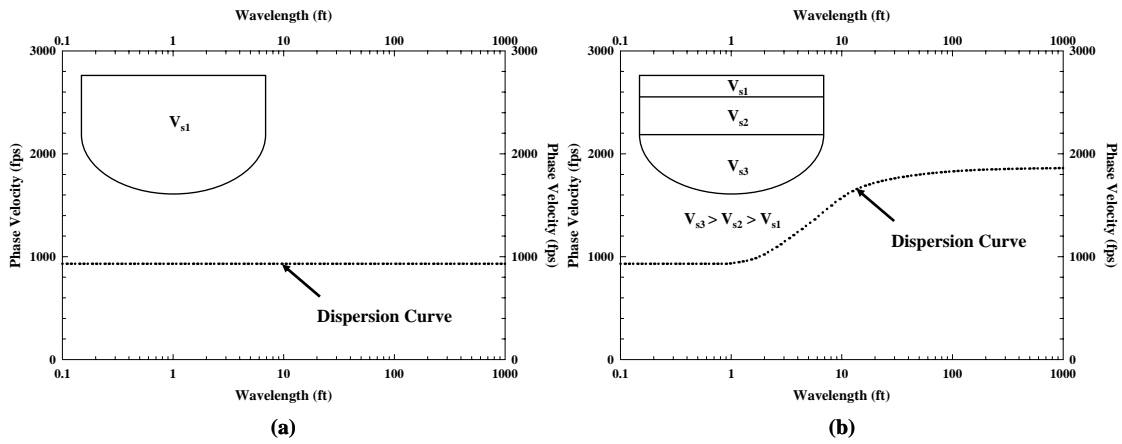
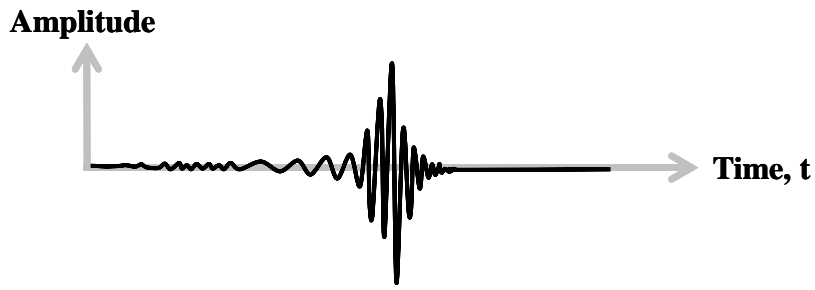
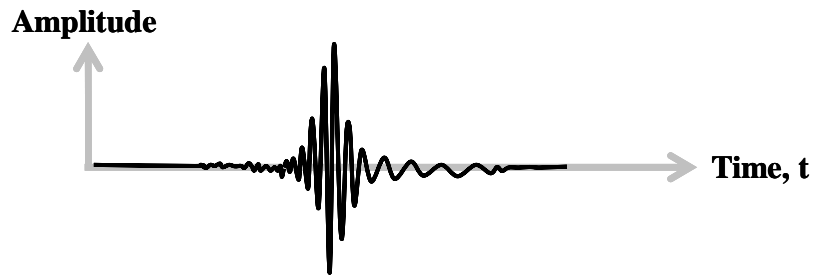


Figure 2.2 Dispersion Curves of Plane Rayleigh Wave Traveling in (a) Isotropic, Homogeneous Half Space and (b) Layered System



(a)



(b)

Figure 2.3 Comparisons of Different Waveforms from (a) Normally Dispersive Geotechnical Site and (b) Inversely Dispersive Pavement Site (Not Real Record, for Illustration Only)

2.2.2 Relationship between Shear and Rayleigh Wave Velocities

The information provided by shear wave velocity profiles has been used in many different ways to help engineers, geologists and seismologists understand the engineering properties of geotechnical sites to make their designs safer and more reliable. For instance, the shear wave velocity profile is directly related to the shear stiffness of a soil/rock profile, so the thickness and depth of different formation/stratum can be determined based on this information as long as there is a noticeable stiffness change between the formations. Also, the V_S profiles can be used to calculate shear modulus, even calculate Young's modulus with a reasonable value of Poisson's Ratio (ν). The information is very important in geotechnical earthquake engineering soil dynamics, and pavement design. Moreover, many structural engineers have adopted shear wave velocity profiles to evaluate the site response for predicting structural response.

The reason why SASW measurements have become so popular is because the shear wave velocity can easily be derived from the Rayleigh wave velocity, and Rayleigh waves measurement are easier and more cost-effective than shear waves measurements as mentioned above. In addition, the SASW method is quickly performed in the field compared to other intrusive profiling methods (i.e. crosshole, downhole and P-S logging methods).

The theoretical relationships between Rayleigh waves and shear waves propagate in an elastic half space can be described by (Richart et al, 1970):

$$\left(\frac{V_R}{V_S}\right)^6 - 8\left(\frac{V_R}{V_S}\right)^4 + (24 - 16\left(\frac{1-2\nu}{2-2\nu}\right))\left(\frac{V_R}{V_S}\right)^2 + 16\left(\left(\frac{1-2\nu}{2-2\nu}\right) - 1\right) = 0 \quad (2.1)$$

The relationship between V_R and V_S is plotted in Figure 2.4 with respect to the Poisson's ratio (ν). As seen in the figure, the ratio of V_R to V_S ranges from 0.874 to 0.955 for

Poisson's ratio ranging from 0 to 0.5, respectively. This range in difference in the ratio of V_R and V_S means the maximum difference or "error" in the value of V_S that is estimated from V_R because of a wrongly assumed Poisson's ratio is no more than 10 %. In other words, the ratio of V_R and V_S is not so sensitive to the Poisson's ratio. In addition, for a reasonable Poisson's range (0.2 to 0.4) which is commonly adopted for all soil and rock except saturated soil, the "error" is less than 5%.

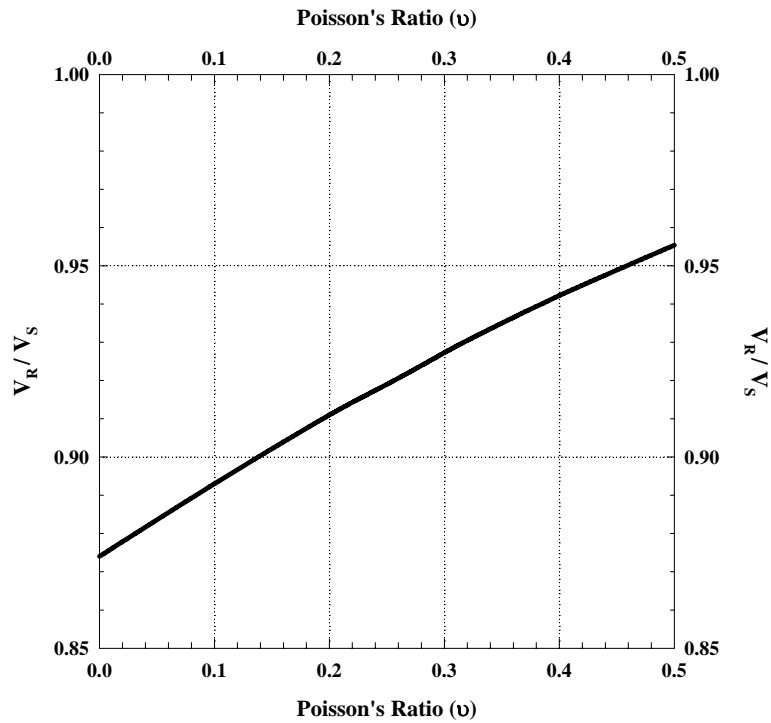


Figure 2.4 Variation of the Ratio of Rayleigh Wave to Shear Wave Velocity with Poisson's Ratio

2.3 REVIEW OF THE DEVELOPMENT OF THE SASW METHOD

Nowadays, several seismic methods are employed to evaluate the wave velocities of geotechnical materials. Either surface waves or body waves are employed in these measurements, with most measurements still involving intrusive methods and body waves. The Spectral-Analysis-of-Surface Waves (SASW) method, one of the increasing used seismic methods, is a non-destructive/intrusive technique used to profile the subsurface. The keys to the SASW method are the generation, measurement and analysis of Rayleigh waves propagating at the test site. Before getting into the SASW method, the steady-state Rayleigh wave method, the predecessor of the SASW method, is discussed below.

2.3.1 Steady-State Rayleigh Wave Method

Rayleigh waves were first introduced in 1885. However, they were not applied to real-world situation until the late 1930s. In 1938, the German Society of Soil Mechanics (DEGEBO) used Rayleigh waves to study the foundation response induced by steady-state vibration and this initialized the application of Rayleigh Waves (Richart et al. 1970, Nazarian 1984 and Roesset 1991). This application also represents the beginning of the steady-state Rayleigh (surface) wave method. In the following decades, the same technique was used by several researchers (Bergstorm and Linderholm (1946), Van der Poel (1951), Nijboer and Van der Poel (1953)) to obtain the material properties of pavement (Roesset et al., 1991). After 1958, the steady-state Rayleigh wave (surface wave) method was extended to survey soil profiles by Jones (1958), Heukelom and Foster (1960), Fry (1963) and Ballard (1964). The steady-state surface wave method was easy to understand but was time-consuming to apply. The field setup and analysis procedures of the steady-state surface wave method are discussed below.

2.3.1.1 Test Setup and Procedures

As mention above, the keys of the SASW method are to excite, measure and analyze Rayleigh waves propagating through the investigating area. These are the same keys to the steady-state Rayleigh wave method. However, the approaches are quite different between the two approaches. The steady-state Rayleigh wave method is described below.

The procedure to perform steady-state Rayleigh wave tests is straightforward. First, one vibrator and two vertical velocity transducers have to be placed in a line (see Figure 2.5) on the ground surface. The vertically excited steady-state vibrator is used to generate a single frequency at a time. This frequency is changed between measurements and testing is performed over a range of frequencies. The wave motion of each single-frequency Rayleigh wave propagating along the test array is monitored by the two transducers and an oscilloscope and recorded by a tape recorder. If the waveforms of the two transducers are not in-phase, the further transducer (sensor at location B in Figure 2.5) has to be moved to the point where the waveforms monitored by both transducers are in-phase (location C in Figure 2.5). For each frequency, sufficient in-phase locations need to be found to calculate the corresponding average wavelength, λ_{avg} , and then the Rayleigh wave velocity ($V_R = f \cdot \lambda_{avg}$) velocity of Rayleigh waves. Also, the test is performed over an adequate frequency range to obtain the Rayleigh velocities over the depths of interest. The next step is to generate the V_S profile of the test site as discussed below.

2.3.1.2 Analysis Procedures

Based on the distance and assumed number of waves between the two sensors that are at in-phase locations for each frequency (f), a plot as shown in Figure 2.6 can be

constructed. The average wavelength of Rayleigh wave (λ_R) for each frequency can be determined from this plot. By using the Equation 2.2, the Rayleigh wave velocity (V_R) of each tested frequency can be computed.

$$V_R = f \cdot \lambda_R \quad (2.2)$$

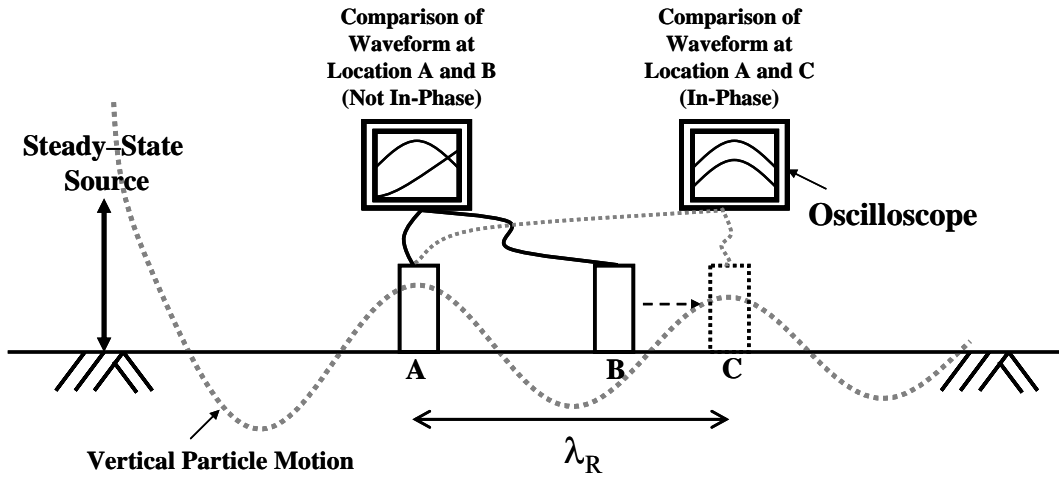


Figure 2.5 Illustration of the Test Setup Used in the Steady-State Rayleigh Wave Method

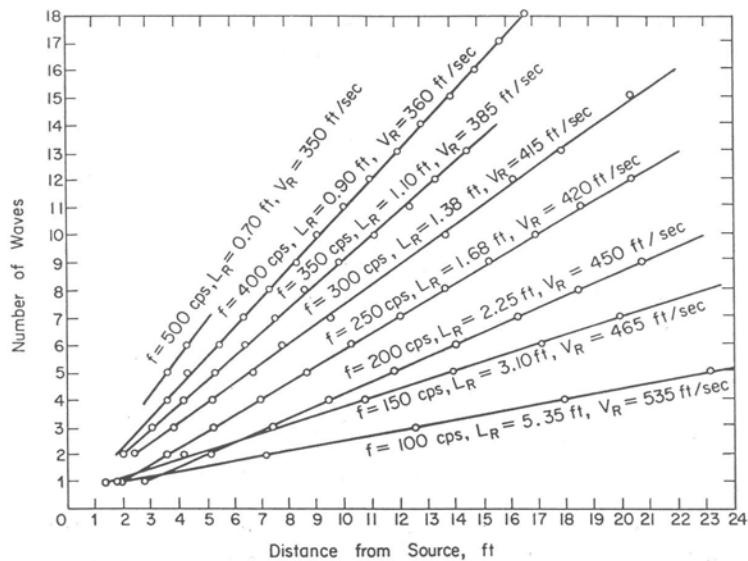


Figure 2.6 Determination of Average Wavelengths of Rayleigh Waves and Associated Rayleigh Wave Velocities (from Richart et al. 1970)

By assuming the shear wave velocity equal to 1.1 times the R-wave velocity and the profiling depth equal to one-half of the corresponding wavelength, a shear wave velocity profile of the test site can be established as shown in Figure 2.7.

The basis of the steady-state Rayleigh wave method is very simple and no complicated theories are involved. However, it is a time-consuming test which takes many hours to profile one site using a few (10 to 25) frequencies. If a higher-resolution V_S profile is needed (for example, for every 1 Hz from 10 to 200 Hz), it may take a day or two to finish the test. So, a more time-efficient profiling method was desired.

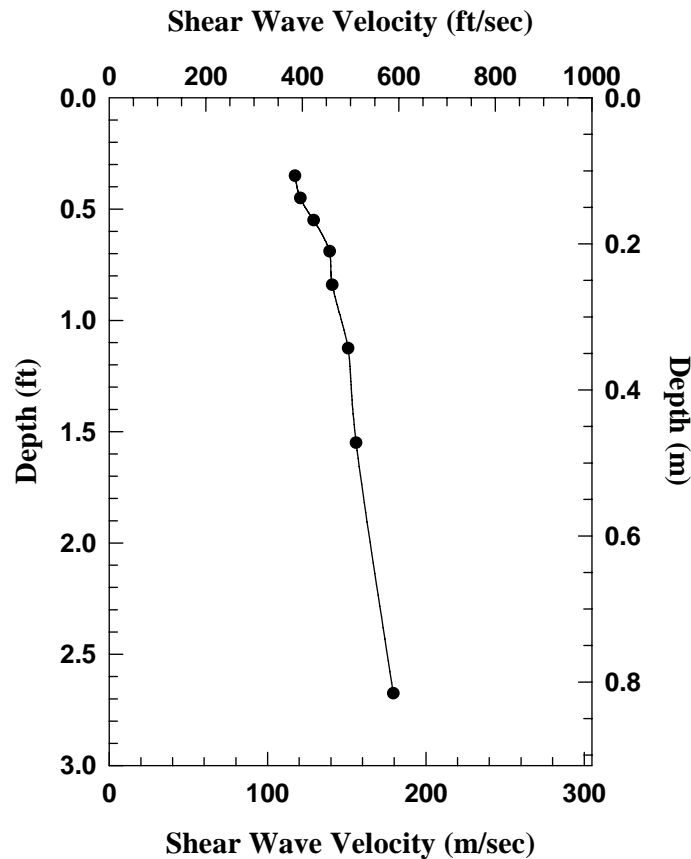


Figure 2.7 Shear Wave Velocity Profile Reduced from Figure 2.6

2.3.2 Development of the SASW Method

In the late 1970s, because of the development of portable digital electronic equipment that could be taken to the field, fast calculation on spectral analysis became possible. With the contribution of the Fast Fourier Transform (FFT) algorithm, the development of the SASW method was initiated.

The idea of the SASW method was formed around the late 1970s. Williams (1981) used broad-band frequency sources (a random noise generator and a drop hammer) and the FFT algorithm to perform spectral analysis to obtain the experimental dispersion curves at two different locations. The spectral analysis is an algorithm used to calculate the phase difference between two adjacent sensors (receivers or transducers) at each frequency. The details are described later. Comparisons between the dispersion curves from spectral analysis and the steady-state surface wave method performed at the same locations showed that these two methods gave similar results. However, this study only focused on the possibility of using spectral analysis to obtain the experimental dispersion curves that are comparable to the ones from the steady-state surface wave method. That is, it did not investigate the relationship between field shear wave velocity profiles and experimental dispersion curves.

Heisey (1981 and 1982) used the spectral-analysis-of-surface-wave to perform seismic tests at two soil sites and two flexible pavement sites. Instead of a tape recorder used in Williams's study, he utilized a spectral analyzer to acquire data and to handle the FFT calculations at the same time. By doing so, the time in the data reduction to determine the dispersion was greatly shortened. Heisey's study was funded by the Texas State Department of Highways and Public Transportation. Heisey's study showed that the shear wave velocity profiles were comparable to crosshole and Falling Weight

Deflectometer (FWD) test results. However, there was no any forward modeling or inversion analysis used to calculate the V_S profiles from the experimental dispersion curves. In Heisey's study, he simply suggested using one-third of the wavelength as the "effective sampling depth" and the values of V_R were divided by 0.94 (or 0.93, depending on the Poisson's ratio from downhole tests) to obtain V_S at the corresponding wavelength to construct the field shear wave velocity profiles for shallow soil layers (less than 30 ft) and the pavement layers. In addition, Heisey investigated which orientation of the receivers is better for the surface wave test and the results showed vertical sensors have better signals than horizontal ones.

In 1984, Nazarian and Stokoe incorporated an inversion technique in the SASW method. The inversion analysis in their study was no longer based on simplified assumptions to acquire the field shear wave velocity profile. Instead, the inversion analysis was theoretically based and made the SASW method more complete. The simplified V_S profiles generated in the past may not be able to determine the actual velocities of each soil layer. That means the V_S value for each layer in the simplified profile could be the value which is averaged with the V_S values of adjacent layers. In other words, the V_S value may be over- or under-estimated. The inversion analysis proposed by Nazarian and Stokoe could overcome this problem and calculate V_S values associated with each of the soil layers. Since then, the SASW method has become more robust and widely accepted to profile the subsurface.

Moreover, there have been several techniques derived from the SASW method by changing the test setup (seismic source types or numbers of sensors) or analysis technique, such as Multichannel Analysis of Surface Waves (MASW) (Park et al., 1999) and controlled source of spectral analysis of surface waves (CXW) methods (Rodriguez-Ordenez, 1994). That shows the flexibility and diversity of the SASW method.

2.4 OVERVIEW OF THE SASW METHOD

2.4.1 Field Equipment

2.4.1.1 Seismic Sources

Several types of devices have been used as seismic sources in the SASW method in this study. Some are very simple, such as a hammer or a drop weight that can generate Rayleigh waves from a vertical impulse over some range of frequencies. Some sophisticated sources can produce Rayleigh waves at each frequency for several seconds to several minutes from high-to-low (or low-to-high) frequencies, called stepped-sine vibration, or “chirp” vibrations, such as vibroseis trucks. Others sources can excite Rayleigh waves over random frequencies, such as bulldozer source. In general, these sources are all broad band seismic sources.

The seismic sources used in this study are broad band frequency sources. They are able to generate surface waves over a broad range in frequencies. The capacity, in terms of energy output and operation frequency, of the seismic source plays an important role in the SASW method. The more energy that the seismic source transmits to the subsurface, the better chance one has of obtaining good quality (or usable) data. The effect of ambient noise can be reduced by larger output energy from the source. In other word, the signal-to-noise ratio is larger. The signal-to-noise ratio is very crucial when performing tests at low frequencies because the maximum profiling depth is based on the low-frequency and ambient noise is often low frequency data. Also, the lower the operational frequency of the seismic source, the deeper can be the maximum profiling depth. The deepest profiling depth for the SASW testing performed in this study is from Site H10 at Hanford, WA. This depth is about 2000 ft.

In terms of the way vibrations are created, there are two different types of sources. One is an active source; the other is a passive source. Active sources are artificial excitations created by vibrators, such as vibroseis trucks, bulldozers or drop weights. Passive sources are ambient noises from natural or human activities, such as geostrophic tremor or traffic. The seismic sources used in the SASW technique are all active sources. Different seismic sources have been employed based on their availability to generate energy and the source-receiver spacings required in the SASW tests. For larger test spacings, usually larger than 25 ft, a more powerful seismic source that can input more energy into the subsurface is required to perform the test, such as vibroseis trucks (Liquidator) or bulldozers. In contrast, for shorter spacings, a sledge or rock hammer is adequate for the SASW source.

There have been six different active sources used for the larger test spacings in the SASW tests performed by University of Texas at Austin. The first one is a bulldozer that was used at some of the Yucca Mountain test sites (Figure 2.8). The second one is a DynaSource (Figure 2.9) which is often used in surface refraction and surface reflection tests. The third one was a large drop weight (4500-lb weight, Figure 2.10) that was developed by Prof. James A. Bay at Utah State University and has been used over past five years but none of the test results are included in this study. The other three are all vibroseis trucks. The first one, a vibroseis (Figure 2.11), is a standard vibroseis truck currently used in exploration industry. The other two are T-Rex and Liquidator which are two of three custom-made vibroseis vehicles for the nees@UTexas project (Figure 2.12). These three vibrators were built by Industrial Vehicles International, Inc. (IVI) for different purposes. T-Rex has the largest output force among the three nees@UTexas project vibrators and can shake in three different directions. Liquidator has more output energy in the low-frequency range (below 3.7 Hz) than the other two so

it is a better seismic source for deep subsurface profiling. Thumper can not output as much energy as the other two vibrators but is the ideal vibroseis truck to perform SASW test in an urban area. In this study, SASW tests performed by Thumper are not included. A comparison of the theoretical output forces of the four different vibroseis systems is presented in Figure 2.13.



Figure 2.8 A bulldozer Used as a Seismic Source to Perform SASW Test at Waste Handling Building (WHB) at Yucca Mountain, NV



Figure 2.9 DynaSource Used as Impact Source at Kung-Chung Elementary School Site (TCU-52) in Taiwan



Figure 2.10 Large Drop Weight Used as Impact Source to Perform SASW Test at LA Fire Station #99, Los Angeles, CA



Figure 2.11 A Traditional Vibroseis Performing the SASW Test at El Centro Array #1 in Imperial Valley, CA



a. High-force, three-axis vibrator called T-Rex



b. Low-frequency, two-axis vibrator called Liquidator



c. High-frequency, three-axis vibrator called Thumper

Figure 2.12 Photographs of the Three Nees@UTexas Mobile Vibrators (from Stokoe et al., 2006)

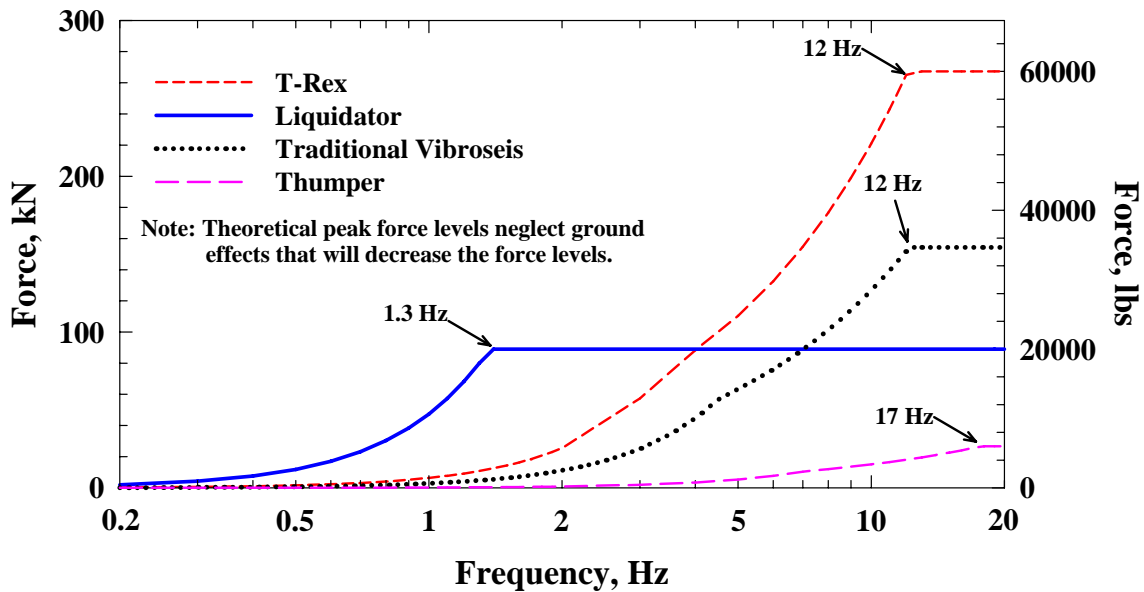


Figure 2.13 Comparison of the Theoretical Output Force Levels in Vertical Shaking of Four Different Vibrators in the Frequency Range of 0.2 to 20 Hz (from Stokoe et al., 2006)

2.4.1.2 Dynamic Signal Analyzer

To handle the Rayleigh-wave-propagation data collected with the sensors placed on the ground (geophones or accelerometers), an Agilent 35670A Dynamic Signal Analyzer (Figure 2.14) is used to record and conduct the calculations for the phase information of the cross-power spectrum in frequency domain in this study. This analyzer has four channels so it can handle data from four different geophones/accelerometers at the same time. Also, a build-in source output of the analyzer is utilized to control the vibroseis trucks to perform a stepped-sine vibration (vibrating at each frequency for several seconds from high-to-low frequencies) or other sine wave vibrations.



Figure 2.14 Photograph of an Agilent 35670A Dynamic Signal Analyzer

2.4.1.3 Transducers/Receivers/Sensors

There are two common types of transducers used in the SASW test. One is the geophone and the other is the accelerometer. Geophones are used at frequencies from about 1 to 500 Hz while accelerometers are used at frequencies from about 20 to 20000 Hz. It is very important to calibrate the transducers to make sure they function well before the test is performed. If the differences between the calibration curves of the transducers are too large within the frequency range of interest, it may result a large error in the test results. Therefore, having these transducers calibrated is crucial to test results.

- **Geophones**

At most geotechnical sites, geophones are used as the signal receivers. Most SASW measurements from long spacings in this study were gathered with Mark Products Model L-4C geophones (Figure 2.15) which have a natural frequency of 1 Hz. These

geophones perform very well in the low frequency range (1 to 300 Hz) which is very important to collecting long-wavelength data.



Figure 2.15 Photograph of 1-Hz Geophone on the Yard of the Brawley Airport in Imperial Valley, CA

- **Accelerometers**

At rock, stiff soil or pavement sites, accelerometers (Figure 2.16) are used instead of geophones to perform (at least portion of) the SASW tests. These accelerometers have better performance in high-frequency range (100 to 20000 Hz) compared to geophones and their frequency ranges are wide enough to monitor all useful data generated by a seismic source at stiff sites.



Figure 2.16 Photograph of an Accelerometer - Wilcoxon Model 736

2.4.2 Analysis Tool

In some studies, a simplified method was adapted to obtain the theoretical dispersion curve from which the shear wave velocity profile was calculated. For instance, an approximate method introduced by Satoh (1991). It is easy to obtain the “estimated” shear wave velocity profile of a test site by this method. However, this method does not take the effects of Poisson’s ratio, ground water table and some other factors into account, including higher modes of Rayleigh waves. Sometimes, these factors have an important impact on the shear wave velocity profile so a theoretically-corrected algorithm or program should be used to reduce the SASW test data. The analysis software used in this study was developed for this purpose. The software is called “WinSASW” and it was developed by Prof. Sung-Ho Joh (1992).

2.4.2.1 Capabilities of WinSASW

WinSASW is a comprehensive software package with which forward modeling, both global- and array-based, and inversion can be performed. Forward modeling incorporated in WinSASW is based on the dynamic stiffness matrix method presented by

Kausel and Roesset (1981) and Kausel and Peek (1982). In this study, WinSASW was used to perform forward modeling. For the vast majority of the analyses, global forward modeling was done. In some cases, array forward modeling was used to investigate the field dispersion curve at largest receiver spacings.

- **Forward Modeling and Inversion Analysis**

There are two methods to obtain the SASW V_S profiles. One of them is forward modeling, and the other is inversion analysis. The difference between these two methods is illustrated Figure 2.17.

The WinSASW program is capable of handling the SASW data recorded by the dynamic signal analyzer. This software has the functions for calculating the phase plot (phase difference between two receivers), masking undesired phase data and generating experimental dispersion curves. It also can determine shear wave velocity profile of the test site by fitting the experimental dispersion curve with a theoretical dispersion curve. The fitting method is an iterative procedure to find the best shear wave velocity profile that fits the dispersion curve evaluated at the test site. This method is also known as forward modeling. The first version of WinSASW could only perform forward modeling but the newer version of WinSASW (version 2) can perform true inversion analysis which was used to compare to the forward modeling results at some test sites from this study.

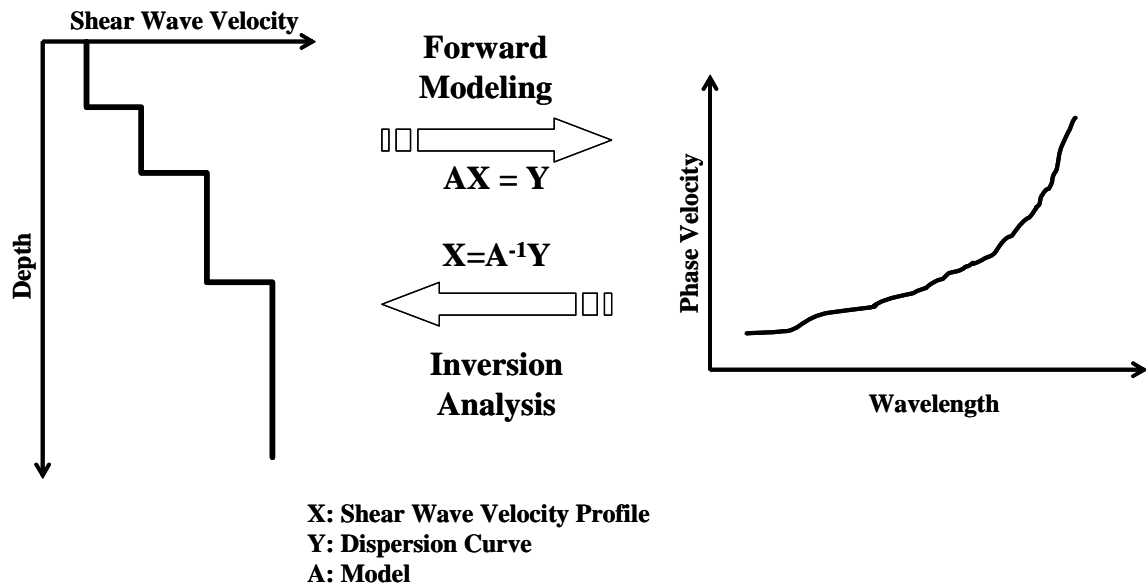


Figure 2.17 Illustration of Difference between Forward Modeling and Inversion Analysis

- **2-D and 3-D Solutions**

In the beginning of the development of the SASW method, only plane Rayleigh waves were considered. Considering only plane R waves means that only the fundamental mode Rayleigh wave was considered and also no reflected or refracted body waves were taken into account. This is called the 2-D solution herein. It may be (or may not be) suitable for some seismic techniques, such as ReMi (Refraction Microtremor) method, that use passive sources to perform the tests because the vibrations generated by passive sources are assumed to be from very far distances. In this case, the effect of reflections and refractions of body waves can be negligible. However, higher-mode R waves may exist as they can with active sources. Because of this reason, a more complete solution, called the 3-D solution, should be adopted to simulate the field

dispersion curve. The WinSASW software adopted in this study is able to conduct both 2-D and 3-D analyses. Only 3-D analyses were used to analyze the data in this study.

- **Fundamental and Higher Modes**

If the shear wave velocities of the soil layers increase smoothly and very gradually with profiling depth, it is likely that only fundamental-mode of Rayleigh waves will appear. However, if there is a rock layer under the soil layers or a softer layer is sandwiched between stiffer layers or if the shear wave velocity increases rapidly between layers, higher modes of the Rayleigh wave may become dominant. In this case, the dispersion curve may be misinterpreted if only the 2-D solution (plane R wave solution) is considered.

The analysis program, WinSASW, used in this study is capable performing the 3-D solution and considers higher modes of Rayleigh waves. Therefore, theoretical dispersion curves can be generated that contain the effects of reflected and refracted body waves and higher-mode Rayleigh waves.

2.4.3 Test Setups for SASW Measurements

As mentioned above, in the SASW method the key are to generate, measure and analyze Rayleigh waves. To generate Rayleigh waves, either an active or passive seismic source is need. In the measurement of Rayleigh waves, two or more transducers (geophones or accelerometers) are used to monitor wave propagating along a radial path from the source. All the measurements are conducted and stored in a dynamic signal analyzer. Regarding the analysis of Rayleigh waves, the appropriate analysis software is required. This software must be able to consider all modes of propagation as discussed earlier.

Based on the location of the centerline of the transducer array or the location of the seismic source, there are several different test setups. Initially, only two sensors were used to detect the ground motion in the SASW test because only two-channel dynamic signal analyzer was available for field use. This generalized configuration of the SASW test is shown in Figure 2.18.

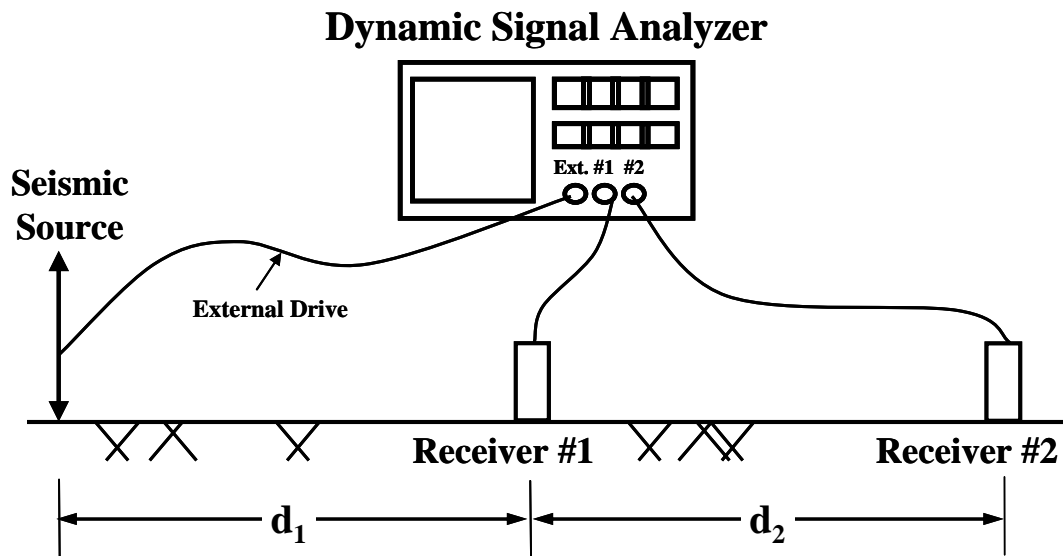


Figure 2.18 Initial Generalized Configuration of the SASW Test Used in the Field

There are two common source-receiver arrangements used in the initial SASW tests. The first one is called the common receiver midpoint (CRMP) geometry (Figure 2.19). The test spacing (X) is doubled from the previous spacing each time the test is performed. In this arrangement, the center line is kept as the midpoint of the receivers of all test spacings. The advantage of this setup is that all the test spacings profile the same area. The disadvantage is that the source and receivers have to move for different test spacings. Some sources are not so easy to move around so they increase the difficulty and time to perform the SASW test. The second test arrangement is called the

common source (CS) geometry. Also, the test spacing (X) is doubled from one spacing to the next. As seen in Figure 2.20, the source is fixed and only the receivers need to be move around. However, in this arrangement, different spacings profile different portions of the test array. If the test site has no significant lateral variability, the test result from these two setups will have little difference.

A study of source and receiver geometry was investigated by Hiltunen and Woods (1989) regarding the testing on pavements. It was found that measurements obtained from these two geometries on the same pavement are nearly identical and the scatter within all the collected data was similar in both geometries.

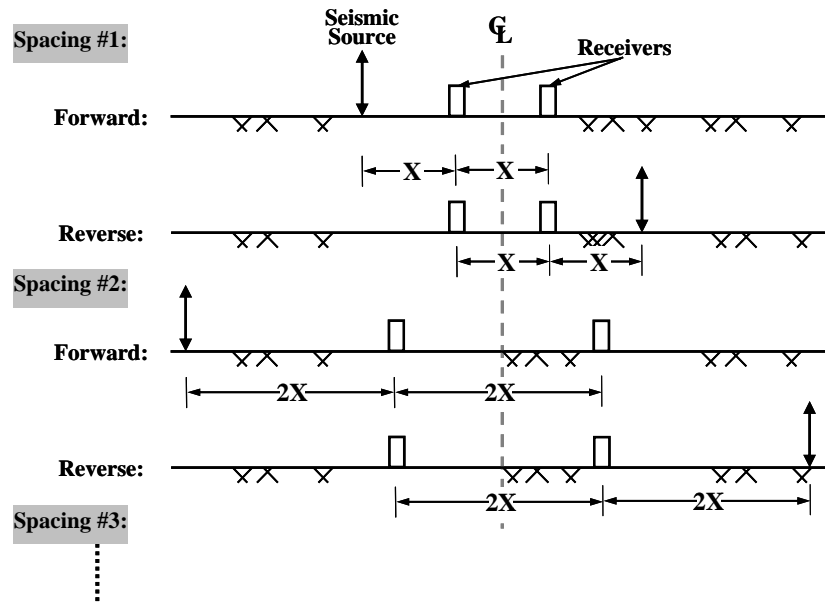


Figure 2.19 Illustration of the Common Receiver Midpoint (CRMP) Geometry Used in Initial SASW Testing with Two Receivers

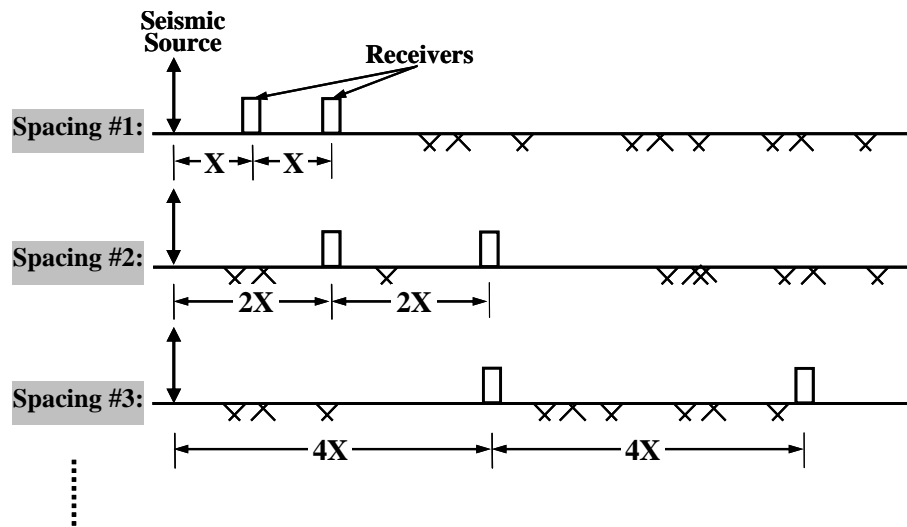


Figure 2.20 Illustration of the Common Source (CS) Geometry Used in Initial SASW Testing with Two Receivers

The arrangement of the source and receivers are not the same at every test site in this study. Sometimes, because of the restriction of space at the test site, the source-receiver arrangements were modified to some extent. However, testing was always performed over the same area of the test site as much possible.

The reason why only two receivers were used in the SASW test in the past is because only a two-channel analyzer was the most available/affordable test equipment at that time. Today, an analyzer is capable of handling four to more than a hundred channels, so more receivers are used in the SASW tests today. By using additional receivers in the SASW test, field testing time is reduced and more information at the test site is obtained because multiple-spacing data are measured at the same time. Again, if there is large lateral variation at the test site, the data from different pair receivers will not be consist with each other. However, this consistency or inconsistency can be used as an “index” to qualitatively estimate the extent of lateral variations. In this study, three receivers were generally used at the test sites. This general arrangement of the source

and receivers is illustrated in Figure 2.21 for shorter spacings (usually less than 25 ft). For larger spacings, only the forward-direction tests were generally conducted.

Within a certain distance from the seismic source of the SASW test, the waveform of the Rayleigh waves has additional characteristics (near-field forms) not taken into account in the data analysis. In the data analysis (WinSASW), only far-field behavior for both Rayleigh waves and body waves from the body waves (P wave and S wave) is assumed. To avoid misinterpreting the SASW test results, these near-field data should be excluded. In an attempt to minimize the inclusion of near-field data, two criteria are applied to the SASW test setups. First criterion is the spacing ratio between source and first receiver and the first and second receivers; the other criterion is the range of acceptable maximum and minimum wavelengths. Several researchers have conducted some studies to find out the best criteria for the SASW test. The results from these studies are listed in Table 2.1.

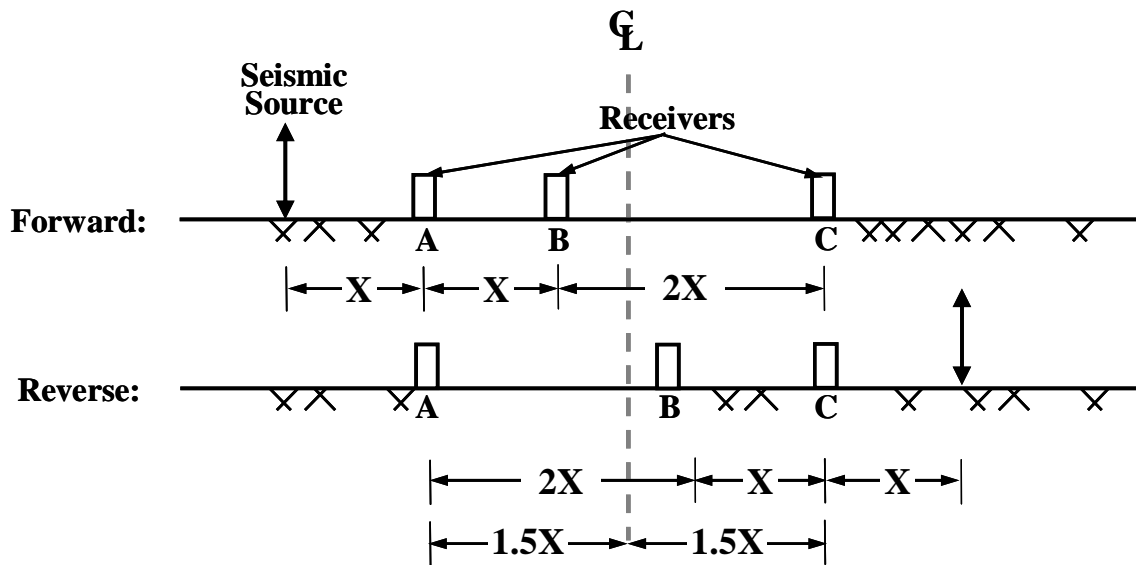


Figure 2.21 Illustration of the General Source-Receiver Arrangement Used in the SASW Tests Performed as Part of this Study

The most common setup is the source-to-first-receiver spacing equal to first-to-second-receiver spacing, and the filtering criterion is wavelength (λ) is less than two times the receiver spacing. In this study, the general setup of the SASW test is that the distance between source and first receiver (d_1) and the distance between the first and second receivers (d_2) are equal and the maximum wavelength used is less than two times the spacing between the receivers ($0.5\lambda < d_1 = d_2$). In some cases, a distance between the source and first receiver was two times the distance between the first and second receivers because of space limitations at the test site. However, the maximum usable wavelength is still the same as the criterion above ($0.5\lambda < d_1$) based on the distance between the source and first receiver. However, in this case, the maximum wavelength becomes four times of the receivers spacing ($0.25\lambda < d_2$).

Table 2.1 Setup and Criteria for Filtering Near-Field Data

Investigator	Setup and Criteria	
Heisey et al. (1982)	$d_1 = d_2$	$1/3 \lambda < d_2 < 2\lambda$
Roesset et al. (1990)	$0.5 \lambda < d_1 < 2\lambda$	$0.5 \lambda < d_2 < \lambda$
Gucunski and Woods (1992)	-	$0.5 \lambda < d_2 < 4\lambda$
Stokoe et al. (1994)	$0.5 \lambda < d_1$	-

d_1 = distance from source to first receiver; d_2 = distance between receivers; λ =wavelength

2.4.4 Procedures to Reduce SASW Data

2.4.4.1 Interpret Experimental/Field Dispersion Curves

The idea of the SASW method is to calculate the Rayleigh wave phase difference with respect to different frequencies/wavelengths for various test spacings at a site so that the field/experimental dispersion curve can be constructed. The field dispersion curve provides the information about the shear wave velocity profile at the test site. The

procedures used to calculate the Rayleigh wave phase velocity and to generate the field dispersion curve are described in the following paragraphs.

First, the FFT algorithm within the dynamic signal analyzer is used to convert the time-domain data from two adjacent receivers (or any pair of receivers) at given locations (receivers A and B or B and C in Figure 2.19) to the frequency domain using:

$$X(f) = \int_{-\infty}^{\infty} x(t) \cdot e^{-i2\pi ft} dt \quad (2.3)$$

$$Y(f) = \int_{-\infty}^{\infty} y(t) \cdot e^{-i2\pi ft} dt \quad (2.4)$$

Where t is time, f is frequency, π is ratio of a circle's circumference to its diameter which is about 3.14159, i is the square-root of negative one, and $X(f)$ and $Y(f)$ are defined as the Fourier transforms of the time-domain records, $x(t)$ and $y(t)$, from first and second receivers, respectively.

Second, cross power spectrum (G_{YX}) or frequency response spectrum (or transfer function) (H_{YX}) of the two frequency-domain records are calculated as:

$$G_{YX}(f) = Y(f) \cdot X^*(f) \quad (2.5)$$

$$H_{YX}(f) = \frac{G_{YX}(f)}{G_{XX}(f)} \quad (2.6)$$

Where G_{XX} is defined as auto power spectrum and $*$ denotes the complex conjugation.

The phase difference data of the Rayleigh waves measured between these two receivers at each tested frequency can be obtained from either the cross power spectrum or transfer function by:

$$\phi(f) = \arctan \cdot \frac{\text{Im}(G_{YX})}{\text{Re}(G_{YX})} = \arctan \cdot \frac{\text{Im}(H_{YX})}{\text{Re}(H_{YX})} \quad (2.7)$$

Where Im means imaginary part of the expression, and Re means the real parts of the expression.

The phase difference information at each frequency is usually presented in a wrapped phase plot as Figure 2.22. In all SASW testing, the procedures described above are performed by the dynamic signal analyzer in the field so that the results can be viewed and checked in the field during data collection. As a result, data collection is improved and the time for post-field-test analysis (or data reduction) is shortened.

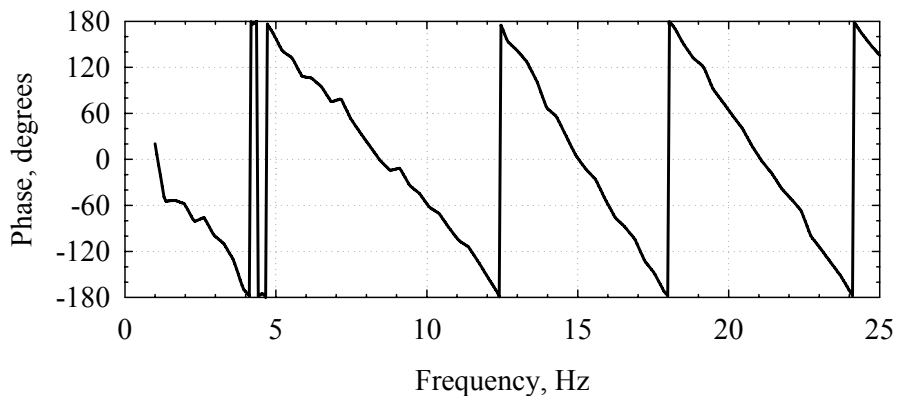


Figure 2.22 Wrapped Phase Plot Determined in the Field from the Cross Power Spectrum Calculated Using Two Adjacent Receivers (or Any Receiver Pairs)

After field testing is completed, the post-field-test analysis can be performed with the WinSASW software. First, the phase velocities of the Rayleigh waves need to be calculated by unwrapping the wrapped phase plot. An unwrapped phase plot is shown in Figure 2.23. This step is automatically done in WinSASW. The next step is to mask/remove the near-field and low-quality data from the phase plot as illustrated in

Figure 2.24. This step has to be performed manually and interactively in WinSASW. Based on the information from the phase plot and the distance between the two receivers, the phase velocity can be calculated for each measured frequency/wavelength. This calculation procedure is explained in Figure 2.25. To make it easier to understand, two examples are shown below.

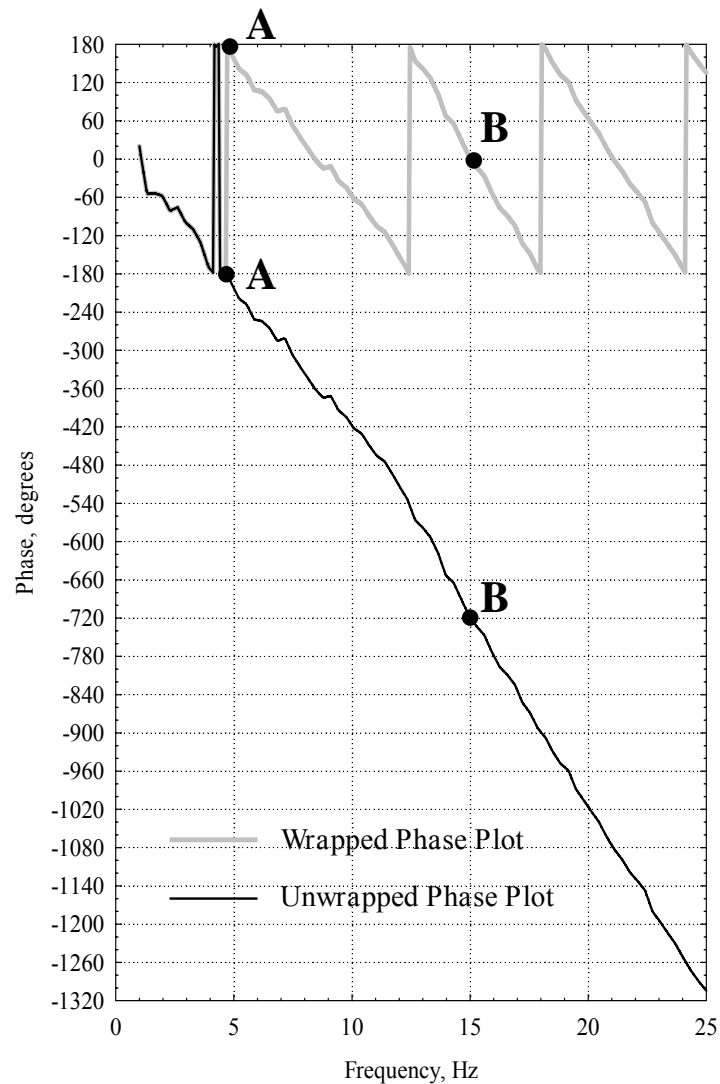


Figure 2.23 Comparison of Wrapped and Unwrapped Phase Plots Determined from the Cross Power Spectrum Evaluated from One Pair of Receivers

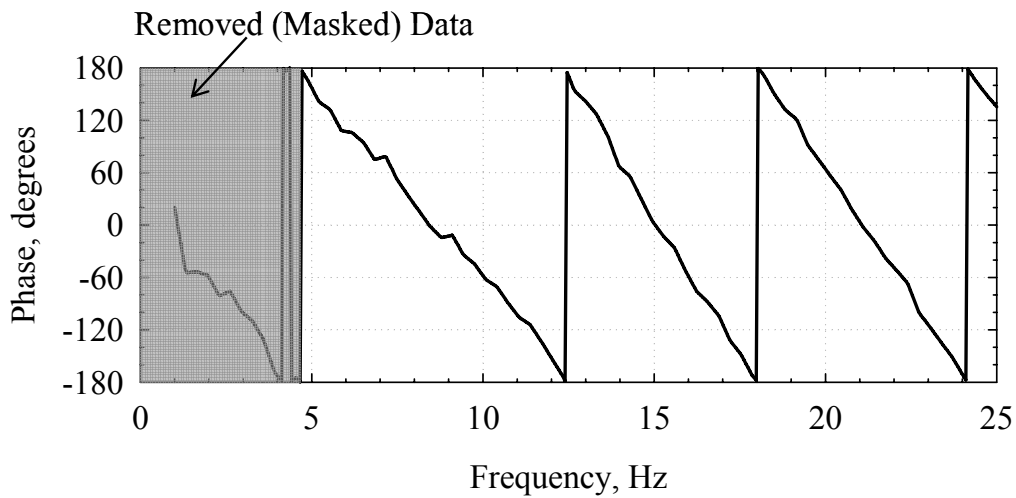


Figure 2.24 Illustration of Masking Undesired Data in a Wrapped Phase Plot

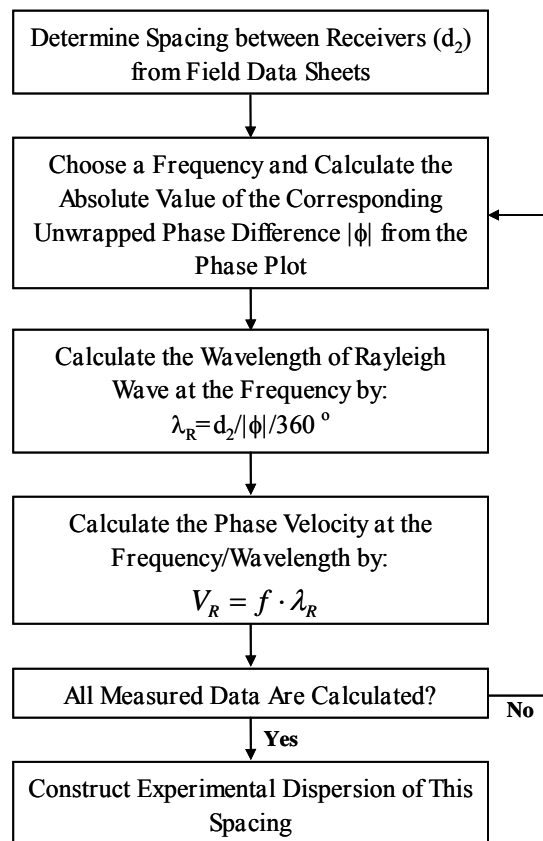


Figure 2.25 Flow Chart of Calculating Wavelengths of Rayleigh Waves and the Corresponding Phase Velocities to Build the Experimental Dispersion Curve

- Example 1:

In Figure 2.23, at Point A in the Unwrapped Phase Plot: $d_2 = 300 \text{ ft}$, $|\phi| = 180^\circ$ and $f = 4.6 \text{ Hz}$.

$$\text{Therefore: } \lambda_R = \frac{d_2}{\frac{|\phi|}{360^\circ}} = \frac{300 \text{ ft}}{\frac{180^\circ}{360^\circ}} = 600 \text{ ft} \quad (2.8)$$

$$\text{And: } V_R = f \cdot \lambda_R = 4.6 \text{ Hz} \cdot 600 \text{ ft} = 2760 \text{ fps} \quad (2.9)$$

The resulting value of V_R and its corresponding λ_R for Point A are plotted in Figure 2.26.

- Example 2:

In Figure 2.23, at Point B in the Unwrapped Phase Plot: $d_2 = 300 \text{ ft}$, $|\phi| = 720^\circ$ and $f = 15 \text{ Hz}$.

$$\text{Therefore: } \lambda_R = \frac{d_2}{\frac{|\phi|}{360^\circ}} = \frac{300 \text{ ft}}{\frac{720^\circ}{360^\circ}} = 150 \text{ ft} \quad (2.10)$$

$$\text{And: } V_R = f \cdot \lambda_R = 15 \text{ Hz} \cdot 150 \text{ ft} = 2250 \text{ fps} \quad (2.11)$$

The resulting value of V_R and its corresponding λ_R for Point B are plotted in Figure 2.26.

After the calculations above are performed for each measured frequency/wavelength, the experimental dispersion curve of the test-spacing being analyzed can be constructed (shown by the black circles in Figure 2.26). This one-spacing consists of 338 data points in this example. After all the data from all test

spacings at the site are calculated, a global/composite experimental dispersion curve (shown by the gray circles in Figure 2.26) is obtained. The composite field curve combines the individual experimental dispersion curves from the different spacings. The composite curve is composed of 3012 data points.

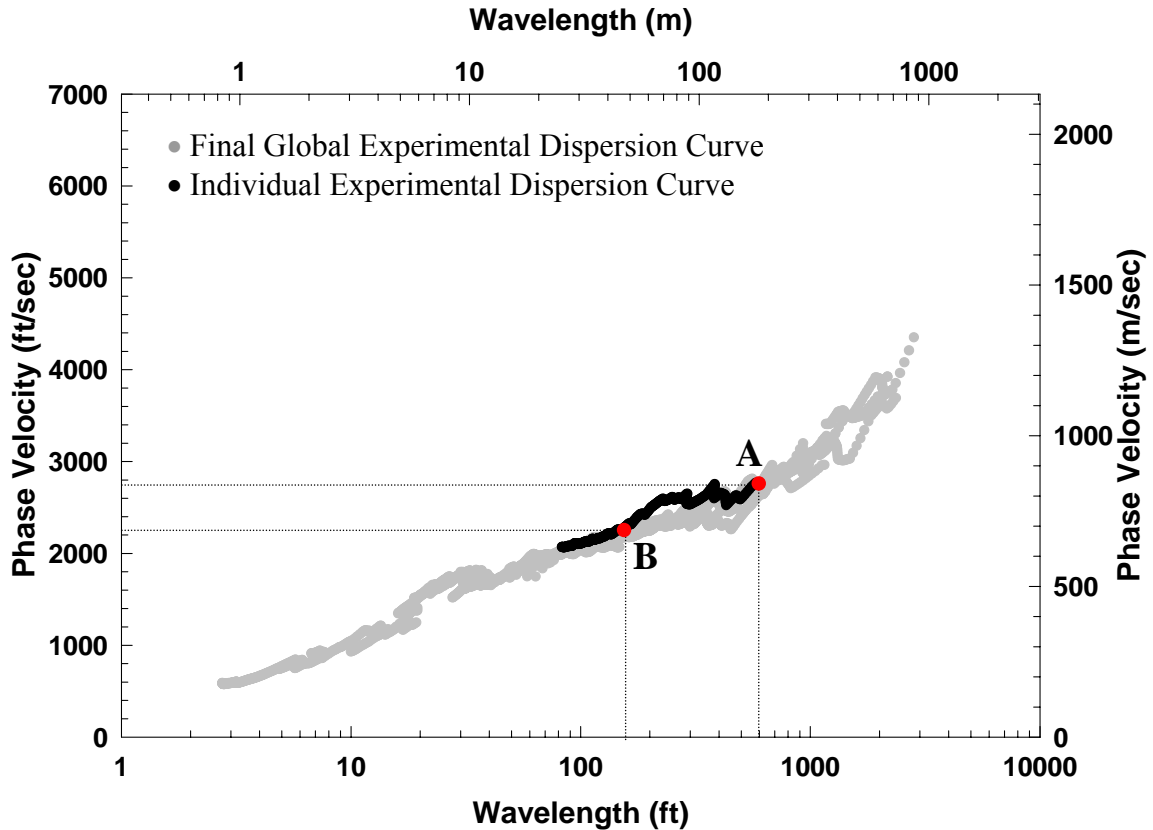


Figure 2.26 Experimental Dispersion Curves Calculated from Figure 2.23 and All Other Receiver Spacings at the Site

Figures 2.27 through 2.52 show: (1) the phase plots for each test spacing from one site in the North Portal Facility area at Yucca Mountain, NV and (2) the corresponding experimental dispersion curves derived from the phase plots. The black and gray circles in each dispersion curve figure represent the individual experimental dispersion curve

from each test spacing (a total of 13 individual curves) and the global experimental dispersion curve determined from all spacings respectively.

One important point in evaluating the appropriateness of the SASW test at a given site is to see how well the individual dispersion curves fit together (in other words, “overlap”) to form the composite dispersion curve. In the case of the individual dispersion curve shown in Figures from 27 to 52 at the Yucca Mountain Site, the overlap between individual curves is excellent, indicating little global variability at this site. As the present forward modeling in WinSASW is used, little global variability is implicitly assumed, which is reasonable in this example.

The next step is to generate the shear wave velocity profile that has a theoretical dispersion curve that fits well the experimental dispersion curve. To achieve this goal, either forward modeling or inversion analysis should be used. In this study, all V_s profiles were determined by forward modeling.

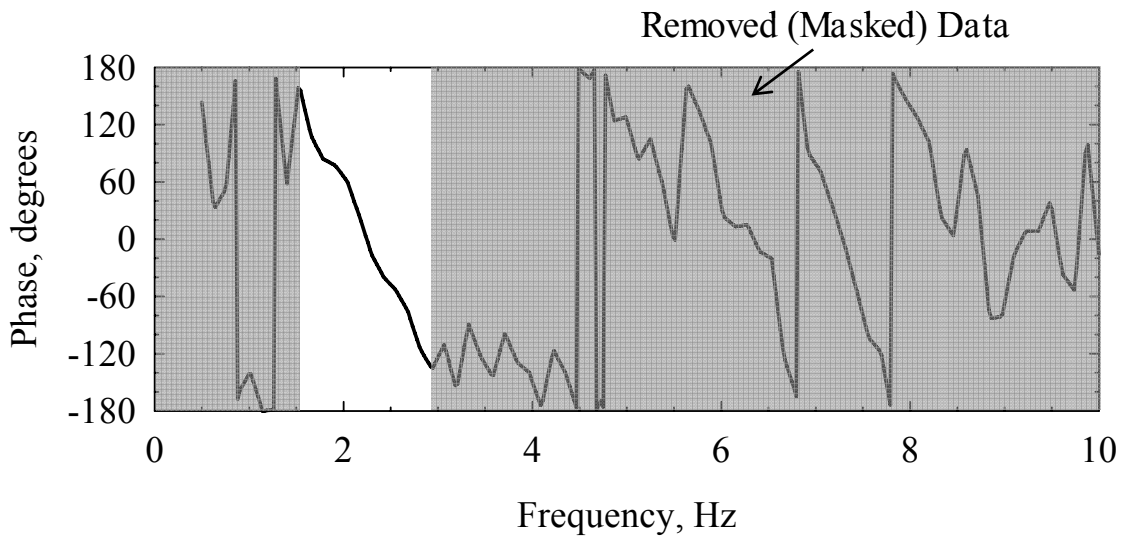


Figure 2.27 Wrapped Phase Plot Measured by SASW Testing with a 1600-ft Receiver at One Yucca Mountain Site

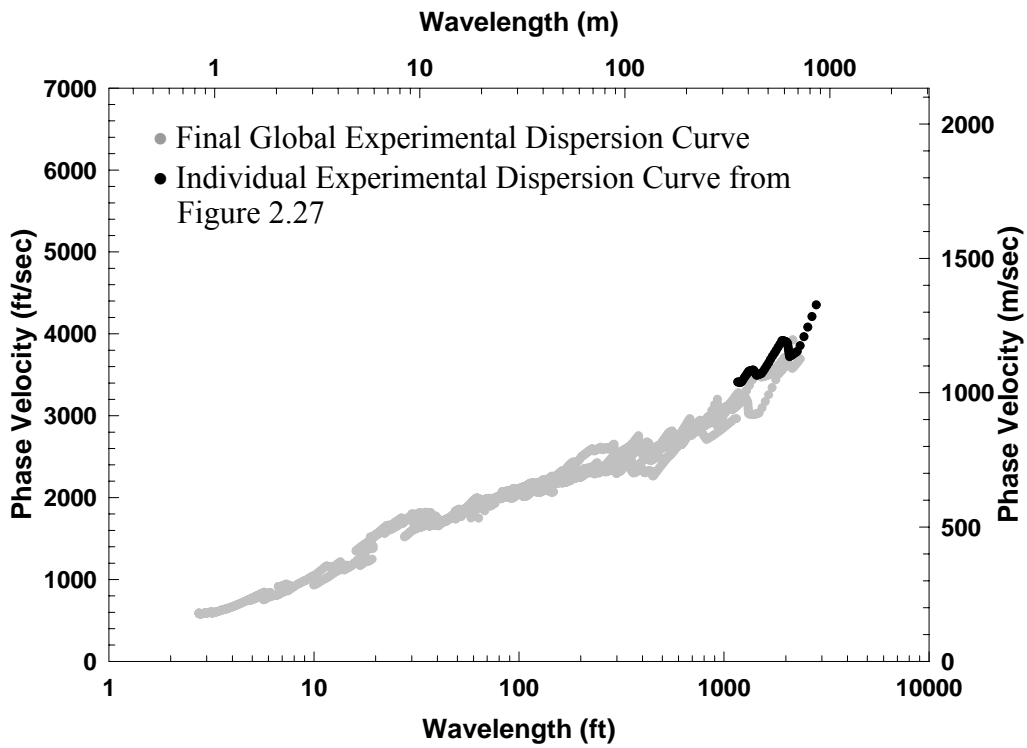


Figure 2.28 Experimental Dispersion Curves Determined from Figure 2.27 and All Other Receiver Spacings at One Yucca Mountain Site

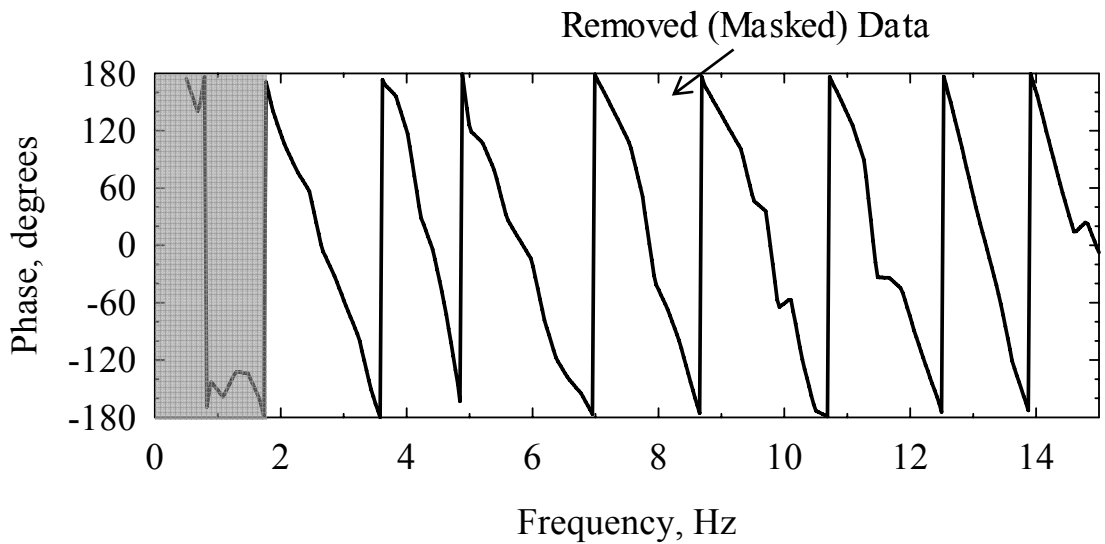


Figure 2.29 Wrapped Phase Plot Measured by SASW Testing with a 1200-ft Receiver at One Yucca Mountain Site

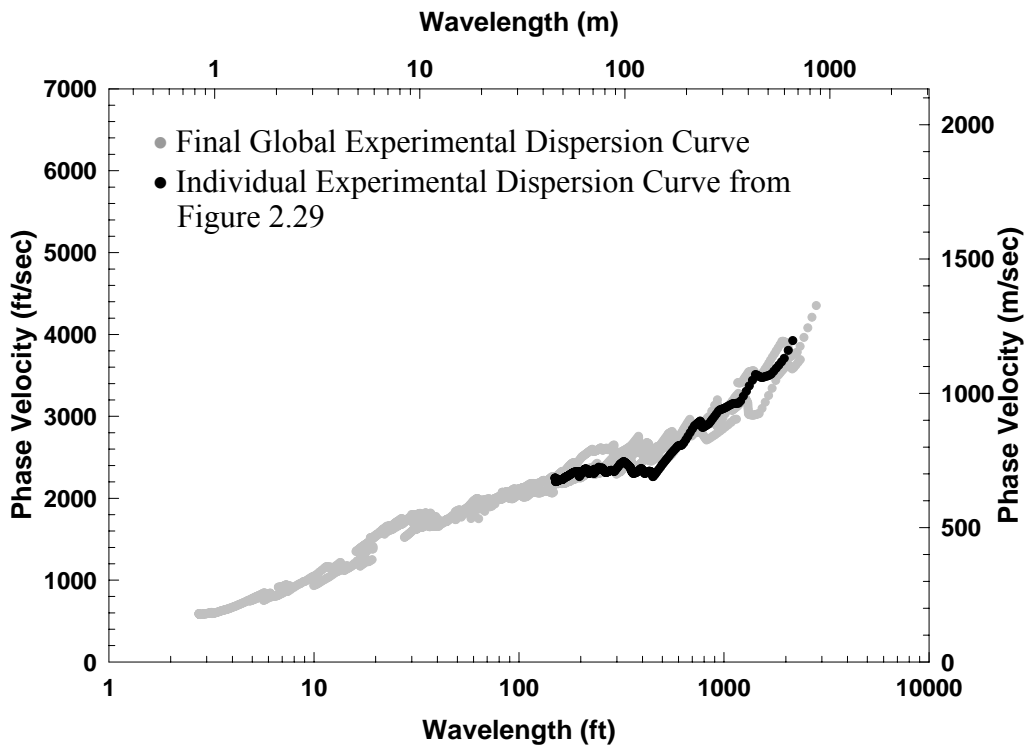


Figure 2.30 Experimental Dispersion Curves Determined from Figure 2.29 and All Other Receiver Spacings at One Yucca Mountain Site

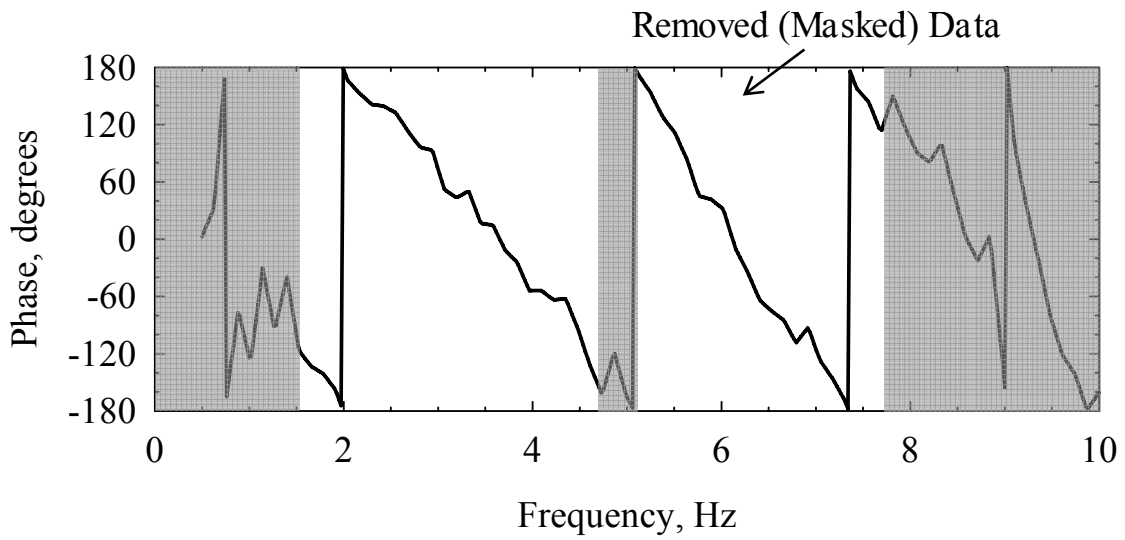


Figure 2.31 Wrapped Phase Plot Measured by SASW Testing with a 800-ft Receiver at One Yucca Mountain Site

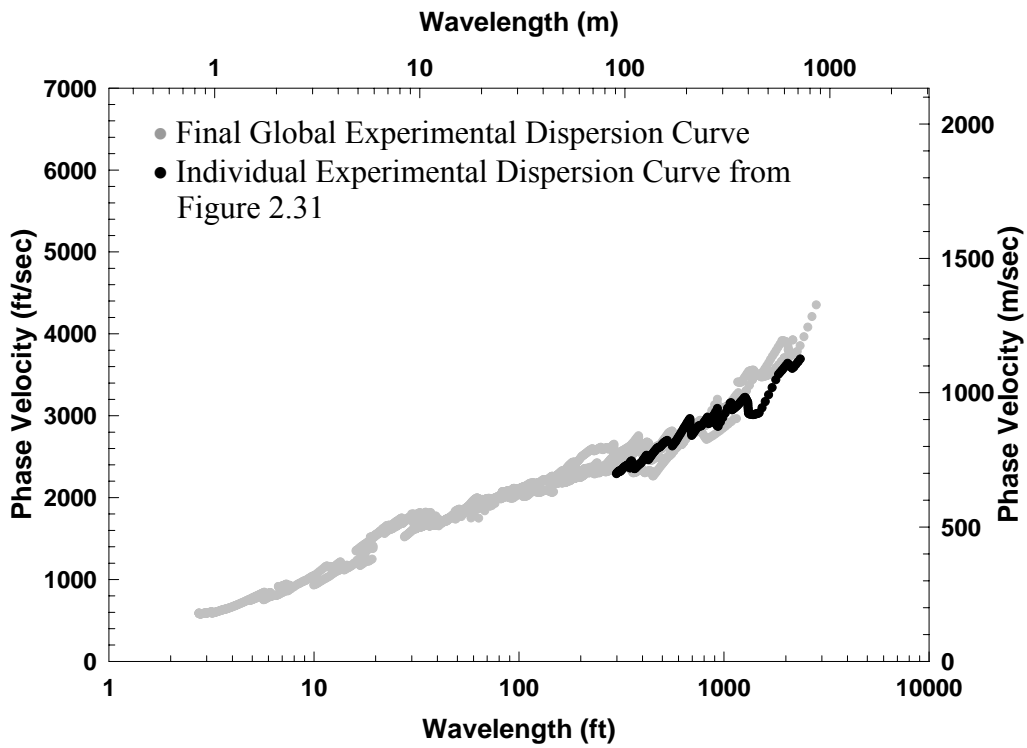


Figure 2.32 Experimental Dispersion Curves Determined from Figure 2.31 and All Other Receiver Spacings at One Yucca Mountain Site

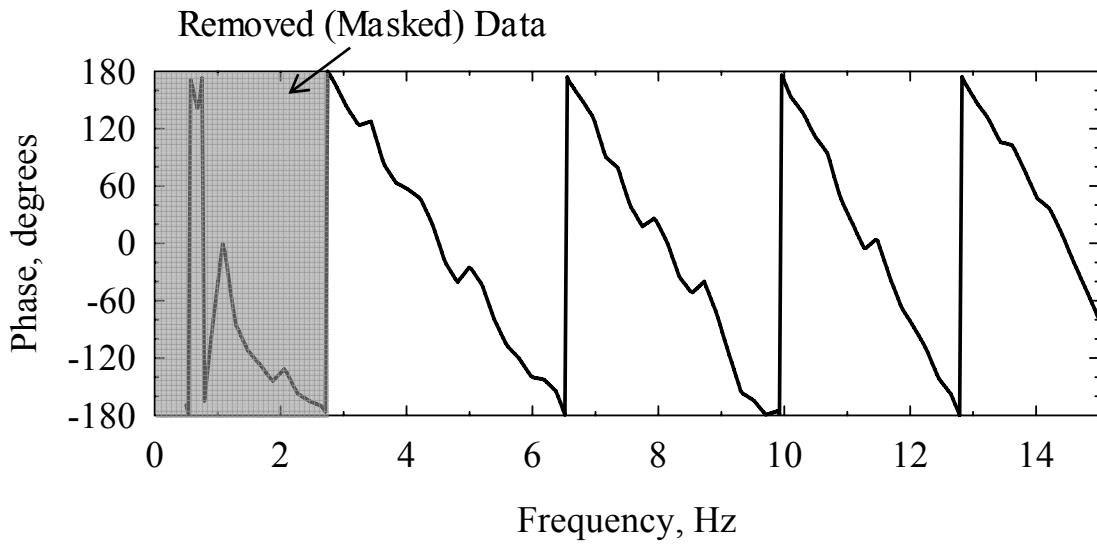


Figure 2.33 Wrapped Phase Plot Measured by SASW Testing with a 600-ft Receiver at One Yucca Mountain Site (from $d_1: d_2 = 600 \text{ ft} : 1200 \text{ ft}$ Setup)

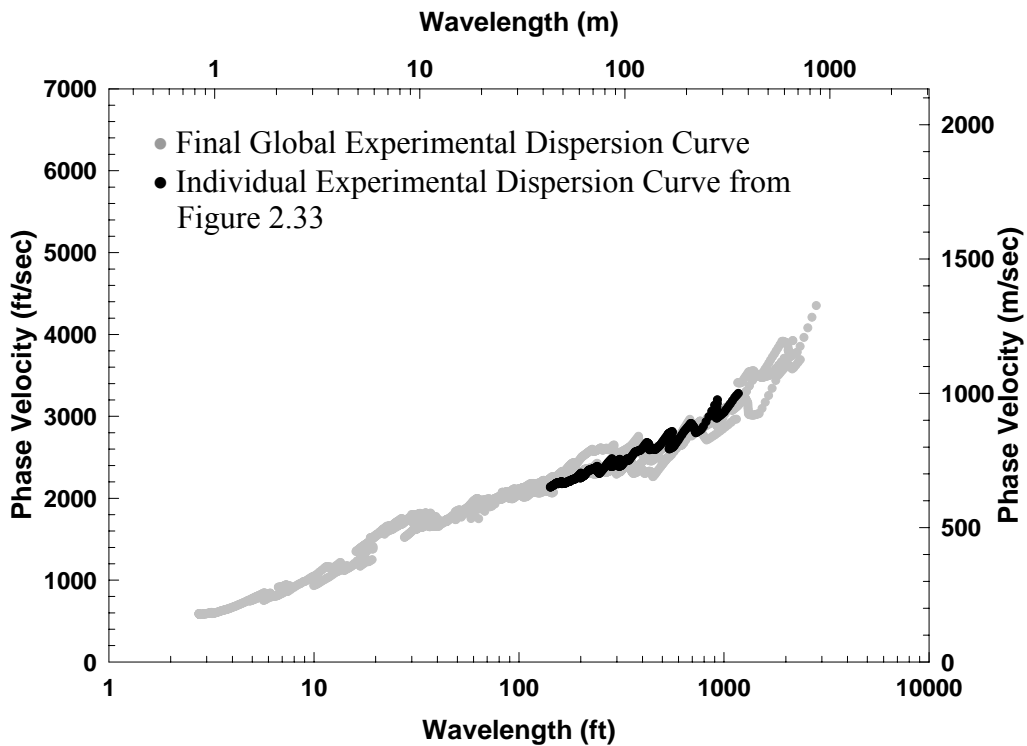


Figure 2.34 Experimental Dispersion Curves Determined from Figure 2.33 and All Other Receiver Spacings at One Yucca Mountain Site

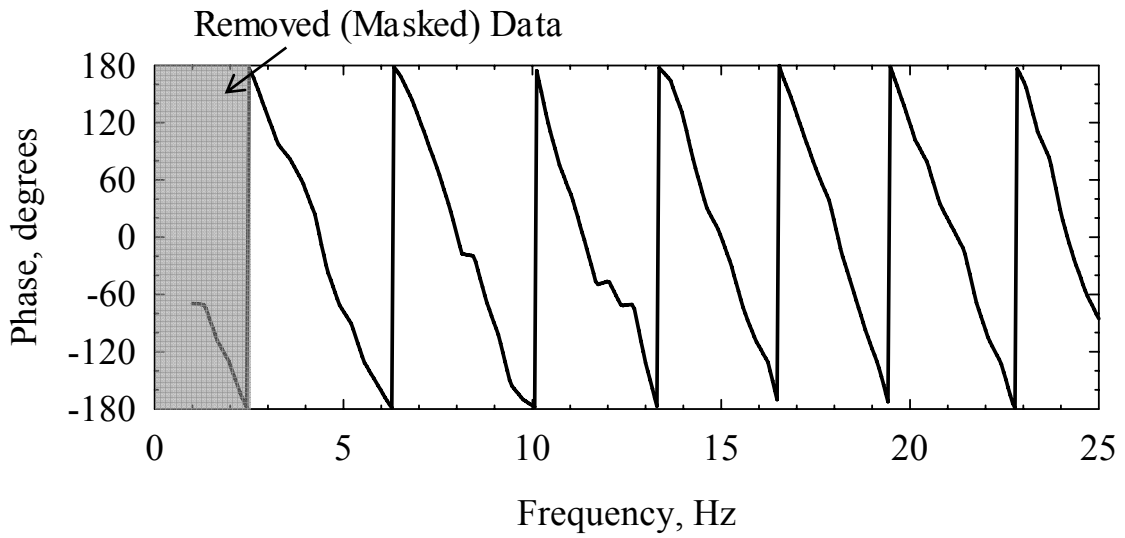


Figure 2.35 Wrapped Phase Plot Measured by SASW Testing with a 600-ft Receiver at One Yucca Mountain Site (from $d_1 : d_2 = 300 \text{ ft} : 600 \text{ ft}$ Setup)

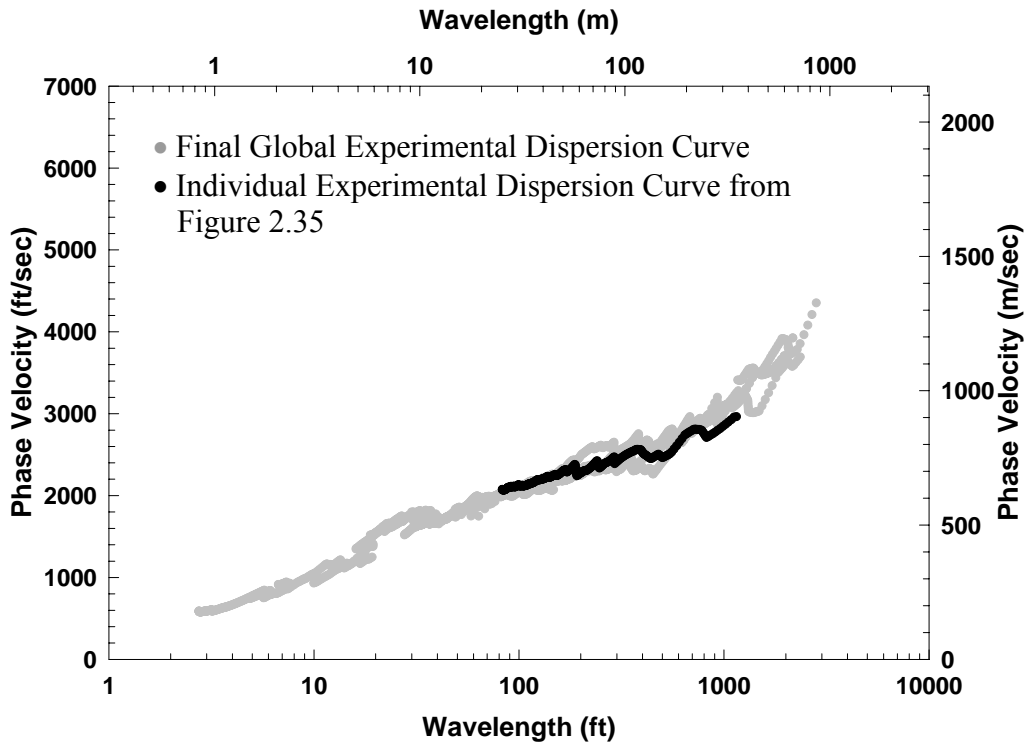


Figure 2.36 Experimental Dispersion Curves Determined from Figure 2.35 and All Other Receiver Spacings at One Yucca Mountain Site

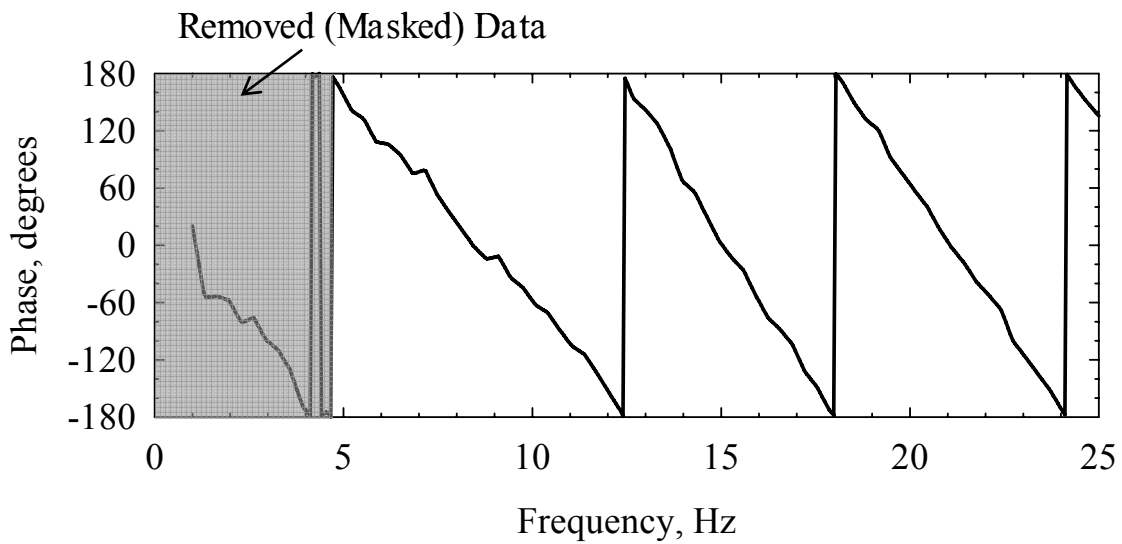


Figure 2.37 Wrapped Phase Plot Measured by SASW Testing with a 300-ft Receiver at One Yucca Mountain Site

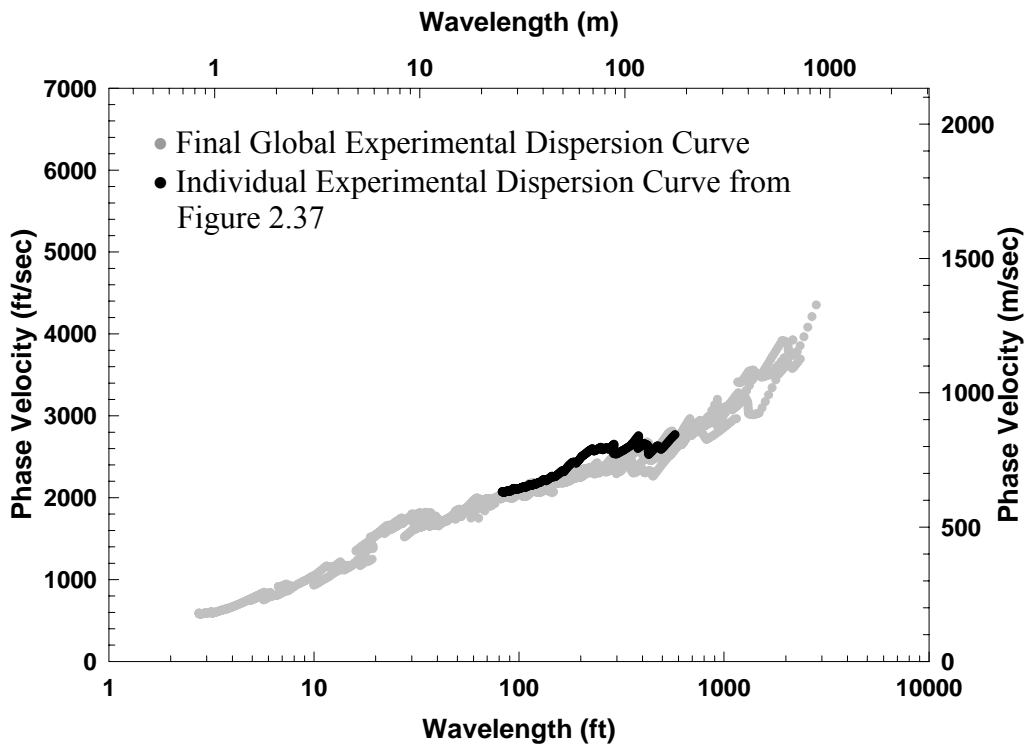


Figure 2.38 Experimental Dispersion Curves Determined from Figure 2.37 and All Other Receiver Spacings at One Yucca Mountain Site

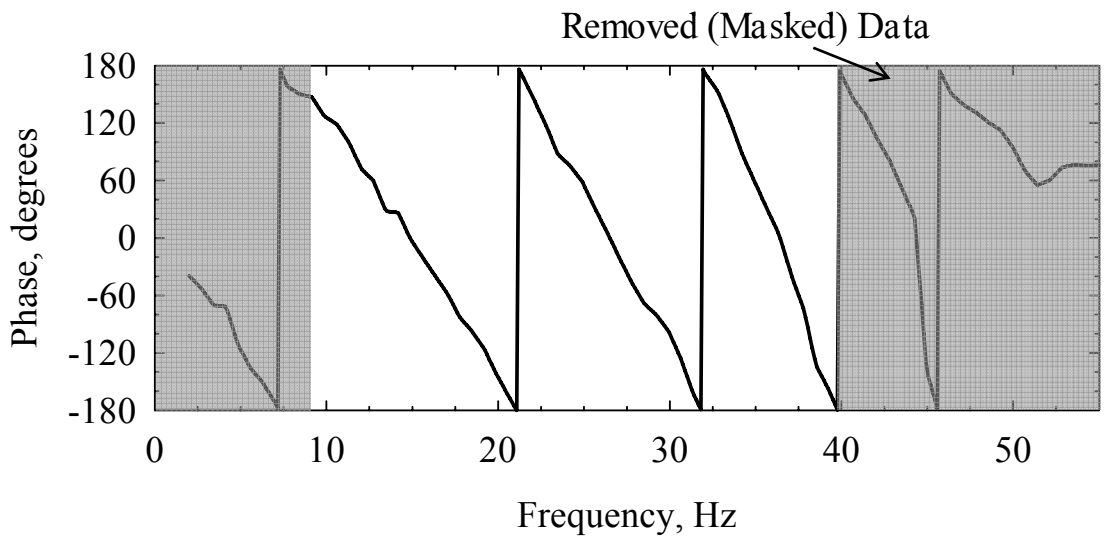


Figure 2.39 Wrapped Phase Plot Measured by SASW Testing with a 150-ft Receiver at One Yucca Mountain Site

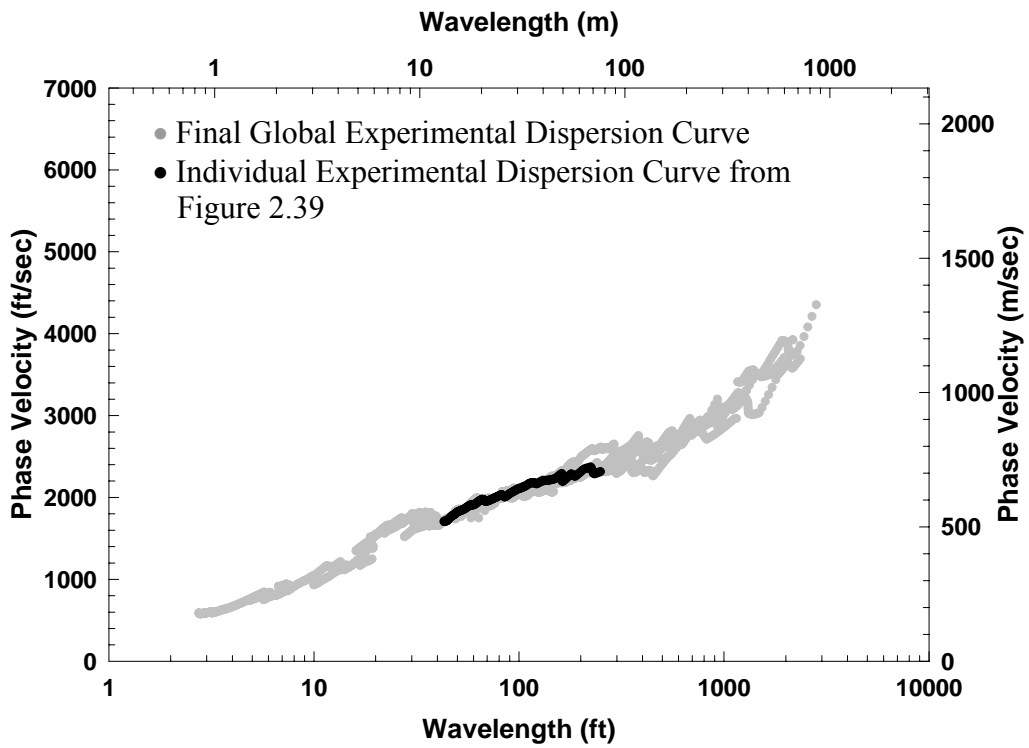


Figure 2.40 Experimental Dispersion Curves Determined from Figure 2.39 and All Other Receiver Spacings at One Yucca Mountain Site

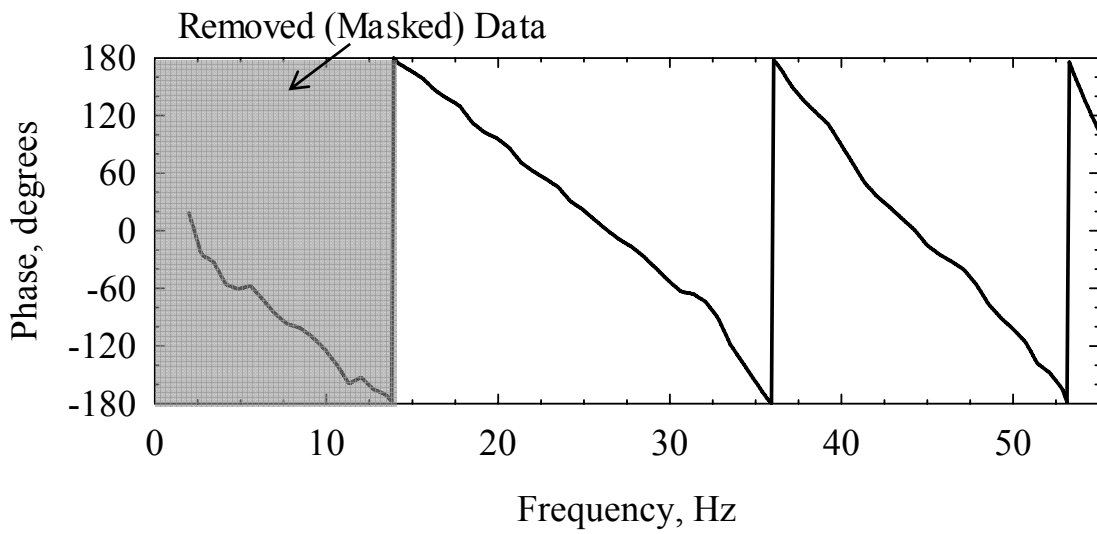


Figure 2.41 Wrapped Phase Plot Measured by SASW Testing with a 75-ft Receiver at One Yucca Mountain Site

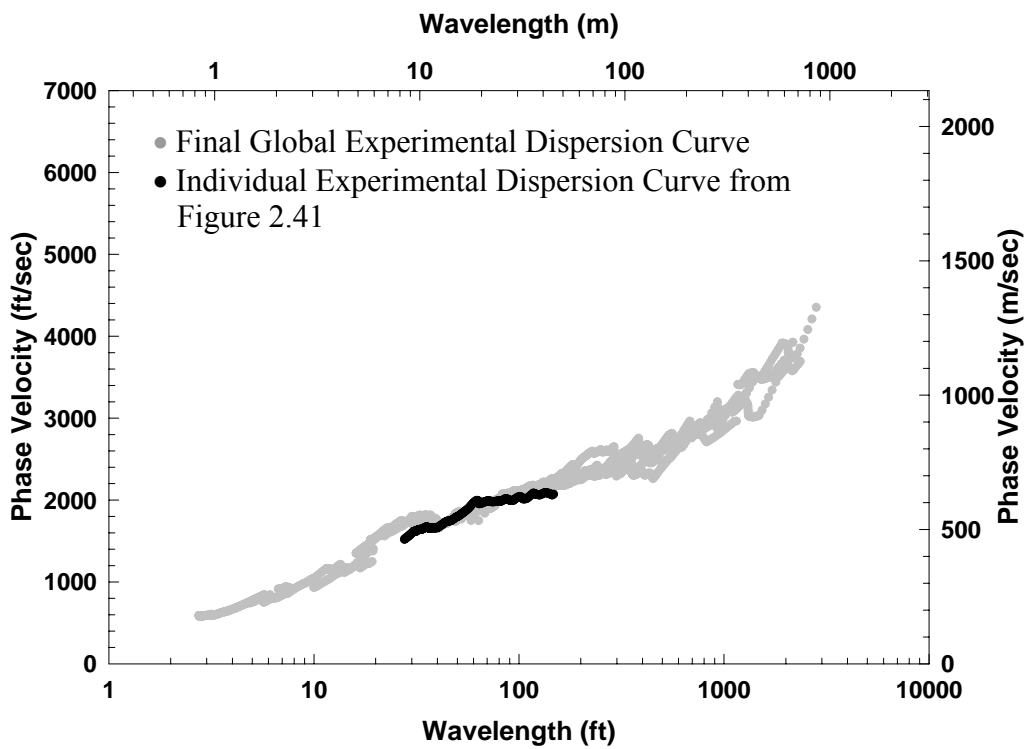


Figure 2.42 Experimental Dispersion Curves Determined from Figure 2.41 and All Other Receiver Spacings at One Yucca Mountain Site

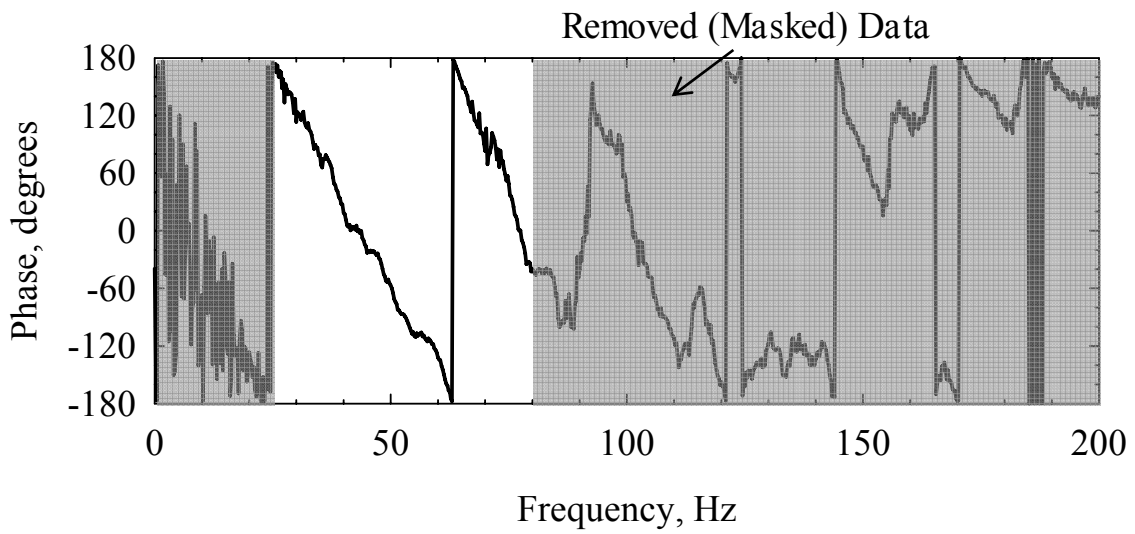


Figure 2.43 Wrapped Phase Plot Measured by SASW Testing with a 40-ft Receiver at One Yucca Mountain Site

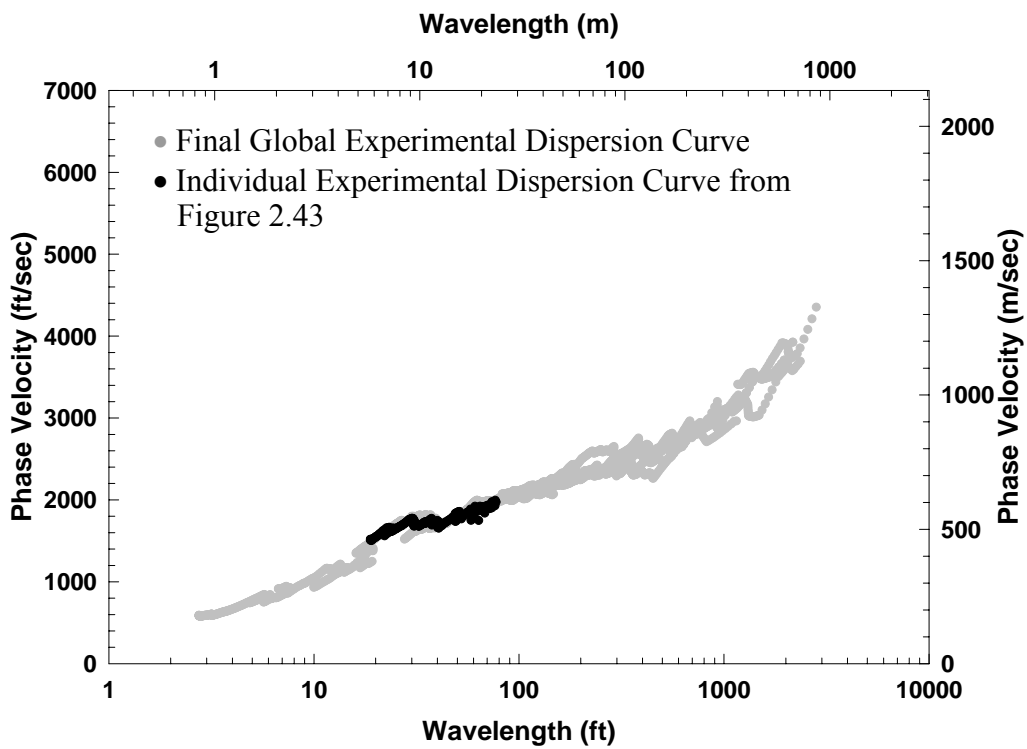


Figure 2.44 Experimental Dispersion Curves Determined from Figure 2.43 and All Other Receiver Spacings at One Yucca Mountain Site

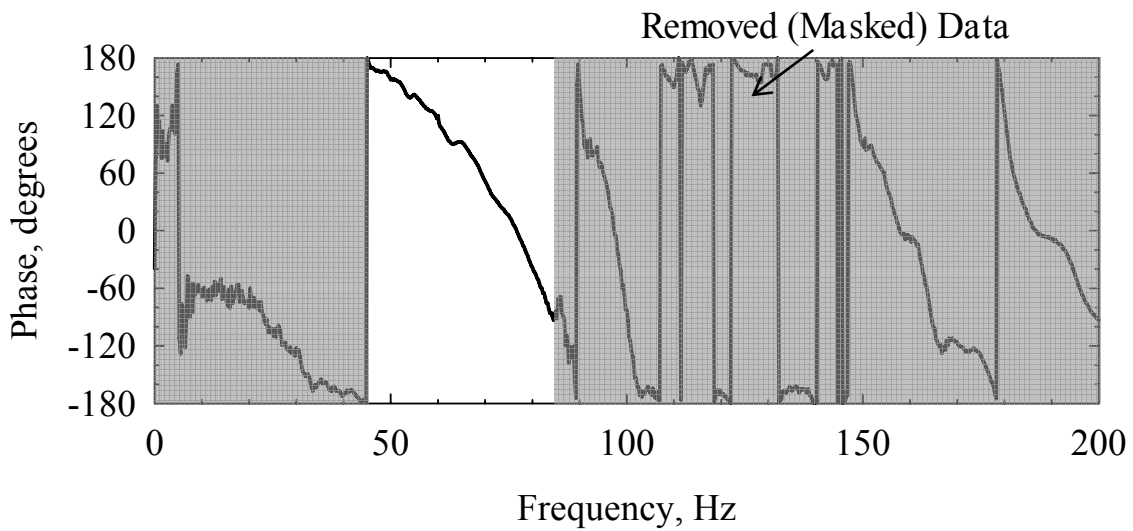


Figure 2.45 Wrapped Phase Plot Measured by SASW Testing with a 20-ft Receiver at One Yucca Mountain Site

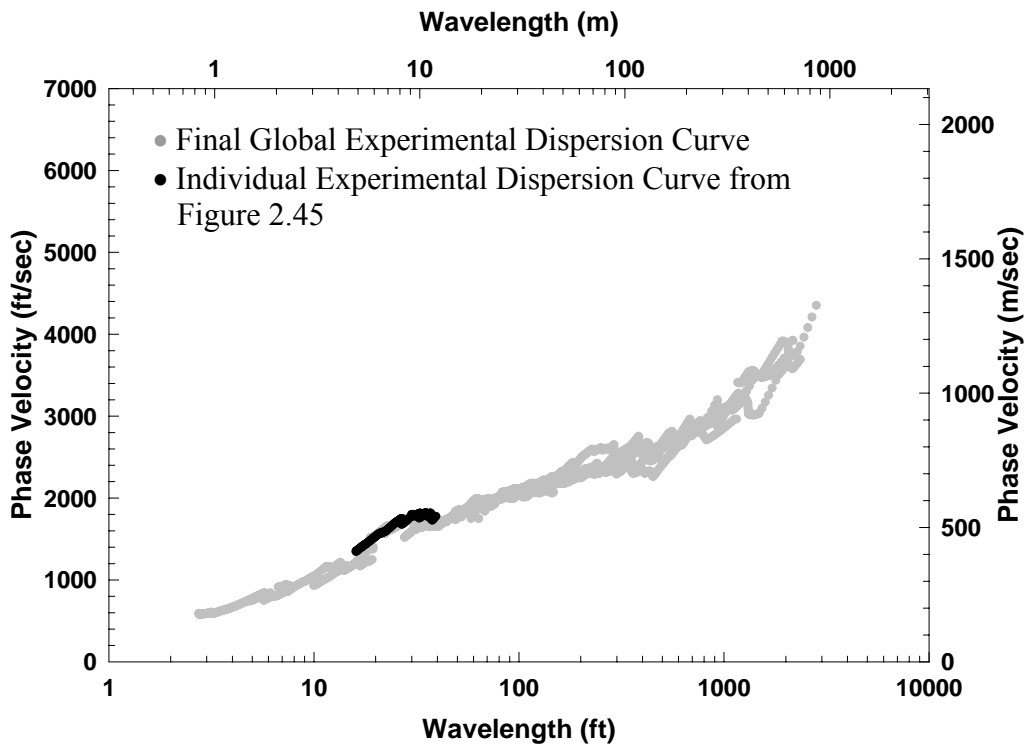


Figure 2.46 Experimental Dispersion Curves Determined from Figure 2.45 and All Other Receiver Spacings at One Yucca Mountain Site

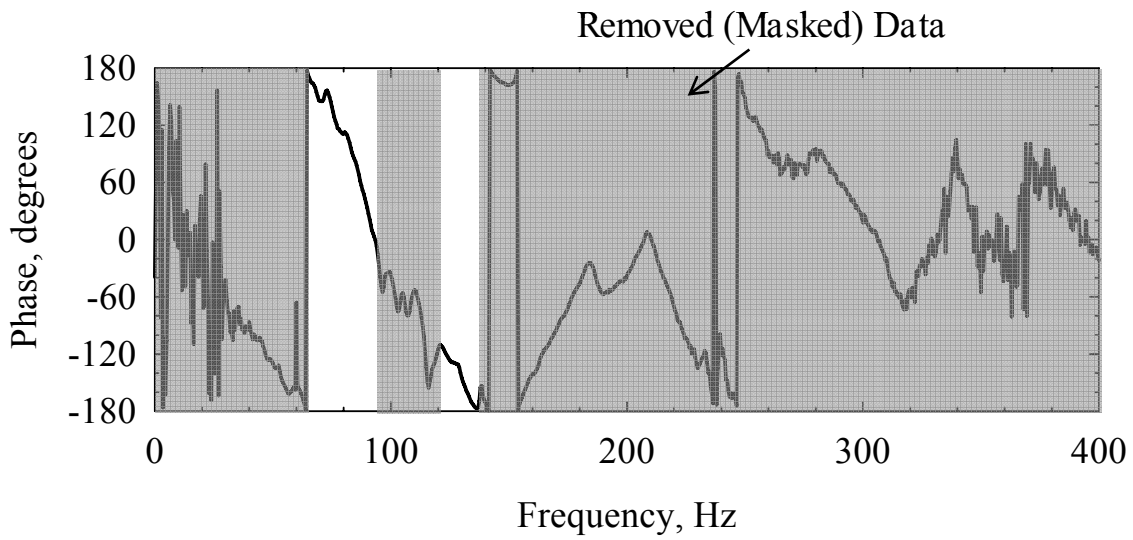


Figure 2.47 Wrapped Phase Plot Measured by SASW Testing with a 10-ft Receiver at One Yucca Mountain Site

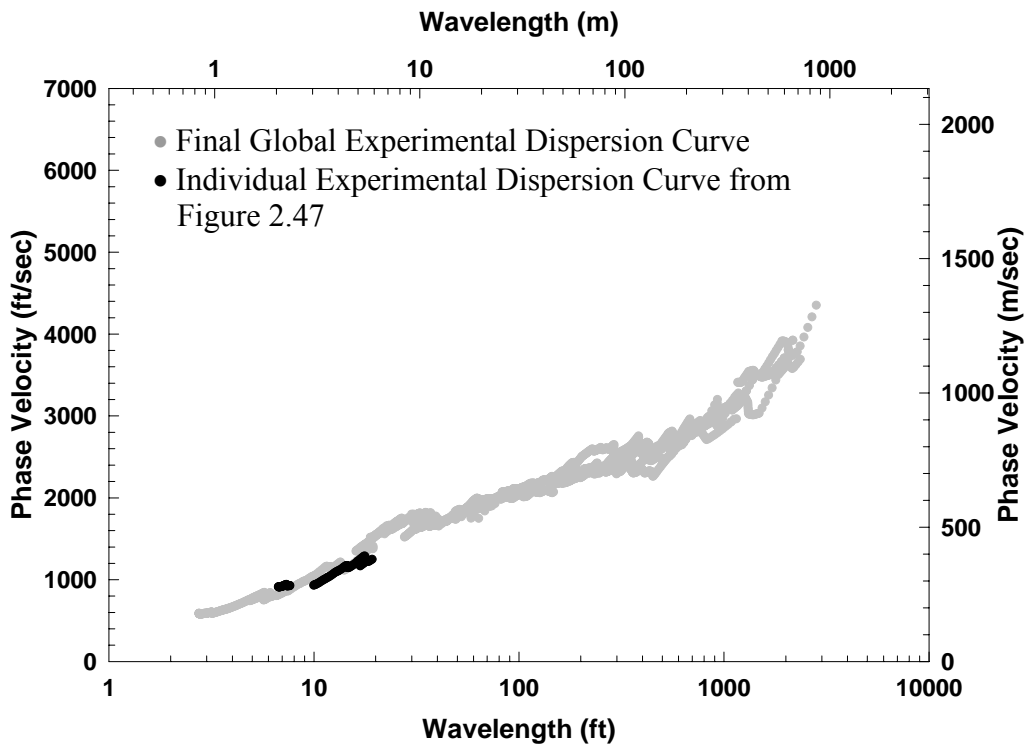


Figure 2.48 Experimental Dispersion Curves Determined from Figure 2.47 and All Other Receiver Spacings at One Yucca Mountain Site

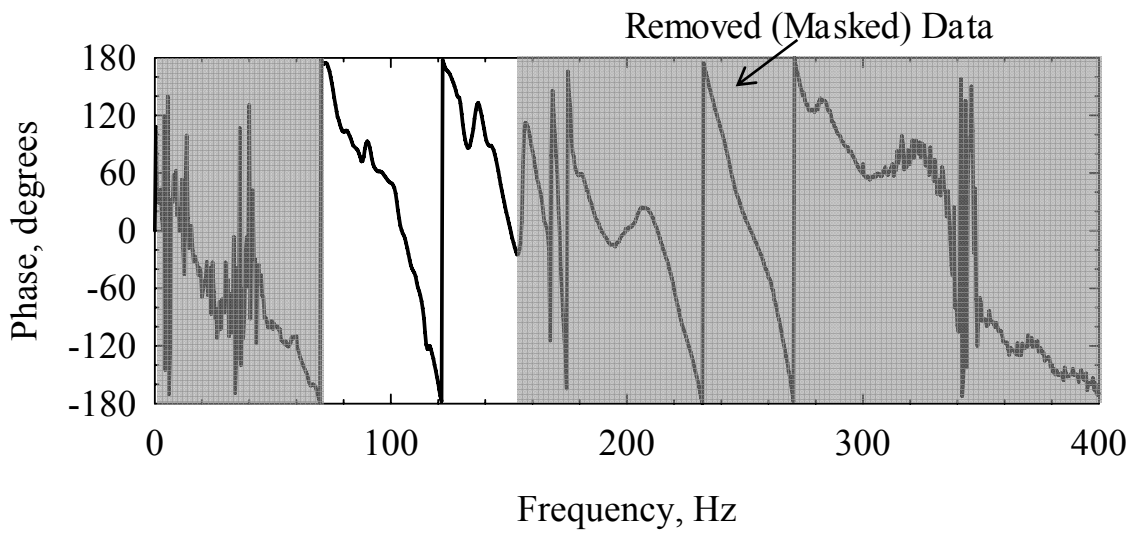


Figure 2.49 Wrapped Phase Plot Measured by SASW Testing with a 10-ft Receiver at One Yucca Mountain Site (from Reverse Direction)

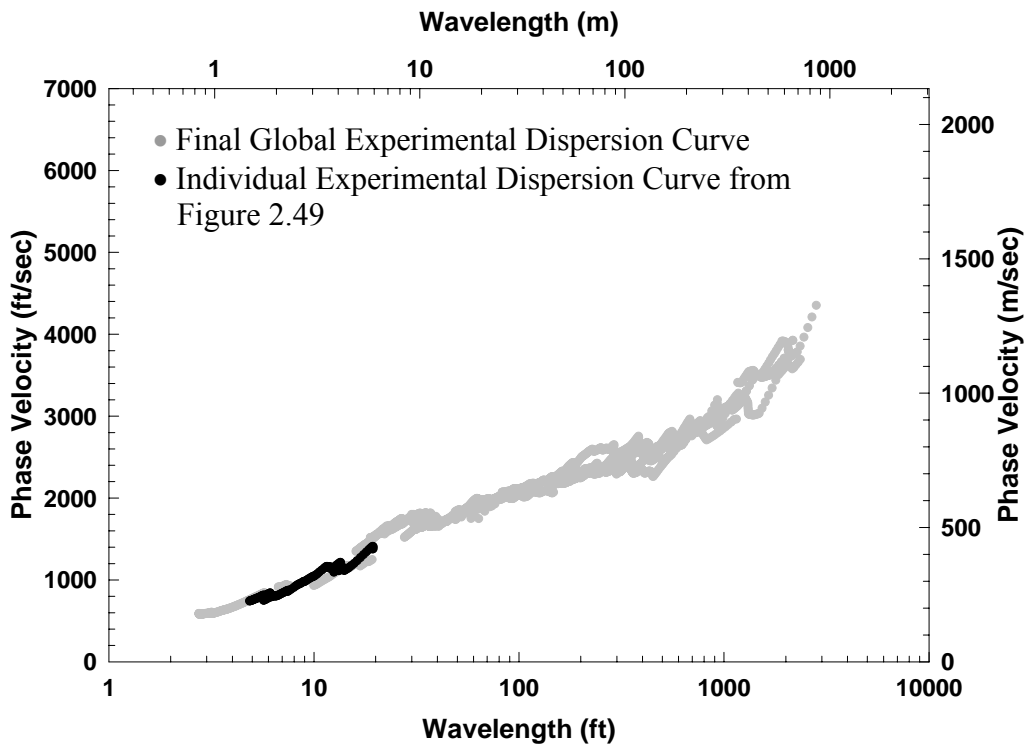


Figure 2.50 Experimental Dispersion Curves Determined from Figure 2.49 and All Other Receiver Spacings at One Yucca Mountain Site

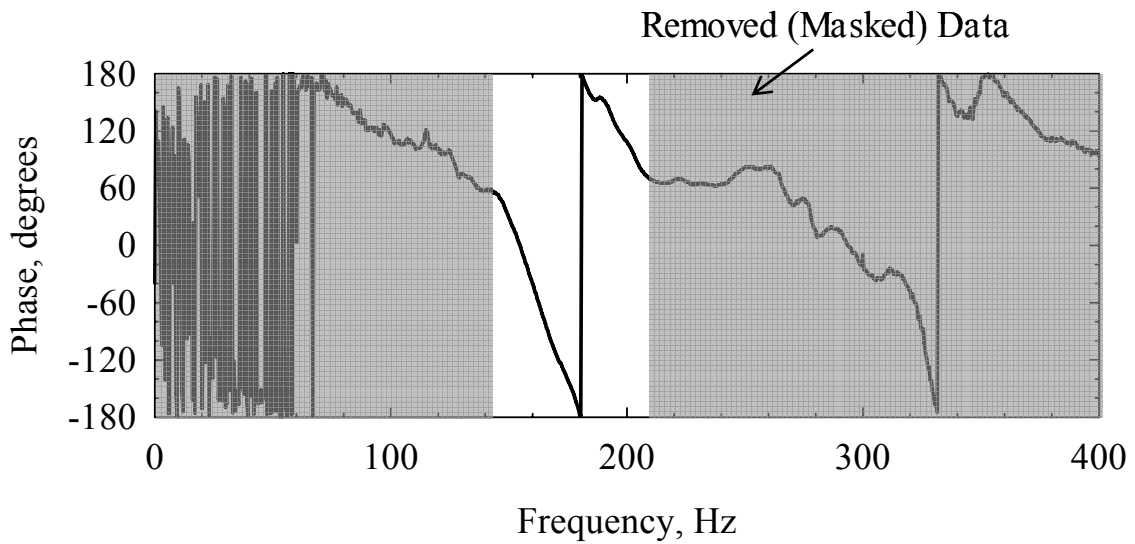


Figure 2.51 Wrapped Phase Plot Measured by SASW Testing with a 5-ft Receiver at One Yucca Mountain Site (from Reverse Direction)

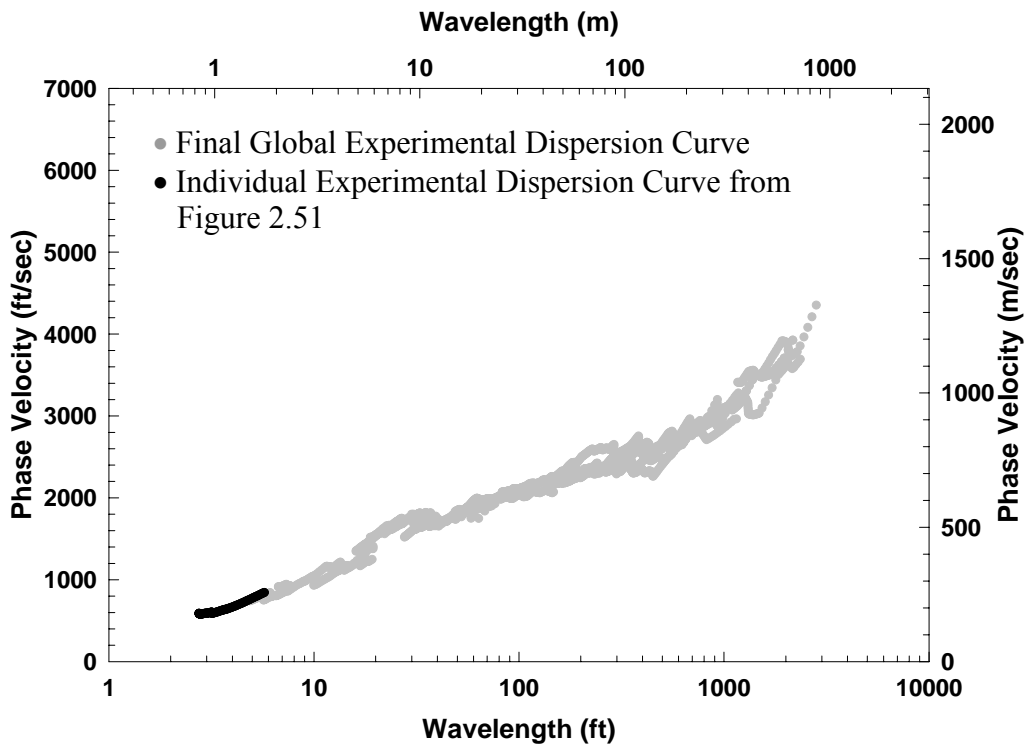


Figure 2.52 Experimental Dispersion Curves Determined from Figure 2.51 and All Other Receiver Spacings at One Yucca Mountain Site

2.4.4.2 Forward Modeling

The SASW V_S profiles used in this study were determined by forward modeling. The forward modeling method employed in WinSASW is a technique with which the person performing the analysis tries to fit the theoretical dispersion curve (generated from an assumed V_S profile and a theoretical model) to the experimental dispersion curve by through an iterative procedure. The procedure of WinSASW forward modeling method is demonstrated.

First, a simple V_S profile (Figure 2.53 (a) and Table 2.2) is assumed to generate the initial theoretical dispersion curve in Figure 2.53 (b). As seen, the theoretical dispersion curve is lower than the experimental dispersion curve in the wavelength range from 3 to 10 ft and 150 to 1500 ft but higher in the wavelength range from 25 to 90 ft.

To improve the fit between the theoretical dispersion curve and the experimental dispersion curve, the first two layers were divided into four layers, their thicknesses were adjusted and their V_S values were also adjusted (based on engineering judgement). The result of these changes is shown in Figure 2.54 (a) and Table 2.3. After the adjustment, the theoretical and experimental dispersion curves in Figure 2.54 (b) matched better in the shorter wavelength range (from 2 to 40 ft).

The next step is to adjust the V_S values in the intermediate wavelength range. The fifth layer was divided into three layers and the thicknesses and V_S values of these layers modified as shown in Figure 2.55 (a) and Table 2.4. As seen in the Figure 2.55 (b), a better match between the theoretical and experimental dispersion curves was achieved. To make the theoretical dispersion curve match better the experimental dispersion curve in the longer wavelength range, the number and V_S values of the deeper layers were changed in Figure 2.56 (a) and Table 2.5. The new theoretical dispersion curve is shown in Figure 2.56 (b) which fit the experimental dispersion curve better than

the previous one (Figure 2.55 (b)). The final fitting and the shear wave velocity profile were presented in Figure 2.57 and Table 2.6.

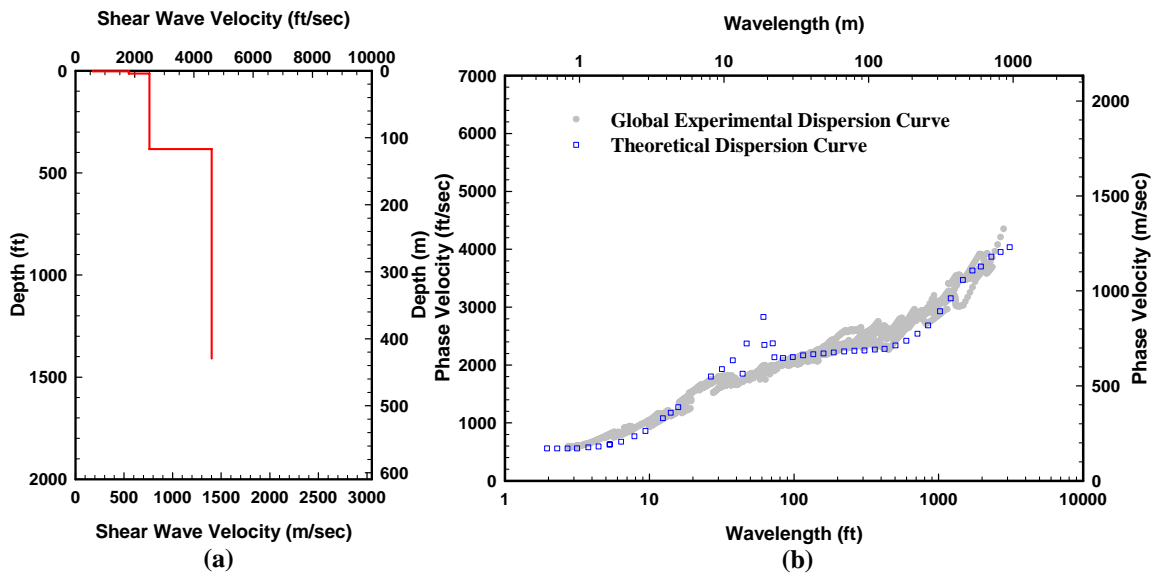


Figure 2.53 Illustration of Forward Modeling – Step 1: (a) Assumed V_S Profile; (b) Comparison of Theoretical Dispersion Curve from Assumed V_S Profile with the Experimental Dispersion Curve

Table 2.2 Profile Parameters Used in Step 1 to Develop the Theoretical Dispersion Curve for the Site at Yucca Mountain

Layer No.	Thickness, ft	Depth to Top of Layer, ft	S-Wave Velocity, ft/s	Assumed Poisson's Ratio	P-Wave Velocity, ft/s	Assumed Mass Density, pcf
1	3	0	590	0.33	1171	120
2	10.5	3	1800	0.33	3573	120
3	370	13.5	2500	0.25	4330	130
4	1100	383.5	4600	0.25	7967	130
5	75	1409	4600 [#]	0.25	7967	130
6	Half Space	1484	5500 [#]	0.20	8982	135

[#] Layer Deeper than Maximum Depth (Maximum Depth = $\lambda_{max}/2$)

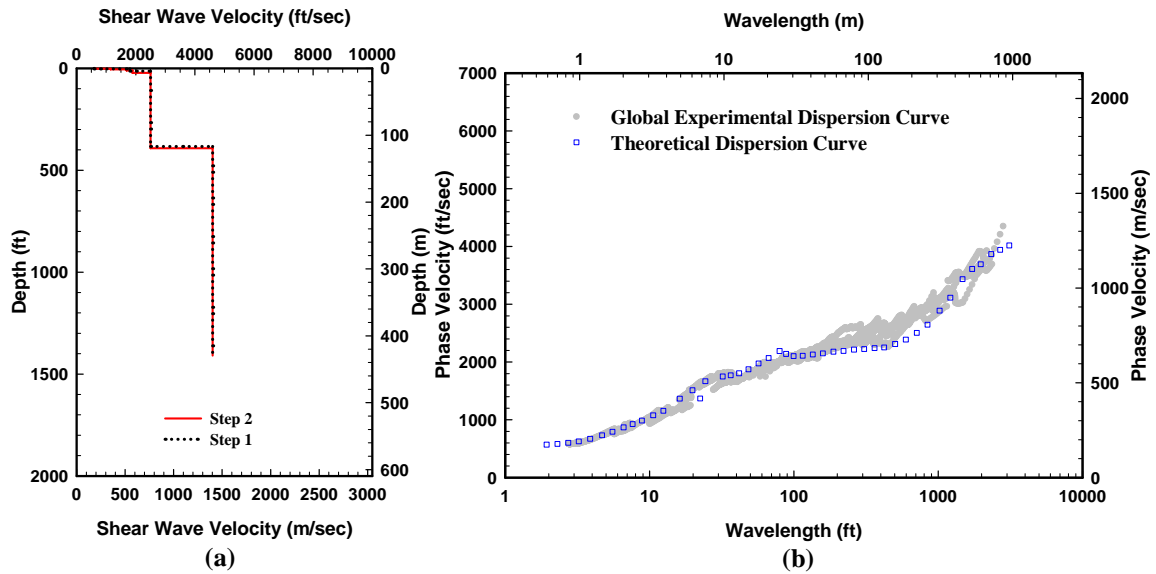


Figure 2.54 Illustration of Forward Modeling – Step 2: (a) Assumed V_S Profile; (b) Comparison of Theoretical Dispersion Curve from Assumed V_S Profile with the Experimental Dispersion Curve

Table 2.3 Profile Parameters Used in Step 2 to Develop the Theoretical Dispersion Curve for the Site at Yucca Mountain

Layer No.	Thickness, ft	Depth to Top of Layer, ft	S-Wave Velocity, ft/s	Assumed Poisson's Ratio	P-Wave Velocity, ft/s	Assumed Mass Density, pcf
1	1.8	0	600	0.33	1191	120
2	3.1	1.8	1150	0.33	2283	120
3	5.4	4.9	1690	0.33	3355	120
4	12	10.3	1890	0.33	3752	120
5	370	22.3	2500	0.25	4330	130
6	1100	392	4600	0.25	7967	130
7	83	1409	4600 [#]	0.25	7967	130
8	Half Space	1492	5500 [#]	0.20	8982	135

[#] Layer Deeper than Maximum Depth (Maximum Depth = $\lambda_{max}/2$)

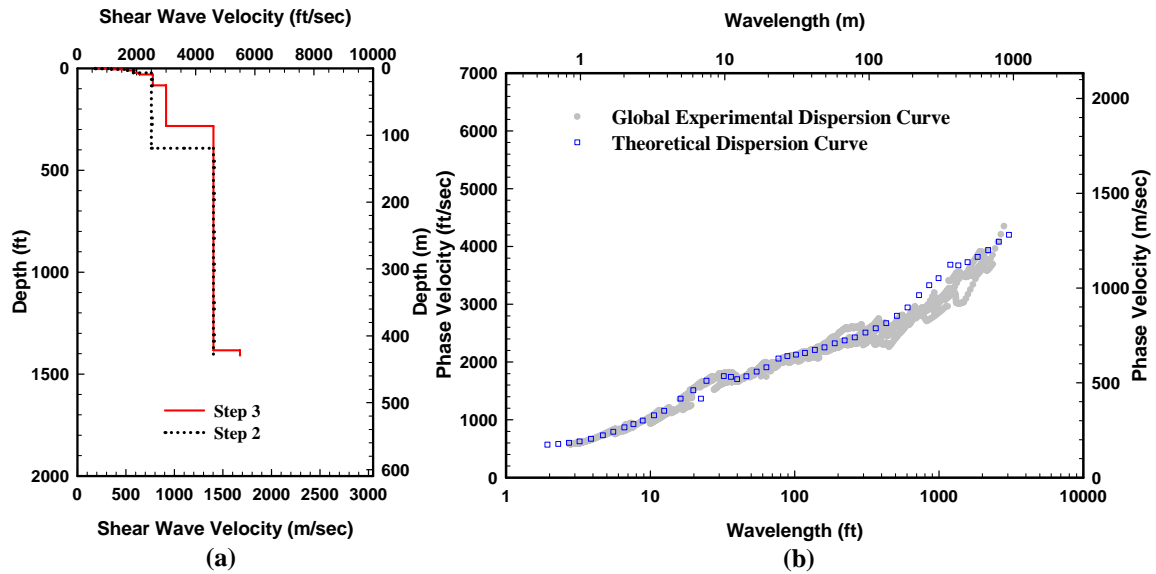


Figure 2.55 Illustration of Forward Modeling – Step 3: (a) Assumed V_S Profile; (b) Comparison of Theoretical Dispersion Curve from Assumed V_S Profile with the Experimental Dispersion Curve

Table 2.4 Profile Parameters Used in Step 3 to Develop the Theoretical Dispersion Curve for the Site at Yucca Mountain

Layer No.	Thickness, ft	Depth to Top of Layer, ft	S-Wave Velocity, ft/s	Assumed Poisson's Ratio	P-Wave Velocity, ft/s	Assumed Mass Density, pcf
1	1.8	0	600	0.33	1191	120
2	3.1	1.8	1150	0.33	2283	120
3	5.4	4.9	1690	0.33	3355	120
4	12	10.3	1890	0.33	3752	120
5	8	22.3	2100	0.20	3429	130
6	53	30	2550	0.25	4417	130
7	200	83	3000	0.25	5196	130
8	1100	283	4600	0.25	7967	130
9	26	1383	5500	0.20	8982	135
10	Half Space	1409	5500 [#]	0.20	8982	135

[#] Layer Deeper than Maximum Depth (Maximum Depth = $\lambda_{max}/2$)

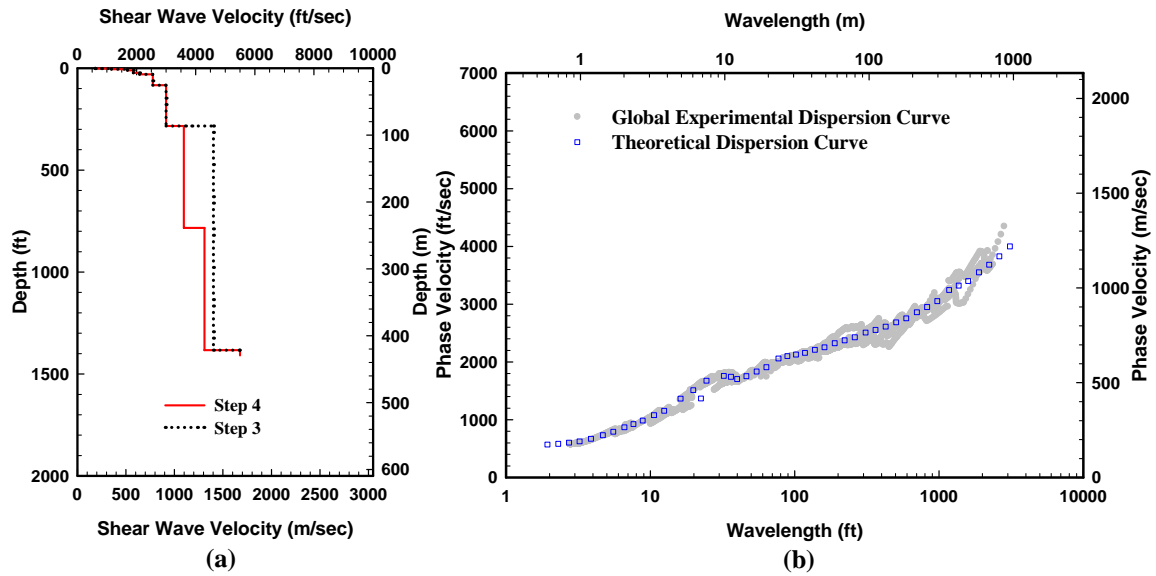


Figure 2.56 Illustration of Forward Modeling – Step 4: (a) Assumed V_S Profile; (b) Comparison of Theoretical Dispersion Curve from Assumed V_S Profile with the Experimental Dispersion Curve

Table 2.5 Profile Parameters Used in Step 4 to Develop the Theoretical Dispersion Curve for the Site at Yucca Mountain

Layer No.	Thickness, ft	Depth to Top of Layer, ft	S-Wave Velocity, ft/s	Assumed Poisson's Ratio	P-Wave Velocity, ft/s	Assumed Mass Density, pcf
1	1.8	0	600	0.33	1191	120
2	3.1	1.8	1150	0.33	2283	120
3	5.4	4.9	1690	0.33	3355	120
4	12	10.3	1890	0.33	3752	120
5	8	22.3	2100	0.20	3429	130
6	53	30.3	2550	0.25	4417	130
7	200	83.3	3000	0.25	5196	130
8	500	283.3	3600	0.25	6235	130
9	600	783.3	4300	0.25	7448	130
10	26	1383.3	5500	0.20	8982	135
11	Half Space	1409	5500 [#]	0.20	8982	135

[#] Layer Deeper than Maximum Depth (Maximum Depth = $\lambda_{max}/2$)

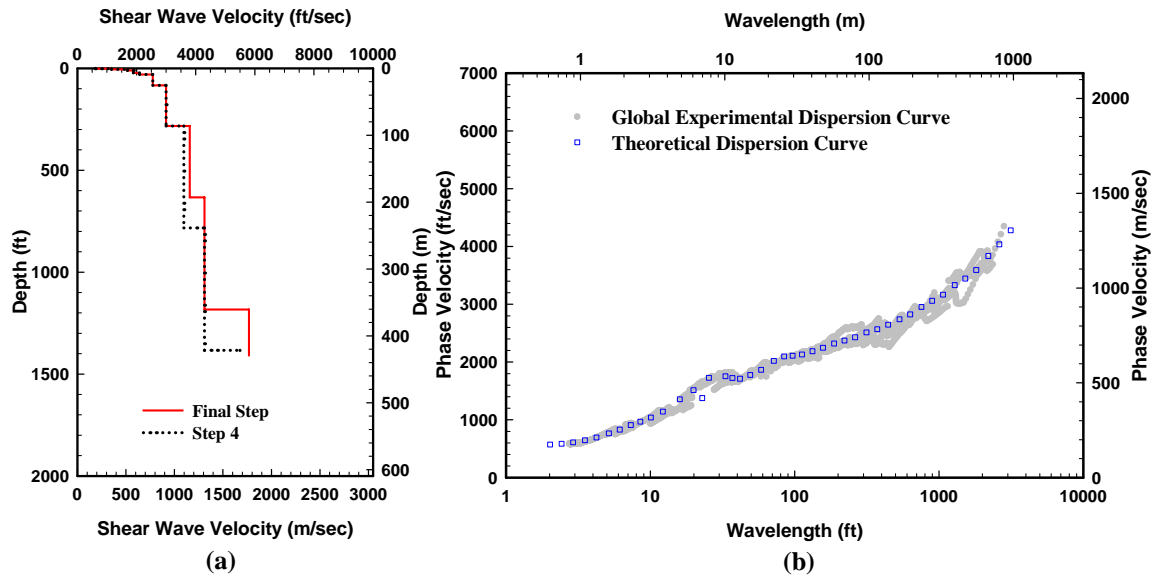


Figure 2.57 Illustration of Forward Modeling – Final Step: (a) Assumed V_S Profile; (b) Comparison of Theoretical Dispersion Curve from Assumed V_S Profile with the Experimental Dispersion Curve

Table 2.6 Profile Parameters Used in Final Step to Develop the Theoretical Dispersion Curve for the Site at Yucca Mountain

Layer No.	Thickness, ft	Depth to Top of Layer, ft	S-Wave Velocity, ft/s	Assumed Poisson's Ratio	P-Wave Velocity, ft/s	Assumed Mass Density, pcf
1	1.8	0	600	0.33	1191	120
2	3.1	1.8	1150	0.33	2283	120
3	5.4	4.9	1690	0.33	3355	120
4	12	10.3	1890	0.33	3752	120
5	8	22	2100	0.2	3429	130
6	53	30	2550	0.25	4417	130
7	200	83	3000	0.25	5196	130
8	350	283	3800	0.25	6582	130
9	550	633	4300	0.25	7448	130
10	226	1183	5800	0.25	10046	130
11	Half Space	1409	5800 [#]	0.25	10046	130

[#] Layer Deeper than Maximum Depth (Maximum Depth = $\lambda_{max}/2$)

The actual number of steps of the data reduction is more than ten times the example presented above. It is not as easy as described above and took three to six hours for the example shown.

All the fitting processes in the forward modeling were judged by eyes and the engineering judgment of an experienced engineer can shorten the time of the data reduction. Good judgment and understanding of the theory behind seismic wave propagation are very important in the forward modeling procedure.

The question also arises as to the accuracy of the final fit shown in Figure 2.57. In other word, how much difference would it be in the final V_S profile if the final fit is close to the upper or lower boundaries of the field dispersion curve in this example? To investigate the difference, two new theoretical dispersion curves were generated to fit the upper and lower boundaries of the field dispersion curve. By comparing the V_S profile that were used to determined the new dispersion curves that fit the upper and lower boundaries the field dispersion curve. The comparisons between the original final V_S profile and the two new V_S profiles and their corresponding theoretical dispersion curves are shown in Figure 5.58. As seen in Table 2.7, the difference between the original and new V_S profiles is less than 5% in average. The maximum difference is 18.3 % but that only happens in a 7-ft thin layer.

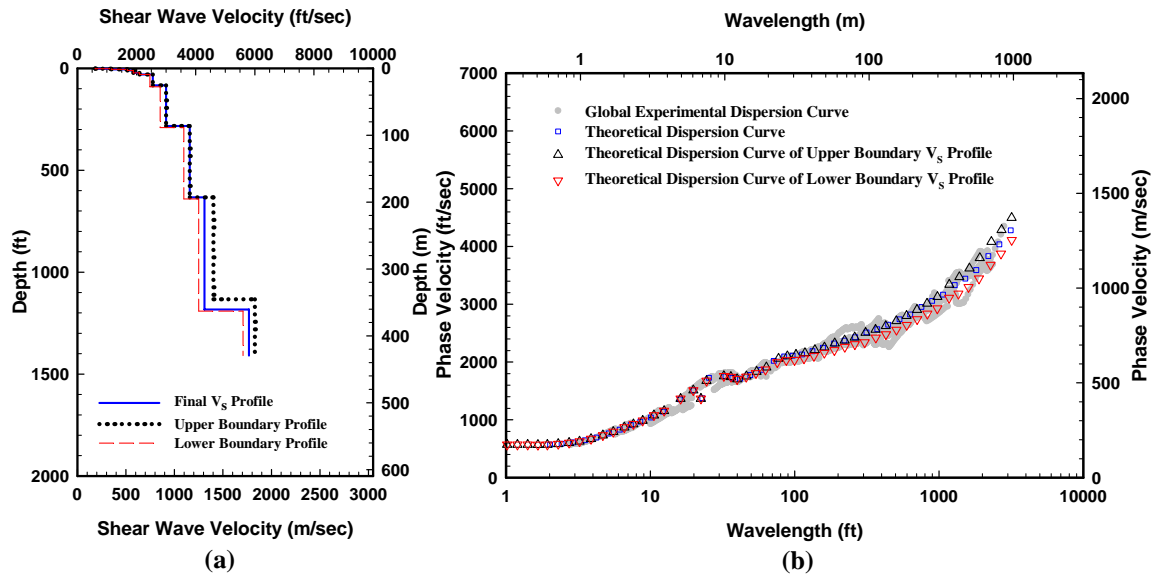


Figure 2.58 Comparisons between V_S Profiles and the Corresponding Theoretical Dispersion Curves That Fit the Average and Upper and Low Boundaries of the Field Dispersion Curve in Figure 5.57

Table 2.7 Comparison of V_S profiles Used to Determine Original and Upper and Lower Boundaries Theoretical Dispersion Curves in Figure 5.58

Depth to the bottom of the Layer(ft)	V_S (ips)			Difference between V_S Profiles	
	Original	Higher boundary	Lower boundary	(2)/(1) - 1	(3)/(1) - 1
	(1)	(2)	(3)		
0	600	600	600	0.0%	0.0%
1.8	600	600	600	0.0%	0.0%
4.9	1150	1150	1150	0.0%	0.0%
10.3	1690	1690	1690	0.0%	0.0%
22.3	1890	1890	1890	0.0%	0.0%
30.3	2100	2100	2100	0.0%	0.0%
83.3	2550	2550	2450	0.0%	-3.9%
90.3	3000	3000	2450	0.0%	-18.3%
283.3	3000	3000	2800	0.0%	-6.7%
633.3	3800	3800	3600	0.0%	-5.3%
1183.3	4300	4600	4100	7.0%	-4.7%
1409	5800	6000	5600	3.4%	-3.4%
	Average V_S:			0.9%	-3.8%
	Weighted Average V_S based on the thickness of each layer :			3.3%	-4.8%

2.5 SUMMARY

The SASW method uses Rayleigh wave measurements in the field to obtain the shear wave velocity profile of geotechnical sites. The V_s profiles provide useful information to engineers, geologists and seismologists in characterizing the site and estimating how different layers in the site respond to loading. Compared to other borehole-required or intrusive profiling tests, the SASW method is time- and cost-efficient.

In this chapter, an overview of the development of the SASW method was presented. It began with an introduction of Rayleigh waves. A review of steady-state Rayleigh wave method, the predecessor of the SASW method was then presented. In the end, the theories, test setups and analysis procedures of the SASW method were described.

Chapter 3 Overview of the Database and the Study Methodology

3.1 INTRODUCTION

The V_S profile of a geotechnical site is an very important parameter in helping engineers make decisions regarding the earthquake response of the site and the behavior of structures of the site. There are many seismic profiling methods that can be used to obtain the V_S profile. In this work, V_S profiles are acquired by the SASW method. These profiles are then used to do classifications and other studies. In addition to the V_S profiles acquired with the SASW method, there are other V_S measurements that were performed at the same geographic locations as the SASW testing. These V_S profiles were determined with two intrusive survey techniques, the downhole and suspension (P-S) logging methods. The V_S profiles from these three different seismic measurements are analyzed and compared in the following chapters. In total, the database consists of more than 5M of field studies performed over six years.

Unlike the SASW method, the downhole and suspension logging methods are intrusive exploration methods which require a borehole to perform the tests. Since their methodologies are different from the SASW method, brief descriptions of the two methods are presented in this chapter as well.

In terms of the site classifications, the criteria in the IBC-2006 (International Building Codes) provisions were adopted in this study. A brief discuss of the IBC-2006 provisions of site classification system is presented in Section 3.4.

Statistical analyses of the V_S profiles are also performed. The methods used to analyze the V_S profile are discussed. These methods should be consistent through the dissertation in the different chapters. For example, the distribution of the shear wave velocity profiles in a family of measurements is assumed either normally or log-normally

distributed. This assumption needs to be clarified. The methodologies adopted in the statistical analysis are described near the end of this chapter.

3.2 OVERVIEW OF THE DATABASE IN THIS STUDY

3.2.1 SASW Measurements

The SASW V_S profiles in this work were acquired on several projects that were funded by different sponsors. Information of the test locations, sponsors and projects are tabulated in Table 3.1. These SASW V_S profiles are from four different geographic regions. They are: (1) Imperial Valley, CA, (2) Taiwan (3) Hanford, WA and (4) Yucca Mountain, NV as seen in Table 3.1. The number of the test sites (or V_S profiles) at each location is shown in the table. The SASW tests conducted at these four locations were performed for different purposes. For example, the SASW tests performed in Imperial Valley and Taiwan were used to survey subsurface conditions at strong motion recording (SMR) sites. Based on the SASW V_S profiles, average shear wave velocities of the top 30 m ($V_{S,30}$) were calculated and site classifications were determined for the sites. Also, the potential of liquefaction at these sites could be evaluated by the SASW V_S profiles at shallow depths. At the Hanford and Yucca Mountain (YM) sites, the SASW measurements were used to survey the soil/rock properties of the planned geologic repository (YM) and the waste treatment facility (Hanford) locations. Because of the importance of these facilities and the depth of planned repository in Yucca Mountain (about 1000 ft deep from the top of the mountain), it was necessary to survey the subsurface as deep as possible with the SASW tests. The deepest SASW V_S profile achieved was about 1500 ft at Yucca Mountain and 2000 ft at Hanford.

All SASW tests mentioned in this study were performed by personnel from the University of Texas at Austin (UTA) led by Dr. Kenneth H. Stokoe. The SASW data

were reduced by the author guided by Dr. Kenneth H. Stokoe, Dr. Sung-Ho Joh and Dr. Brent L. Rosenblad, except for tests performed during 2000 and 2001 at Yucca Mountain which were reduced by Dr. Rosenblad.

Table 3.1 Information about the SASW V_s Profiles Used in This Study

Test Location	Number of Site Tested	Project Name	Sponsor
Imperial Valley, CA	31	Application of SASW to US SMR Sites – 2C01	Pacific Earthquake Engineering Research Center (PEER)
Taiwan	26	SMR Site Characterization in Taiwan-SASW – 2A02C	
Hanford, WA	10	Shear Wave Profiling at the Waste Treatment Plant Site, Hanford, WA	Pacific Northwest National Laboratory Richland, WA
Yucca Mountain, NV	114 Surface sites 50 Tunnel sites	Yucca Mountain Site Characterization	Bechtel SAIC Company (BSC)

*SMR = strong-motion recording

3.2.2 Other Seismic Measurements

In addition to the SASW profiles, some downhole and suspension (P-S) logging test results are also available. These tests were performed at the same locations or very near the locations where the SASW tests were carried out. The downhole and P-S logging data were mainly gathered and reduced by Redpath Geophysics, GEOVision Inc., USGS (U.S. Geological Survey) and NCREE (National Center for Research on Earthquake Engineering, Taiwan). The testing setups and equipment of the downhole and suspension logging methods is discussed later in this chapter.

In total, 264 V_S profiles from three different survey techniques performed on ground surface and in boreholes are used in this work. In addition, there are 50 shallow SASW V_S profiles (no deeper than 20 ft) acquired in the tunnels beneath Yucca Mountain. Statistical analyses of the distribution of these data from surface sites are presented in Figure 3.1, 3.2 and 3.3. As seen in Figure 3.1, most data are from Yucca Mountain and the SASW data contributed almost 70% of the total available data. There are more downhole data than P-S logging data but neither of them is available at every geographic site. One thing that needs to be mentioned here is that most available P-S logging profiles do not have any data until they reach certain depths. If a P-S profile has no data in the top 30 ft (10 m) or less, the profile is still used in this study. For that portion of the P-S logging profile where the P-S logging data are not available, the profile was replaced by downhole profiles, if available, measured at the same boreholes and at the same depths to make the site classification analysis possible.

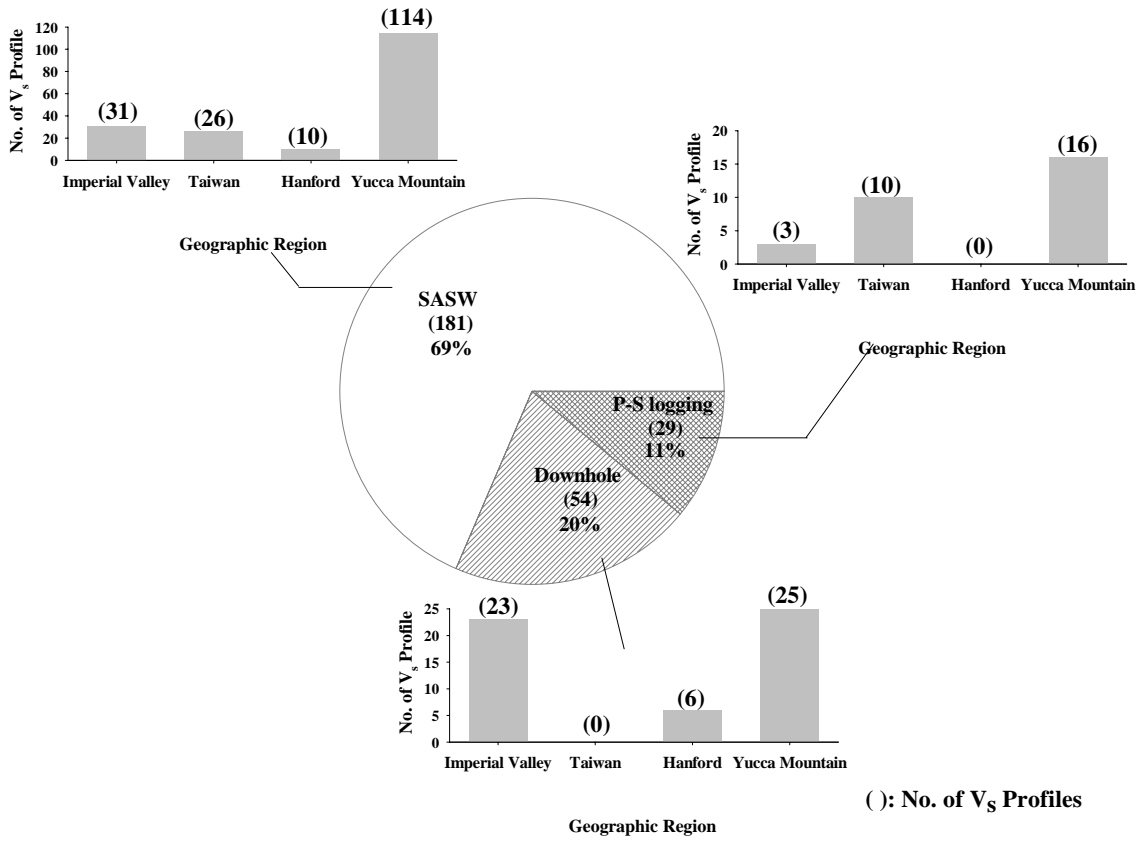


Figure 3.1 Distribution of V_s Profiles Measured at Surface Sites with Respect to Survey Technique and Geographic Location

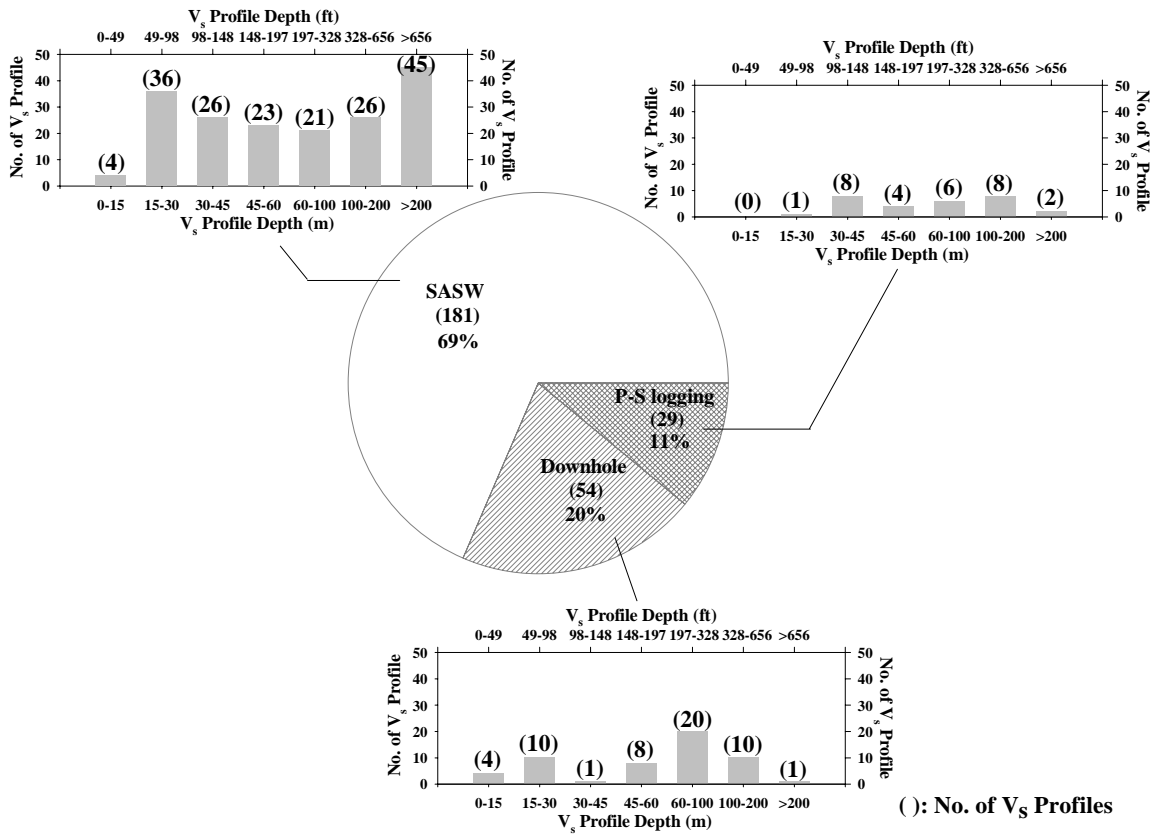


Figure 3.2 Distribution of V_S Profiles Measured at Surface Sites with Respect to Survey Technique and Profiling Depth

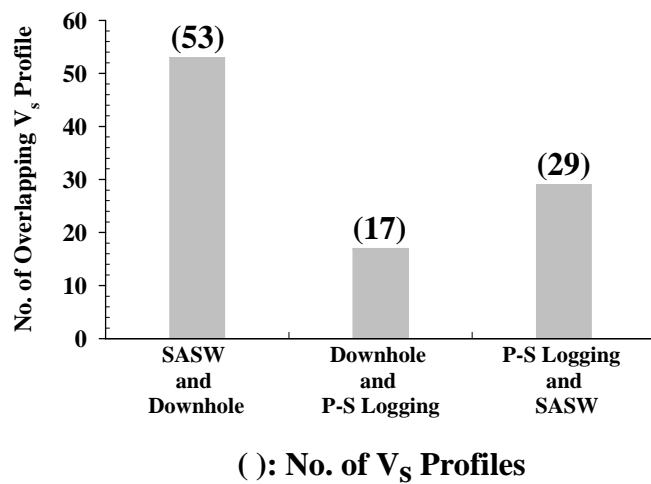


Figure 3.3 Histogram of Common Test Sites for the Different Survey Techniques

Generally speaking, the average depth of the SASW V_S profiles presented in this study is deeper than the V_S profiles of the downhole and P-S measurements (Figure 3.2). One reason is that most of the SASW V_S profiles were acquired at the Yucca Mountain test site (over 50%) and, on average, these profiles are deeper than the other test sites because of the depth of nuclear waste repository. The other reason is that the downhole and P-S logging survey depths are restricted by the depths of boreholes where the test was performed and the average depth of these boreholes is generally in the range of 60 to 100 m.

As shown in Figure 3.3, 53 out of the 181 SASW test sites have downhole data. However, only 29 sites among the 181 SASW test sites have P-S logging data. This comparison shows the advantage of the SASW method in that, unlike the downhole and P-S logging methods, it is free from the restriction of available boreholes.

3.3 OVERVIEW OF OTHER SEISMIC TECHNIQUES

The SASW technique is reviewed in Chapter 2. In this section, the downhole and P-S logging are briefly discussed.

3.3.1 Downhole Method

The downhole method has been widely used as subsurface profiling technique for more than 40 years. This technique requires only one borehole to perform the test. If soil is too weak or the rock is too fracture to support the borehole remaining open, a PVC casing is often grouted in place.

The basic idea of the downhole method is to generate compression waves (P waves) and shear waves (S waves) by hitting the source block vertically and in two opposite horizontal directions. The key is to detect the arrival of these waves with an in-hole receiver(s) from which the travel time of the body waves between the trigger and

receiver(s) is determined. With the travel time and travel distance, the body wave velocities of the soil layers at different depths are calculated. In the downhole method, the need to measure the arrivals of both P- and S- waves requires the use of at least one three-directional (3-D) transducer (geophone) in the test. Usually, the sampling depth interval is from 1.5 to 6 m (5 to 20 ft). A schematic diagram of the general downhole setup is presented in Figure 3.4. The data are analyzed in the form illustrated in Figure 3.5(a) to determine average P-wave (or S-wave) velocity. Body wave velocity profiles are then constructed as shown in Figure 3.5(b).

In terms of the number of the receivers used, there are two common configurations that are employed. The first configuration is exactly the same as shown in Figure 3.4 in which one 3-D receiver is used. The second configuration, which is presented in Figure 3.6, utilizes two (or more) 3-D receivers to perform a test.

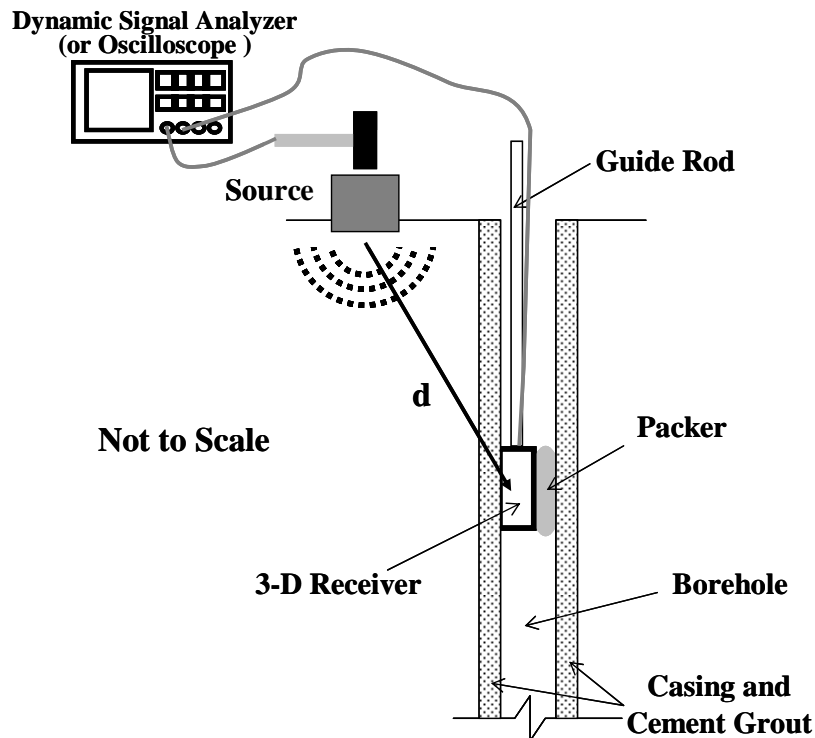


Figure 3.4 General Configuration of Downhole Testing

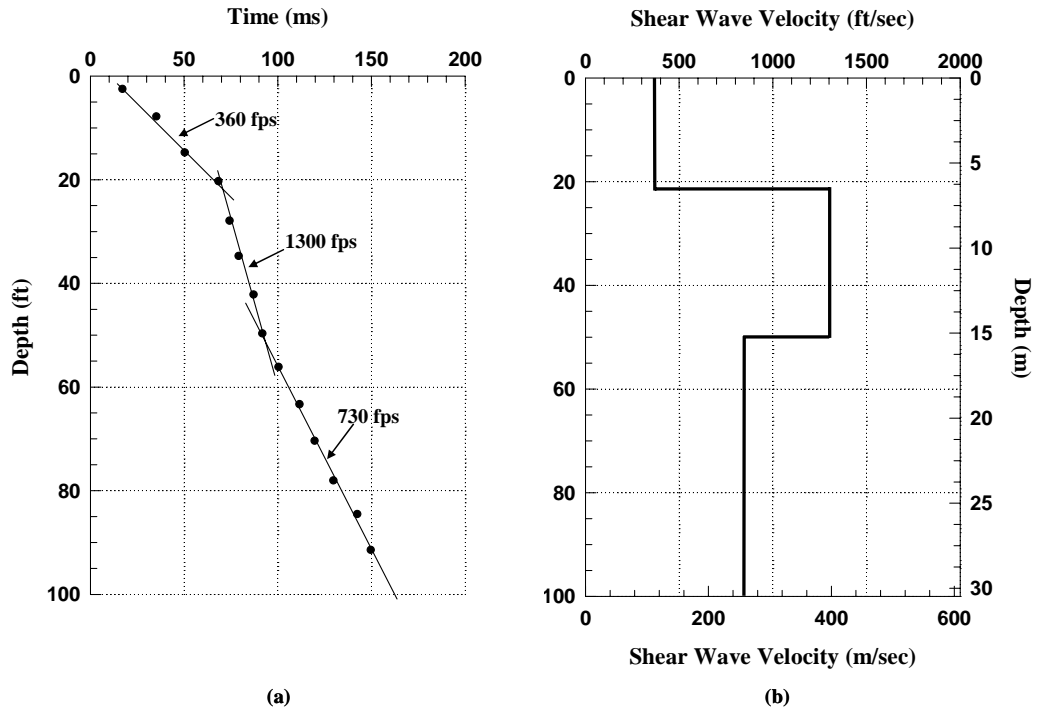


Figure 3.5 Downhole Travel Time Measurements and Resulting Shear Wave Velocity Profile

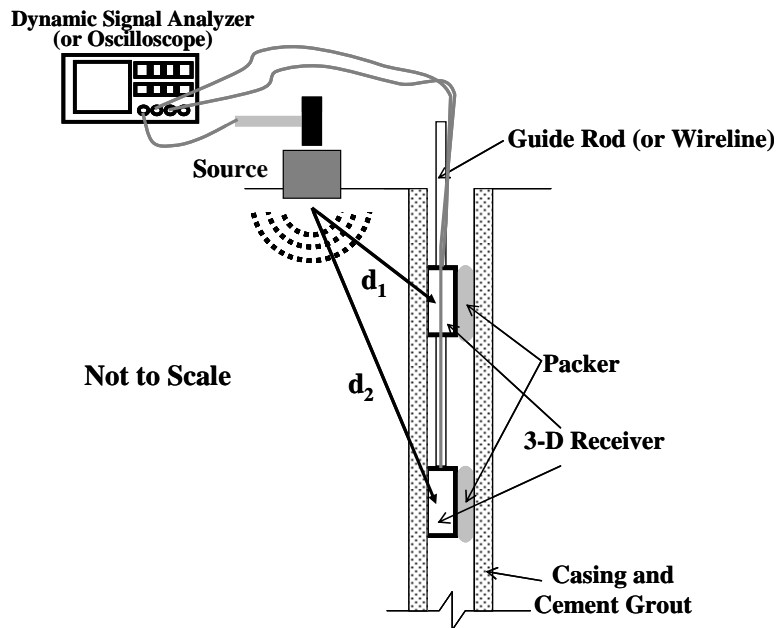
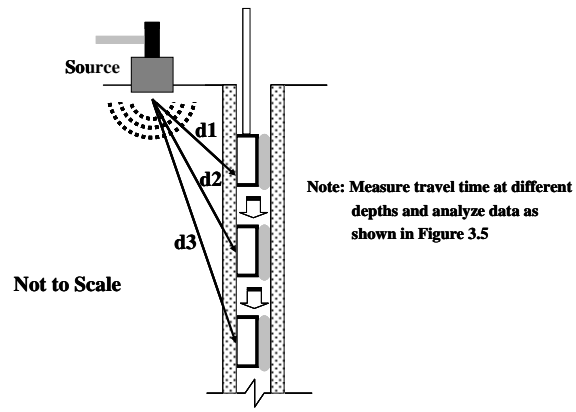


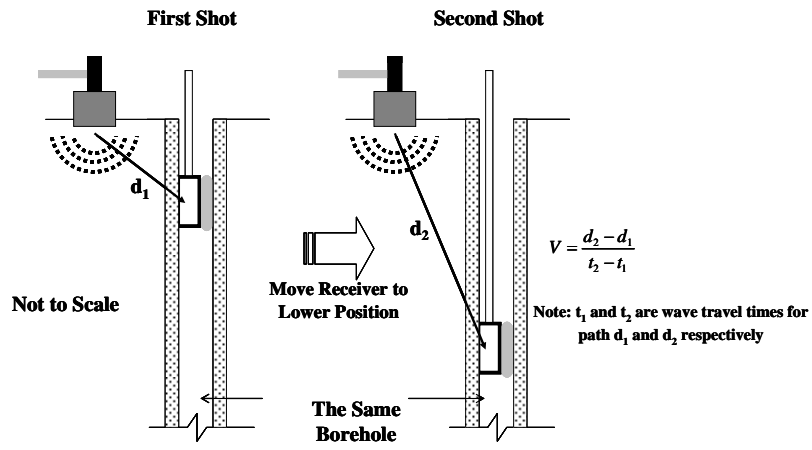
Figure 3.6 Setup of Downhole Testing with Two (or more) Receivers

The approach to calculating body wave velocities can vary with the data collection. There are three different ways to interpret the shear or compression wave velocity of the soil profile. They are: (1) direct measurements from which average velocities are calculated, (2) pseudo-interval measurements and (3) true-interval measurements. The differences between these three methods are illustrated in Figure 3.7. The advantage of first two methods is lower equipment cost. The advantage of the third method is that it is faster to perform. The most widely used approach is shown in Figure 3.7 (a) to collect the data and Figure 3.5 to analyze the data. Today, multi-channel analyzers (four or more) and receivers are more affordable so it is possible to utilize more receivers to conduct the downhole testing to save test time and to increase profile resolution.

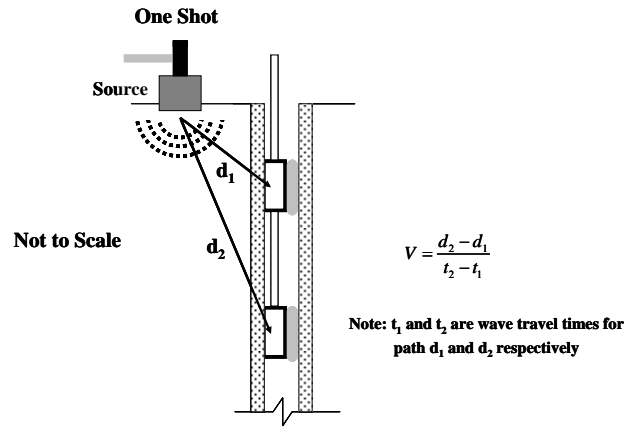
There are some disadvantages of downhole seismic method. First, because of the requirement of the borehole, the downhole method is more costly and compared to the SASW method. Secondly, poor coupling between the casing pipe and soil may cause low-quality data that could be hard to interpret. Moreover, if steel (metal) casing is used, it may causes problems in measuring and interpreting the data. Sometimes, body waves from the source can propagate along the casing instead of the soil layers. In this case, the wave arrival may be misinterpreted, often resulting in overestimating the wave velocity. Last, the profiling depth of the downhole method is restricted by the depth of the borehole where the test is performed. It can also be restricted by the energy level generated by the seismic source.



(a) Direct Measurements for Average Values



(b) Pseudo-Interval Measurements (Two shots)



(c) True-Interval Measurements (One Shot Only)

Figure 3.7 Different Downhole Measurements: (a) Direct Measurements, (b) Pseudo-Interval Measurements, and (c) True-Interval Measurements

3.3.2 Suspension (P-S) Logging Method

The suspension P-S velocity logging method was developed in the mid-1970's by OYO company in Japan. After a decade or two of development, it gained acceptance in Japan. Later, the method was introduced in the United States. Like downhole testing, this method requires a borehole to perform the test. An uncased borehole is preferred. In addition, the borehole has to be filled with drilling mud or water.

The basic setup of the suspension logging method is shown in Figure 3.8. The key device of this method is a 7-m long probe that is connected to a cable designed to support the probe and transmit signals from the probe to a recorder on surface. The probe is equipped with one reversible polarity solenoid source near its bottom end and two biaxial geophones on its top half, with one meter between them. The frequency range of the solenoid source is between 500 and 5000 Hz. Usually, higher frequencies (around 3000 Hz) are used for the P-wave measurements and lower frequencies (around 1000 Hz) are applied to the S-wave detection.

The procedures of the P-S logging measurement are very simple. First, immerse the probe completely into the liquid-filled borehole with nylon whiskers to center the probe in the borehole to avoid it contacting the borehole wall directly. Then, by activating the source in two opposite directions, the P wave and S wave are detected by the two biaxial geophones and the signals are transmitted to and recorded by the device on surface. The recorded data for a single depth are illustrated in Figure 3.9 and the reduced velocity profiles of body waves are shown in Figure 3.10. Usually, the interval of sampling rate is from 0.5 to 1 m.

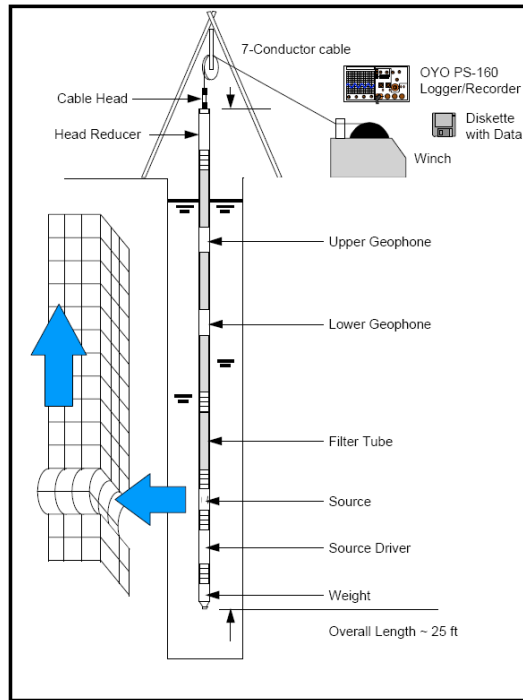


Figure 3.8 Illustration of the Setup of the Suspension Logging Method (from http://www.geovision.com/PDF/M_PS_Logging.PDF)

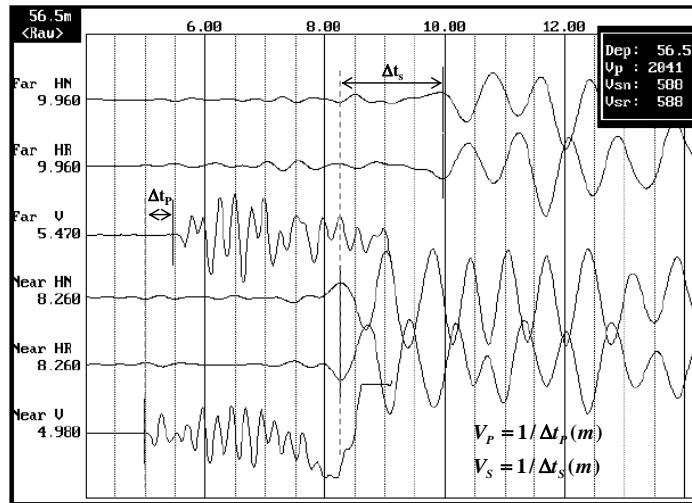


Figure 3.9 An Example of a Single Depth Data of Suspension Logging Test (Modified from http://www.geovision.com/PDF/M_PS_Logging.PDF)

GOLDEN GATE BRIDGE HOLE B6 SUSPENSION LOGGING
P and S Wave Velocities; Data collected December 14-15, 1991

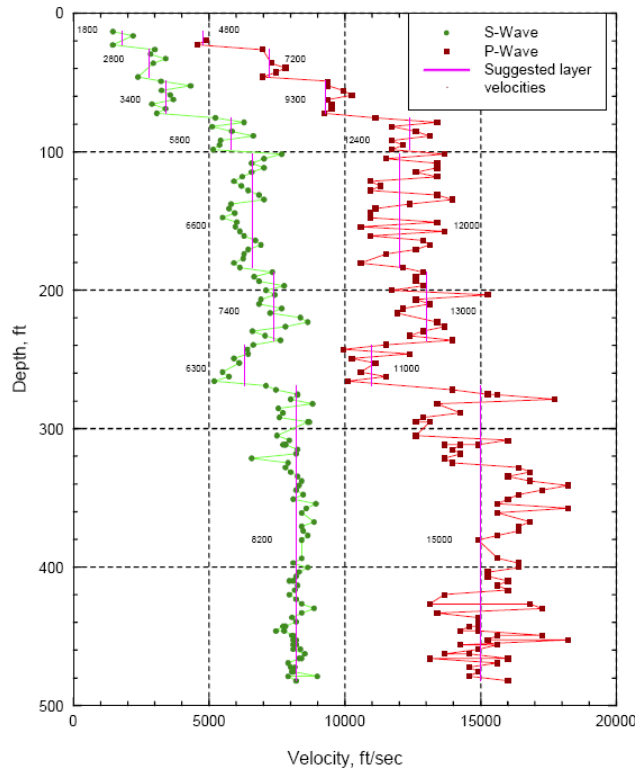


Figure 3.10 Example of S- and P-Wave Velocity Profiles from the Suspension Logging Test (from http://www.geovision.com/PDF/M_PS_Logging.PDF)

Compared to other profiling method, the suspension logging method has some advantages. The resolution of the P-S logging measurements can be as high as 20 cm so thin layers which have big contrast in engineering/geologic properties to the adjacent layers can be resolved. Because this method can measure V_S and V_P profiles from a borehole, it is possible to calculate shear modulus, bulk modulus, compressibility, and Poisson's ratio based on the P-S logging measurements.

However, there are some disadvantages of the suspension logging method, too. This method does not always obtain good results near the surface (about top 5 meters) because of ambiguous signals at low confining pressures around the borehole and/or because of interference from the casing (coupling condition with soil or steel casing) at

these shallow depths. Also, it has the same disadvantages as the downhole method mentioned above. It is claimed that this method can survey to depths of 2,000 ft (GEOVision, http://www.geovision.com/PDF/M_PS_Logging.PDF). However, of course the cost of the borehole where the P-S logging would be performed could be expensive.

3.4 SITE CLASSIFICATION SYSTEM

Nowadays, earthquake engineers used the top 30-m V_S profile ($V_{S,30}$) to classify the site (based on Uniform Building Code (UBC-97), National Earthquake Hazards Reduction Program (NEHRP-94) procedure or most current International Building Code (IBC-2006) provisions) and obtain the predicted site response or ground motion for design purposes. The site class criteria for IBC-2006 are tabulated in Table 3.2. The reason to use the V_S profile in the top 30 m is because this depth is a common depth of many boreholes and, in the past, most V_S profiles were obtained by downhole or other borehole required tests that were generally in the top 30 to 45 m. The value of $V_{S,30}$ can be obtained by Equation 3.1:

$$V_{s,30} = \frac{30m}{\sum_{i=1}^N \frac{h_i}{V_i}} \quad (3.1)$$

Where i = data number, N = total number of data, h = thickness of each soil layer and $\sum_{i=1}^N h_i = 30$ m.

In this work, the $V_{S,30}$ and site class reduced from different profiling techniques at the same areas are compared. According to the results of these comparisons, the similarity or difference in the profiling data between these methods of can be observed.

Table 3.2 Site Class Definitions (IBC-2006)

Site Class	Soil Profile Name	Average Properties in Top 100 feet (30 meter)		
		Soil Shear Wave Velocity, V_S (ft/s)	Standard Penetration Resistance, \bar{N}	Soil Undrained Shear Strength, \bar{S}_u (psf)
A	Hard rock	$V_S > 5000$	N/A	N/A
B	Rock	$2500 < V_S \leq 5000$	N/A	N/A
C	Very dense soil and soft rock	$1200 < V_S \leq 2500$	$\bar{N} > 50$	$\bar{S}_u > 2000$
D	Stiff soil profile	$600 \leq V_S \leq 1200$	$15 \leq \bar{N} \leq 50$	$1000 \leq \bar{S}_u \leq 2000$
E	Soft soil profile	$V_S < 600$	$\bar{N} < 15$	$\bar{S}_u < 1000$
E	-	Any profile with more than 10 feet of soil having the following characteristics: 1. Plasticity index $PI > 20$, 2. Moisture content $w \geq 40\%$, and 3. Undrained shear strength $\bar{S}_u < 500$ psf		
F	-	Any profile containing soils having one or more of the following characteristics: 1. Soils vulnerable to potential failure or collapse under seismic loading such as liquefiable soils, quick and highly sensitive clays, collapsible weakly cemented soils. 2. Peats and/or highly organic clays ($H > 10$ feet of peat highly organic clay where H = thickness of soil) 3. Very high plasticity clays ($H > 25$ feet with plasticity index $PI > 75$) 4. Very thick soft/medium stiff clays ($H > 120$ feet)		

For SI: 1 foot = 304.8 mm, 1 square foot = 0.0929 m², 1 pound per square foot = 0.0479 KPa. N/A = Not applicable

3.5 CLARIFICATION OF ANALYSIS METHODOLOGY

3.5.1 Data Distribution and Parameters used in Statistical Study

Different databases may have different types of distributions and the distribution of the data may affect the way the statistical analysis is performed.

To investigate what kind of the distribution exists in the V_S profiles used in this study, the histograms were examined on a foot by foot basis. No dominant distribution

in the histograms was found. The reason may be the number of data points is not large enough to show the distribution. Based on the opinions of some geologists and seismologists and some reports (e.g. Andrus et al. 2005), the distribution of V_S profiles in this dissertation is assumed to be a log-normal distribution.

In addition, the median and corresponding 16th and 84th percentile boundaries are three important “indices” used as a standard to compare the representative V_S profiles acquired from different techniques at the same area. Also, the coefficient of variation (COV), the ratio of the standard deviation to the mean, of a test site is investigated. The COV may be able to be used as an index of the uniformity of a site. One thing that needs to be mentioned here is that the calculations of the four parameters cited above only apply to three or more V_S profiles from the same technique at the same area. In fact, it is preferable to have five or more profiles whenever possible.

Also, before conducting the statistical analysis, if there is more than one profile at the same site by the same method, these profiles are averaged to calculate the representative profile of this site for this method. By doing so, one avoids putting too much weight on the same site where multiple profiles from the same profiling method have been acquired. Because of this process, the number of V_S profiles in some tables may more than that shown in the “No. of Profiles” figures. For example, there are 23 downhole V_S profiles from 21 sites in Imperial Valley so 23 profiles are listed in Table 4.3 but the “No. of Profiles” in Figure 4.4 is 21.

3.5.2 Criteria for Comparing V_S Profiles

In Chapter 4 through Chapter 7, the profession often compares V_S profiles in a general sense; that is without considering important details. To illustrate this point, the V_S comparisons are performed at three levels of detail in this study.

First, on a global level, all available V_S profiles acquired in the same region from different techniques are compared. This is called a general comparison or an “apples-to-oranges-comparison”. Secondly, the comparisons are made only for the profiles from the common sites where different measurements were performed. This comparison is called a common site comparison or a “green-apples-to-red-apples comparison”. The last comparison is called an identical-site-and-depth comparison over identical sites and depths (or a “green-apples-to-green-apples comparison”) because only the V_S profiles from the common sites and common depths are studied.

The V_S profiles obtained from the SASW method provides more global site information than the downhole and suspension logging methods. In contrast, the downhole measurements are rather localized and the suspension logging measurements are very localized. Therefore, there should be some difference between the measurements from the SASW, downhole and suspension logging methods. However, the difference should be small if the “green-apples-to-green apples” comparisons are used and if the three methods have similar precision in their measurements.

3.6 SUMMARY

In this chapter, an overview of the database used in this work is given. The test arrangements, procedures and the data reduction processes associated with the downhole and suspension logging methods are described. In addition, the advantages and disadvantages of downhole and suspension logging methods are discussed. Also, the site classification criteria adopted in this work is presented. In the end, the parameters, in terms of the statistical analyses, used to compare different survey techniques are defined.

Chapter 4 SASW Testing in Imperial Valley, California

4.1 BACKGROUND OF TEST SITE

Imperial Valley is a region in southeastern California, between the Salton Sea, the largest (saltwater) lake in California, and the border of Mexico. Most of this area is below sea level. Since 1872, several big earthquakes have occurred in this region, with most of them having a magnitude over 6 (Table 4.1). As seen in Table 4.1, the largest earthquake occurred in 1940 with a magnitude 7.1. These earthquakes resulted in severe damage to structures and induced liquefaction in the area. To less serious property damage and loss of life in the future, it is important to study the usefulness of site classification and the site response during future earthquakes in this region.

Table 4.1 Table of Major Earthquakes happen in Imperial Valley, California (from United States Geological Survey, USGS)

DATE	MAGNITUDE
May 3, 1872	5.75
April 19, 1906	6.2
June 23, 1915	6.0
June 23, 1915	5.9
May 19, 1940	7.1
October 15, 1979	6.5

4.2 REVIEW OF SASW TESTING PERFORMED IN IMPERIAL VALLEY, CA

In this study, SASW tests that were performed in Imperial Valley, CA were sponsored by the Pacific Earthquake Engineering Research Center (PEER) Lifelines Program under the project: Application of SASW to US SMR Sites - 2C01. The goal of this project was to apply the SASW method to profile the subsurface of selected strong-motion recording (SMR) sites in Imperial Valley, CA and use the top 30 m of the V_S

profiles ($V_{s,30}$) obtained from the SASW tests to classify these sites based on the IBC-2006 provisions. Furthermore, the upper portion of the SASW V_s profiles (top 30 ft or so) can be used to evaluate of the liquefaction potential of some of these sites. According to the information from the SASW measurements, engineers can estimate the site response and liquefaction potential at planned important facilities, such as transformer stations, during an earthquake.

Maps of the approximate locations of test sites are shown in Figures 4.1 and 4.2. The area covered by SASW testing is about 60 mi. by 30 mi. The SASW tests were performed at 30 arrays by personnel (Dr .Kenneth H. Stokoe, II, Brent L. Rosenblad, Hyung Choon Park, and the author) from the University of Texas at Austin (UTA) between May 13 and May 22, 2002 in Imperial Valley, CA. A traditional vibroseis truck was used as the seismic source for the SASW tests. In addition, one more SASW test was performed in August 17, 2005 at the Wildlife Liquefaction Array (WLA) by Kenneth H. Stokoe, II, Mr. Min Jae Jung, Brady R. Cox and Cecil Hoffpauir from UTA. The T-Rex vibrator, one of the three custom-made vibrators of the nees@UTexas project, was employed to be the active source for this test. In total, 31 SASW V_s profiles were obtained.

Generally, receiver spacings of 5, 10, 20, 40, 80, 160, 320 ft were used. For spacings of receivers 1 and 2 of no more than 20 ft, the SASW testing was performed in both forward and reverse directions with an impact source. For other spacings, the SASW testing was only conducted in the forward direction with the vibroseis.

As to the testing equipment, two active seismic sources mentioned above are for large SASW test spacings (for distance between receivers 1 and 2 larger than 40 ft). For shorter spacings, a sledge hammer was employed to perform the tests. Three 1-Hz geophones (Mark Products, Model L-4C) were used to monitor the surface waves which

were recorded and conducted by a four-channel analyzer (Agilent 35670A Dynamic Signal Analyzer).

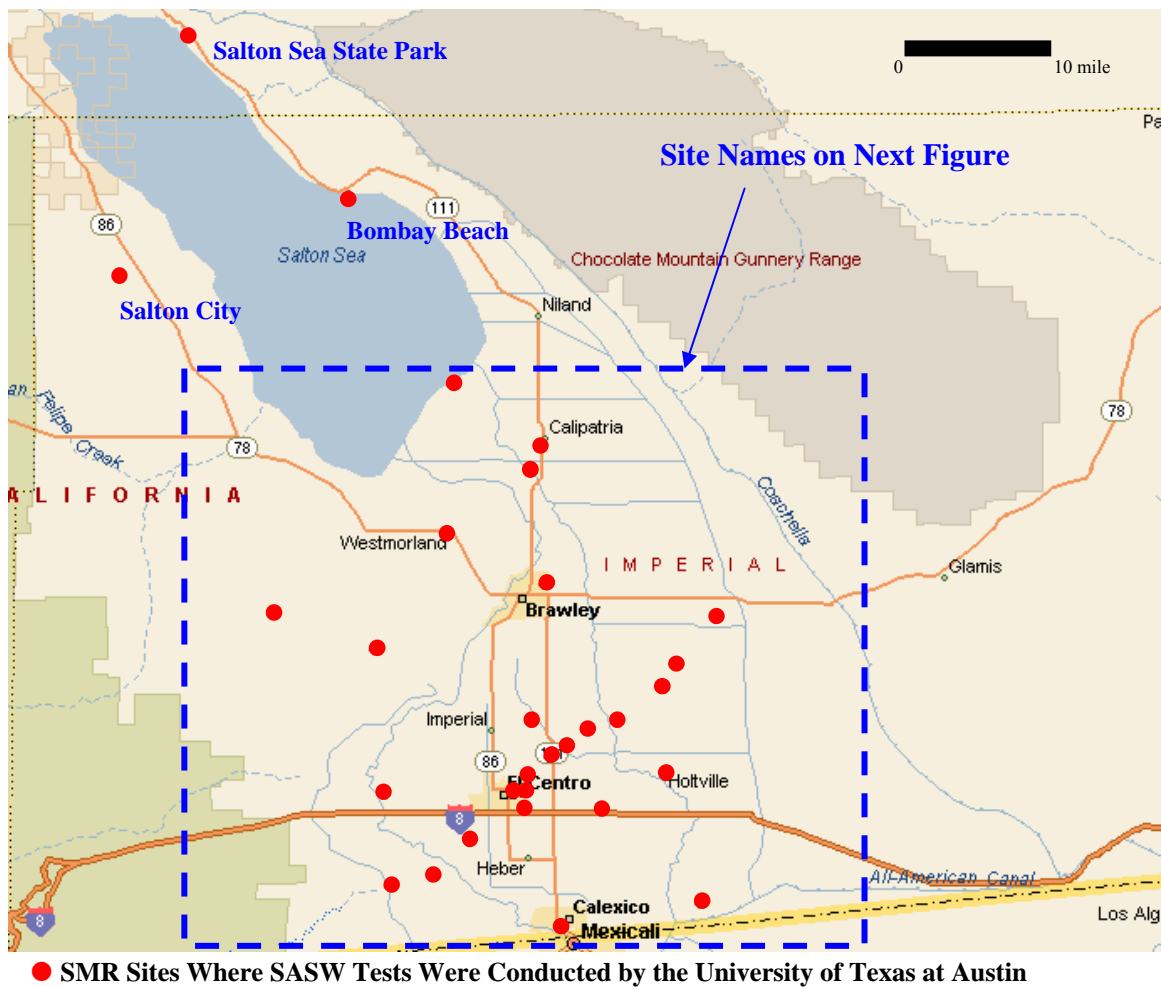


Figure 4.1 Approximate Locations of 31 SASW Testing Sites Superimposed on a Map of Imperial Valley, CA

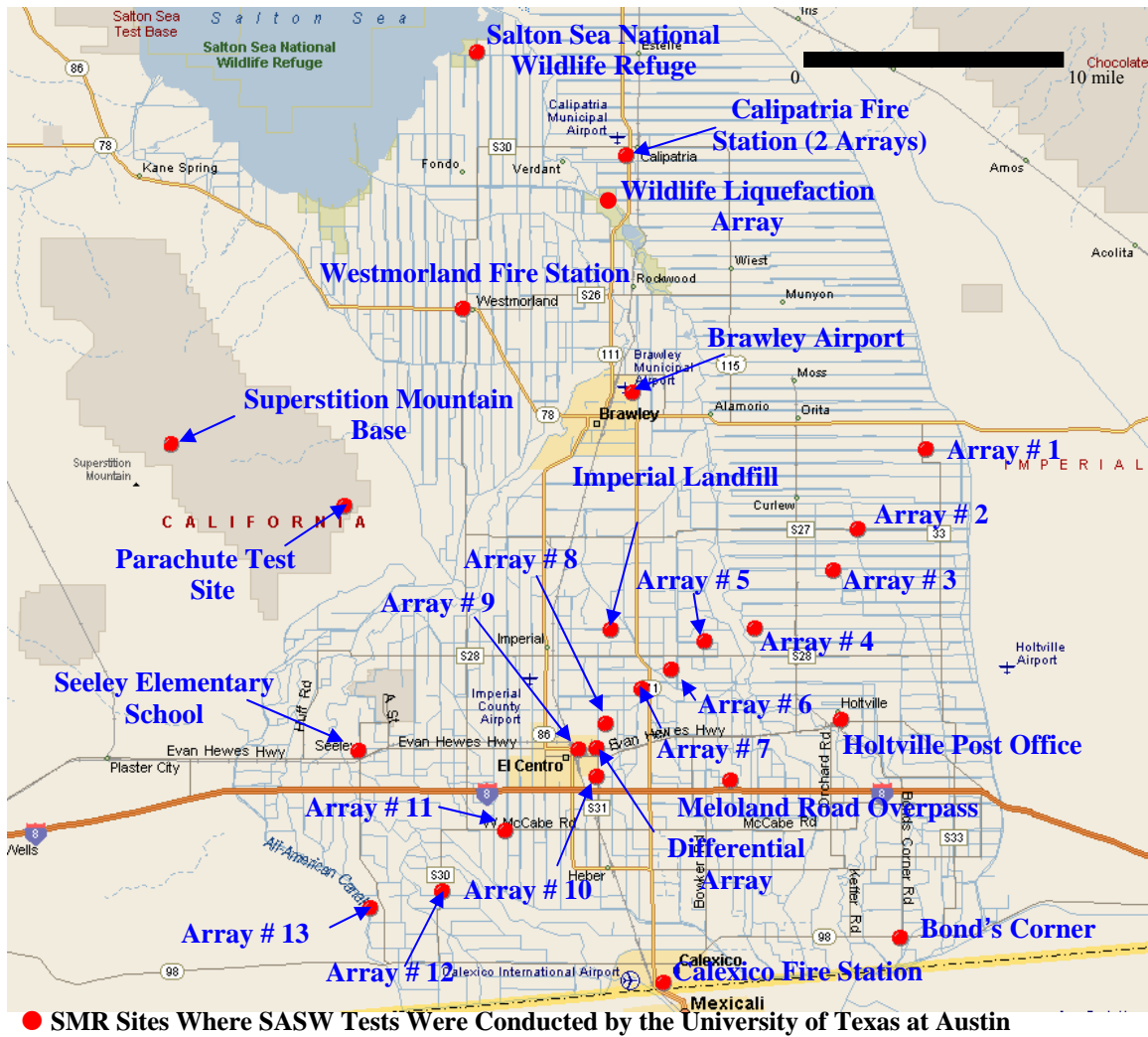


Figure 4.2 Approximate Locations of SASW Testing Sites Superimposed on a Map of Imperial Valley, CA (Continued)

4.3 TESTING RESULTS

4.3.1 SASW Testing

A list of the SASW test sites is tabulated in Table 4.2. The V_s profiles are presented in Figure 4.3 which also includes information about the median, 16th and 84th percentile boundaries, COV and depth of the 31 profiles. The deepest V_s profile is

316 ft at the Wildlife Liquefaction Array; the shallowest one is 64 ft at the New Calipatria Fire Station site. Among the 31 sites, only four sites (El Centro Array #2, El Centro Array #3, Imperial Landfill, and Wildlife Liquefaction Array sites) are classified as “E” sites and the rest are “D” sites based on the $V_{s,30}$ obtained from SASW tests and IBC-2006 provisions. The “E” sites may have the potential to liquefy during future earthquakes. Further information are needed to determine the liquefaction potential. The information of other available seismic test results is also listed in the Table 4.2.

Table 4.2 Information of SASW Test Sites in Imperial Valley, CA

No.	Site Name	Station No.	Profile Depth (ft)	$V_{s,30}$ (fps)	Site Class	Test Date	Test Performer	Other Test	
								Downhole	P-S Logging
1	El Centro Array # 1	USGS 5056	119	779	D	15-May-02	UTA		
2	El Centro Array # 2	USGS 5115	91	592	E*	14-May-02	UTA	1	
3	El Centro Array # 3 (Pine Union School)	USGS 5057	150	568	E	16-May-02	UTA	1	
4	El Centro Array # 4	USGS 955	128	707	D	14-May-02	UTA	1	
5	El Centro Array # 5	USGS 952	104	638	D	15-May-02	UTA	1	
6	El Centro Array # 6	USGS 5158	115	657	D	15-May-02	UTA	1	
7	El Centro Array # 7 (Imperial Valley College)	USGS 5028	100	633	D	14-May-02	UTA	1	1
8	El Centro Array # 8	USGS 958	104	671	D	18-May-02	UTA	1	
9	El Centro Array # 9 (El Centro 1940)	USGS 117	83	670	D*	13-May-02	UTA	1	
10	El Centro Array # 10 (Regional Hospital)	USGS 412	175	672	D	18-May-02	UTA	1	
11	El Centro Array # 11 (McCabe School)	USGS 5058	132	646	D	17-May-02	UTA	1	
12	El Centro Array # 12 (Meloland Cattle Co.)	USGS 931	104	646	D	17-May-02	UTA	1	
13	El Centro Array # 13	USGS 5059	138	887	D	18-May-02	UTA	1	
14	Bombay Beach	USGS 5271	256	843	D	22-May-02	UTA		
15	Bond's Corner	USGS 5054	100	777	D	16-May-02	UTA	1	
16	Brawley Airport	USGS 5060	129	617	D	20-May-02	UTA	1	
17	Calexico Fire Station	USGS 5053	114	650	D	17-May-02	UTA	1	
18	Calipatria Fire Station (New)	USGS 5061	64	707	D*	21-May-02	UTA		
19	Calipatria Fire Station (Old)	USGS 5061	83	675	D*	21-May-02	UTA	1	
20	El Centro Differential Array	USGS 5165	100	628	D	13-May-02	UTA	2	
21	Holtville Post Office	USGS 5055	118	693	D	16-May-02	UTA	1	
22	Imperial Landfill	USGS 5413	150	588	E	18-May-02	UTA		
23	Meloland Road Overpass	CDMG 5155	103	650	D	19-May-02	UTA		1
24	Parachute Test Site	USGS 5051	258	1144	D	19-May-02	UTA	2	
25	Salton City	CSMIP 11628	242	1064	D	22-May-02	UTA		
26	Salton Sea State Park	CSMIP 11613	186	870	D	22-May-02	UTA		
27	Salton Sea Wild Life Refuge	USGS 5062	102	627	D	21-May-02	UTA	1	
28	Seeley Elementary School	USGS 5273	152	656	D	20-May-02	UTA		
29	Superstition Mountain Base	USGS 5274	262	1084	D	20-May-02	UTA		
30	Westmorland Fire Station	USGS 5169	75	670	D*	21-May-02	UTA	1	
31	Wildlife Liquefaction Array	WLA	316	562	E	3-Feb-02	UTA		1

*Based on extrapolated data

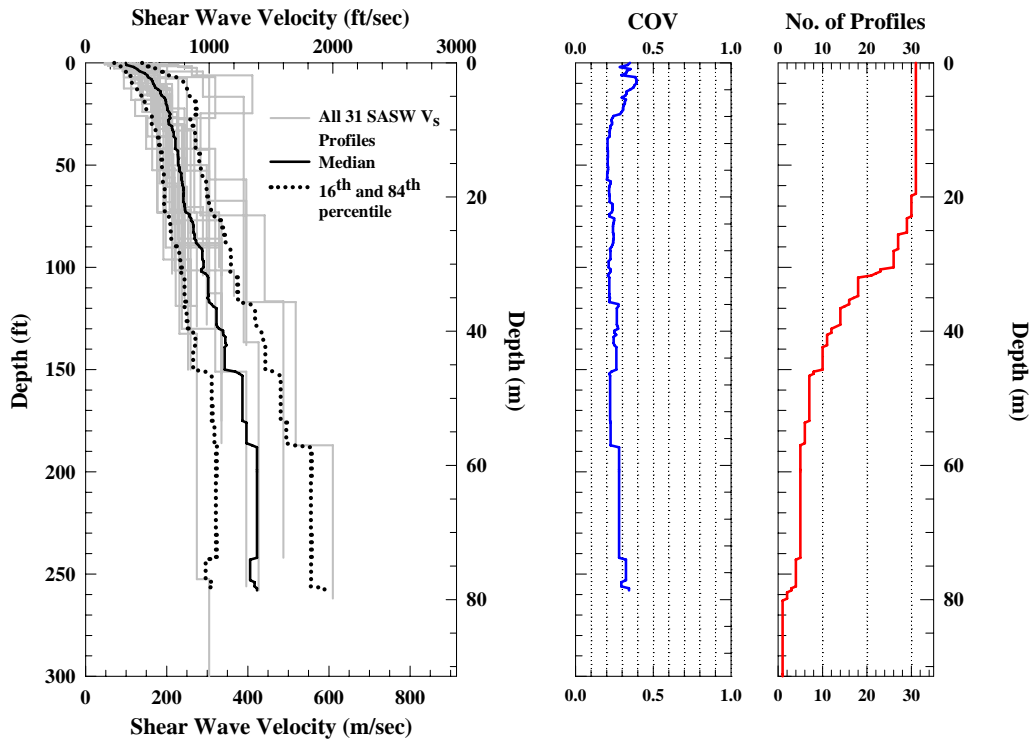


Figure 4.3 Individual Profile and Statistical Information of 31 SASW V_s Profiles from Imperial Valley, CA

4.3.2 Downhole Testing

In addition to the SASW testing, there are 23 downhole V_s profiles available from 21 of the 31 SASW test sites. These downhole measurements were conducted by USGS (Porcella, 1984), Hansen et al., and GEOVision in 2001. Most of these downhole measurements were performed in the beginning of 1980s. A detailed list is presented in Table 4.3. The deepest downhole V_s profile is 802 ft and this profile was measured at the El Centro Array #9 Site. In contrast, the shallowest profile is 79 ft at the old Calipatria Fire Station site. Unlike the SASW profiles which have “D” or “E” sites only, the downhole results have one “C” site, two “E” sites and 20 “D” sites which are classified based on the 23 downhole V_s profiles (from 21 sites). It is interesting that,

at the Parachute test site, two downhole tests were performed in the same borehole but with different results and two different site classes were (or $V_{s,30}$) determined. The reasons for this difference are discussed in Section 4.4.5. The 23 shear wave velocity profiles of downhole measurements are plotted in Figure 4.4 with the same statistical information as shown in the Figure 4.3 for the SASW profiles.

Table 4.3 Information of Available Downhole Test Sites in Imperial Valley, CA

No.	Site Name	Profile Depth (ft)	$V_{s,30}$ (fps)	Site Class	Test Date	Test Performer
1	El Centro Array # 2	247	621	D	29-Jan-81	USGS
2	El Centro Array # 3 (Pine Union School)	222	538	E	7-Feb-81	USGS
3	El Centro Array # 4	242	681	D	27-Jan-81	USGS
4	El Centro Array # 5	225	673	D	16-Jan-81	USGS
5	El Centro Array # 6	230	662	D	15-Jan-81	USGS
6	El Centro Array # 7 (Imperial Valley College)	189	697	D	11-Feb-81	USGS
7	El Centro Array # 8	238	681	D	26-Jan-81	USGS
8	El Centro Array # 9 (El Centro 1940)	802	700	D	4-Apr-81	USGS
9	El Centro Array # 10 (Regional Hospital)	233	669	D	13-Jan-81	USGS
10	El Centro Array # 11 (McCabe School)	205	648	D	23-Jan-81	USGS
11	El Centro Array # 12 (Meloland Cattle Co.)	90	674	D*	28-Jan-81	USGS
12	El Centro Array # 13	236	825	D	15-Feb-81	USGS
13	Bond's Corner	180	731	D	17-Feb-81	USGS
14	Brawley Airport	126	684	D	14-Jan-81	USGS
15	Calexico Fire Station	248	759	D	6-Feb-81	USGS
16	Calipatria Fire Station (Old)	79	665	D*	1-Mar-82	USGS
17	El Centro Differential Array	240	656	D	25-Jan-81	USGS
		250	663	D	(?)	Hansen et al.
18	Holtville Post Office	246	661	D	16-Feb-81	USGS
19	Parachute Test Site	94	1205	C*	4-Mar-82	USGS
		94	1131	D*	14-Jun-01	GEOVision
20	Salton Sea Wild Life Refuge	91	552	E*	2-Mar-82	USGS
21	Westmorland Fire Station	98	641	D	3-Mar-82	USGS

*Based on extrapolated data

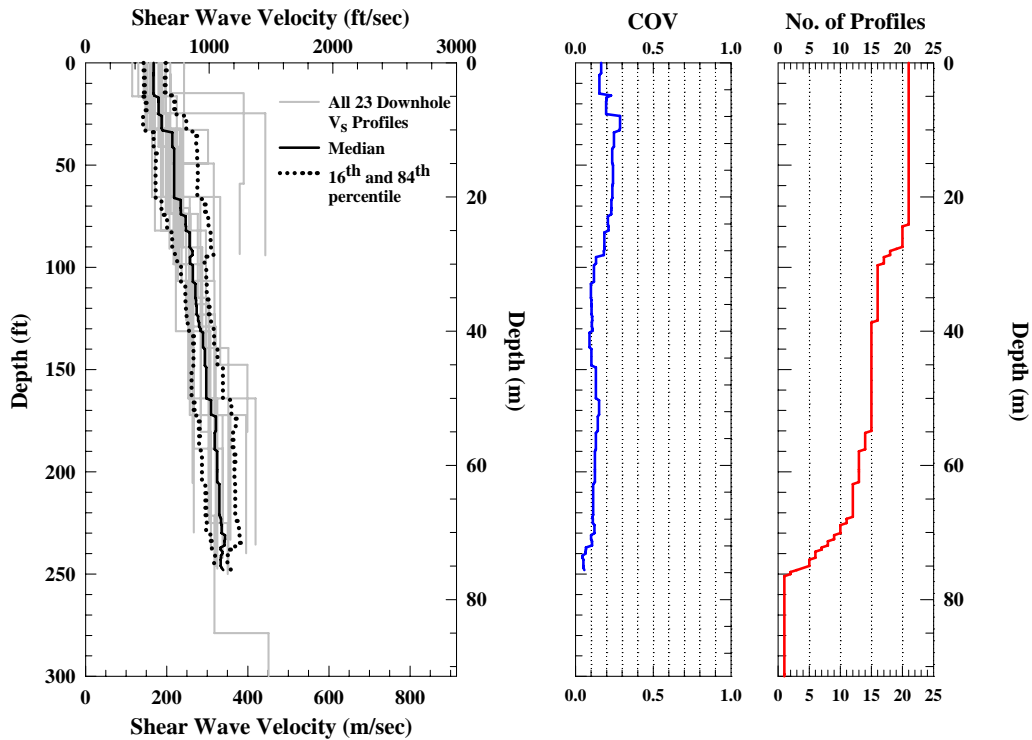


Figure 4.4 Individual Profile and Statistical Information of 23 Downhole V_S profiles (From 21 Sites) from Imperial Valley, CA

4.3.3 Suspension Logging

Three suspension logging V_S profiles were measured in the same area. These profiles are listed in Table 4.4. These tests were conducted by Kajima and GEOVision Inc. All three profiles are deeper than 300 ft and each site classifies as a “D” site. The three shear wave velocity profiles determined by suspension logging are presented in Figure 4.5. The median, 16th and 84th percentile boundaries, COV and depth information are also included in the figure. At some depths, one or two of the three P-S logging V_S profiles have no data. This causes the profile number in Figure 4.5 jumping between 1 and 3 dramatically at the range of the depth from 100 to 325 ft.

Table 4.4 Information of Three Suspension Logging Test Sites in Imperial Valley, CA

No.	Site Name	Profile Depth (ft)	$V_{s,30}$ (fps)	Site Class	Test Date	Test Performer
1	El Centro Array # 7 (Imperial Valley College)	339	747	D	1999-2000	Kajima
2	Meloland Road Overpass	799	730	D	29-Oct-97	GEOVision
3	Wildlife Liquefaction Array	322	657	D	20-Nov-03	GEOVision

*Based on extrapolated data

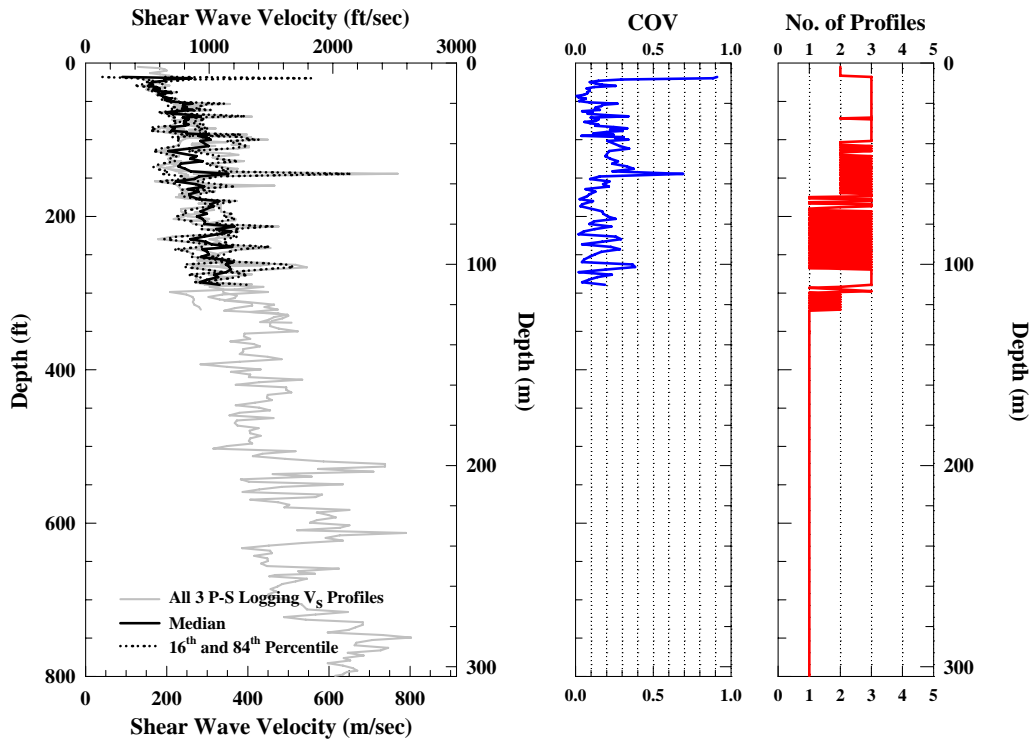


Figure 4.5 Individual Profiles and Statistical Information of Three Suspension Logging V_s Profiles from Imperial Valley, CA

4.4 STATISTICAL ANALYSES AND COMPARISONS

Generally speaking, most of the V_s profiles are very similar, except some sites (Parachute Test Site, Superstition Mountain Base and Salton City) that are at or close to

mountain areas. The values of the $V_{S,30}$ of these sites are always around 1200 fps which is much higher than the other sites.

In the following sections, many different comparisons are made based on the criteria stated in Section 3.5.2. These comparisons are general comparisons (or “apples-to-oranges” comparisons), common site comparisons (or “green-apples-to-red-apples” comparisons), and identical-site-and-depth comparisons (or “green-apples-to-green apples” comparisons).

Some other geologic/geographic factors are also taken into account to do some advance studies for each comparisons described in Chapter 3. By excluding the three sites at the mountain area (Parachute Test Site, Superstition Mountain Base and Salton City) or/and the five sites on the edge of Imperial Valley (El Centro Array #1, El Centro Array #13, Bombay Beach, Bond’s Corner and Salton Sea State Park), more objective comparisons can be observed.

In addition, because only a few of suspension logging profiles are available, three in total, these samples may not be sufficient to draw an objective conclusion. Therefore, most comparisons made in this chapter are between the SASW and downhole V_S profiles.

4.4.1 General Comparisons (Apples-to-Oranges Comparisons)

There are 31 SASW, 23 downhole and 3 suspension logging V_S profiles available in Imperial Valley for this study. As stated above, most comparisons made here are between the SASW and downhole measurements because only three suspension logging profiles are available.

The general comparison of the SASW and downhole V_S profiles is shown in Figure 4.6. As seen, there are some minor differences between the medians of the two methods in the top 90 ft. As the depth increases, the differences between them continue to increase. From Tables 4.2 and 4.3, it can be easily observed that the V_S profiles

acquired from the mountain area have higher velocities than the profiles in the valley area. Moreover, there are three SASW test sites (Parachute Test Site, Superstition Mountain Base and Salton City) in the mountain areas but only one downhole profile (Parachute Test Site) located in the same area so values of V_S in the mountain profiles have more weight on the median SASW profile than the median downhole profile. This difference also can be seen in the COV values in Figure 4.6, with the COV of the SASW profiles almost two times larger than the values in the downhole profiles below 100 ft.

To eliminate the bias in the data, the profiles from mountain area are removed and the two sets of V_S profiles are compared again. The statistical results are presented in Figure 4.7. Now, the median profiles from the two methods are very similar. So are the COV profiles. The primary difference in the COV profile is the larger values of the COV in the top 25 ft found in the SASW V_S profiles. This variability is felt to result from the higher resolution of the SASW test at shallow depths. Furthermore, if the five sites on the perimeter of Imperial Valley are excluded, an even better comparison can be obtained between the two measurements in terms of their median and COV values is found as seen in Figure 4.8. The five sites are Sites El Centro Array #1, El Centro Array #13, Bombay Beach, Bond's Corner and Salton Sea State Park. The average COV values are about 0.10 for the downhole profiles and 0.15 for the SASW profiles, and both of the values are smaller than in the previous two comparisons. The reason for removing the five sites is that these sites are likely in the transition zone between the mountain and valley areas. In addition, among these five (SASW) sites, only two sites have downhole measurements so the five sites put more weight, in terms of the transition zone profiles, on the SASW profiles than the downhole profiles.

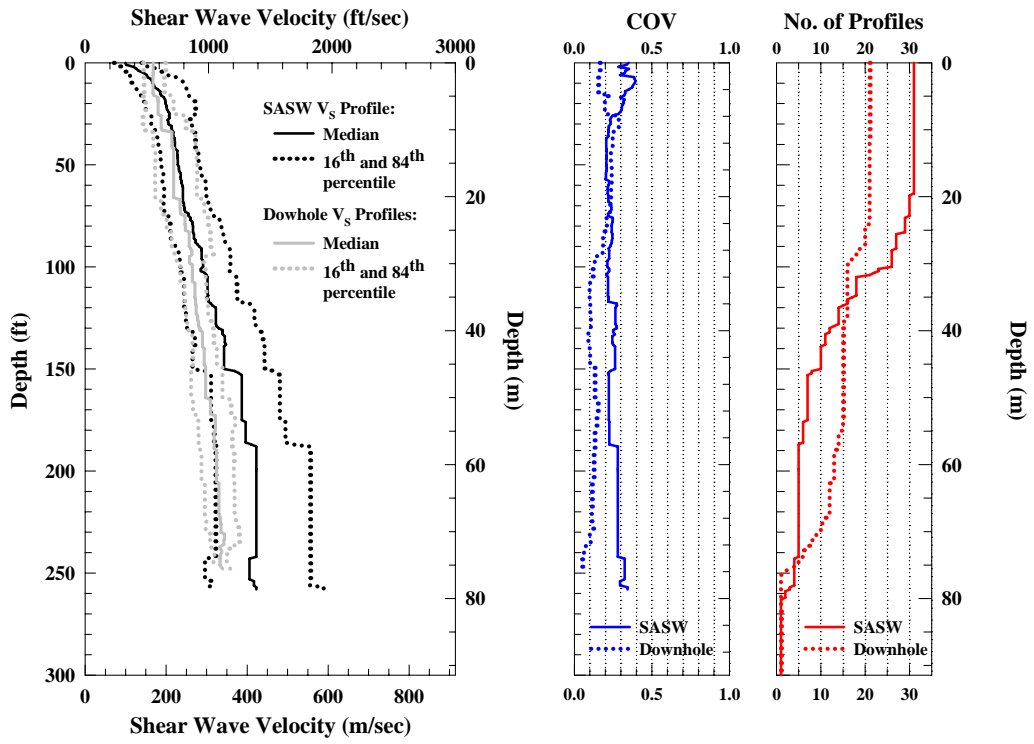


Figure 4.6 Comparison of the Median and 16th and 84th Percentile Boundaries of All Available 31 SASW and 21 Downhole V_S Profiles Measured in Imperial Valley, CA

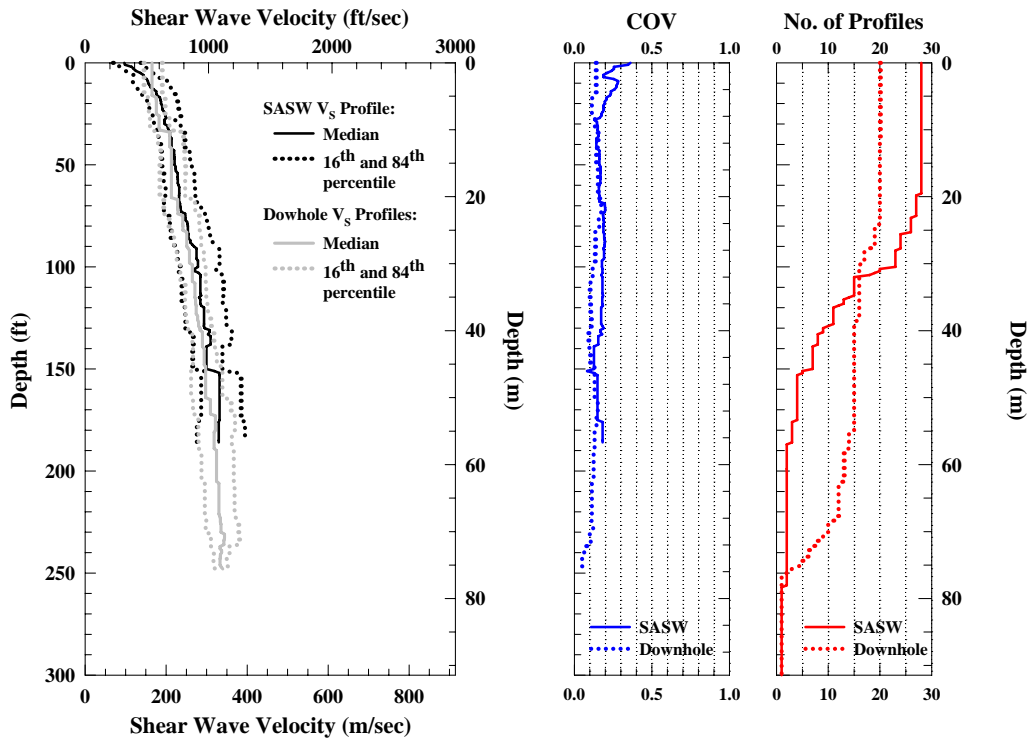


Figure 4.7 Comparison of the Median and 16th and 84th Percentile Boundaries of V_s Profiles of 28 SASW and 20 Downhole Test Sites not in the Mountain Areas of Imperial Valley, CA

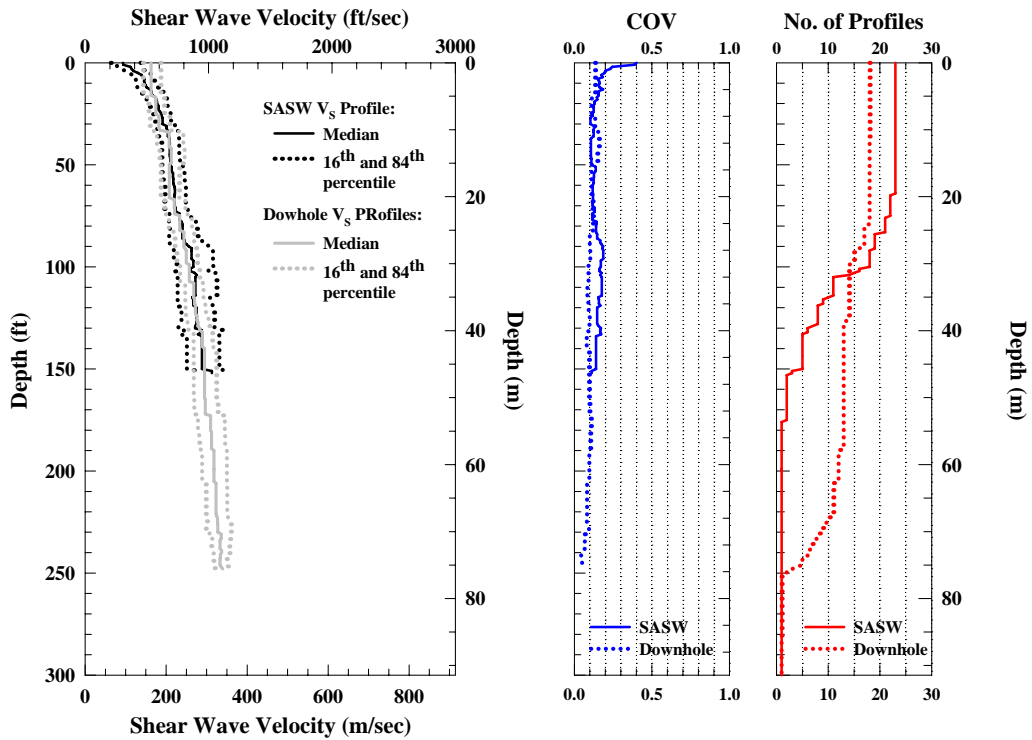


Figure 4.8 Comparison of the Median and 16th and 84th Percentile Boundaries of V_s Profiles of 23 SASW and 18 Downhole Test Sites in the Central Valley Area of Imperial Valley, CA

Although there are too few P-S logging data to do an objective comparison, these profiles are still compared in Figure 4.9 (without the 16th and 84th percentile boundaries) with the SASW and downhole results presented in Figure 4.8. The comparison shows the three measurements have very similar median values, even though there are some differences in the COV values. The reason could be that these profiles from three different techniques were all acquired in the central valley area but the number of P-S logging profiles is too few to lower the COV values.

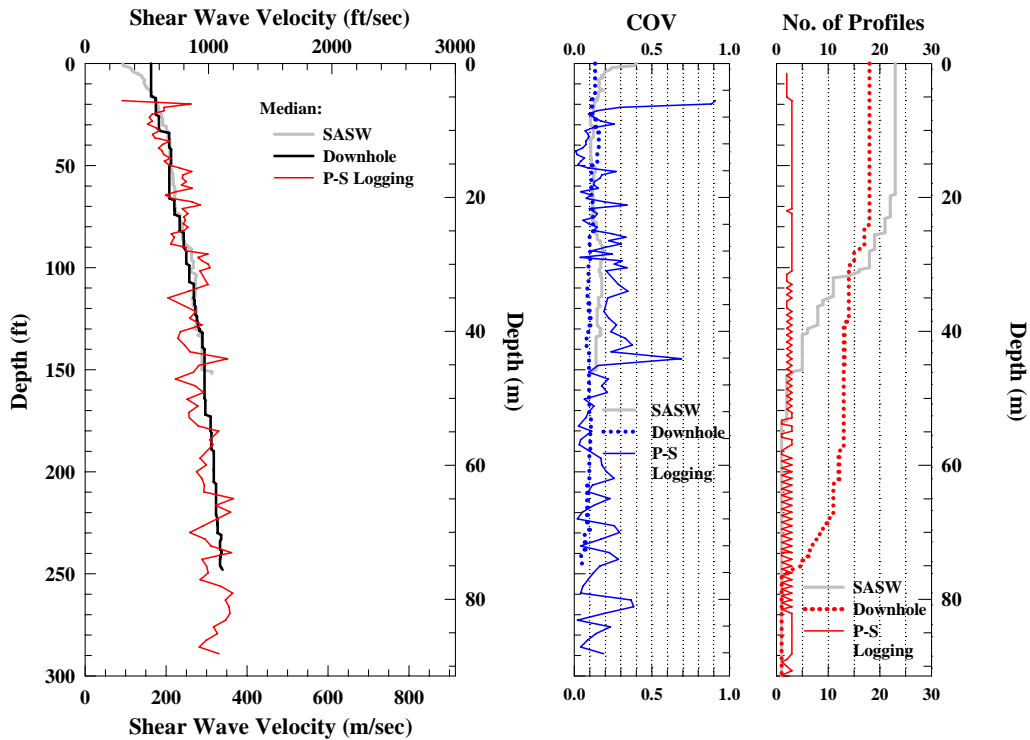


Figure 4.9 Comparison of the Median and 16th and 84th Percentile Boundaries of 23 SASW, 19 Downhole and Three P-S Logging V_s Profiles in the Central Valley Areas in Imperial Valley, CA

4.4.2 Common Site Comparisons (Green-Apples-to-Red-Apples Comparisons)

There are 21 common sites between the SASW and downhole test sites in Imperial Valley. The same comparison sequences used in the previous section are repeated here, but they are used to study the relationship between the uniformity of the soil deposit and the COV of V_s profiles instead of removing bias data. Actually, there is no bias data in this comparison as there was in the previous one.

First, all the V_s profiles from the SASW and downhole measurements at the 21 sites are compared in Figure 4.10. The median and COV values of these two methods are similar in the top 90 ft but differ below that depth. However, the difference is

smaller than the difference shown in Figure 4.6. This outcome is expected, as long as the different profiling methods have a similar degree of accuracy for the same test sites.

Because one profile was obtained in the mountain area in this set of 21 sites is quite different from the other 20 profiles in this comparison, it may have an effect on the median and COV values. Therefore, it is proper to remove it (Parachute Test Site) and to perform the comparison with the remaining 20 sites. This new comparison is presented in Figure 4.11. As expected, more similar results are observed in terms of the median and COV profiles and values determined with the two different techniques.

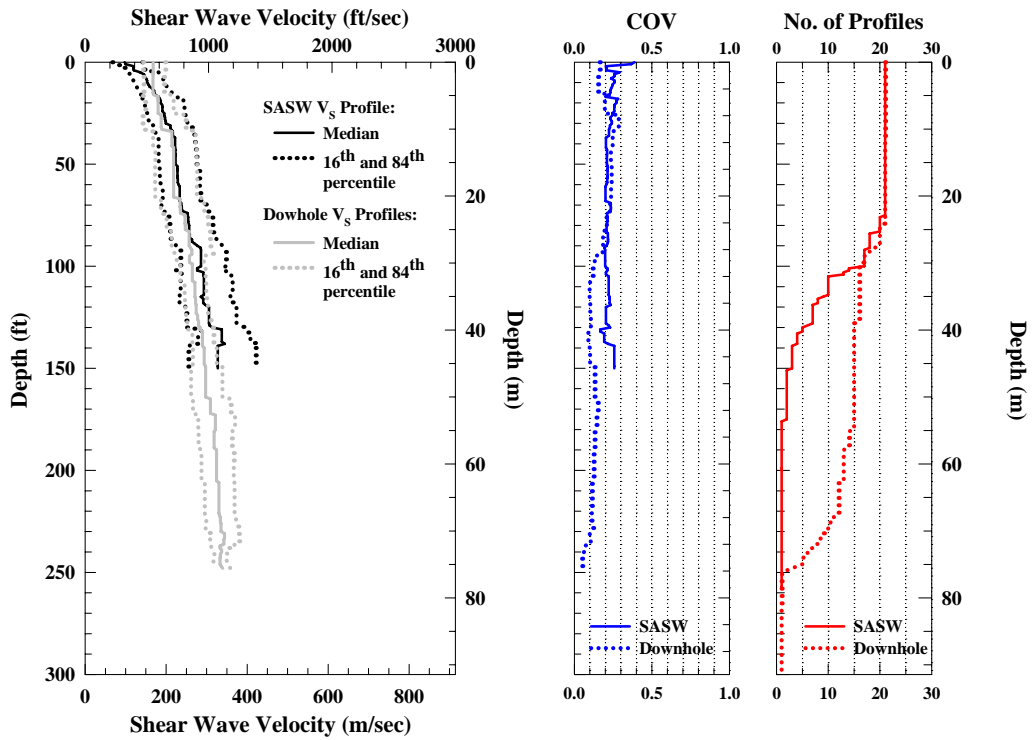


Figure 4.10 Comparison of the Median and 16th and 84th Percentile Boundaries of Available SASW and Downhole V_s Profiles from 21 Common Sites in Imperial Valley, CA

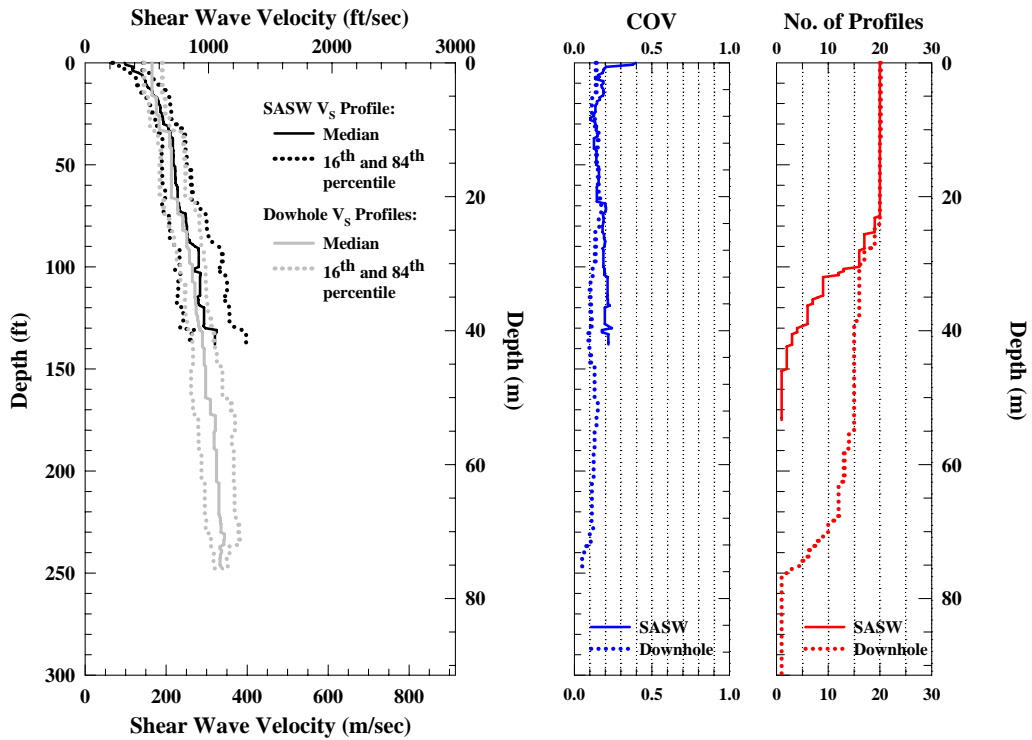


Figure 4.11 Comparison of the Median and 16th and 84th Percentile Boundaries of Available SASW and Downhole V_s Profiles from 20 Common Sites not in the Mountain Areas in Imperial Valley, CA

Next, if the two profiles (El Centro #13 Array and Bond's Corner) measured from the perimeter areas of the valley are excluded from the comparison, the new results (Figure 4.12) show an even more consistence between the SASW and downhole median and COV profiles and values.

A comparison between the SASW and suspension logging profiles at the three common sites is shown in Figure 4.13. Surprisingly, the values of the median and COV are very consistent. This close comparison likely occurs because these sites have very similar properties with little vertical variation so that the lower resolution at depth of the SASW method relative to the suspension logger does not enter the comparison.

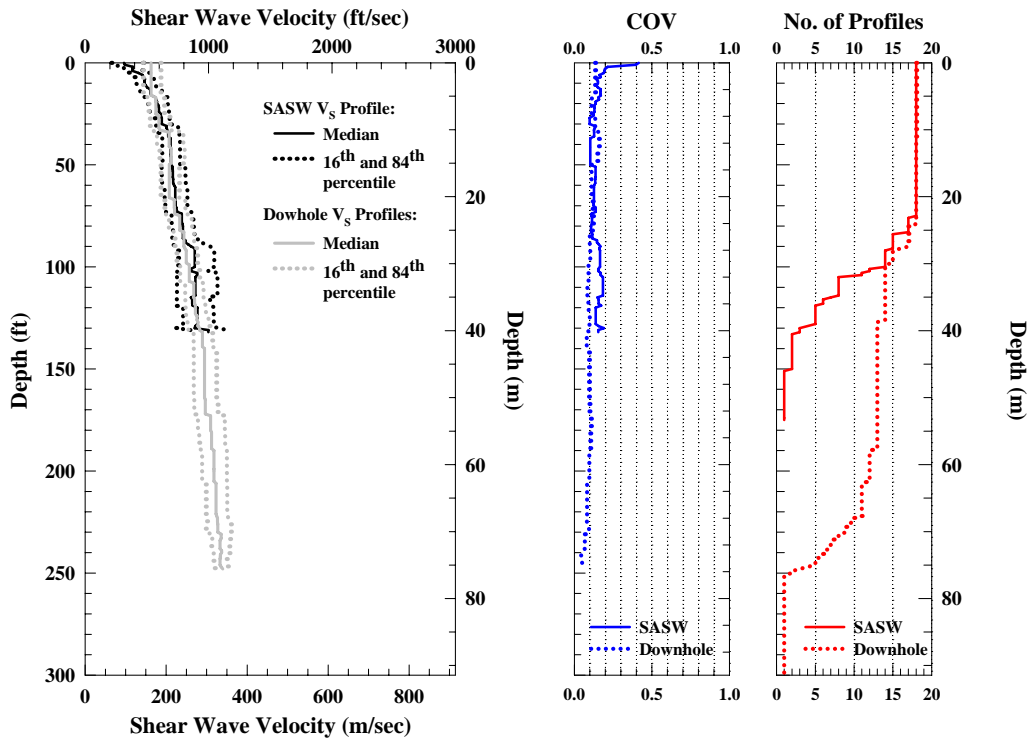


Figure 4.12 Comparison of the Median and 16th and 84th Percentile Boundaries of Available SASW and Downhole V_s Profiles from 18 Common Sites in the Central Valley Area of Imperial Valley, CA

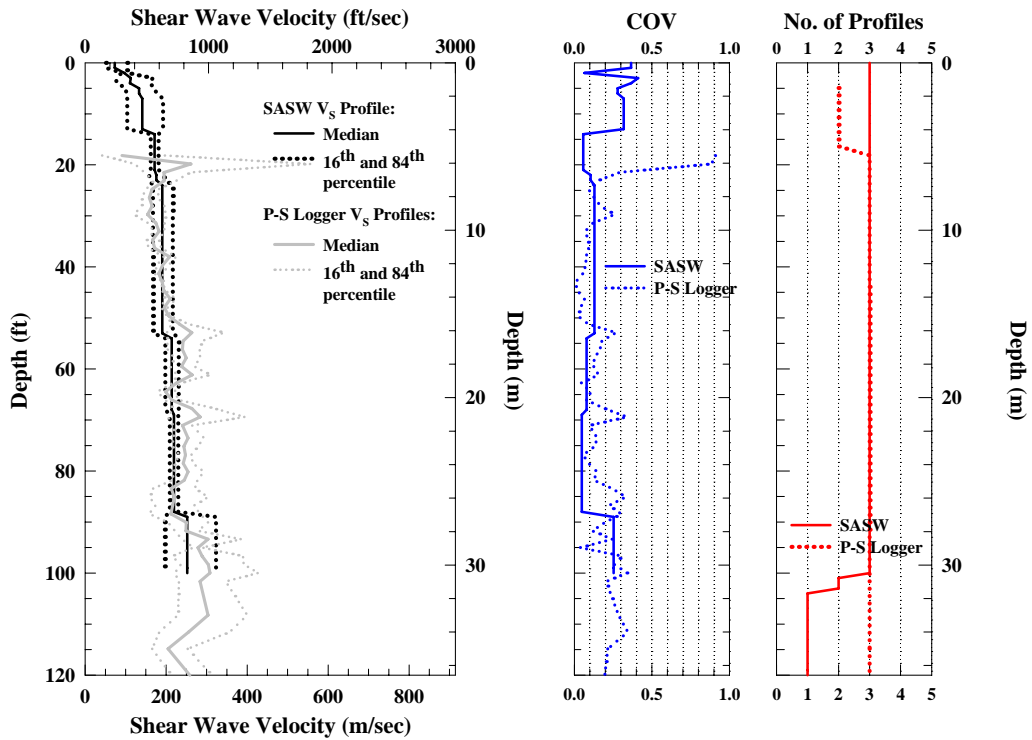


Figure 4.13 Comparison of the Median and 16th and 84th Percentile Boundaries of Available SASW and P-S Logging V_s Profiles from Three Common Sites in Imperial Valley, CA

4.4.3 Identical-site-and-depth comparisons (Green-Apples-to-Green-Apples Comparisons)

To perform more objective comparisons between different survey methods, only profiles from common sites and common depths (hence, common soil layers) are compared in this section.

First, the V_s profiles from 16 common sites of the SASW and downhole methods are again used. Instead of using the whole measured profiles, only the profiles at common depths are used. This approach means that the compared profiles are from the same depth ranges which have both SASW and downhole measurements. These results are plotted in Figure 4.14. As seen in the figure, the curves representing the number of

profiles from SASW and downhole tests are identical. This is why this type of comparison is called an identical-site-and-depth comparison or comparison of “green apples to green apples”. The median and COV values and profiles in Figure 4.14 are very similar to the ones in Figure 4.10. The reason is that the comparison in Figure 4.10 is an “identical” comparison in about the top 100 ft. The average COV values of the SASW and downhole V_s profiles are 0.22 and 0.21, respectively in the top 100 ft in Figure 4.14.

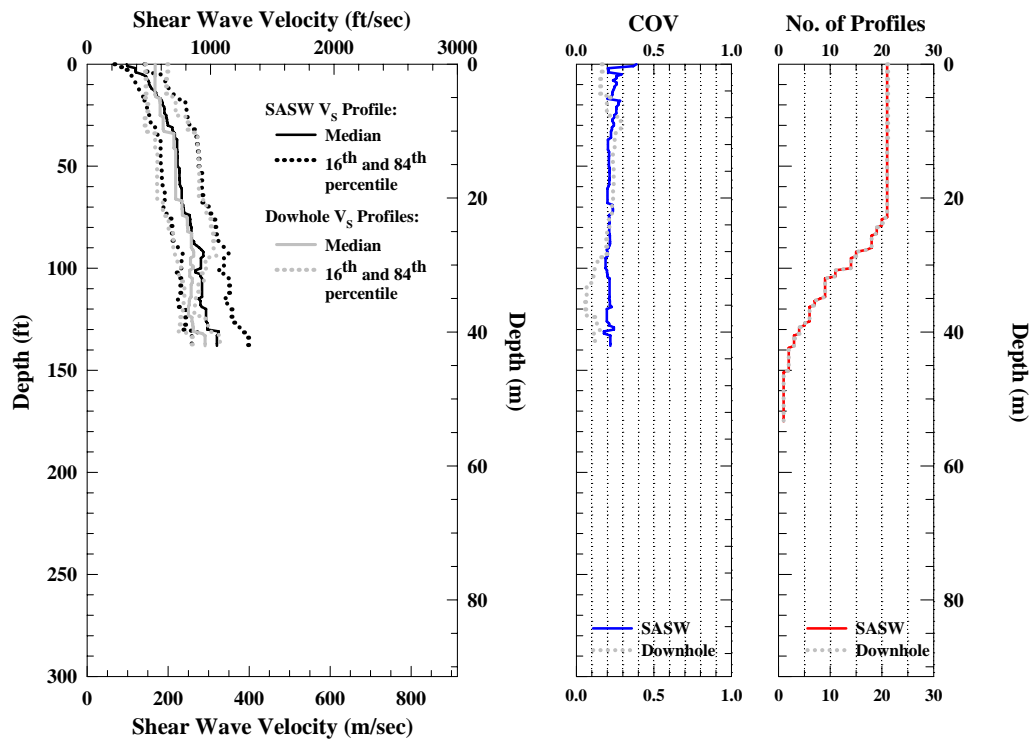


Figure 4.14 Comparison of the Median and 16th and 84th Percentile Boundaries of Available SASW and P-S Logging V_s Profiles at the Identical Depths from 21 Common Sites in Imperial Valley, CA

Second, the profile from the Parachute Test Site is removed to make the comparison even more objective. These results are presented in Figure 4.15. The median profiles become slightly slower compared to the one in Figure 4.14 in the top 94

ft (the common V_s depths of the Parachute Test Site) but still very similar to each other. However, the COV values are much lower, 0.15 in average, in the top 5 to 70 ft in Figure 4.15.

Lastly, by excluding the two sites (El Centro #13 Array and Bond's Corner) on the perimeter areas of Imperial Valley, the difference between the median and COV values and profiles is further reduced as shown in Figure 4.16. The main reason is believed to be that the remaining 18 sites have very similar properties and the vertical and lateral uniformities at these 18 sites do not show the decrease in resolving power of the SASW at these depths.

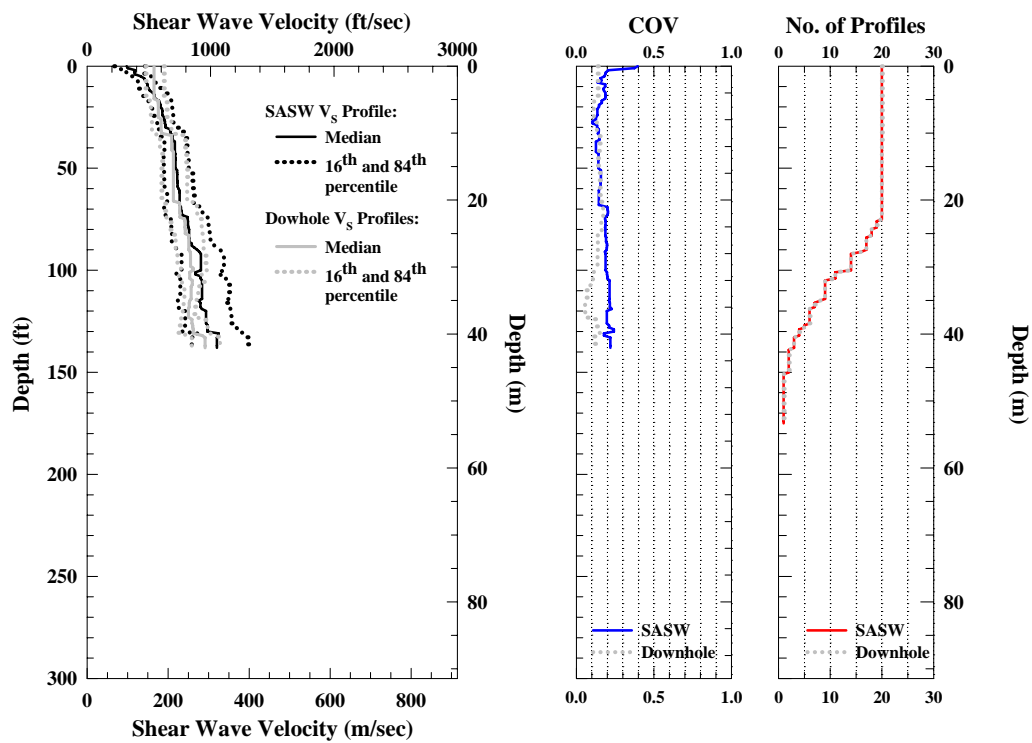


Figure 4.15 Comparison of the Median and 16th and 84th Percentile Boundaries of Available SASW and P-S Logging V_s Profiles at the Identical Depths from 20 Common Sites not in the Mountain Areas of Imperial Valley, CA

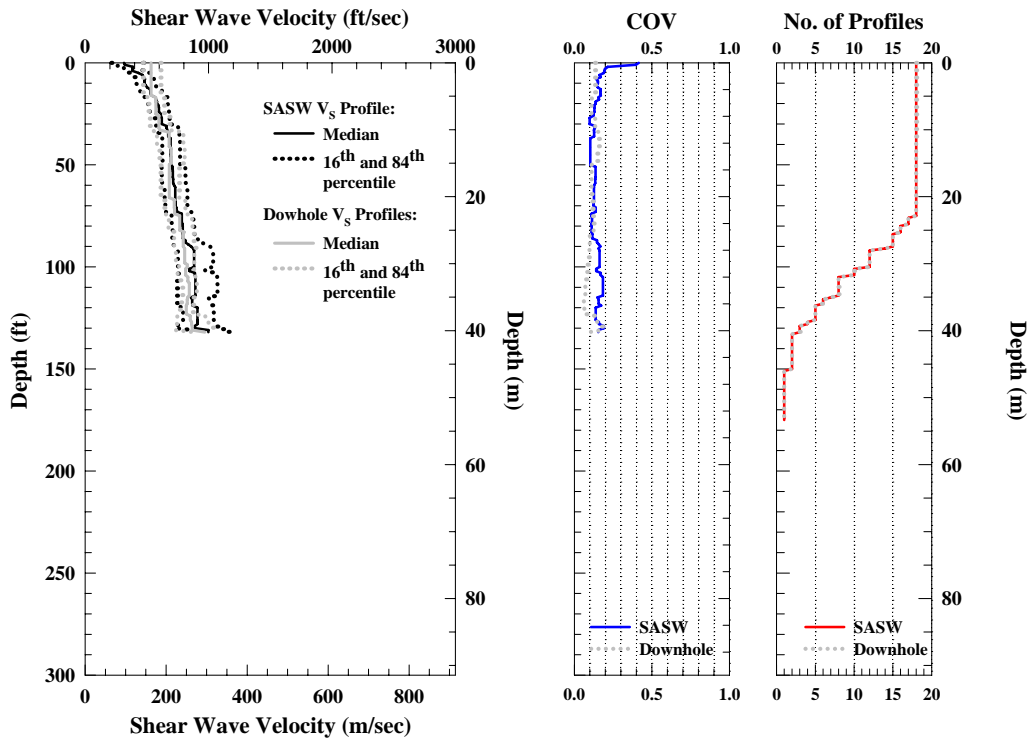


Figure 4.16 Comparison of the Median and 16th and 84th Percentile Boundaries of Available SASW and P-S Logging V_s Profiles at the Identical Depths from 18 Common Sites in Central Valley Area of Imperial Valley, CA

4.4.4 Comparisons of COV Values

As observed in Figures 4.6 to 4.16, the average COV values of the SASW measurements are from 0.15 (central valley sites only) to 0.26 (all 31 sites). The downhole measurements have the same trend but with a smaller COV range, which is from 0.10 to 0.17. A list of average COV value with the different comparison criteria used in Section 4.4.1 to 4.4.3 is tabulated in Table 4.5.

Table 4.5 Average COV Values with Different Comparison Criteria

Comparison Criteria		COV (Coefficient of Variation)					
		SASW	Range of Compared Depth (ft)	Downhole	Range of Compared Depth (ft)	P-S Logging	Range of Compared Depth (ft)
General Comparisons	All Available V_s Profiles	0.26 (31)*	258	0.15 (21)	248	0.19 (3)	289
	Excluding Mountain Sites	0.20 (28)	186	0.12 (20)	248	0.19 (3)	289
	Central Valley Sites Only	0.15 (23)	152	0.10 (18)	248	0.19 (3)	289
Common Site Comparisons	21 Common sites	0.22 (21)	150	0.15 (21)	248	0.19 (3)	289
	Excluding Mountain Sites	0.18 (20)	138	0.12 (20)	248	0.19 (3)	289
	Central Valley Sites Only	0.15 (18)	132	0.10 (18)	248	0.19 (3)	289
	Three P-S Logging Sites Only	0.14 (3)	100	-		0.19 (3)	289
Identical Comparisons	21 Common sites	0.22 (21)	138	0.17 (21)	138	-	
	Excluding Mountain Sites	0.18 (20)	138	0.12 (20)	138	-	
	Central Valley Sites Only	0.15 (18)	132	0.10 (18)	132	-	

*(): Number of Sites Involved

As the V_s profiles from the mountain areas and the perimeter areas of the valley are excluded, the COV values become smaller which indicates that the V_s profiles in the central valley area are very similar. That is, the soil deposit/formation is very uniform in the central valley area. In fact, the $V_{s,30}$ values of all these sites are about 650 fps. Based on the calculated (average) COV values in this chapter for the SASW measurements, it seems that a uniform geotechnical site may have an average COV value of no more than 0.15. The final conclusion is drawn in Chapter 9 after other geographic areas are also considered.

4.4.5 Comparisons of Site Classification

Three different site classes were determined for the test site in Imperial Valley based on three different seismic testing. They are classes “C”, “D” and “E” sites. The range of $V_{s,30}$ values are from about 560 to 1210 fps. A list of the test sites and the corresponding $V_{s,30}$ and site class from all three seismic techniques are presented in Table 4.6. As seen in the table, most sites (18 out 21 common sites) have the same site

class when comparing the classifications based the SASW and downhole profiles. There are slightly different $V_{S,30}$ values (average less than 10%, and a maximum of 18% with respect to the SASW $V_{S,30}$ values) for the SASW and downhole measurements. There are three sites (El Centro Array # 2, Parachute Test Site and Salton Sea Wildlife Refuge) that have different site classes according to the $V_{S,30}$ calculated from the SASW and downhole profiling measurements. Only one site, Wildlife Liquefaction Array, has different site classes between the SASW and P-S logging methods. However, the difference between their $V_{S,30}$ from different measurements are in the range from 5 to 17% based on the $V_{S,30}$ of SASW profiles. The site class difference at the same site is the result of $V_{S,30}$ at these sites being close to the boundaries between different site classes and, hence, small differences in $V_{S,30}$ changing the site classification. For example, the $V_{S,30}$ value of Site El Centro Array #2 from the downhole profile is 621 fps which is only 21 fps higher than the lower boundary (600 fps) of “D” sites. In contrast, the $V_{S,30}$ value of the SASW profile at the same site is 592 fps which is only 8 fps less than the lower boundary of “D” sites. Basically, there is not much difference between the two different measurements in terms of the $V_{S,30}$ values. The same scenario could happen to a site where has multiple profiles from the same survey technique. For instance, there are two $V_{S,30}$ values of the Parachute Test Site from downhole tests performed at different times. One of them is 1205 fps and the other is 1131 fps. Unfortunately, the upper boundary of “D” site (1200 fps) is right between these two numbers so this site has two different site classes determined by the same profiling technique.

To avoiding misleading the reader, it would be best to show the $V_{S,30}$ values as well when presenting the site classification.

Table 4.6 Comparisons of $V_{s,30}$ and Site Class Classification determined by Different Seismic Profiling Techniques

No.	Site Name	SASW		Dowhole		P-S Logging	
		$V_{s,30}$ (fps)	Site Class	$V_{s,30}$ (fps)	Site Class	$V_{s,30}$ (fps)	Site Class
1	El Centro Array # 1	779	D				
2	El Centro Array # 2	592	E*	621	D		
3	El Centro Array # 3 (Pine Union School)	568	E	538	E		
4	El Centro Array # 4	707	D	681	D		
5	El Centro Array # 5	638	D	673	D		
6	El Centro Array # 6	657	D	662	D		
7	El Centro Array # 7 (Imperial Valley College)	633	D	697	D	747	D
8	El Centro Array # 8	671	D	681	D		
9	El Centro Array # 9 (El Centro 1940)	670	D*	700	D		
10	El Centro Array # 10 (Regional Hospital)	672	D	669	D		
11	El Centro Array # 11 (McCabe School)	646	D	648	D		
12	El Centro Array # 12 (Meloland Cattle Co.)	646	D	674	D*		
13	El Centro Array # 13	887	D	825	D		
14	Bombay Beach	843	D				
15	Bond's Corner	777	D	731	D		
16	Brawley Airport	617	D	684	D		
17	Calexico Fire Station	650	D	759	D		
18	Calipatria Fire Station (New)	707	D*				
19	Calipatria Fire Station (Old)	675	D*	665	D*		
20	El Centro Differential Array	628	D	656 663	D D		
21	Holtville Post Office	693	D	661	D		
22	Imperial Landfill	588	E				
23	Meloland Road Overpass	650	D			730	D
24	Parachute Test Site	1144	D	1205 1131	C* D*		
25	Salton City	1064	D				
26	Salton Sea State Park	870	D				
27	Salton Sea Wild Life Refuge	627	D	552	E*		
28	Seeley Elementary School	656	D				
29	Superstition Mountain Base	1084	D				
30	Westmorland Fire Station	670	D*	641	D		
31	Wildlife Liquefaction Array	562	E			657	D

*Based on extrapolated data

4.5 CALCULATION OF REPRESENTATIVE FIELD SHEAR MODULI VALUES

Based on the SASW V_s profiles from the central valley area, representative field shear moduli at small strain (G_{max}) with respect to depth can be calculated over the measurement depths with the assumed unit weight (120 pcf) used to perform forward modeling in WinSASW software. The field shear modulus can be calculated from:

$$G_{max} = V_s^2 \cdot \rho \quad (4.1)$$

where ρ is soil density.

It is important to know field G_{max} profiles of the central valley because the most population is growing and construction is increasing. The 23 SASW V_S profiles, therefore, were used to calculate a median, and 16th and 84th percentile boundaries for the field G_{max} profile. These results are shown in Figure 4.17.

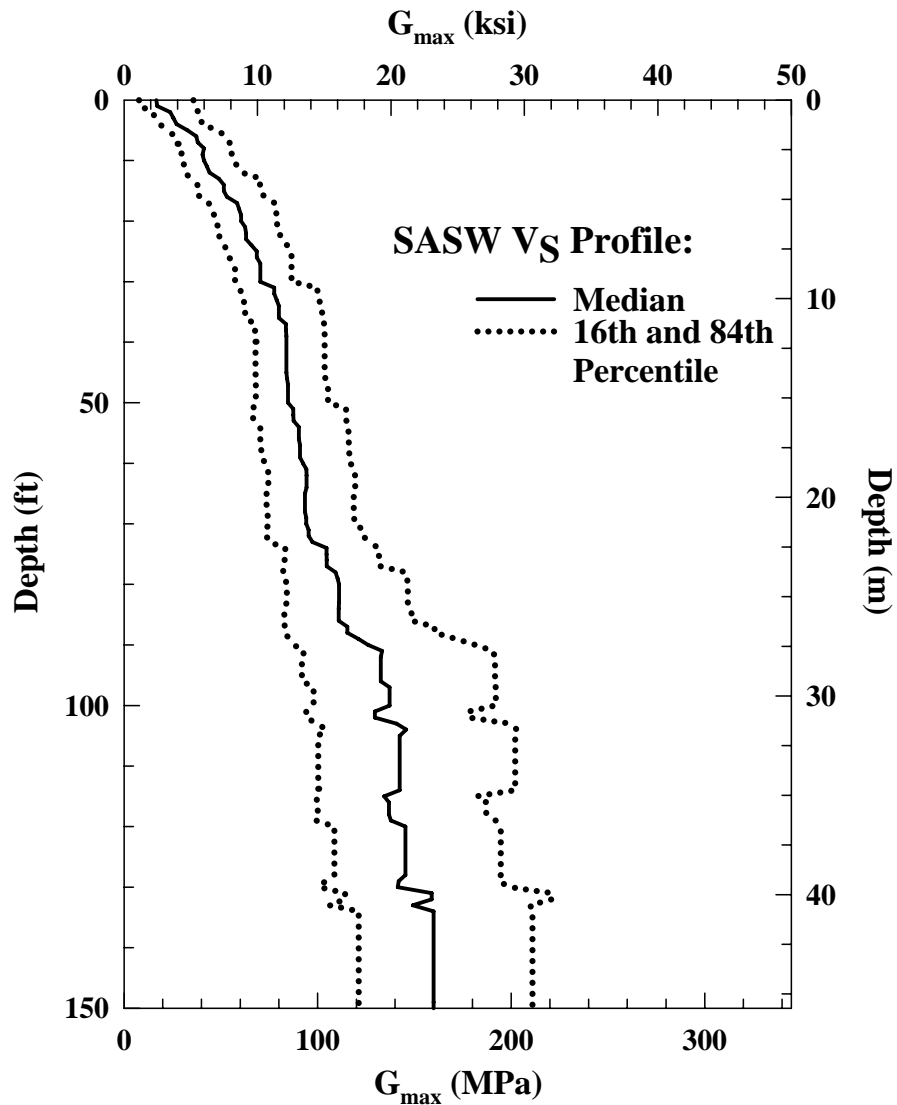


Figure 4.17 Field G_{max} Profiles Calculated from Representative V_S Profile Determined from 23 SASW Test Sites in the Central Valley Area

4.6 SUMMARY

In this chapter, the test sites in Imperial Valley are presented where 31 SASW, 23 downhole and three P-S suspension logging test were performed. Since SASW testing was performed in this area by the University of Texas team and since the most sites were tested by the SASW method, the review concentrates on the SASW measurements. The V_S profiles obtained from the SASW, downhole and suspension logging measurements are presented and they are compared in several different aspects. The results show the measurements from the SASW method are consistent with the downhole and P-S logging methods and vice versa. The COV and site classification of different measurements were investigated as well.

Based on the different comparison (“apples-to-oranges”, “green-apples-to-red-apples” and “green-apples-to-green-apples” comparisons), the “green-apples-to-green-apples” comparisons (identical-site-and-depth comparisons) have the best consistency between the SASW and downhole measurements, especially when the V_S profiles obtained in mountain area and at the perimeter area of the valley were excluded. As to the SASW COV profiles, smaller average COV values are observed in the “green-apples-to-green-apples” comparisons (identical-site-and-depth comparisons). The smallest average value is 0.15 based on the SASW profiles determined at the central valley area. There are larger variations at the shallow COV profile of SASW profiles compared to the downhole measurements. The high resolution of the SASW method at shallow depths should be the reason of the phenomenon. In average, according to the V_S profiles studied in this chapter, the suspension logging has larger COV values and the downhole testing has lower COV values.

Although, there are only three P-S logging V_S profiles, the median V_S of the three P-S logging profiles agrees to the SASW measurements very well as seen in Figure 4.14 .

The reason can be that the vertical and lateral variations at these three sites are very minor and these three sites are located in a smaller area compared to the central valley area.

One thing need to mention here is that in the top 15 ft of the median profile, the downhole measurements always higher than SASW profiles. The reason may be as stated in Section 3.3.1. The reason of lack of data on the top 5 to 20 ft of suspension logging measurements was also explained in Section 3.3.2.

Chapter 5 SASW Testing in Taiwan

5.1 BACKGROUND OF TEST SITE

Taiwan is an island in the western Pacific Ocean near the eastern coast of Asia. It is separated from the southeastern coast of mainland China by the Taiwan Strait. In terms of Geological location, Taiwan is on the boundary between the Philippine Sea Plate and the Eurasian Plate (or Asiatic Plate in Figure 5.1) where the tectonic movement is extremely active. Because of these special geologic conditions, Taiwan was formed by the mountain building activity resulting from the pushing between the Plates. The Plate movement also developed the Jade Mountain, the highest mountain in the eastern Asia, and numerous earthquakes. Unfortunately, the population density is very high in Taiwan and the current tallest building (Taipei 101) is in this earthquake prone region.

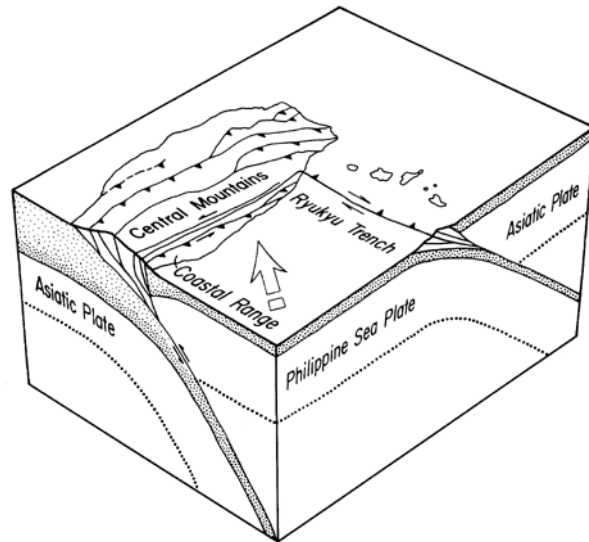


Figure 5.1 Schematic diagram showing present plate tectonic configuration of Taiwan (from Ernst et al., 1985)

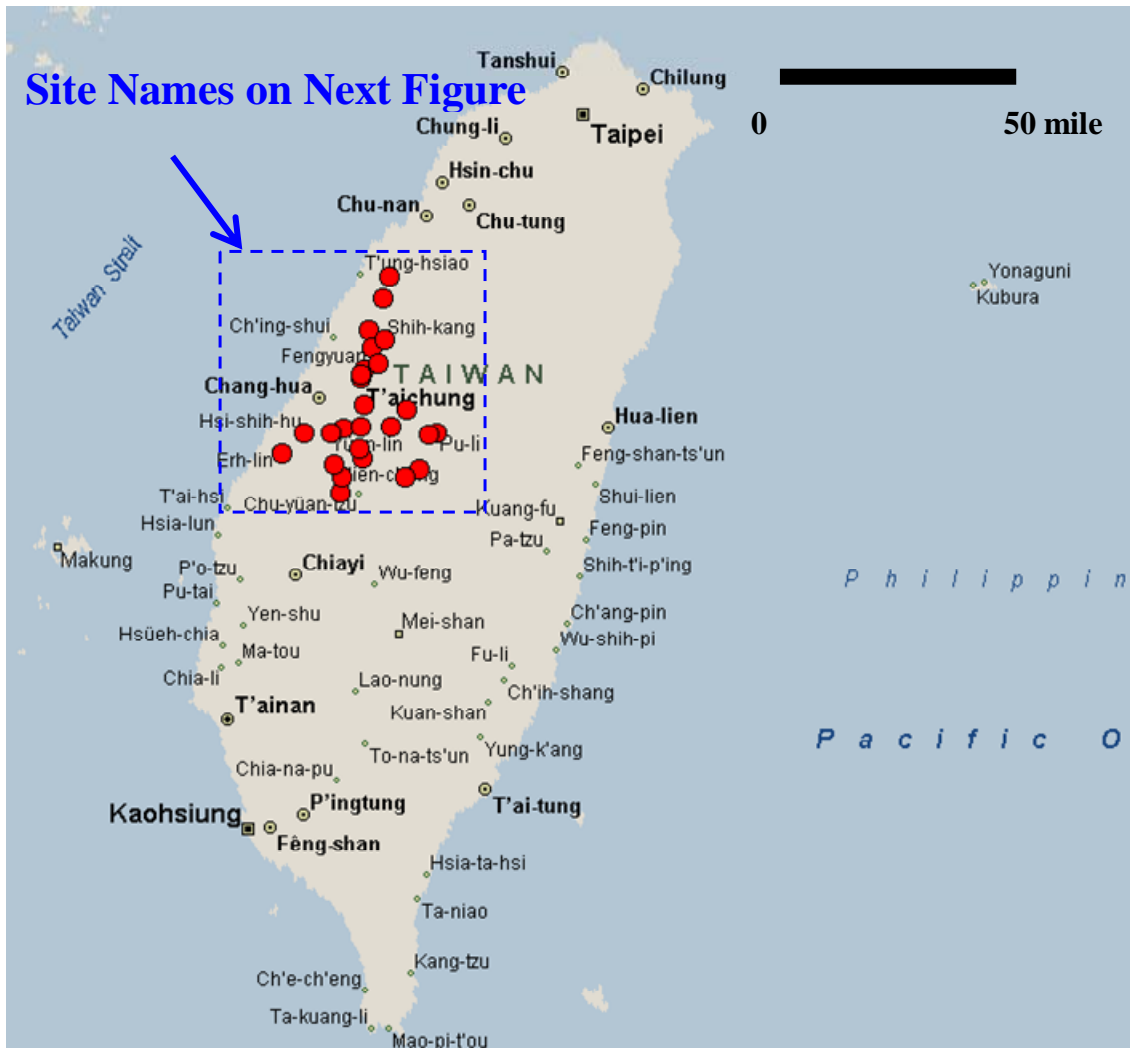
On September 21 1999, the Chi-Chi Earthquake (measured 7.3 on the Richter scale) caused severe damage in Taiwan, especially in the west-central region. In total,

2415 lives were lost, 11,305 people were injured, 51,711 houses were completely destroyed and 53,768 houses were partially destroyed. To avoid a similar tragedy from happening again, it is necessary to re-evaluate the building codes and site responses for earthquake designs in this region.

5.2 REVIEW OF SASW TESTING PERFORMED IN TAIWAN

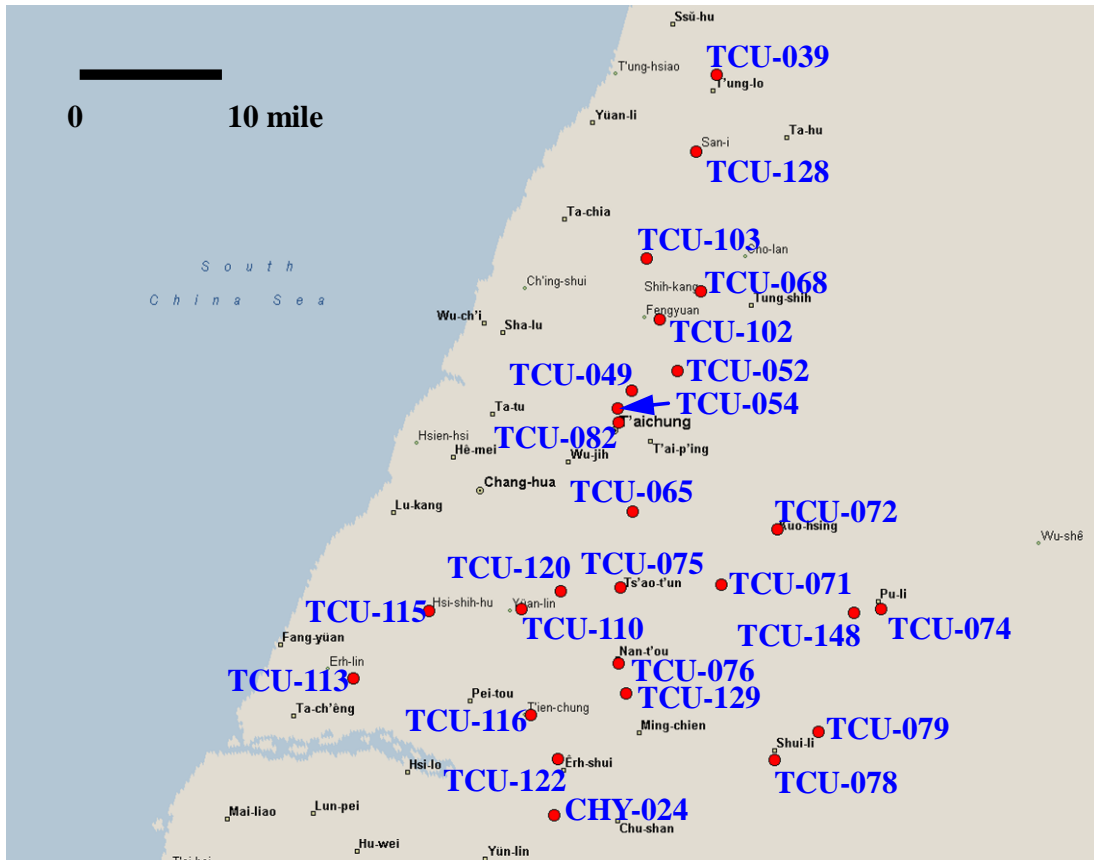
SASW testing was carried out in Taiwan during January 2003. This work was sponsored by the Pacific Earthquake Engineering Research Center (PEER) Lifelines Program under project: SMR Site Characterization in Taiwan-SASW – 2A02C. A total of 26 test sites were studied. The locations of 26 SASW tests are shown on the maps in Figures 5.2 and 5.3. As seen in Figure 5.2, most of the test sites are located in west-central Taiwan. This area is about 50 mi. by 40 mi. in plan. A more detailed map of the test site is shown in Figure 5.3.

The goal of the seismic investigations in Taiwan was to determine shear wave velocity profiles to a depth of about 30 m (100 ft) at each test site. The 26 sites were selected because of their proximity to strong-motion recording (SMR) stations that recorded ground motions during the 1999 Chi-Chi Earthquake. Dr. Kenneth H. Stokoe, II, Brent L. Rosenblad and Farn-Yuh Menq from UT-Austin performed the SASW tests from January 16 through January 23, 2003. In addition to the personnel from University of Texas at Austin, there were other researchers from two universities in Taiwan helping conduct the SASW tests. They were Dr. Sheng-huoo Ni from National Cheng Kung University (NCKU) and Dr. Ding-Shing Cheng from Chung Cheng Institute of Technology (CCIT). Many of their graduate students were also involved in this project.



● SMR Sites where SASW Tests were Conducted by the University of Texas at Austin

Figure 5.2 Approximate Locations of SASW Testing Sites Superimposed on a Map of Taiwan



● SMR Sites where SASW Tests were Conducted by the University of Texas at Austin

Figure 5.3 Approximate Locations of SASW Testing Sites Superimposed on a Map of Taiwan (Continued)

Most of the field testing was performed in or near elementary schools and close to classrooms. To avoid the noise from the impact source disturbing the students, an efficient arrangement of source and receivers was adopted to minimize testing time around the schools. In this arrangement, three geophones were used to perform SASW testing. Figure 2.19 (Chapter 2) shows the arrangement need with the shorter test spacings ($2X < \text{less than } 25 \text{ ft}$). Due to limited space at the schools and attempting to minimize disturbance from noise, only forward-direction testing was performed for

longer receiver spacings (distance between first and second receivers larger than 25 ft). This forward-direction testing arrangement is illustrated in Figure 5.4 which is a kind of modified common-source (CS) arrangement.

The major advantage of adopting these configurations was limiting the time the large source was required near the schools because two sets of data were obtained from each source location.

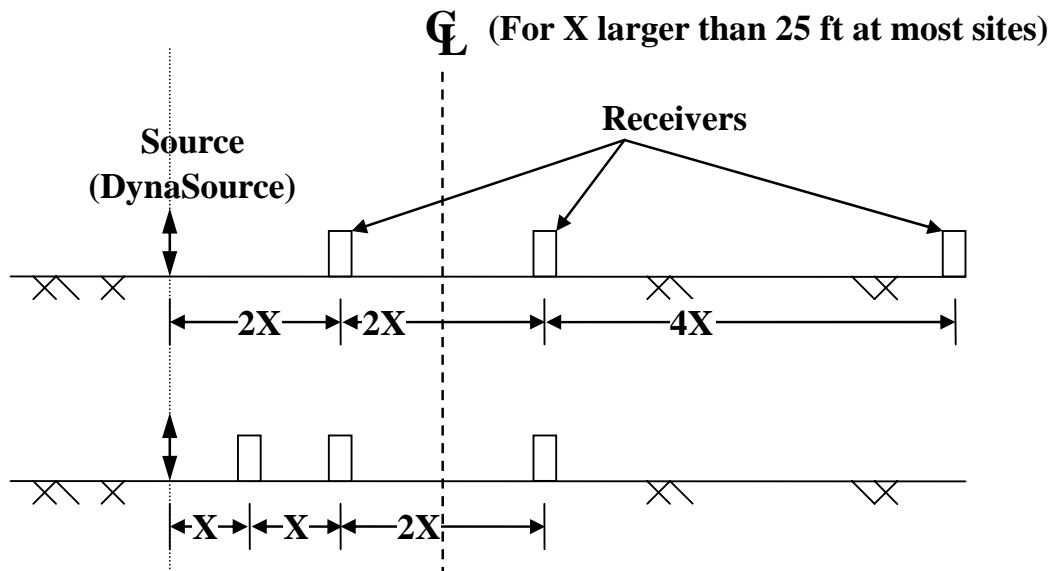


Figure 5.4 Modified Source-Receiver Geometry Used with the Large DynaSource and Larger Receiver Spacings in Taiwan

Generally, receiver spacings of 3, 6, 12, 25, 50, 75, 100 ft were used. However, maximum distances between the second and third receivers varied, depending on the available space at the test site. The maximum spacing was 125 ft (38 m) at Si-Kon Elementary School (TGU-068) and Cheng - Jung Elementary School (TCU-128). The shortest distance between the first receiver and the second receiver was 3 ft at most sites. This number and progression of receiver spacings resulted in extensive overlapping of

individual dispersion curves used to develop the composite field curve which enhanced the test reliability

Two types of sources were used in these SASW tests. At the shorter receiver spacings, a sledge hammer was used to generate Rayleigh waves over the interested frequency ranges of interest. At larger receiver spacings, a DynaSource (Figure 2.9) was employed which is often used in surface refraction and surface reflection tests.

A four-channel analyzer, Agilent 35670A Dynamic Signal Analyzer, was used to record data and to perform the FFT of the SASW time-domain measurements to obtain the phase plots as described in Chapter 2. Based on these phase plots, the test operator could subjectively evaluate the data from different receiver pairs (R1-R2 and R2-R3) to determine if they are consistent or not.

5.3 TESTING RESULTS

Although there are no available downhole measurements at some of the sites where the SASW tests were conducted, ten suspension logging V_s profiles performed by NCREE (National Center for Research on Earthquake Engineering, Taiwan) are provided to be compared.

5.3.1 SASW Testing

Information about the 26 SASW test sites is listed in Table 5.1. As seen in the table, the deepest V_s profile is 127 ft which was evaluated at Kuo-Sing Elementary School (TCU-072) and the shallowest profile is 45 ft at the Suan - Don Elementary School (TCU-071). One thing that should be mentioned here is that most of these site classes were calculated with extrapolated V_s profiles because the profiling depths at most sites were close to but not deeper than 100 ft. The reason could be: (1) the energy generated by the DynaSource was not large enough to give good quality data from the

largest spacing (100 ft) in the low frequency ranges; (2) there are many different types of pavement materials and objects on the surface, for example sandy or PU (polyurethane) runway, concrete pavement in school yards, that can absorb, attenuate or redirect the wave energy generated by the DynaSource; (3) the limitations of test space, that is, largest test spacing was not able to be larger than 100 ft. Therefore, most site classes from the SASW measurements were determined by extrapolation.

Table 5.1 Information on the 26 SASW Test Sites in Taiwan

No.	Site Name	Station No.	Profile Depth (ft)	$V_{s,30}$ (fps)	Site Class	Test Date	Test Performer	Other Test
								P-S Logging
1	Lin - Chong Elementary School	CHY-024	82	1283	C*	21-Jan-03	UTA	
2	Ton - Lo Elementary School	TCU-039	93	1791	C*	17-Jan-03	UTA	
3	Cheou - Shio Elementary School	TCU-049	74	1477	C*	16-Jan-03	UTA	1
4	Kung - Chung Elementary School	TCU-052	86	1280	C*	16-Jan-03	UTA	
5	Sin - San Elementary School	TCU-054	87	1653	C*	18-Jan-03	UTA	1
6	Wu - Fon Elementary School	TCU-065	116	797	D	18-Jan-03	UTA	1
7	Si - Kon Elementary School	TCU-068	46	1415	C*	18-Jan-03 23-Jan-03	UTA	
8	Suan - Don Elementary School	TCU-071	45	1913	C*	20-Jan-03	UTA	
9	Kuo- Sing Elementary School	TCU-072	127	1361	C	20-Jan-03	UTA	1
10	Nan - Kon Elementary School	TCU-074	95.5	1364	C*	20-Jan-03	UTA	
11	Chiou - Tun Elementary School	TCU-075	46	1707	C*	19-Jan-03	UTA	1
12	Nan - To Elementary School	TCU-076	87	1645	C*	19-Jan-03	UTA	1
13	Shai - Li Elementary School	TCU-078	68	1530	C*	21-Jan-03	UTA	
14	Tor - Se Elementary School	TCU-079	89	1378	C*	21-Jan-03	UTA	
15	Tai - Chung Weather Station	TCU-082	78	1297	C*	16-Jan-03	UTA	1
16	Fon - Ton High School	TCU-102	114	1756	C	18-Jan-03	UTA	1
17	Nai - Pu Elementary School	TCU-103	85	2013	C*	17-Jan-03	UTA	
18	Yuan - Lin Elementary School	TCU-110	70	692	D*	19-Jan-03	UTA	1
19	Sin - Hua Elementary School	TCU-113	69	773	D*	22-Jan-03	UTA	
20	Si - Hu Elementary School	TCU-115	87	735	D*	22-Jan-03	UTA	
21	Ten - Chong High School	TCU-116	92	1232	C*	22-Jan-03	UTA	
22	Ton - Ang Elementary School	TCU-120	65	1295	C*	19-Jan-03	UTA	
23	A - Sua Elementary School	TCU-122	88	1554	C*	22-Jan-03	UTA	
24	Cheng - Jung Elementary School	TCU-128	67	1714	C*	17-Jan-03	UTA	
25	Sin - Jai Elementary School	TCU-129	89	2146	C*	21-Jan-03	UTA	
26	Chi - Nan University	TCU-148	95	1361	C*	20-Jan-03 21-Jan-03	UTA	1

*Based on extrapolated data

In Figure 5.5, the 26 V_S profiles are shown with their median values and 16th and 84th percentile boundaries. Obviously, there are two groups of V_S profiles with a distinct gap between them. If Figure 5.5 is re-plotted based on the different site classes (Figure 5.6 (a) and 5.6(b)), it can be seen that the slower V_S group includes all four “D” sites from the SASW measurements and the remaining 22 “C” sites are composed of the

higher V_S values. Further discussing with the V_S profiles from the suspension logging measurements is presented later in this chapter.

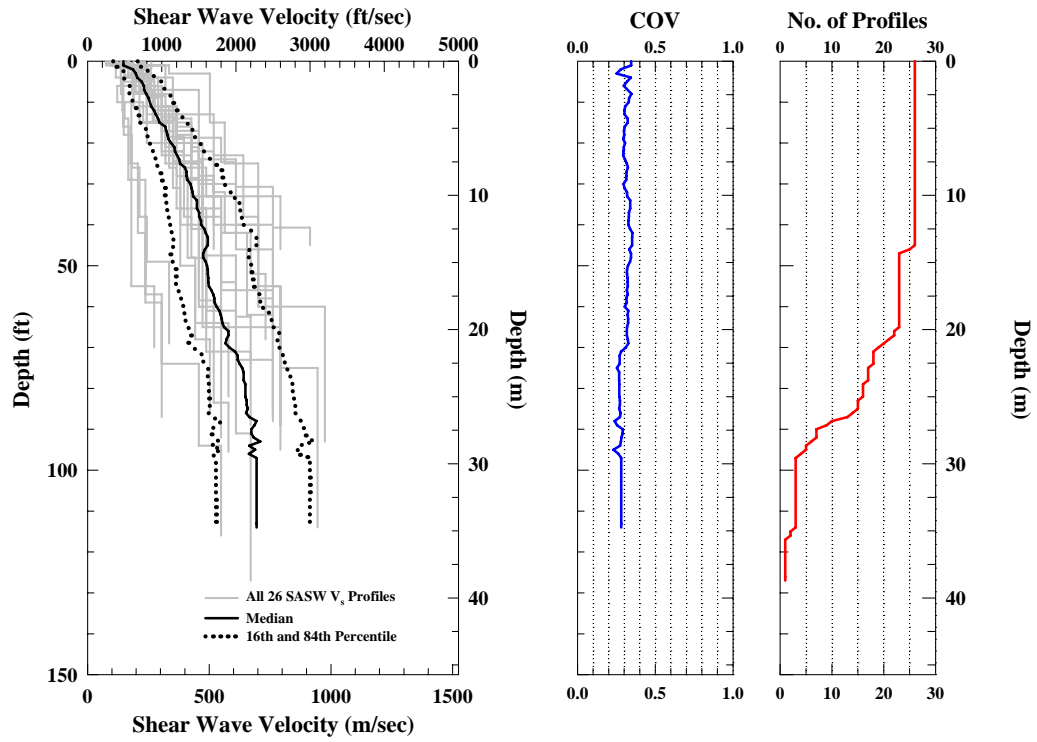


Figure 5.5 Individual Profiles and Statistical Information of the 26 SASW V_S Profiles from Taiwan Test Sites

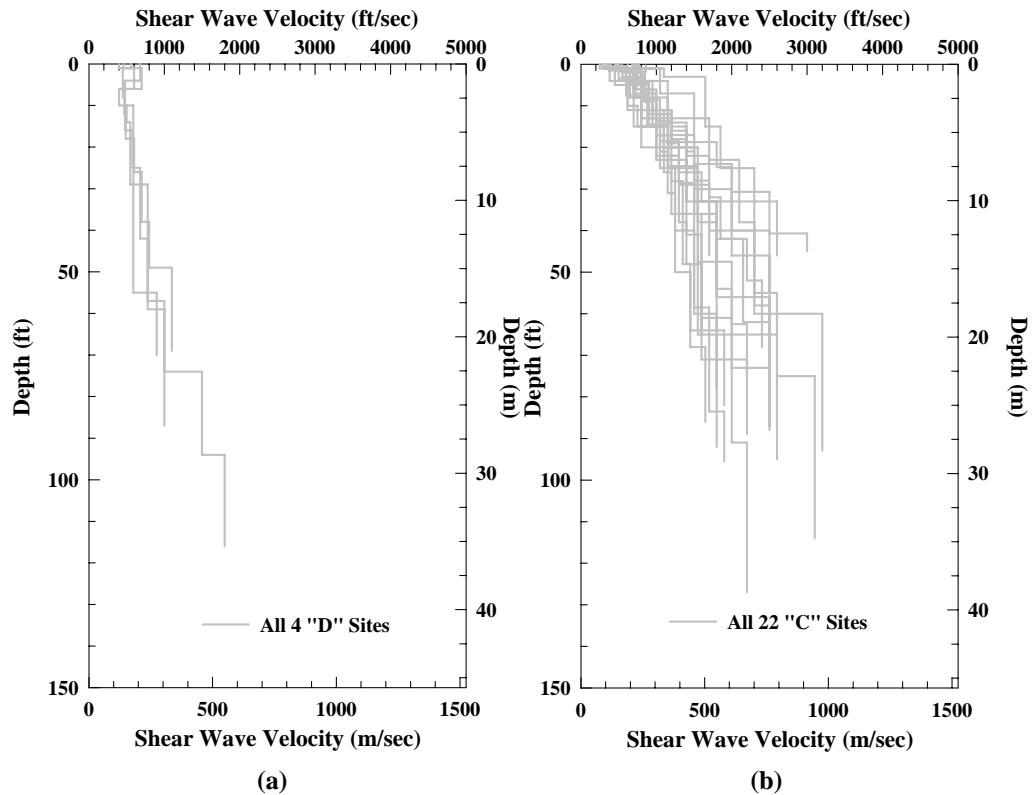


Figure 5.6 Illustration of : (a) Low-Velocity Group: Four “D” Sites, and (b) Higher-Velocity Group: 22 “C” Sites Determined by SASW Tests in Taiwan

Also, the site classification shows that there are four “D” sites and 22 “C” sites. Interestingly, the $V_{S,30}$ of these four “D” sites are all less than 800 fps which is in the lower one-third portion of the shear wave velocity range of “D” sites. These low V_S values mean the engineering properties of the sites are much different than the “C” sites which were also classified by the SASW method. In other words, the four “D” sites are distributed in the alluvium plain area but the “C” sites are in the hill or mountain areas. The difference between these two class sites can also be observed in Figure 5.7.

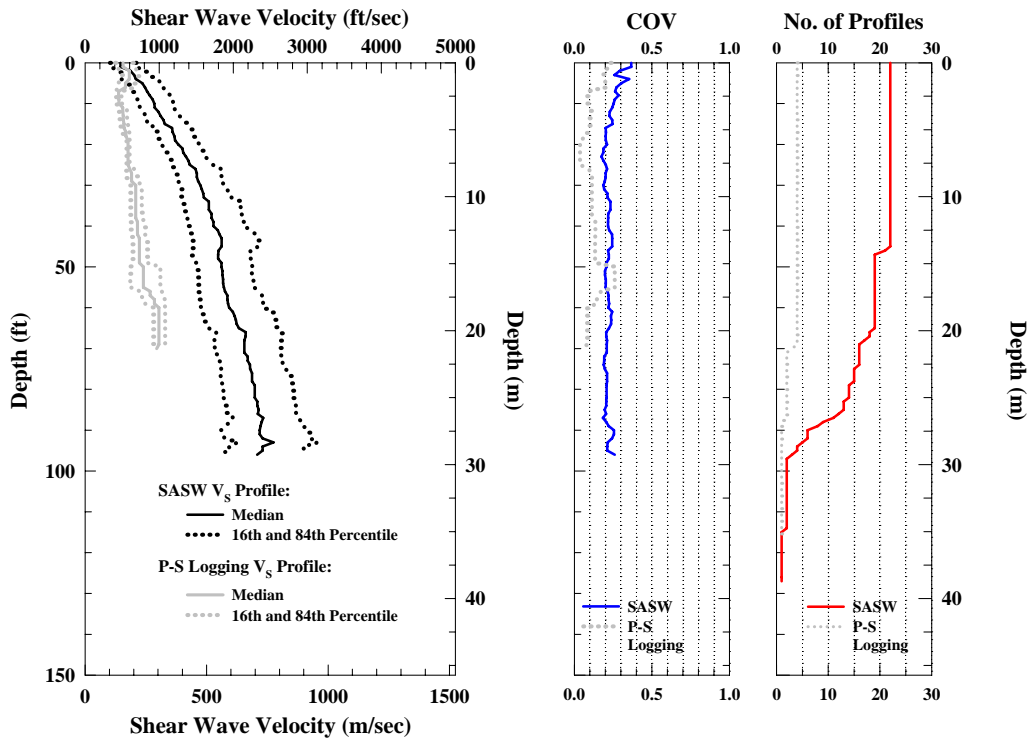


Figure 5.7 Comparisons of Statistical Information of “C” and “D” Sites Determined by SASW Tests in Taiwan

5.3.2 Suspension Logging Tests

In addition to the 26 SASW profiles, NCREE performed ten suspension logging measurements among the 26 SASW test locations near the end of 2002. Table 5.2 shows the general information of these ten P-S logging sites. In the table, it shows the deepest profile is 320 ft measured at the Wu - Fon Elementary School (TCU-065) and, in contrast, the shallowest one, 100 ft deep, is obtained at the Yuan - Lin Elementary School (TCU-110).

Table 5.2 Information on the Ten Suspension Logging Sites in Taiwan

No.	Site Name	Station No.	Profile Depth (ft)	$V_{s,30}$ (fps)	Site Class	Test Date	Test Performer
1	Cheou - Shio Elementary School	TCU-049	108	1615	C	12-Sep-02	NCREE
2	Sin - San Elementary School	TCU-054	108	1506	C	12-Sep-02	NCREE
3	Wu - Fon Elementary School	TCU-065	320	998	D	4-Nov-02	NCREE
4	Kuo- Sing Elementary School	TCU-072	254	1742	C	25-Oct-02	NCREE
5	Chiou - Tun Elementary School	TCU-075	105	1763	C	14-Sep-02	NCREE
6	Nan - To Elementary School	TCU-076	103	1935	C	5-Nov-02	NCREE
7	Tai - Chung Weather Station	TCU-082	107	1568	C	5-Nov-02	NCREE
8	Fon - Ton High School	TCU-102	105	2442	C	11-Sep-02	NCREE
9	Yuan - Lin Elementary School	TCU-110	100	669	D	13-Sep-02	NCREE
10	Chi - Nan University	TCU-148	107	1818	C	4-Nov-02	NCREE

The V_s profiles from the ten suspension logging sites are shown in Figure 5.8. As observed in the SASW V_s profiles, the P-S logging measurements seem to have two velocity groups. However, the two groups are not as obvious as the SASW profiles in Figure 5.5. If Figure 5.8 is re-plotted based on the site classes, the high velocity group is formed by eight suspension logging V_s profiles from the “C” sites and the low velocity group is composed of the two suspension logging V_s profiles from the “D” sites as shown in Figure 5.9.

5.4 STATISTICAL ANALYSES AND COMPARISONS

In general, the trends shown in the SASW and suspension logging V_s profiles are very similar. Both of the profiling techniques have higher and lower velocity groups. Moreover, each group is formed by either “C” or “D” sites only. In the following sections, the V_s profiles acquired by these two methods are compared in different terms.

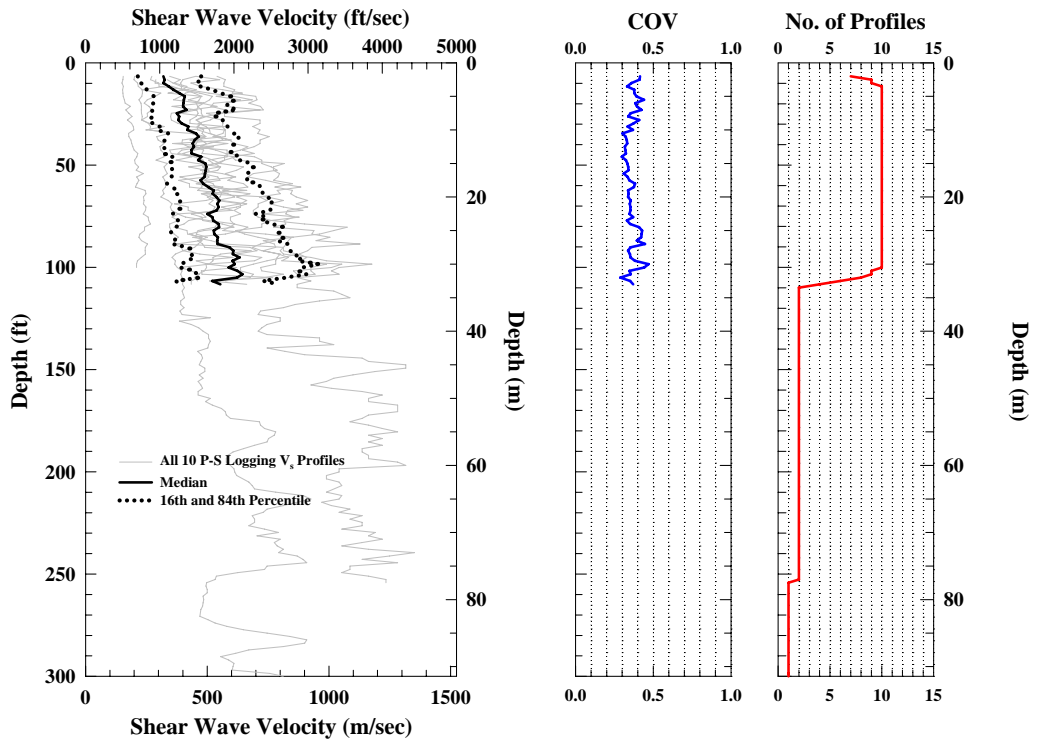


Figure 5.8 Individual Profiles and Statistical Information of the Ten Suspension Logging V_s Profiles from the Taiwan Test Sites

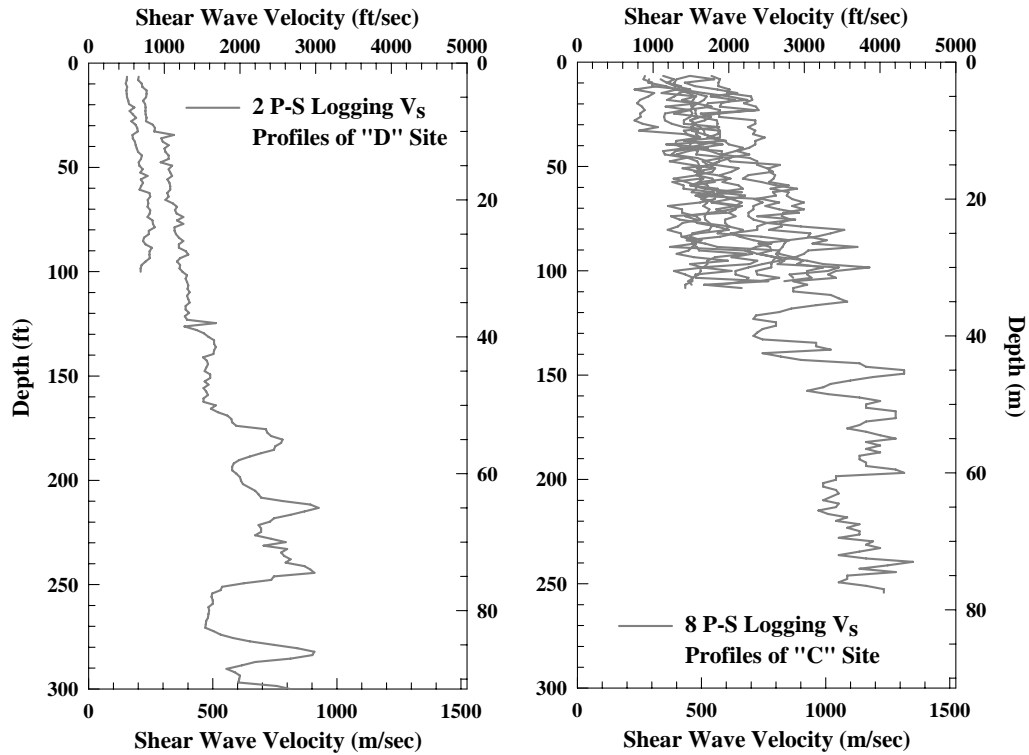


Figure 5.9 Illustration of : (a) Low-Velocity Group: Two “D” Sites, and (b) Higher-Velocity Group: Eight “C” Sites Determined by P-S Logging Tests in Taiwan

5.4.1 General Comparisons (Apples-to-Oranges Comparisons)

First, all 26 SASW and ten P-S logging V_s profiles are compared in terms of the median and 16th and 84th percentile boundaries in Figure 5.9. In the top 25 ft the suspension logging measurements are higher than the SASW profiles. This also observed in Figure 5.8 from the individual P-S logging profiles. These profiles always start at around 1000 fps at the depth of 6 to 10 ft. Several of them even start at over 1500 fps. The reason for the no-data zone in the top 6 to 10 ft and the reason the V_s profiles acquired by P-S logging method are always higher than the SASW method near the surface may be a casing-related issue; that is, the casing and grout are affecting the P-

and S-waves in suspension logging in this soft material. In contrast, at the depths from 25 to 70 ft the median values of both measurements agree very well. Below 70 ft, however, the two measurements differ again. The median V_S value of the P-S logging profiles is lower than the SASW measurements in the 70- to 110-ft depth range. As observed, the COV values of the P-S logging data are larger than the SASW data at this depth range as well. To investigate if the difference is caused by the two “D” sites in the P-S logging profiles, the “D” sites were removed in the next comparison. In addition, four of the 26 SASW test sites were also removed. Therefore, to make the comparison more objective, only “C” sites are used.

The comparison without the “D” sites is shown in Figure 5.10. Some differences in the top 25 ft and at the depths below 70 ft are still observed. These differences mean that the “D” sites in the suspension logging measurements are not the only reason for this inconsistency. Therefore, further comparisons are made the following sections.

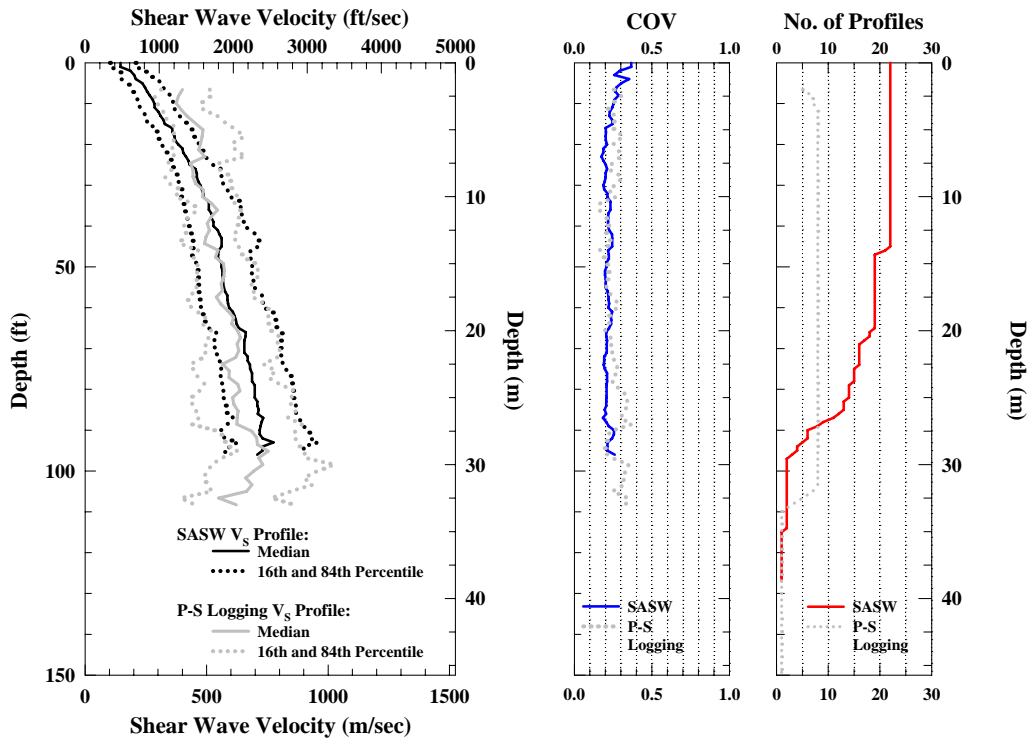


Figure 5.10 Comparison of the Median and 16th and 84th Percentile Boundaries of the 22 SASW and 8 Suspension Logging V_s Profiles from “C” Sites Measured in Taiwan

5.4.2 Common Site Comparisons (Green-Apples-to Red-Apples Comparisons)

To reduce the differences in the comparisons due to mixing sites where only the SASW profiles are available, only the ten common sites used in the comparison where both the SASW and P-S logging measurements are made. The comparison of the ten common sites is presented in Figure 5.11. Again, the difference between the two measurements below 70 ft is still noticeable. Next, the two “D” sites among the ten common sites are removed to make another comparison (Figure 5.12). As seen in the figure, these “D” sites do not have much contribution to the inconsistency as the results shows in Figure 5.10. The reason causing the difference is discussed below

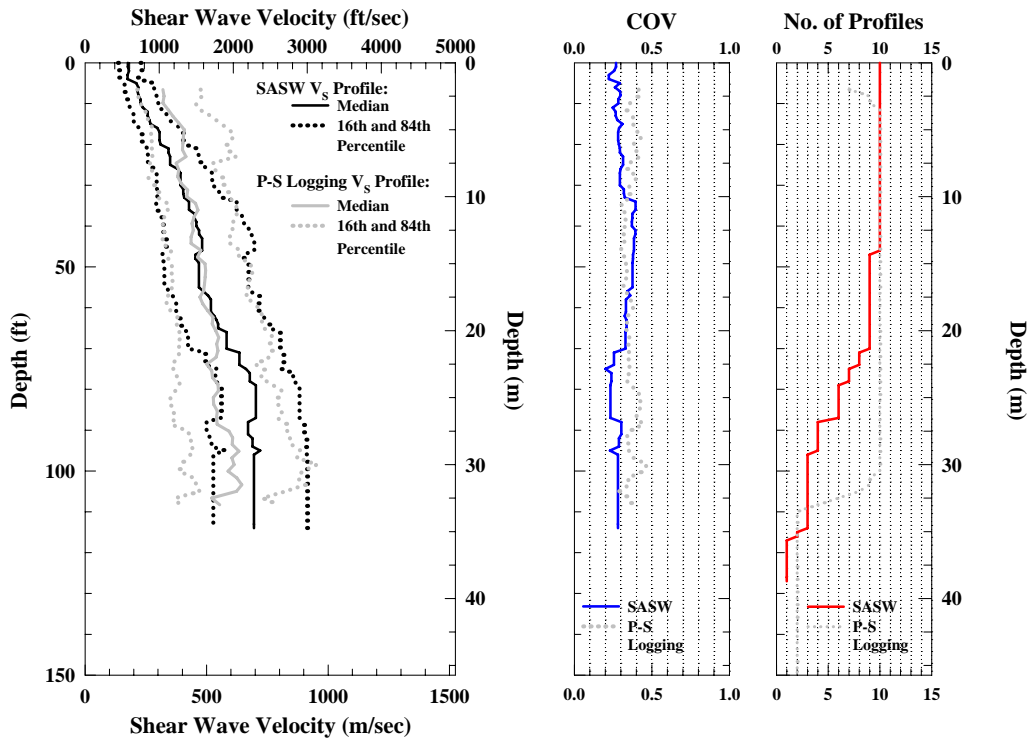


Figure 5.11 Comparison of the Median and 16th and 84th Percentile Boundaries of the SASW and Suspension Logging V_s Profiles at Ten Common Sites in Taiwan

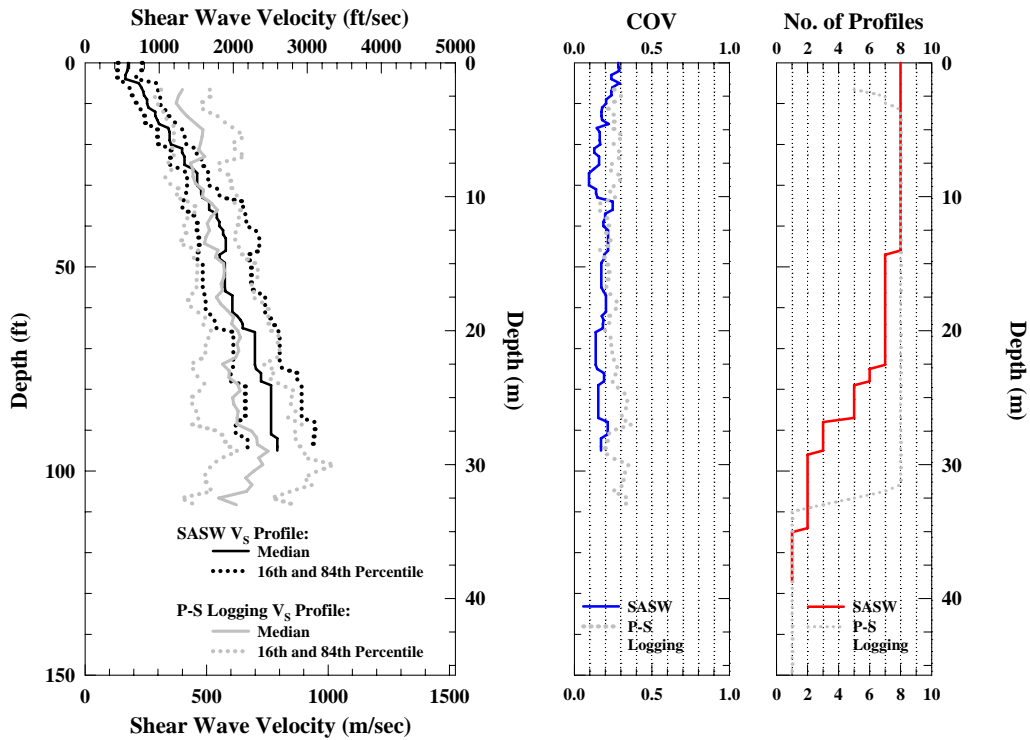


Figure 5.12 Comparison of the Median and 16th and 84th Percentile Boundaries of the SASW and Suspension Logging V_s Profiles at Eight Common “C” Sites in Taiwan

5.4.3 Identical-Site-and-Depth Comparisons (Green-Apples-to-Green-Apples Comparisons)

Based on the global and common comparisons above, the only possibility of the inconsistency left is the profile depth differences at each common location. To do this comparison, both SASW and P-S logging profiles in the same boreholes and over the same profiling depths are compared. Twenty profiles from ten common sites are involved in this comparison with identical depths from each profile at each common site. These results are presented in Figure 5.13. There is some improvement compared to Figure 5.11 but it is not over the complete profile. Therefore, the different site classes are taken into account by removing the two “D” sites from the ten common sites to make

comparison. This comparison is shown in Figure 5.14. However, the inconsistency between the medians from the two different measurements still does not disappear as had occurred in the downhole and SASW comparisons in Section 5.4.2 for the eight sites.

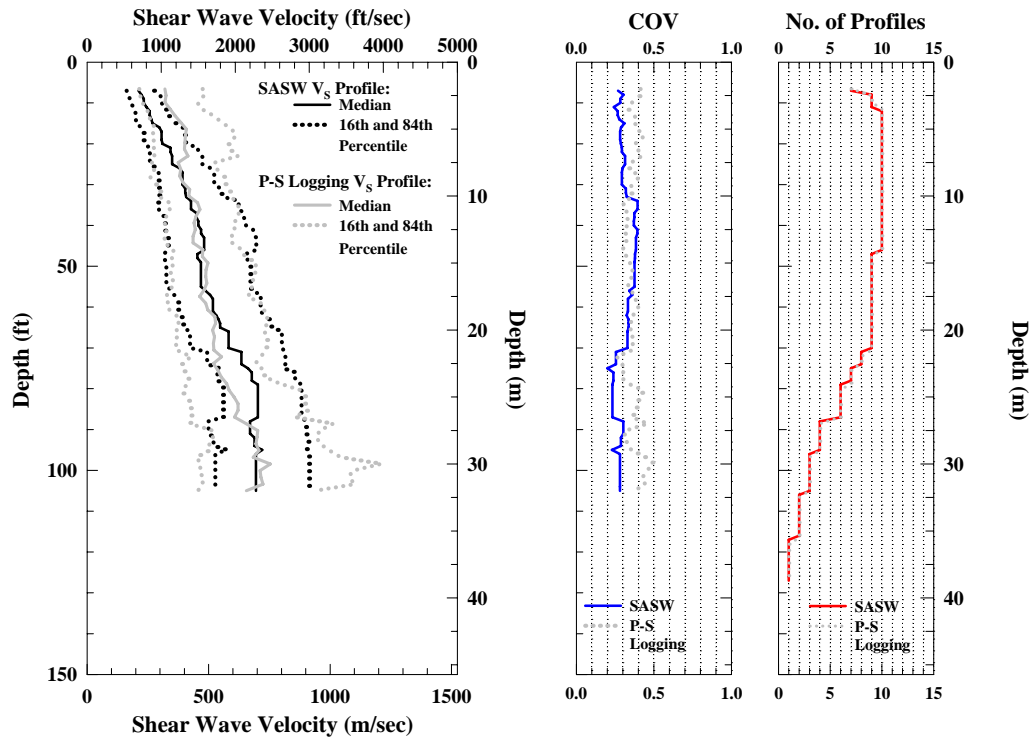


Figure 5.13 Comparison of the Median and 16th and 84th Percentile Boundaries of the Available SASW and P-S Logging V_s Profiles over Identical Depths from Ten Common Sites in Taiwan

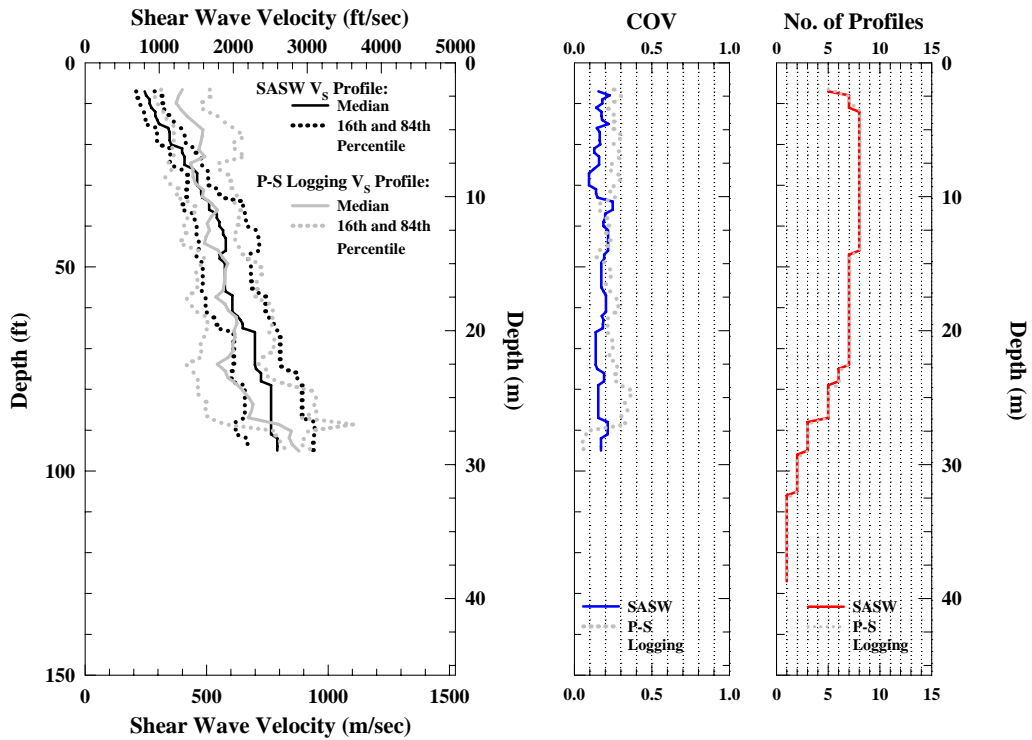


Figure 5.14 Comparison of the Median and 16th and 84th Percentile Boundaries of the Available SASW and P-S Logging V_s Profiles over Identical Depths from Eight Common “C” Sites in Taiwan

5.4.4 Comparisons of COV

The COV values of the SASW V_s profiles are rather uniform at the Taiwan sites. With the “C” and “D” sites together, the average COV values of SASW profiles are always about 0.30. If only the “C” sites are compared, the COV values are around 0.20 for the SASW measurements. Although there are too few profiles of the “D” sites to draw an objective conclusion, according to Figure 5.7, it can be seen that the four “D” sites are very uniform with a COV value about 0.1 for most depths. Comparing to the COV values calculated from the “D” sites in Imperial Valley, this value is about 30% smaller.

As to the suspension logging profiles, their COV values are always slightly higher than the values of SASW profiles at many depths, but the differences are larger in the top 25 ft and below 70 ft compared to the SASW results. The reason could be the natures of these two methods that the SASW method shows more general information in the V_S profiles but the P-S logging shows more localized variation in the V_S profiles due to its higher resolution. Therefore, the COV values of the P-S logging V_S measurements are always higher than the SASW method.

5.4.5 Comparisons of Site Classifications

There are only two site classes determined for the seismic profiling in Taiwan. These site classes are “C” and “D” sites (Table 5.3). The site classes determined by the SASW and suspension logging techniques are consistent at the ten common sites. However, the values of $V_{S,30}$ determined from these two methods show some differences. The range of the difference is from 9 % (the Cheou-Shio and Sin-San Elementary Schools) to 39% (the Fon-Ton High School), with the values from P-S logging results usually larger than the SASW profiles. This difference seems to suggest that there is a difference between the two techniques. This difference is expected because the V_S profiles of the P-S logging method are always higher than the SASW method in the top 25 ft which results in the calculation of higher $V_{S,30}$ values from the suspension logging measurements. As concluded in Chapter 4, it would be better to present the site class information along with the corresponding V_S values.

5.4.6 Comparisons of G_{max}

Based on the V_S profile acquired by the SASW method, the small-strain field shear modulus (G_{max}) profile can be calculated with Equation 5.1 and an assumed unit

weight. For V_s values in the profile less than 2000 fps, the assumed unit weight is 120 pcf. The values of G_{max} is:

$$G_{max} = V_s^2 \cdot \rho \quad (5.1)$$

where ρ is soil density (total unit weight divided by gravity).

Table 5.3 Comparisons of Site Classifications and $V_{s,30}$ between the SASW and P-S Logging Measurements

No.	Site Name	Station No.	SASW		P-S Logging		Diff. (%)
			$V_{s,30}$ (fps)	Site Class	$V_{s,30}$ (fps)	Site Class	(1)-(2)
			(1)		(2)		(1)
1	Lin - Chong Elementary School	CHY-024	1283	C*			
2	Ton - Lo Elementary School	TCU-039	1791	C*			
3	Cheou - Shio Elementary School	TCU-049	1477	C*	1615	C	-9%
4	Kung - Chung Elementary School	TCU-052	1280	C*			
5	Sin - San Elementary School	TCU-054	1653	C*	1506	C	9%
6	Wu - Fon Elementary School	TCU-065	797	D	998	D	-25%
7	Si - Kon Elementary School	TCU-068	1415	C*			
8	Suan - Don Elementary School	TCU-071	1913	C*			
9	Kuo - Sing Elementary School	TCU-072	1361	C	1742	C	-28%
10	Nan - Kon Elementary School	TCU-074	1364	C*			
11	Chiou - Tun Elementary School	TCU-075	1707	C*	1763	C	-3%
12	Nan - To Elementary School	TCU-076	1645	C*	1935	C	-18%
13	Shai - Li Elementary School	TCU-078	1530	C*			
14	Tor - Se Elementary School	TCU-079	1378	C*			
15	Tai - Chung Weather Station	TCU-082	1297	C*	1568	C	-21%
16	Fon - Ton High School	TCU-102	1756	C	2442	C	-39%
17	Nai - Pu Elementary School	TCU-103	2013	C*			
18	Yuan - Lin Elementary School	TCU-110	692	D*	669	D	3%
19	Sin - Hua Elementary School	TCU-113	773	D*			
20	Si - Hu Elementary School	TCU-115	735	D*			
21	Ten - Chong High School	TCU-116	1232	C*			
22	Ton - Ang Elementary School	TCU-120	1295	C*			
23	A - Sua Elementary School	TCU-122	1554	C*			
24	Cheng - Jung Elementary School	TCU-128	1714	C*			
25	Sin - Jai Elementary School	TCU-129	2146	C*			
26	Chi - Nan University	TCU-148	1361	C*	1818	C	-34%

*Based on extrapolated data

To compare objectively the SASW G_{max} profiles from this study with the other studies (Lin et al. 2000) conducted in the Taichung Basin (in the center of the SASW test sites near TCU-082) for gravelly cobble deposits, 22 SASW V_s profiles of the “C” sites were used make a comparison but at the depths where the V_s profile larger than 2000 fps was removed. The reason to remove these profiles is that the V_s profiles over 2000 fps

may be composed of soft or weathered rock or stiff rock, not gravels. Regarding excluding the softer “D” sites, these sites are more like alluvium than gravel deposits so their profiles are not included in this comparison. The studies performed by Lin et al. (2000) include not only downhole but also cyclic triaxial tests. Figure 5.15 shows the G_{max} comparisons between the SASW, downhole and laboratory results for gravel materials and these results agree to each other very well.

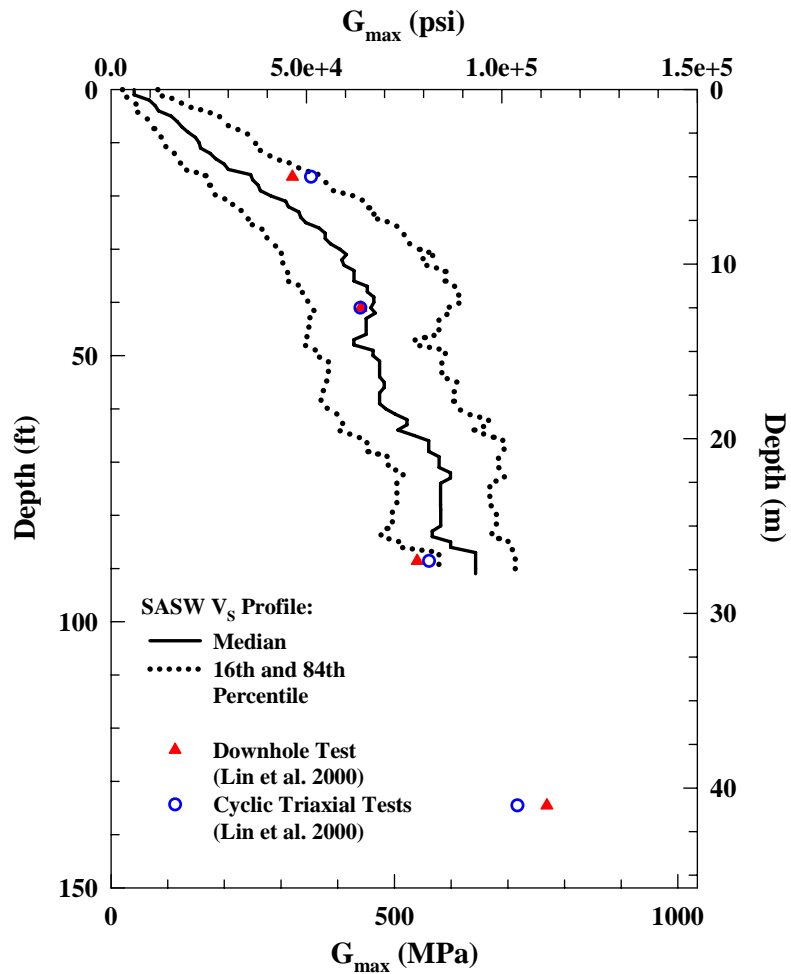


Figure 5.15 Comparison of Gravel Material between SASW, Downhole and Cyclic Triaxial Tests Results

5.5 SUMMARY AND CONCLUSIONS

The background of test sites in Taiwan was described in Section 5.1. The SASW measurements and the V_S results from all available profiles, including suspension logging measurements, are then reviewed.

Based on three different comparing criteria described in Chapter 3, the profiles reduced from SASW and P-S logging methods were analyzed. It always shows the profiles of P-S logging measurements have higher V_S on top 25 ft and lower V_S profiles below 70 ft than the SASW results. At the depths from 25 to 70 ft, these two measurements, however, have very similar median values, especially in the “green-apples-to-green-apples” comparisons. The inconsistency in the top 25 ft may be caused by the casing and grout near the borehole surface. In contrast, the difference below 70 ft between the two median may be due to the different wavelengths used in the SASW and suspension logging methods to profile the soil layers. Interestingly, the COV values of the P-S logging measurements below 70 ft are always larger than SASW profiles. The reason may be due to the lateral averaging at depth inherent in the SASW method.

As to the COV values associated with the measured V_S profiles, at most depths, the SASW results show smaller COV values than the P-S logging profiles, especially in the top 25 ft and below 70 ft. This difference is expected below 70 ft due to the “global-type” measurement at depth in SASW testing.

The comparison of site classification between different seismic measurements shows the two techniques are consistent in terms of determining the site class at all ten common sites. However, the values of $V_{S,30}$ do not agree closely with each other. This difference seems to result from the higher P-S logging measurements in the top 25 ft.

The field shear modulus was also studied here. Based on the results acquired at Taichung Basin, it shows the SASW measurements are consistent to the downhole and cyclic triaxial tests.

Chapter 6 SASW Testing at Hanford, WA

6.1 BACKGROUND OF TEST SITE

Hanford, a federal government owned area, is located in the south-central Washington by the Columbia River. This location is famous for the Manhattan Project in the 1940s and the following Cold War era. Since then, various nuclear-related projects have been conducted there and numerous facilities have been constructed to support these research activities. Nowadays, these nuclear-related projects have been slowly phased out at Hanford and “replaced” by a cleanup project. The goals of this cleanup project is to handle and deal with the radioactive waste generated from the Manhattan Project and other projects of the Cold War era, and to lower the radiation level at Hanford to conform to governmental regulations. Because of this project, many waste treatment facilities have been built. To keep these facilities safe during future earthquakes and to prevent the high-level nuclear waste from escaping into to the natural environment, it is important to dynamically characterize the soil deposits and rock formations at Hanford. Therefore, ten sites were selected at Hanford where SASW testing was conducted with the goal of deep V_s profiling.

6.2 REVIEW OF SASW TESTING PERFORMED AT HANFORD

SASW tests were conducted at Hanford, WA for the Pacific Northwest National Laboratory (PNL) in Richland, WA. The goal of these seismic investigations is to use the SASW technique to profile the subsurface of ten sites around the Waste Treatment Plant (WTP) near the 200 East Area of Hanford. The general locations of the ten SASW sites are shown in Figure 6.1. As seen in the map, the area covered by the

majority of the SASW testing sites (not including Site H10) are about 6000 ft long and 8000 ft wide. Site H10 is about six miles northwest from this area.

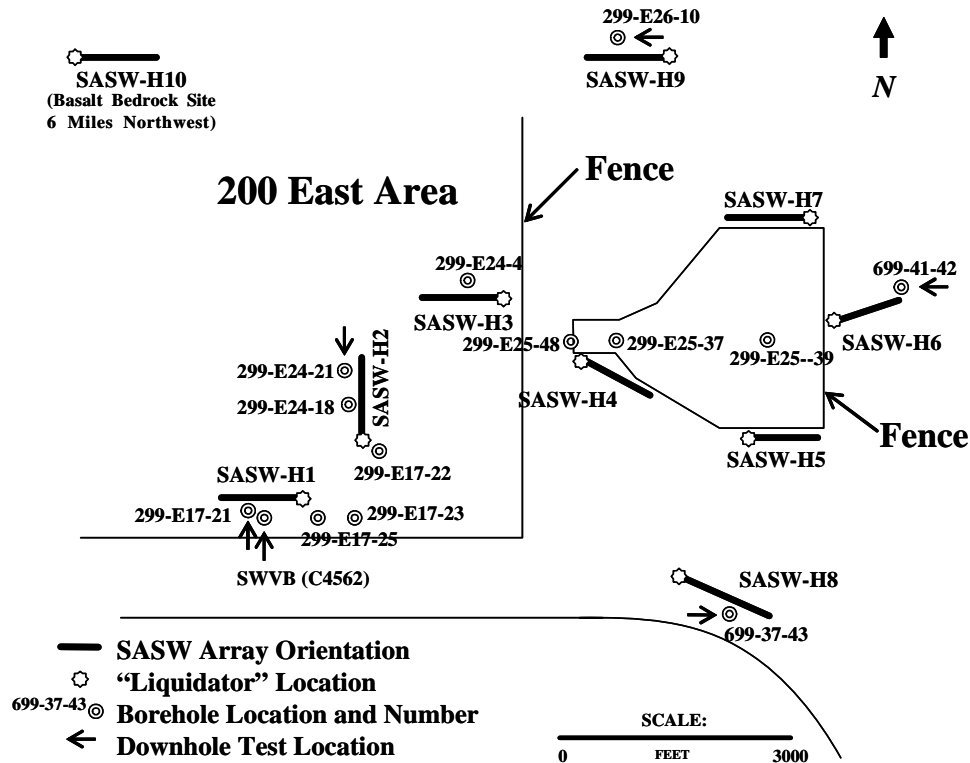


Figure 6.1 Map of Approximate Locations of SASW Testing Arrays at Hanford, WA

Testing was conducted between September 8 and 12, 2004. Dr. Kenneth H. Stokoe, II and personnel (Mr. Min Jae Jung, Brady R. Cox and Cecil Hoffpauir and Ms. Asli Kurtulus) from University of Texas at Austin performed the SASW tests in the field, and the data were reduced as part of this research by the writer. A total of ten SASW test arrays were evaluated at locations near the Waste Treatment Plant at Hanford.

The general configuration of the source and receivers used in field testing at each array location is illustrated in Figure 6.2 for shorter spacings (less than 25 ft between first

and second receiver). Three receivers were used at each source-receivers setup. This arrangement enabled two sets of SASW test results to be obtained at the same time, thereby cutting testing time in half as compared to using only two receivers. The middle receiver (receiver #2) was located at the center line of the test array at all times. When different spacings were used and/or reverse directions were tested, only receivers #1 and #3 and the source were moved. For these shorter spacings, SASW tests were performed in both the forward and reverse directions using a sledge hammer for an impact source. For the larger spacings, testing was performed only in the forward direction using a large vibroseis truck (called “Liquidator”) as the source. Reverse direction testing was not performed with Liquidator due to the difficulty of finding multiple locations to place this large machine (weight of about 70,000 lb) and the damage/disruption to vegetation at the sites by driving Liquidator multiple times over the array location.

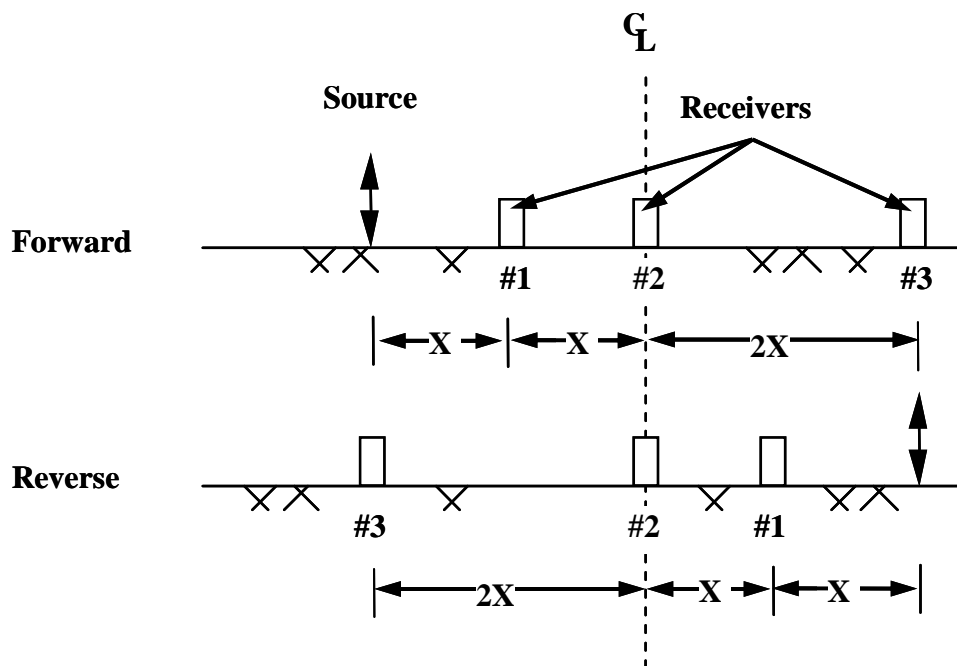


Figure 6.2 Common-Middle-Receiver Geometry Used in SASW Testing at Hanford Sites

Distances between receivers of 5, 10, 25, 50, 75, 150, 300, 450 and 600 ft were typically used when space considerations allowed. This number and progression of receiver spacings resulted in extensive overlapping of the individual dispersion curves used to develop a composite field curve, thereby enhancing the test reliability and confirming global lateral uniformity over the test array. The longest spacing used in the SASW arrays at Hanford was 1000 ft at Site H10. Regardless of the spacing between receivers, at no point in the data analyses were wavelengths considered that were longer than twice the distance between the source and the first receiver in the receiver pair. This geometry resulted in minimizing near-field effects while simultaneously recording long wavelengths.

Vertical velocity transducers, Mark Products Model L-4C geophones, were used as receivers. These geophones have a natural frequency of 1 Hz and good performance over frequencies from 1 Hz to 300 Hz.

The recording device used in these tests was a Hewlett-Packard (HP) 35670A Dynamic Signal Analyzer, a four-channel analyzer. The dynamic signal analyzer was used to record the geophone output and to perform calculations in the frequency domain so that the relative phase of the cross-power spectrum was reviewed in the field during data collection. In addition, the source output of the analyzer was used to control the vibration frequency and amplitude of Liquidator. SASW tests with Liquidator were performed in a stepped-sine mode (from high to low frequencies at the Hanford sites), where the source signal was swept over the frequencies of interest and the relative phase and coherence were determined at each frequency. This process also allowed the operator to evaluate subjectively the data being collected in the field to assure consistency with the expected Rayleigh wave propagation in a layered half space.

6.3 TEST RESULTS

In addition to the ten SASW sites, V_s profiles from six downhole and one P-S suspension logging tests are available among the 10 SASW test sites. However, the top 316 ft of the P-S logging profile has no data. Therefore, this P-S logging profile is not included in this study.

For the forward modeling analysis, the unit weight was assumed by the following criteria. If the shear wave velocity larger than 2000 fps the unit weight was assumed to be 125 pcf. If the shear wave velocity is between 2000 fps and 5000 fps, the unit weight was assumed to be 130 pcf above the water table and 135 below the water table. For the shear wave velocity over 5000 fps, the unit weight was assumed to be 145 pcf, regardless if the measurements were above or below the water table.

6.3.1 SASW Testing

Information of these ten sites is tabulated in Table 6.1. The number of available downhole measurements at each SASW test site is also included in the table. As seen, the shallowest profile extends to a depth of 522 ft at Site H6; in contrast, the deepest profile is 1990 ft acquired at Site H10. The difference in depth is almost four times. The reason for the very deep profile at Site H10 is that testing was performed directly on hard basalt.

The profiling depths of the SASW testing at these sites are much deeper than the SASW measurements in Imperial Valley and Taiwan. In the extreme case, the difference is more than 40 times (Suan-Don elementary school in Taiwan and Site H10 site at Hanford, WA). The reasons are: (1) the operation frequency, (2) energy output of the source, (3) the V_s values of the soil/rock formations, and (4) damping of the soil/rock formations. Of course, the maximum feasible test spacing can be another reason.

Table 6.1 Information of SASW Testing at Hanford, WA

No.	Site Name	Profile Depth (ft)	$V_{s,30}$ (fps)	Site Class	Test Date	Test Performer	Other Tests
							Downhole
1	H1	878	1241	C	8-Sep-04	UTA	2
2	H2	869	1328	C	11-Sep-04	UTA	1
3	H3	584	1234	C	9-Sep-04	UTA	
4	H4	1173	1293	C	11-Sep-04	UTA	
5	H5	541	1140	D	10-Sep-04	UTA	
6	H6	522	1298	C	10-Sep-04	UTA	1
7	H7	606	1295	C	10-Sep-04	UTA	
8	H8	889	1013	D	9-Sep-04	UTA	1
9	H9	705	1526	C	9-Sep-04	UTA	1
10	H10	1990	2042	C	12-Sep-04	UTA	

All ten SASW V_S profiles and the values of their median and 16th and 84th percentile ranges are shown in Figure 6.3. Among these ten sites, most V_S profiles are consistent with each other, except the one at Site H10. Actually, the geologic characteristics of Site H10 are different from the others. The basalt layer at Site H10 is exposed at the ground; however, at the other sites, the top of the basalt layer occurs below a depth of at least 205 ft. After removing Site H10, the remaining 9 SASW V_S profiles and their median and 16th and 84th percentile ranges are shown in Figure 6.4. In general, the COV values are much smaller compared to Figure 6.3. However, the COV at the depths from 200 to 450 ft is obviously larger than the other depths. The reason is that the basalt formation begins to appear at different depths at the SASW test locations.

Based on the V_S profile in the top 30 m (100 ft) profiles in the SASW measurements, the ten SASW sites are classified as eight “C” sites and two “D” sites using the IBC-2006 provisions. Except for Site H10, the $V_{S,30}$ of the remaining nine sites are very similar which is around 1200 fps. This value is the boundary ($V_S = 1200$ fps) between “C” and “D” sites so some of these sites are classified as “C” site but the others are determined as “D” sites.

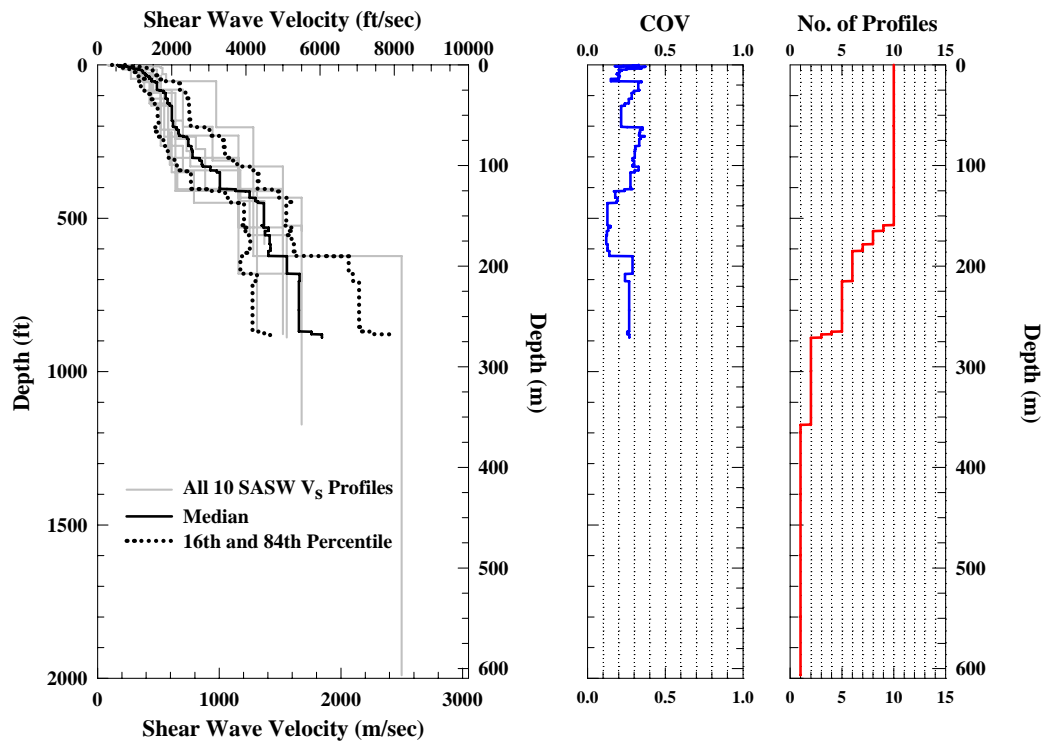


Figure 6.3 Individual Profiles and Statistical Information of Ten SASW V_s profiles from the Hanford Test Sites

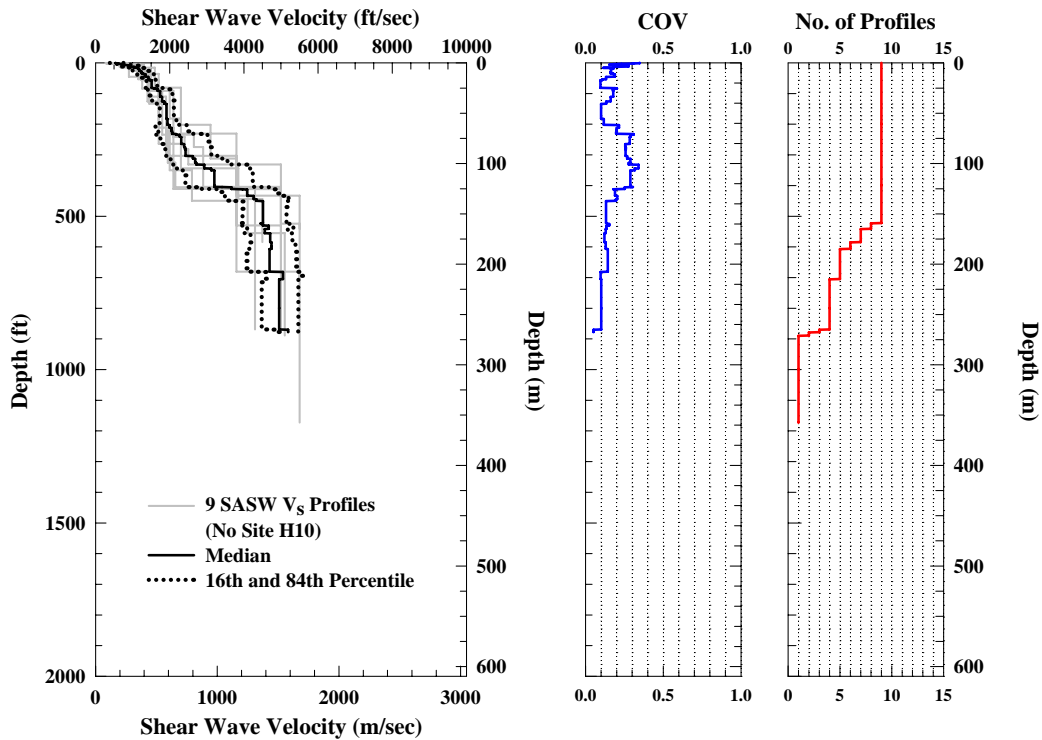


Figure 6.4 Individual Profiles and Statistical Information of Nine SASW V_s Profiles from the Hanford Test Sites; Each Site has Soil Layers over Basalt.

6.3.2 Downhole Testing

Six downhole measurements were performed in six different boreholes near five of the SASW test sites (see Figure 6.1). These downhole tests were performed from June 22 to June 27 in 2004 by Tom Williams of Northland Geophysical and Bruce Redpath of Redpath Geophysics. The information of these downhole measurements and the corresponding SASW sites are shown in Table 6.2. As observed, the depths of these downhole profiles are not as deep as the SASW profiles. The deepest one is 530 ft from borehole SWVB (C4562) near SASW Site H1. In contrast, the shallowest one is 180 ft from borehole 299-E26-10 close to SASW Site H9. The profiling depth was governed by borehole depth and/or the decision not to profile into potential polluted zones.

Figure 6.5 presents all six downhole V_s profiles as well as their median and 16th and 84th percentile boundaries. These downhole profiles are not deep enough to show the larger variations in the COV values caused by the varying-depth basalt layer. The larger variations are observed in the SASW COV profile at depths from 200 to 450 ft in Figure 6.4. However, the larger variations at these depths can be somewhat observed in the two deeper individual downhole profiles.

Table 6.2 Information of Downhole Testing at Hanford, WA

No.	SASW Site Name	Nearby Borehole	Profile Depth (ft)	$V_{s,30}$ (fps)	Site Class	Test Date	Test Performer
1	H1	299-E17-21	200	1412	C	27-Jun-04	#
2	H1	SWVB(C4562)	530	1422	C	26-Jun-04	#
						27-Jun-04	#
3	H2	299-E24-21	230	1287	C	22-Jun-04	#
4	H6	699-41-42	260	1377	C	24-Jun-04	#
5	H8	699-37-43	250	1005	D	25-Jun-04	#
6	H9	299-E26-10	180	1586	C	23-Jun-04	#

Tom Williams of Northland Geophysical and Bruce Redpath of Redpath Geophysics

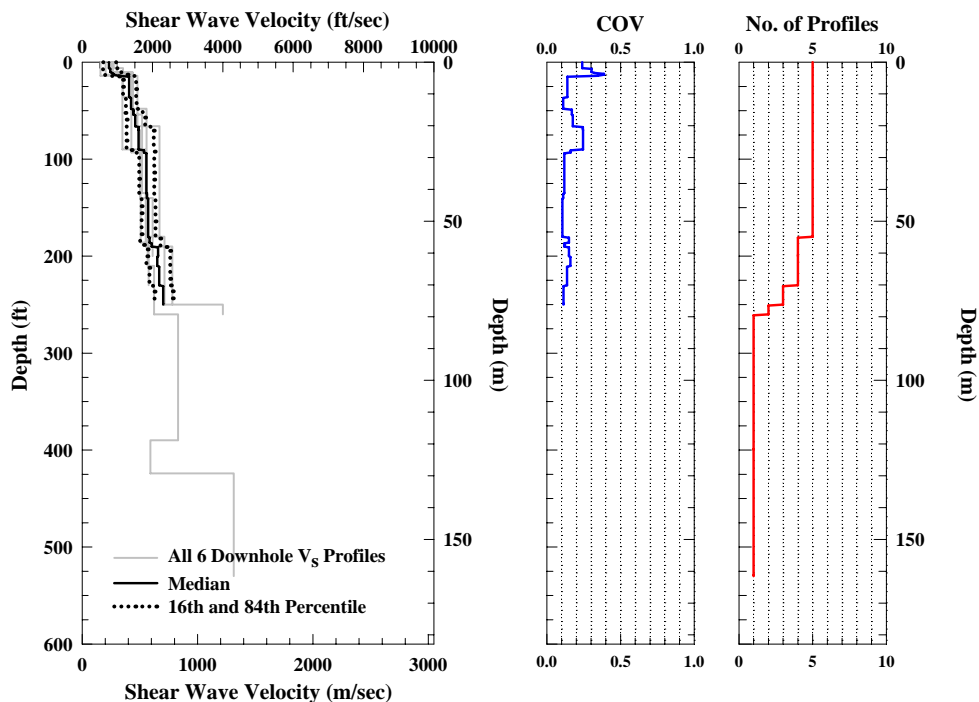


Figure 6.5 Individual Profiles and Statistical Information of Six Downhole V_s Profiles (from Five Sites) at the Hanford Test Sites

Among the five common (SASW and downhole) sites, only one site (Site H8 or Borehole 699-37-43) is classified as a “D” site based on the $V_{S,30}$ value from the downhole profiles. The remaining four sites are all “C” sites.

6.4 STATISTICAL ANALYSES AND COMPARISONS

The general comparison of the individual profiles from the SASW and downhole measurements is presented in Figure 6.6. Site H10, the basalt site, has been excluded from the comparison in Figure 6.6 (b). As seen in Figure 6.6 (b), on the top 250 ft, the two measurements agree very well.

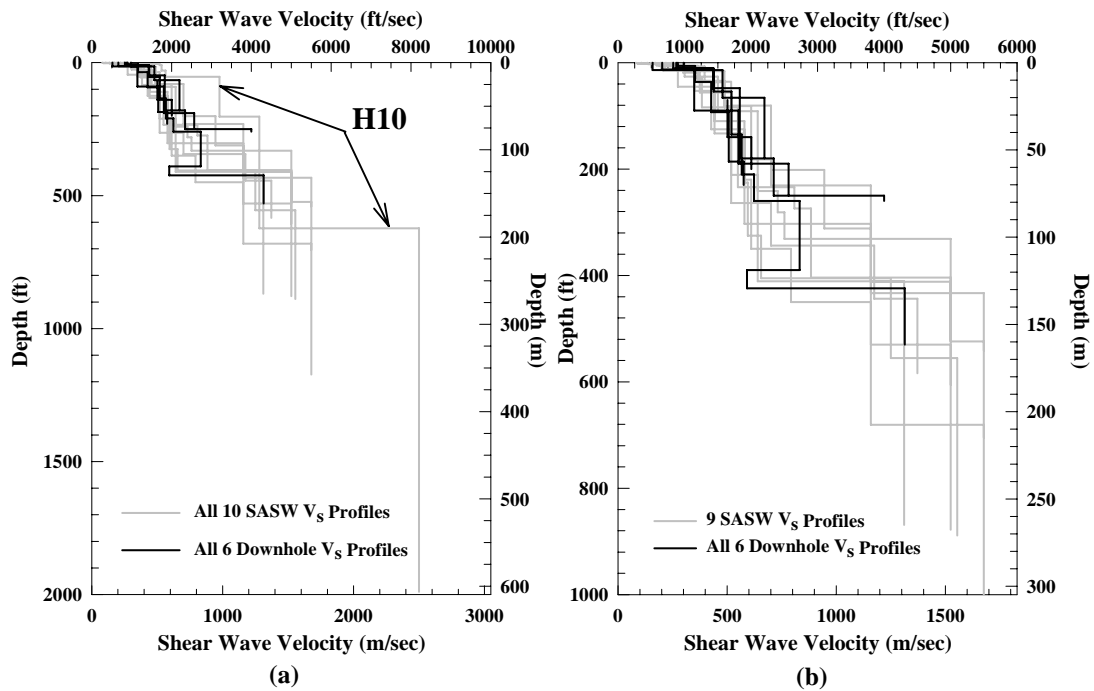


Figure 6.6 General Comparison of Individual SASW and Downhole V_S Profiles: (a) with Site H10 and (b) without Site H10 at Hanford, WA

Before performing the comparisons, one thing needs to be mentioned. When performing the statistical analysis, the two downhole profiles (at Boreholes 299-E17-21 and SWVB (C4562)) near the SASW Site H1 were averaged to represent the downhole

profile at Site H1. By doing so, the weight of the downhole profile at Site H1 is not two times the other sites/profiles.

In addition to the comparisons based on the site locations and profiling depths, some other comparisons with respect to geologic profiles are made in this section. A table (Stokoe et al., 2005a) of geologic profiles at each SASW test site is presented in Table 6.3.

Table 6.3 Geologic Profile of the Ten SASW Test Sites at Hanford, WA

No.	Site Name	Name of Geological Formation								
		Hanford Formation		Ringold Formation				Columbia River Basalt		
		Sand Sequence	Gravel Sequence	Fine Grained	Unit E	Lower Mud (Silt)	Unit A	Saddle Mountains Basalt	Wanapum Basalt	Grande Ronde Basalt
1	H1	0'-247'	247'-323'	Not Present	323'-376'	376'-438'	438'-496'	537'-1300'+		No Data
2	H2	0'-268'	268'-420'	Not Present				420'-1200'+		No Data
3	H3	0'-270' ¹	270'-381'	Not Present				381'-1000'+		No Data
4	H4	0'-165' ¹	165'-263'	Not Present			263'-405'	405'-1200'+		No Data
5	H5	0'-170' ¹	170'-275'	Not Present		275'-300'	300'-385'	385'-1000'+		No Data
6	H6	0'-185' ²	185'-265'	Not Present		265'-292'	292'-375'	375'-1200'+		No Data
7	H7	0'-95' ¹	95'-190' ³	Not Present			190'-270'	270'-1000'+		No Data
8	H8	0'-180'	180'-275'	Not Present	275'-330'	330'-420'	420'-480'	480'-1200'+		No Data
9	H9	0'-205' ¹		Not Present				205'-900'+		No Data
10	H10	Not Present		Not Present				0'-550'	550'-1660'	1660'-?

¹ Hanford sand interbedded gravel

² Mixed with silt

³ Contain some sand layers

6.4.1 General Comparisons (Apples-to-Oranges Comparisons)

The median and 16th and 84th percentile boundaries of the ten SASW and six downhole profiles acquired at Hanford are compared in Figure 6.7. The comparison shows the two median profiles are consistent with each other (even with Site H10 in them). The COV profiles of SASW measurements, however, are much larger than the downhole results. This results from the profile of the Site H10. To remove the bias from the Site H10 profile, the remaining nine profiles are compared to the five downhole profiles (two V_s profiles were averaged at Site H1) in Figure 6.8. As expected, the COV profile for the SASW measurements is much smaller and the two median profiles also agree better after the Site H10 profile is removed. The comparison shown in Figure 6.8 is considered the “Apples-to-Oranges” comparison discussed in Section 3.5.2.

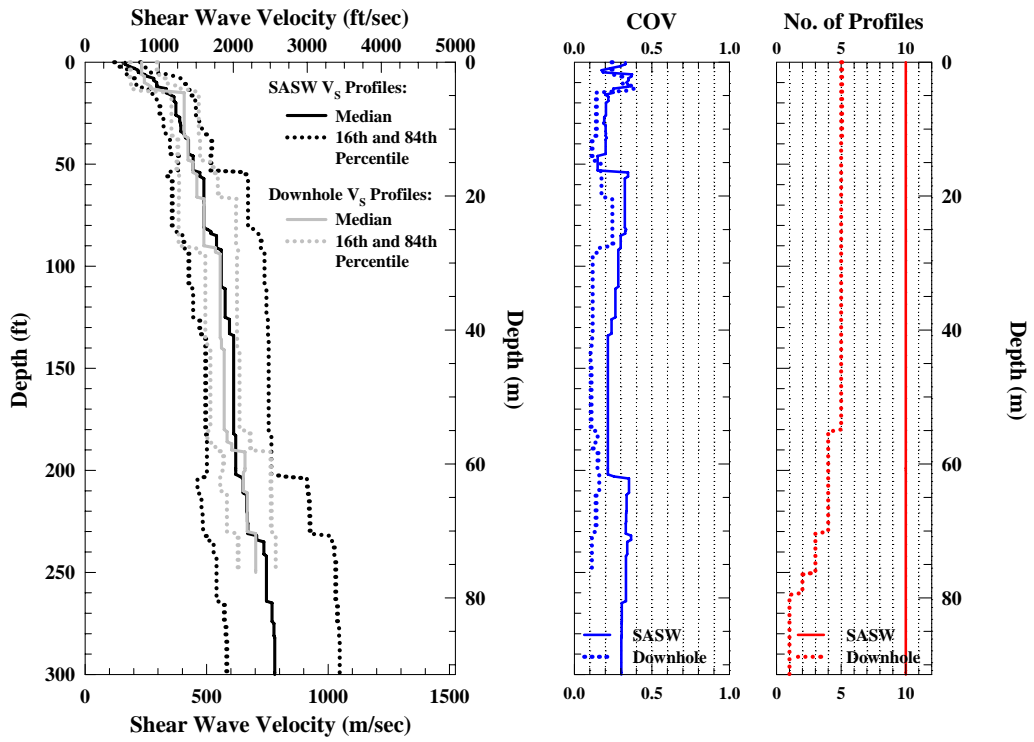


Figure 6.7 Comparison of the Median and 16th and 84th Percentile Boundaries of All Ten SASW and Five Downhole V_s Profiles Measured at Hanford, WA

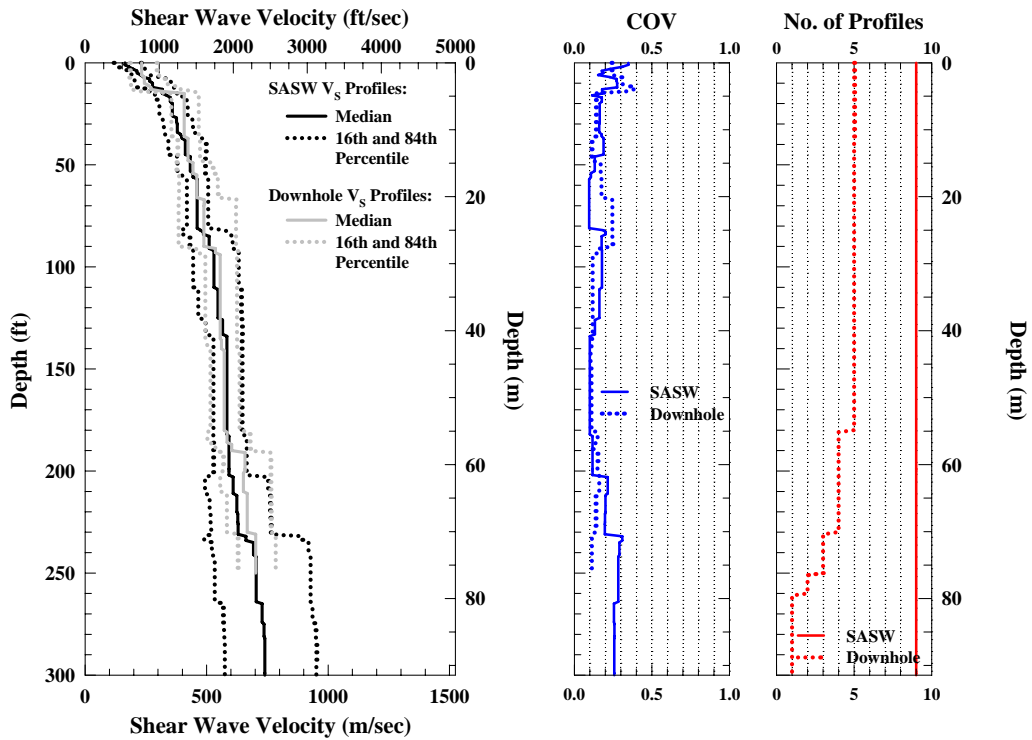


Figure 6.8 Comparison of the Median and 16th and 84th Percentile Boundaries of Nine SASW and Five Downhole V_S Profiles Measured at Hanford, WA

6.4.2 Common Site Comparisons (Green-Apples-to-Red-Apples Comparisons)

To make a more objective comparison between the SASW and downhole profiles, the sites that have both measurements are compared here. These common sites are Sites H1, H2, H6, H8 and H9. Figure 6.9 shows the comparison of the medians and 16th and 84th percentile boundaries of SASW and downhole profiles. (This comparison is the “green-apples-to-red-apples” comparison discussed earlier.) On average, the COV profiles of both methods are no more than 0.20, except the SASW results below 230 ft which is caused by basalt layers as discussed below. There are some larger COV values (slightly larger than 0.20) as seen at the depths from 20 to 120 ft in both COV profiles.

This larger variation results from the various depths of the boundary of Hanford and Ringold formations at each test site as discussed below.

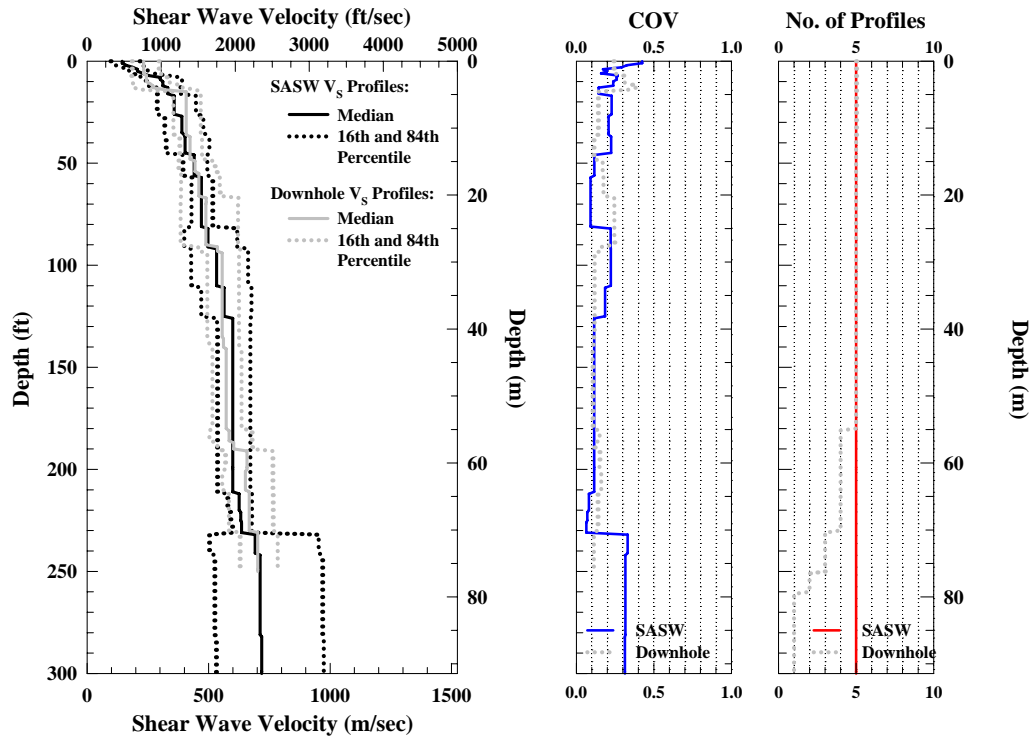


Figure 6.9 Comparison of the Median and 16th and 84th Percentile Boundaries of SASW and Downhole V_S Profiles Measured at Five Common Sites at Hanford, WA

6.4.3 Identical Comparisons (Green-Apples-to-Green-Apples Comparisons)

To keep from biasing the difference in the profiling depths (hence materials) between the SASW and downhole measurements at the same test location, each pair of profiles from the SASW and downhole methods were compared from the identical profiling depths at each of the five common sites. The comparisons of these five identical profiles are presented in Figure 6.10. As seen, the number of profiles of two different techniques at each depth is the same. Figures 6.9 and 6.10 are almost identical,

except for the disappearance of the large variation in the SASW profile below 230 ft because the downhole profiles did not penetrate the basalt layer. As seen in the figure, there is good agreement between: (1) the median profiles, (2) the 16th and 84th percentile boundaries, and (3) the COV profiles. Also, the COV values now average about 0.14.

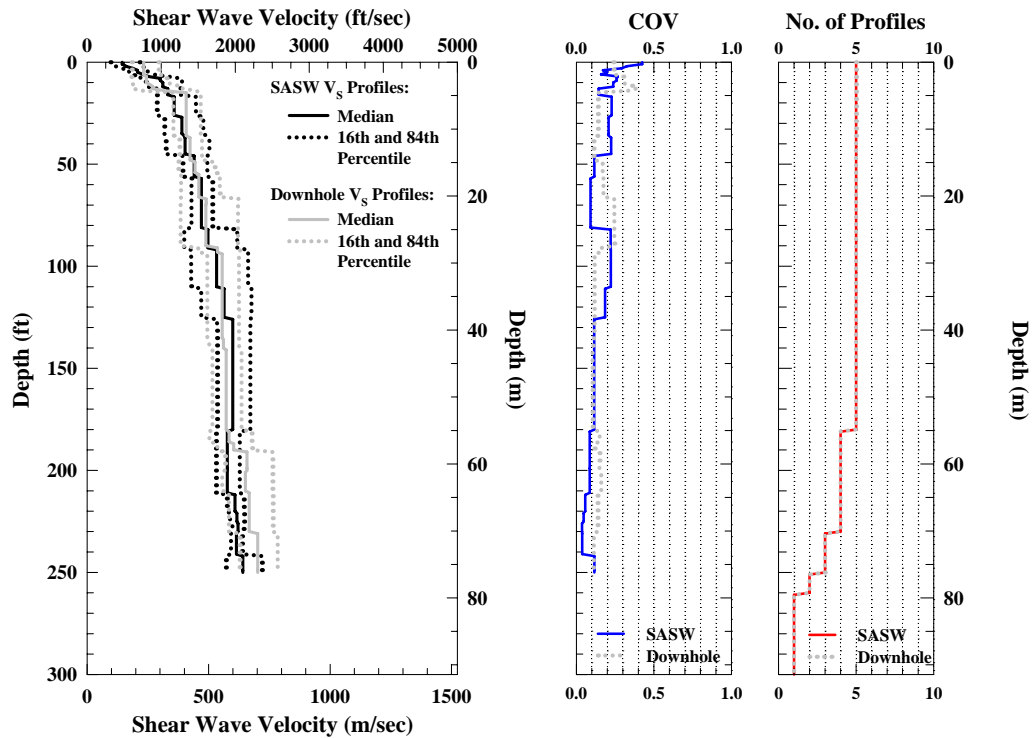


Figure 6.10 Comparison of the Median and 16th and 84th Percentile Boundaries of SASW and Downhole V_s Profiles over Identical Depths at Five Common Sites at Hanford, WA

6.4.4 Statistical Analyses and Comparisons Based on Geologic Information

The geologic profiles at each SASW test site are available in this study (see Table 6.3) so some comparisons based on this information can be studied. Because the depths of the downhole profiles are too short to make comparisons of all formations, only sand sequence of the Hanford formation and the whole Hanford formation (sand and gravel

sequences) are studied. In addition, only the site where the depth of downhole profiles are at least 85% of the thicknesses of studied formations of the same site are included the comparisons. For example, the thickness of the sand sequence (Hanford formation) at Site H2 is 268 ft and the downhole profile at this site is 230 ft deep, which is 86% of the thickness of the sand sequence so this profile is included in sand sequence comparison. However, the same downhole profile is less than 85% thickness of the whole Hanford formation (sand and gravel sequences) so the downhole profile is not included in the comparison of whole Hanford formation.

The gravel sequence of the Hanford formation is not studied here because it is hard to make an objective comparison based on the corresponding V_S profile at the original or top-aligned (start at the same level) depths. However, a study of gravel sequence of Hanford formation regardless of the depth and thickness is also presented in below.

Based on the criteria stated above, only two comparisons are studied. One is for the Hanford formation (sand and gravel sequences) and the other is for the sand sequence.

- ***Hanford Formation (Sand and Gravel Sequences)***

The first comparison for the sand and gravel sequences is presented in Figure 6.11. This comparison includes four downhole profiles from Sites H1, H6, H8 and H9 and nine SASW profile from Sites H1 through H9. As observed, the median and COV profiles of both techniques are very similar except for the COV profile of downhole tests at depths from 50 to 90 ft is larger than average and the median downhole V_S profile increases in the depth range of about 190 to 250 ft. The reasons are discussed in the sand sequence comparison.

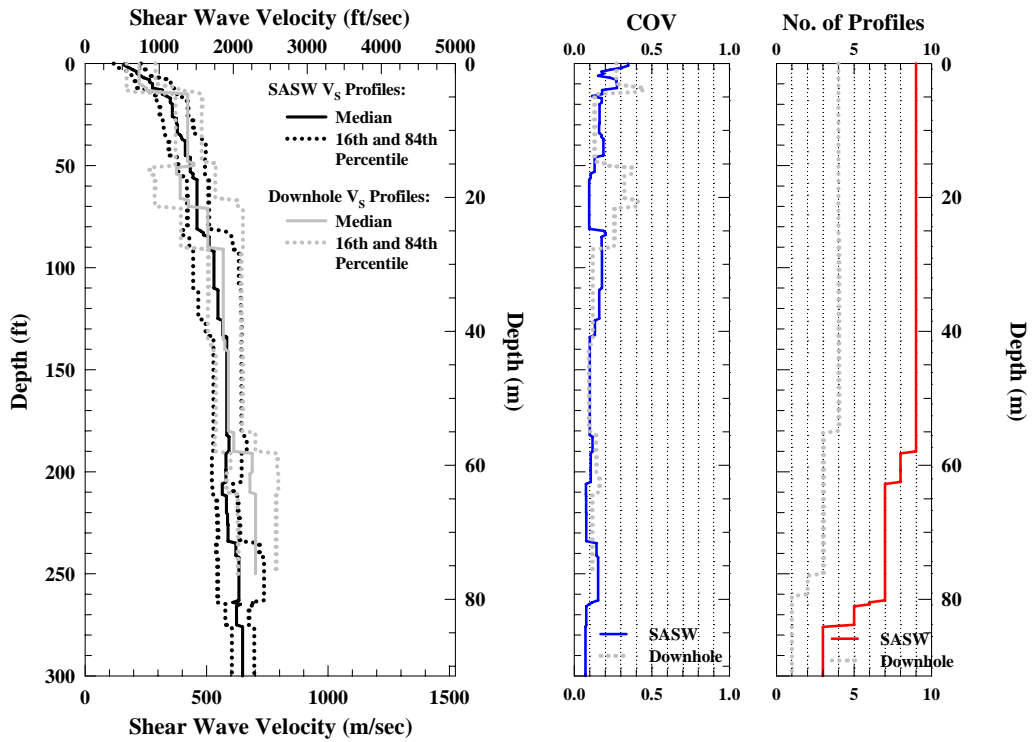


Figure 6.11 Comparison of the Median and 16th and 84th Percentile Boundaries of Nine SASW and Four Downhole V_S Profiles of Hanford Formation (Sand and Gravel Sequences) at Hanford Test Sites

Then a “green-apples-to-red-apples” comparison is made between the SASW and downhole tests from four common sites (Sites H1, H6, H8 and H9). As seen, in Figure 6.12, the median V_S profiles of the SASW and downhole method have less differences but the COV values of the SASW measurements become larger in the top 50 ft and at the depths from 80 to 125 ft. It is because fewer SASW V_S profiles are included in Figure 6.12 than Figure 6.11 so the variations between the thickness and depths of the sand and gravel sequences become larger.

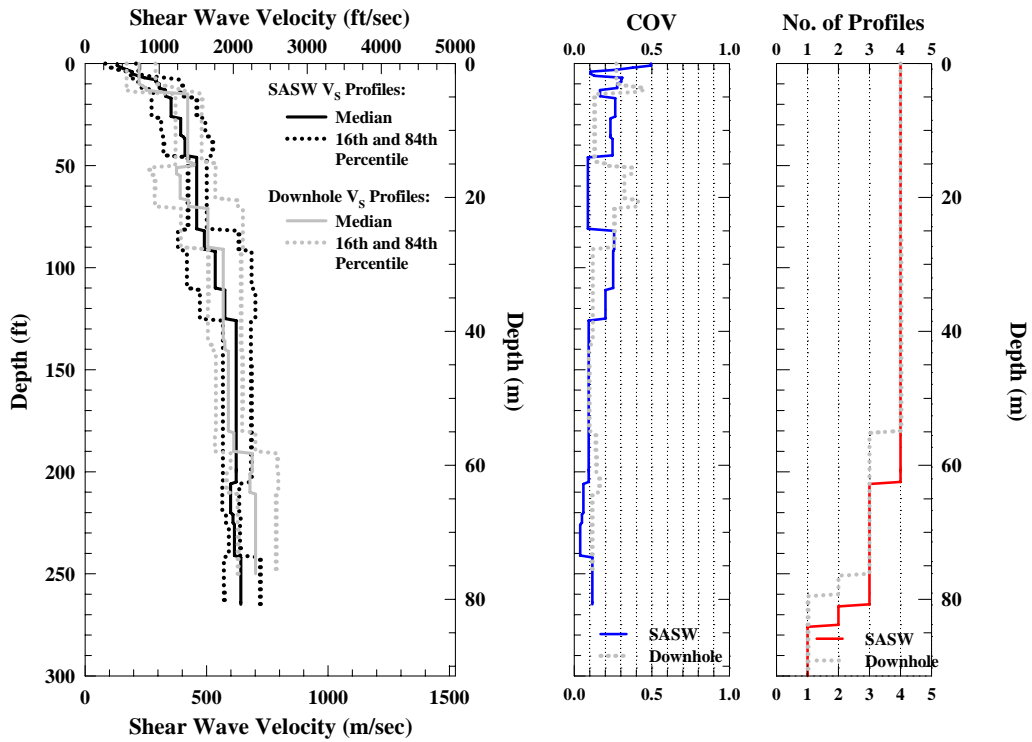


Figure 6.12 Comparison of the Median and 16th and 84th Percentile Boundaries of the SASW and Downhole V_S Profiles of Hanford Formation (Sand and Gravel Sequences) at Four Common Sites at Hanford

Finally, the two measurements were compared based on the “green-apples-to-green-apples” comparison. The results are shown in Figure 6.13. There is no difference between Figures 6.12 and 6.13 in the top 180 ft because the same number of V_S profiles is used in the depth range. Below 180 ft, the two median V_S profiles are closer in Figure 6.13 than in Figure 6.12.

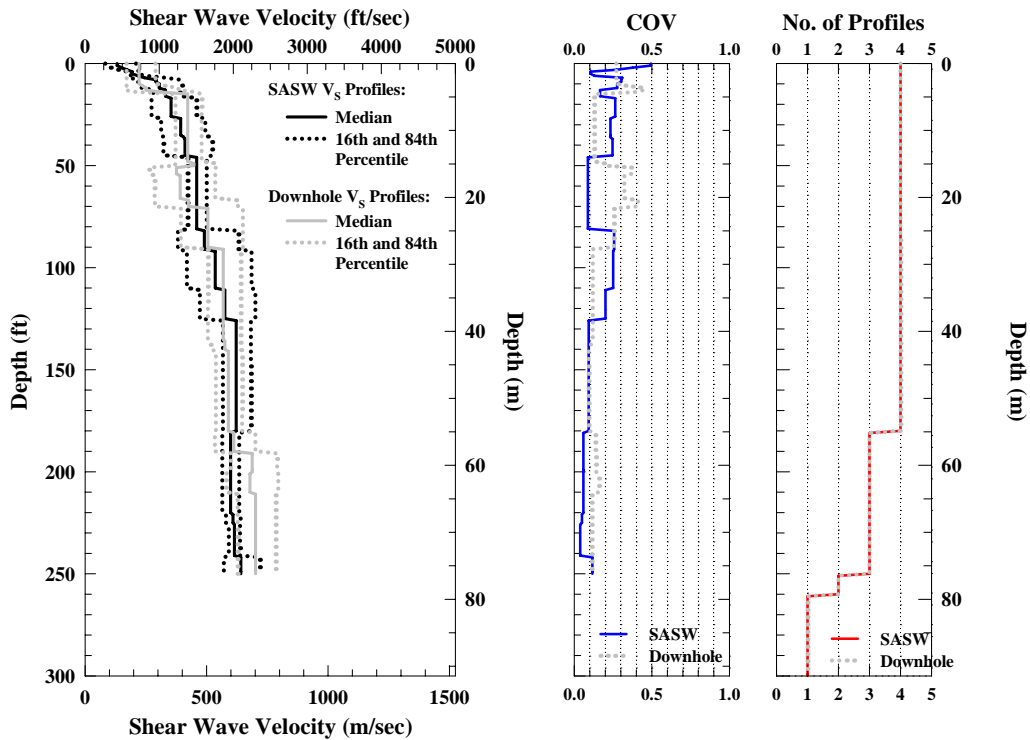


Figure 6.13 Comparison of the Median and 16th and 84th Percentile Boundaries of the SASW and Downhole V_S Profiles of Hanford Formation (Sand and Gravel Sequences) over Identical Depths at Four Common Sites at Hanford

- ***Sand Sequence of Hanford Formation***

The second comparison, the comparison of sand sequence, is shown in Figure 6.14. In this case, nine SASW from Sites H1 through H9 and four downhole profiles from Sites H1, H2, H6 and H8 are compared. Again, the figure shows the two profiling methods have very similar results but the abnormal COV values in the downhole profile at depths from 50 to 90 ft observed in Figure 6.11 become much smaller here. The reason could result from the downhole profile from Site H9 because the difference between the sites studied in the first and second comparisons is Site H2 and H9 and according to the geologic profile of Site H9, the Hanford formation at this site is sand and

gravel interbedded. Unlike Site H9, Site H2 has two distinct layers, the top one for sand and the bottom one for gravel.

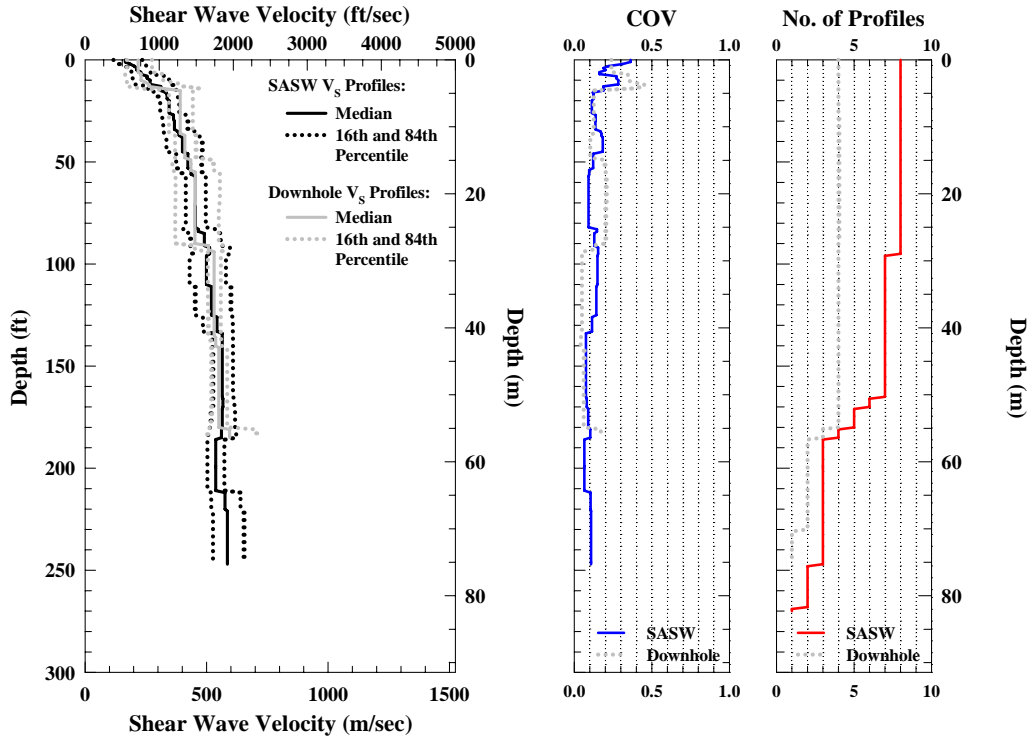


Figure 6.14 Comparison of Median and 16th and 84th Percentile Boundaries of Nine SASW and Four Downhole V_S Profiles of Sand Sequence of Hanford Formation at Hanford Test Sites

A “green-apples-to-red-apples” comparison is made between the SASW and downhole tests from four common sites (Sites H1, H2, H6 and H8) for the sand sequence in Figure 6.15. Based on the average ratio of the downhole V_S to the SASW V_S in the top 185 ft, the median V_S profiles of the SASW and downhole method have less differences in Figure 6.15 than Figure 6.14. The average ratio of the downhole V_S to the SASW V_S in the top 185 ft are 1.02 and 1.01 in Figure 6.14 and Figure 6.15, respectively. The COV values of the SASW measurements become larger at the depths

from 15 to 48 ft and 90 to 125 ft compared to Figure 6.14. The reason is as stated in the common site comparison in Section 6.4.4.1.

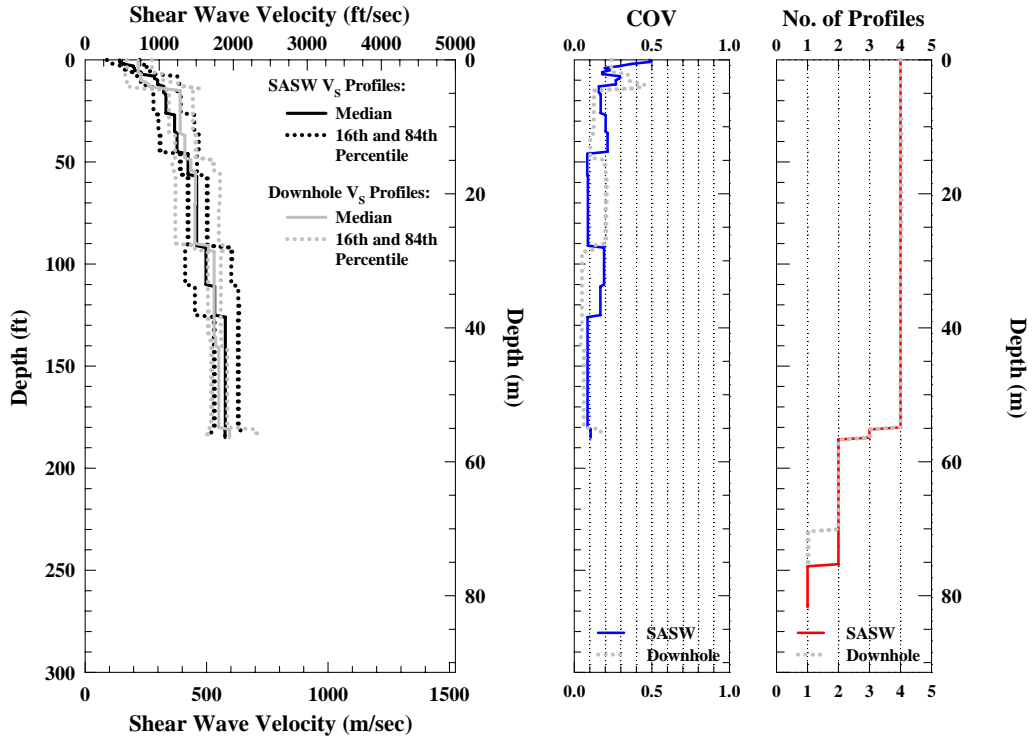


Figure 6.15 Comparison of the Median and 16th and 84th Percentile Boundaries of the SASW and Downhole V_S Profiles Sand Sequence of Hanford Formation at Four Common Sites at Hanford

As to “green-apples-to-green-apples” comparison, the results are presented in Figure 6.16. Actually, the Figure is identical to Figure 6.15, except for the profile number of the SASW measurement below 230 ft. This is because the profile number of both SASW and downhole V_S measurements are less than three at the depth of 185 ft where the profiles stop being compared but their profile number start to differ at 230 ft. Therefore, the “green-apples-to-green-apples” and “green-apples-to-red-apples” comparisons are the same in this case.

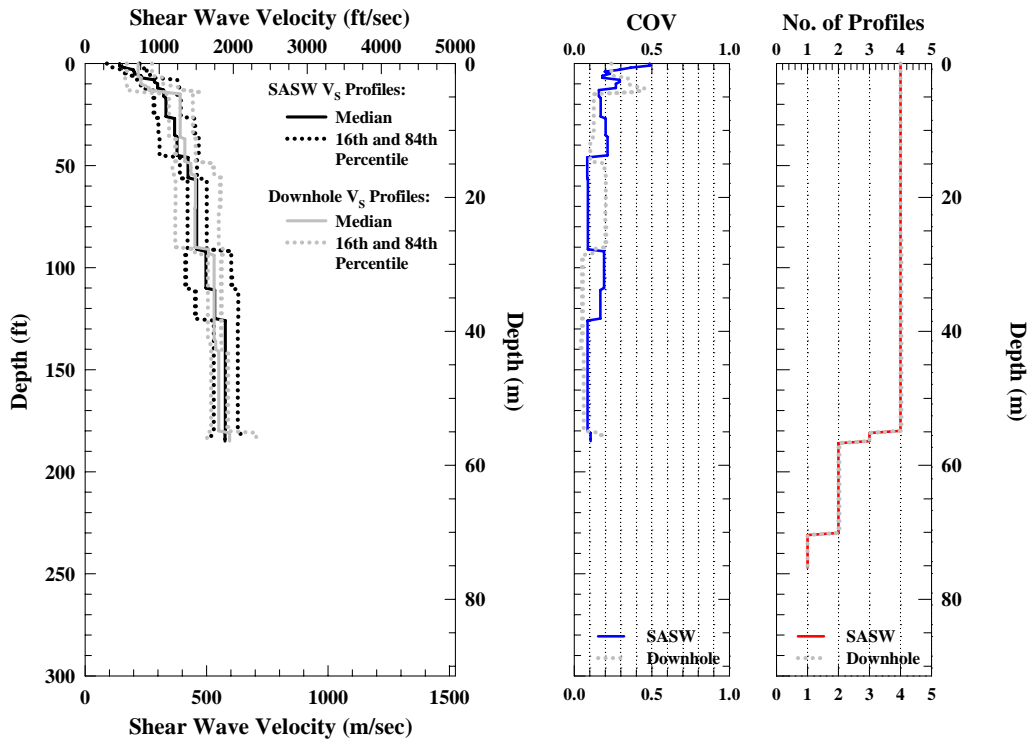


Figure 6.16 Comparison of the Median and 16th and 84th Percentile Boundaries of the SASW and Downhole V_S Profiles of Sand Sequence of Hanford Formation over Identical Depths at Four Common Sites at Hanford

- **Basalt Formation**

The basalt layer is a very important stratum at Hanford, WA. However, the downhole profile is not deep enough to compare with the SASW profiles in this formation. There are three basalt strata, Saddle Mountain, Wannapum and Grande Ronde basalts, observed in the geologic profiles (see Table 6.3). However, only the Saddle Mountain basalt is within the profiling depths of all ten SASW sites. In addition, even the geologic profile indicates that the Saddle Mountain basalt at Site H10 starts at the ground surface and goes to the depth of 550 ft, the top 53 ft at Site H10 could be a weathered basalt. Therefore, the top 53 ft in the SASW profile at Site H10 was removed and the remainder of the profile was aligned to the ground surface with the other nine

profiles to perform statistical analysis which is presented in Figure 6.17. As seen, the Saddle Mountain basalt has a median V_S value of about 4500 fps. Moreover, based on the average COV value in the profile, about 0.15, the Saddle Mountain basalt at these ten sites is very similar.

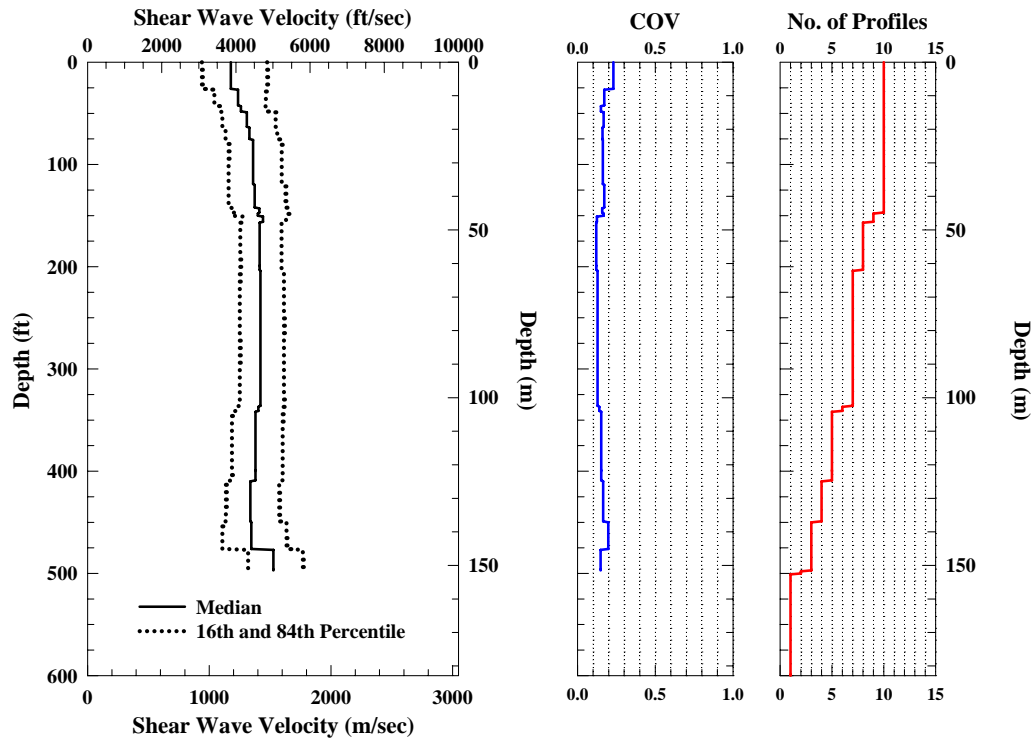


Figure 6.17 Statistical Analysis of Ten, Top-Aligned SASW Profiles of Saddle Mountain Basalt at the Hanford Test Sites

- ***Comparisons Regardless of Thickness and Depth of Each Formation***

The comparisons of shear wave velocity regardless of the depth and thickness of each formation are also studied here. The shear wave velocities are averaged over the depths of each formation with respect to the corresponding geologic profile at each site. Then, the median and 16th and 84th percentile boundaries of each formation are calculated based on the average V_S values of this formation from each site and the assumption of a

log-normal distribution. Because this comparison is regardless of the thickness and depth of each formation, it is easy to make a comparison in the gravel sequence of the Hanford formation. The results are shown in Figure 6.18 which indicates the result from SASW and downhole tests are very close to each other, except the downhole values are higher than SASW results in the gravel sequence of Hanford formation. Again, because of the shortness of downhole profiles, only SASW results are presented for Ringold and Saddle Mountain basalt.

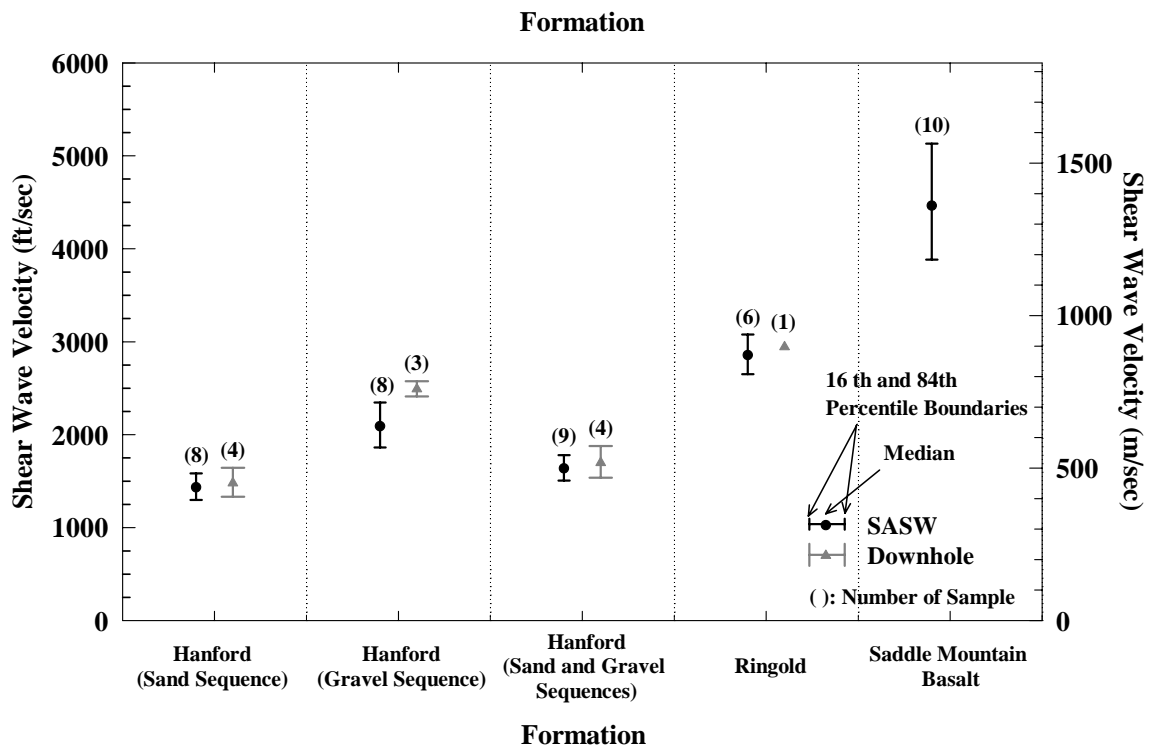


Figure 6.18 Comparison of the SASW and Downhole Average V_s Regardless of Depth and Thickness of the Five Formations at Hanford Test Sites

6.4.5 Comparison of Site Classification

Table 6.4 shows the information of the $V_{s,30}$ and site classification between the SASW and downhole measurements. In terms of the site class, both profiling methods

have the same results. The difference between these two methods is less than 15 % according to the $V_{s,30}$ value at each site. In the five common sites, both methods determined Site H8 as a “D” site and the remaining four sites as “C” sites. Even Site H8 is in a different site class, it still has similar soil properties to the other eight SASW test sites (except Site H10). This can be observed according to the SASW $V_{s,30}$ values of SASW Sites H1 through H7 and H9. In general, the SASW and downhole measurements agree well with respect to site class and $V_{s,30}$.

Table 6.4 Comparisons of Site Classification and $V_{s,30}$ between SASW and Downhole Measurements

No.	Site Name	SASW		Downhole		Difference $\frac{(2)-(1)}{(1)}$
		$V_{s,30}$ (fps) (1)	Site Class	$V_{s,30}$ (fps) (2)	Site Class	
1	H1	1241	C	1412	C	14%
				1422	C	15%
2	H2	1328	C	1287	C	-3%
3	H3	1234	C			
4	H4	1293	C			
5	H5	1140	D			
6	H6	1298	C	1377	C	6%
7	H7	1295	C			
8	H8	1013	D	1005	D	-1%
9	H9	1526	C	1586	C	4%
10	H10	2042	C			

6.5 CALCULATION OF FIELD SHEAR MODULUS

Based on the criteria described in Section 6.3, for the unit weight used in the forward modeling of the SASW method and the median SASW V_s profiles calculated from some different formations and their combinations, the field shear modulus (G_{max}) can be obtained using Equation 4.1. The results are shown in Figures 6.19 to 6.22 for different (combination of) formations. First, Figure 6.19 shows the representative shear modulus profile which includes most formations discussed in this work (Hanford, Ringold and Saddle Mountain formations) at the WTP (Waste Treatment Plant) area.

The representative shear modulus profile is calculated from nine SASW V_S profiles acquired in this area. That means the SASW profile of Site H10 is not included in this figure. As seen, there is a big contrast in the depth range from 400 to 450 ft because of the appearance of the basalt layers at different depths. Second, the nine SASW profiles at the WTP area with only the profiles within the Hanford formation (sand and gravel sequences) are used. These results are presented in Figure 6.20. There is a constant shear modulus (100 ksi) in the depth range from 140 to 240 ft where the general boundary between the sand and gravel sequences occurs in the Hanford formation. Figure 6.21 shows the statistical information of the shear modulus of the sand sequence of the Hanford formation. In general, the shear modulus increases with the depth above the top 140 ft in the profile. The last figure, Figure 6.22, presents the median and 46th and 84th boundaries of the shear modulus of the Saddle Mountain basalt based on ten SASW sites. On average, the field shear modulus of Saddle Mountain basalt is about 600 ksi.

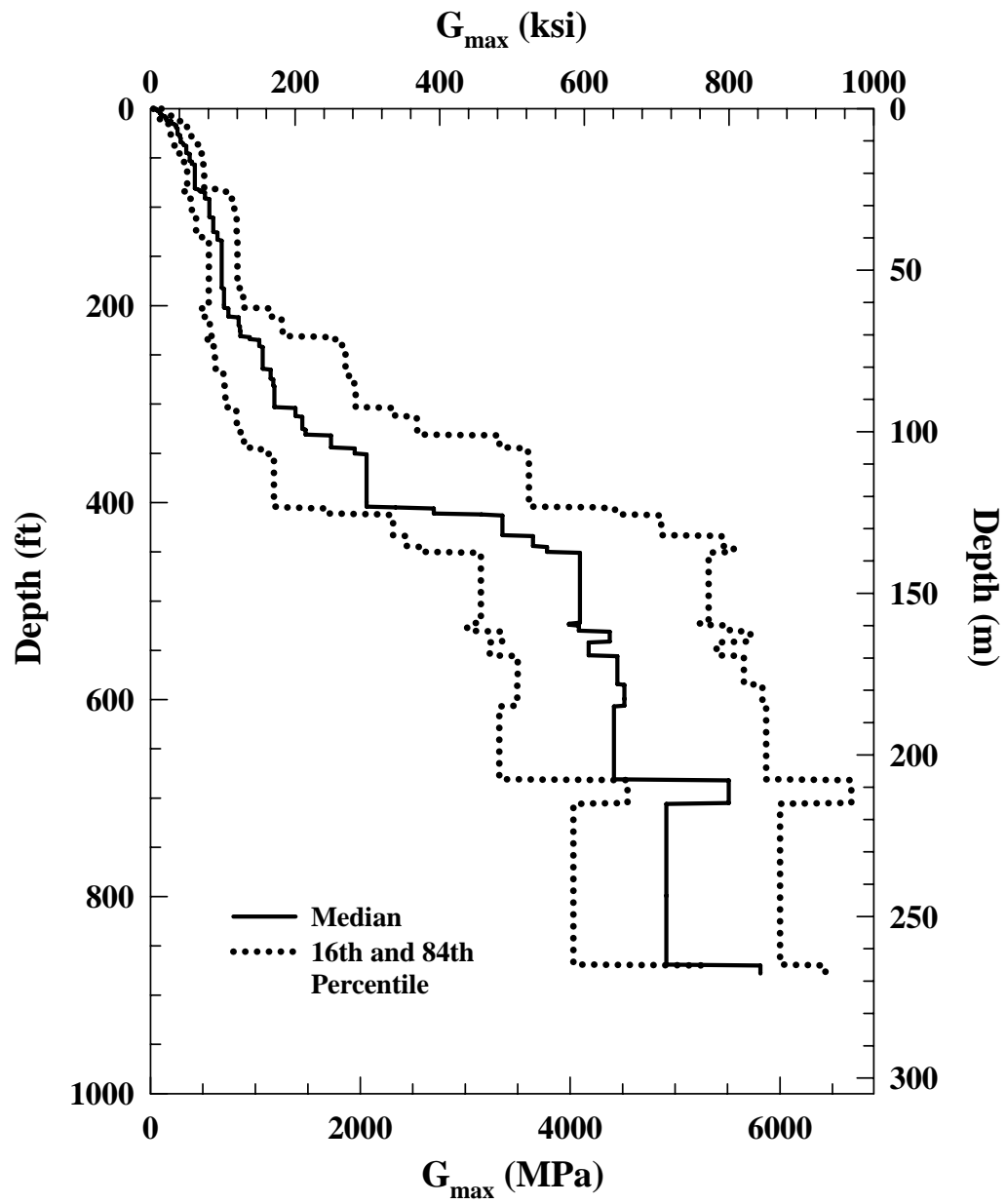


Figure 6.19 Field Shear Modulus of the Waste Treatment Plant Area Based on Nine SASW V_s Profiles (H1 through H9) Acquired at Hanford, WA

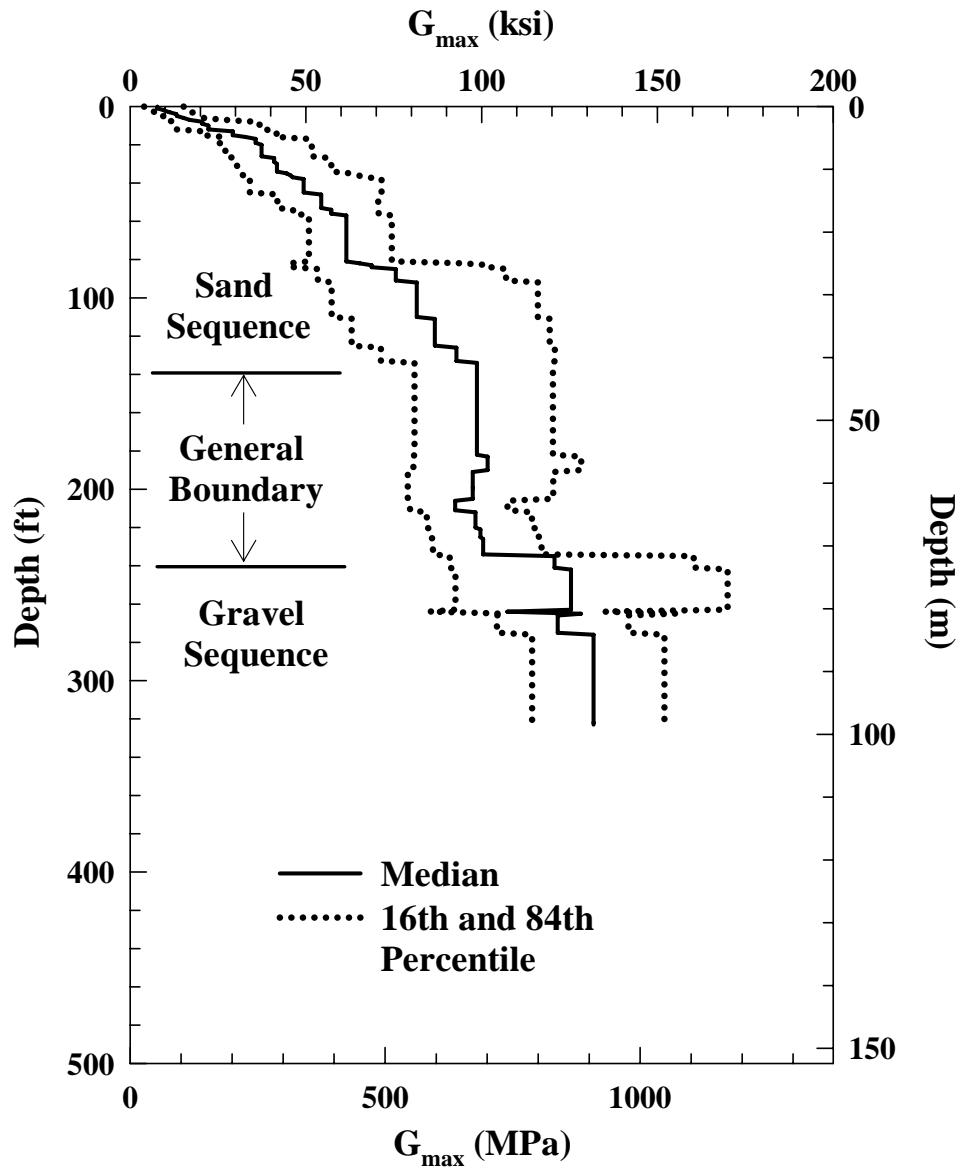


Figure 6.20 Field Shear Modulus of the Hanford Formation (Sand and Gravel Sequences) at the Waste Treatment Plant Area Based on Nine SASW V_S Profiles (H1 through H9) Acquired at Hanford, WA

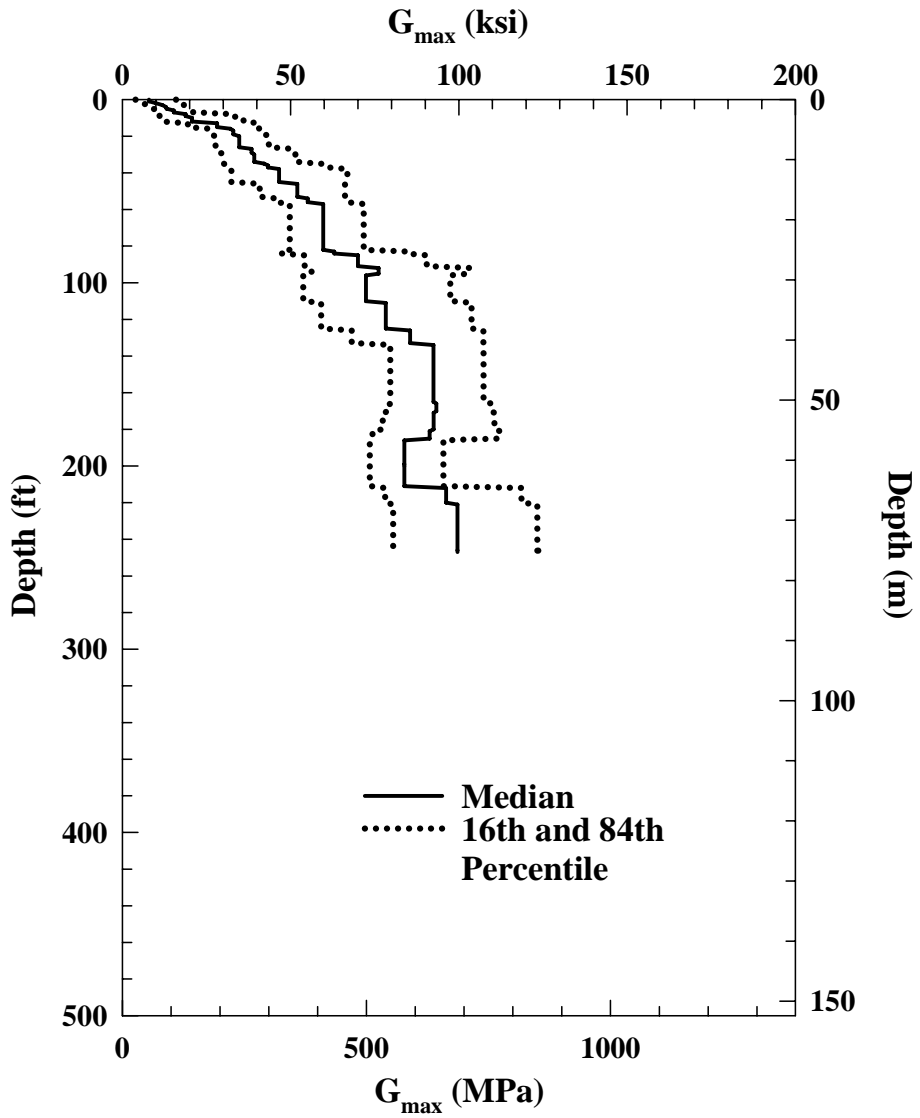


Figure 6.21 Field Shear Modulus of the Sand Sequence of the Hanford Formation at the Waste Treatment Plant Area Based on Nine SASW V_S Profiles (H1 through H9) Acquired at Hanford, WA

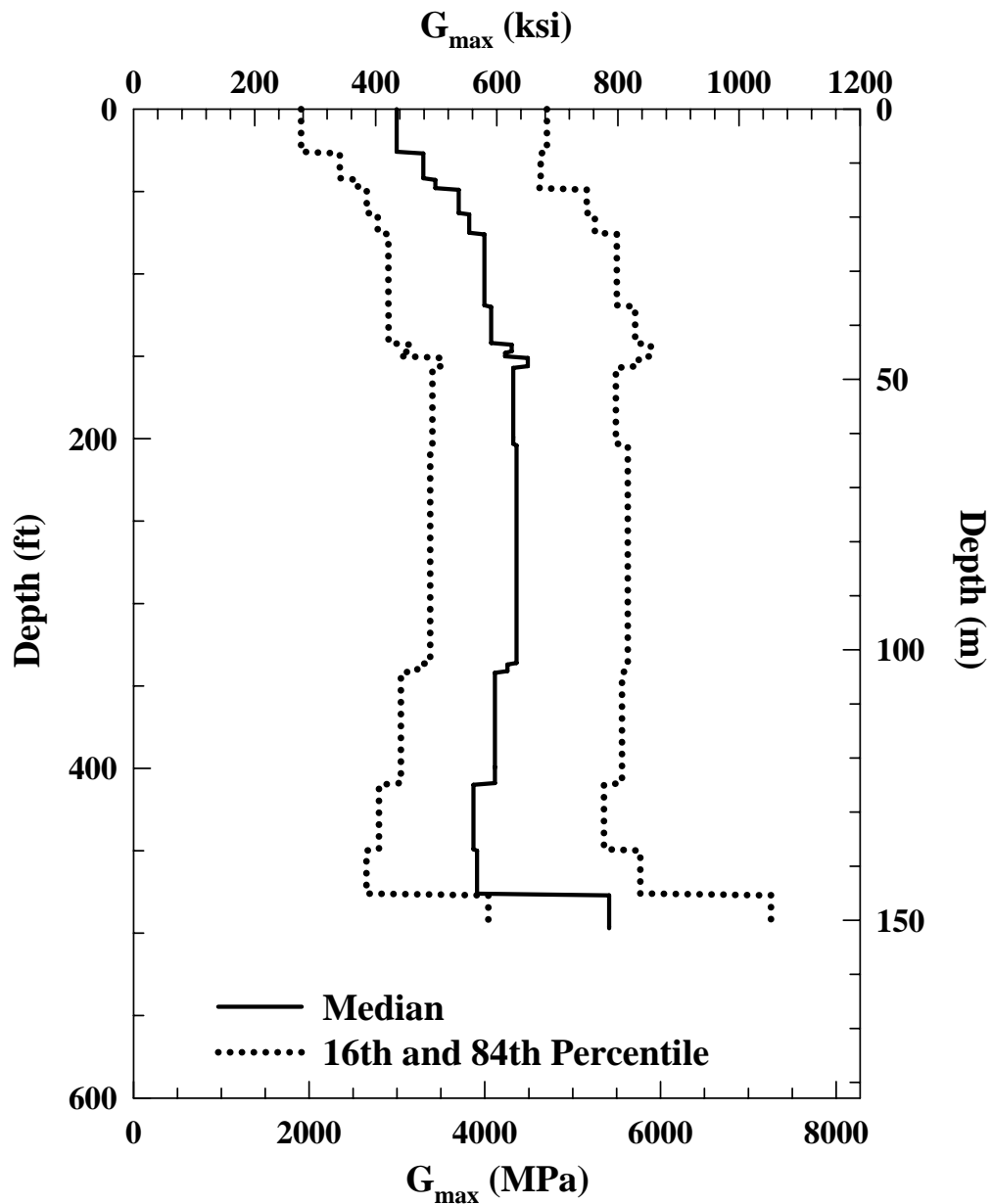


Figure 6.22 Field Shear Modulus of the Saddle Mountain Basalt Based on Ten SASW V_s Profiles Acquired at Hanford, WA

6.6 SUMMARY

In this chapter, the background of the Hanford test site is introduced. The SASW test setups and equipment used at Hanford are described. Also, testing results

from the SASW and downhole measurements are reviewed. The comparisons between the SASW and downhole V_S profiles are studied based on several different criteria stated in Section 3.5.2. Some other comparisons between the SASW and downhole V_S profiles are made based on the geologic profile. Different types of formations and some of their combinations are compared. IN general, the “green-apples-to-green-apples” comparisons have best agreement between the SASW and downhole median V_S profiles. However, the smallest average COV values do not occur in the “green-apples-to-green-apples” comparisons. The reason is that in the “green-apples-to-green-apples” comparisons, fewer V_S profiles are involved so if the included profiles are not very similar (i.e. not very close to the median V_S profile of the nine SASW V_S profiles), the differences between these profiles can increase the COV values to some extent with respect to “green-apples-to-red-apples” or “apples-to-oranges” comparisons. Comparisons, regardless of the thicknesses and depths of different formations, of different formations and some of their combinations between the SASW and downhole measurements are made. The results show that the SASW and downhole measurements are very consistent, except in the gravel sequence of the Hanford formation, the V_S range of downhole profiles is higher than the SASW measurements.

At the end of the chapter, the small-strain field shear modulus (G_{max}) was studied as well. The representative shear moduli of the WTP area were calculated based on the whole profiling depth, Hanford formation and sand formation of Hanford formation of nine SASW V_S profiles. These comparisons show that the median G_{max} of sand sequence of the Hanford formation is about 10 ksi at the surface and increases gradually to around 100 ksi at the depth of 140 ft. Between the range of depths from 140 and 240 ft, a constant G_{max} value (100 ksi) is observed. This is a general boundary of the sand and gravel sequences of the Hanford formation. The reason of the constant G_{max} value

should result from the averaged G_{\max} number of the sand and gravel sequences within this depth range. In addition, the G_{\max} of Saddle Mountain basalt was calculated from the all ten SASW V_s profiles and the result shows the median G_{\max} value of Saddle Mountain basalt is about 600 ksi. These G_{\max} values can offer some crucial information to geotechnical or earthquake engineers for design purpose.

Chapter 7 SASW Testing in Yucca Mountain, NV

7.1 BACKGROUND OF TEST SITE

For decades, the U.S. government has been looking for the appropriate place to build a long-term repository for high-level radioactive waste in the United States. Among several potential locations, Yucca Mountain, NV was selected for this repository. Yucca Mountain is located in a remote desert, approximately 100 miles northwest of Las Vegas, Nevada (Figure 7.1). This area, which is secured and controlled by the federal government, is an excellent candidate compared to many others. Since 1978, the U.S. Department of Energy (DOE) has done numerous studies of Yucca Mountain to determine if it is feasible to build the nation's first long-term geologic repository for high-level radioactive waste there. The high-level radioactive waste, produced from nuclear power generation and national defense programs, is currently stored at numerous (more than 120) temporary repositories around the nation. DOE has already obtained permission to take the next step in building a safe repository to store the radioactive waste and is preparing a license application to obtain the Nuclear Regulatory Commission license to construct the repository.

In addition to the location of Yucca Mountain, the geologic setting of this area is an important factor in choosing Yucca Mountain to be the first high-level radioactive waste repository. The major geologic formation at Yucca Mountain area is several different types of tuffs. Some experts believe the special physical, chemical and thermal characteristics of tuff make it an ideal material to store radioactive waste for the million of years needed for the radioactive waste to become stable and safe through the radioactive decay process. As shown is the lithostratigraphic profile in Figure 7.2, the potential repository location is in the Paint Brush group which is mainly made up of Tiva

Canyon Tuff and Topopah Spring Tuff. To be precise, the high-level radioactive waste will be stored in the Topopah Spring Tuff.

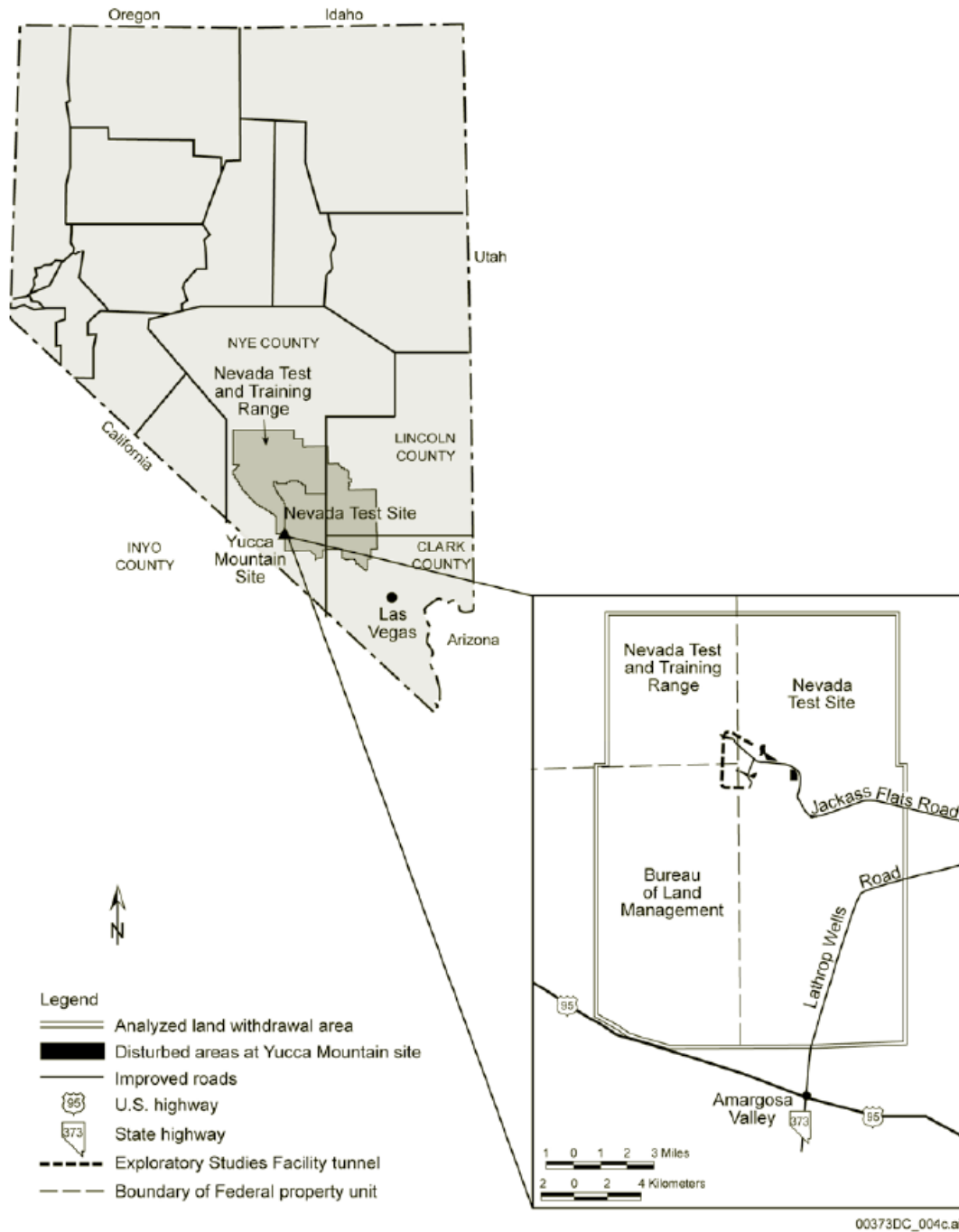
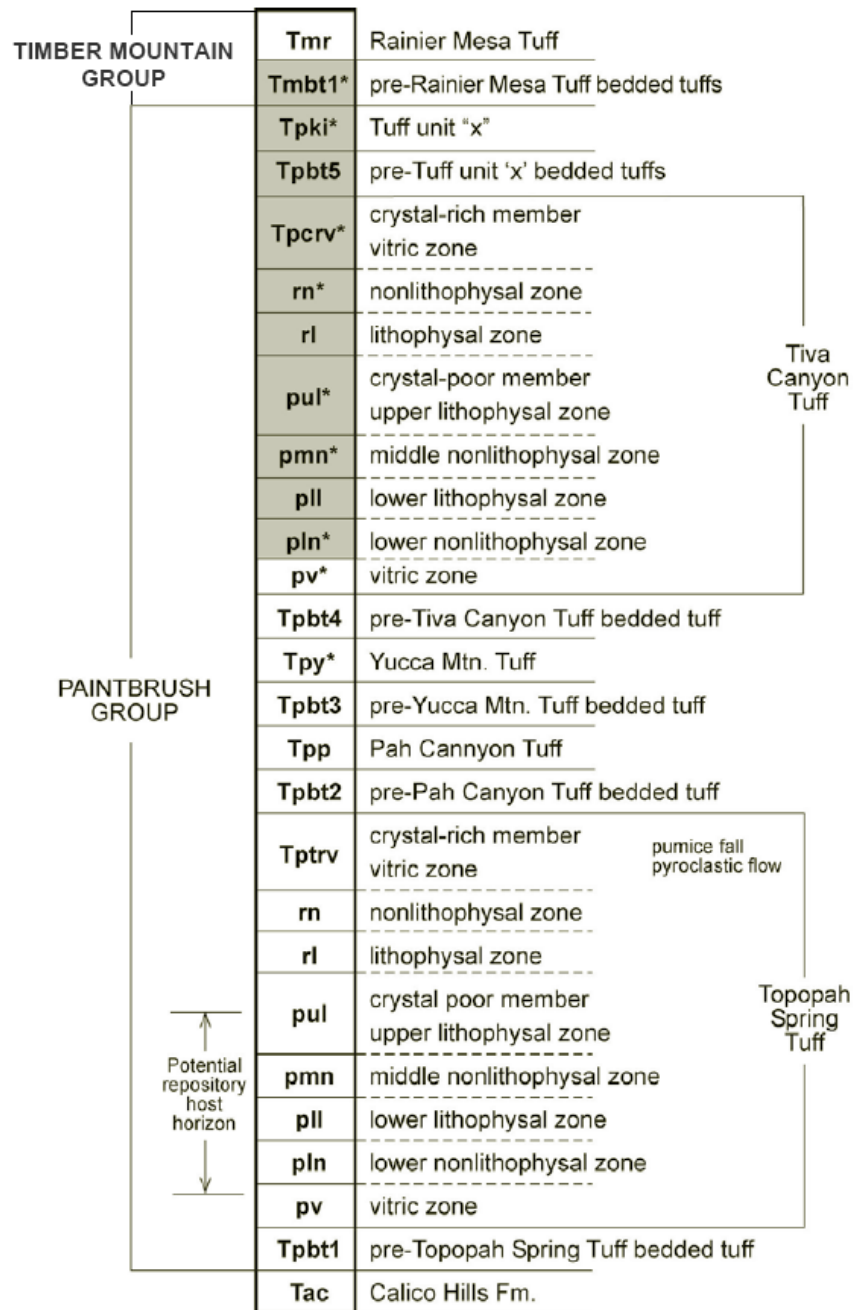


Figure 7.1 Location of Yucca Mountain, NV (Simmons, 2004)



Source: BSC 2002a [DIRS 157829], Figure 233

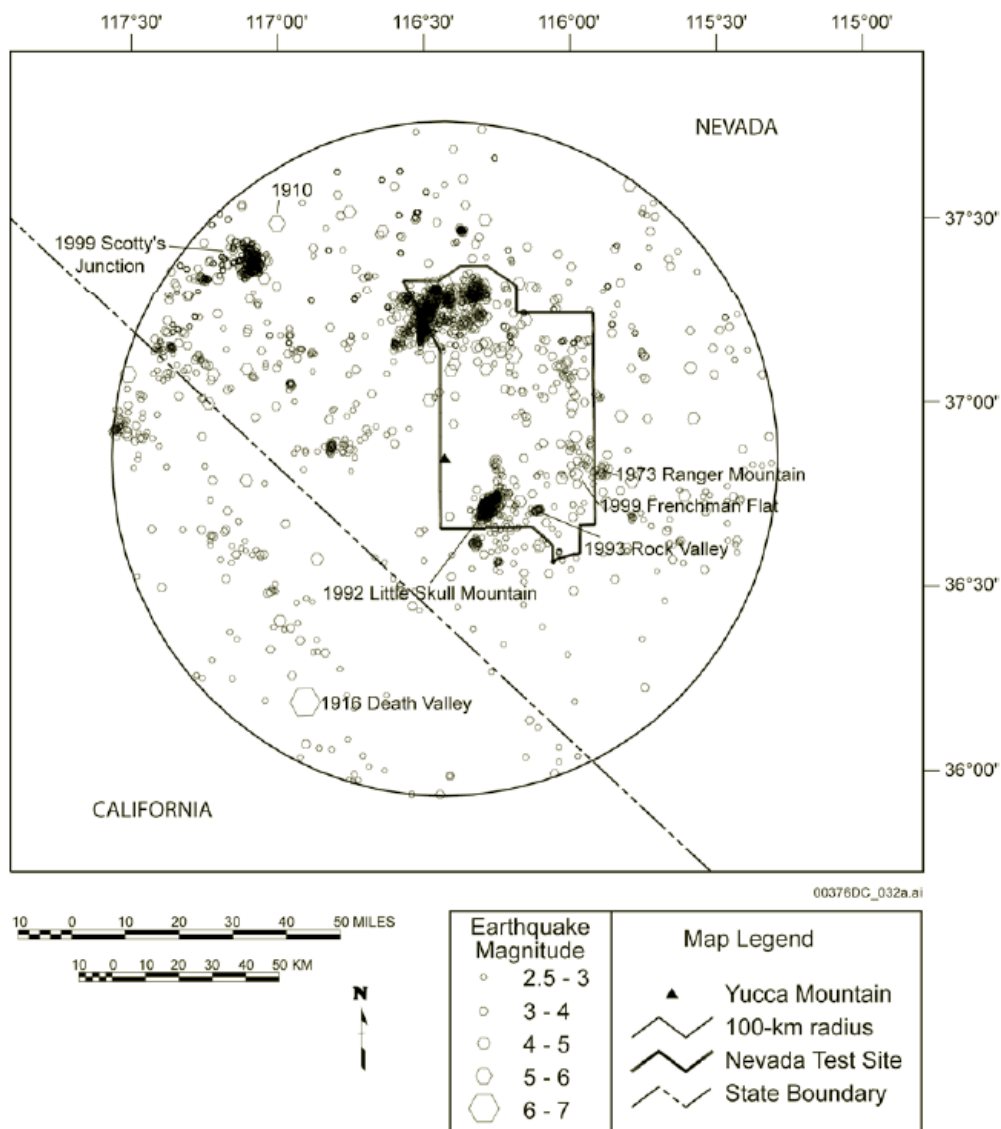
- NOTES: 1. Gray-shaded areas indicate the units that were evaluated in BSC 2002a [DIRS 157829].
 2. Dynamic laboratory tests available for units marked with *.

Figure 7.2 Generalized Lithostratigraphic Column of the Paintbrush Group at Yucca Mountain (Simmons, 2004)

Earthquakes are a safety concern for the location of the long-term repository and Nevada ranks third in the United States for current seismic activity (<http://www.state.nv.us/nucwaste/yucca/seismo01.htm>). Although the threat from earthquakes is not as high as some other regions in the United States, the effects of earthquakes at this site still need to be evaluated because higher safety standard is required on this important project. The history of earthquakes that have happened within 100 km of Yucca Mountain is shown in Figure 7.3

7.2 REVIEW OF SASW TESTING PERFORMED AT YUCCA MOUNTAIN, NV

Because of the importance of this repository, several different profiling techniques have been employed to explore seismically the subsurface in the vicinity of Yucca Mountain. The SASW method, a non-intrusive subsurface exploration technique, is one of these seismic profiling methods requiring no boreholes to perform the survey. All SASW profiles shown here are for the Yucca Mountain Site Characterization Project (YMP). The purpose of the YMP is to use the SASW method to survey the rock (tuff) stiffness in terms of V_s profiles at the proposed repository depth and at associated designated facility locations. The SASW profiles are added to the results from different profiling methods to make the characterization of the repository more complete and robust.



DTNs: MO9906COV99279.000 [DIRS 166582]; MO0006COV00226.000 [DIRS 166581]

Source: CRWMS M&O 2000 [DIRS 151945]

NOTES: Shown are earthquakes from 1904 to 1998. Earthquakes associated with the 1999 Scotty's Junction and 1999 Frenchman Flat sequences are also shown. Significant earthquakes or earthquake sequences are shown with years of occurrence. Activity in the northwestern corner of the Nevada Test Site is related to underground nuclear testing.

Figure 7.3 Earthquake History within 100 km of Yucca Mountain (Simmons, 2004)

7.2.1 SASW Testing Performed between 2000 and 2001

In 2000 and 2001, SASW testing was carried out at two different areas at Yucca Mountain, NV as shown in Figure 7.4 through Figure 7.6. One area is on/near the ridge of Yucca Mountain; the other one is at the potential location of Waste Handling Building (WHB) area. Totally, there were 30 SASW test sites on/near the top of Yucca Mountain (C, D and S sites in Figure 7.4) and 35 SASW sites (Sites SASW-1 through SASW-37 (three of them were combined with other arrays) and one D site in Figure 7.5) at the WHB area. In addition, there were five more SASW testing (Sites T1 through T5 in Figure 7.6) conducted in the Exploratory Study Facility (ESF) tunnel. These tests were performed by the personnel from the University of Texas at Austin lead by Dr. Kenneth H. Stokoe.

In the earlier SASW tests (2000-2001), a two-channel analyzer (HP 3265A) was used to perform the tests. Because only two channels could be used at a time, unlike the SASW test setups described in the other chapters, these SASW tests only utilized two receivers at a time instead of three. At surface sites, Mark Products Model L-4C and L-10 geophones, which have natural frequencies of 1 and 4.5 Hz respectively, were used in the SASW tests. These geophones have excellent performance in the low-frequency range. Especially, the Mark Products Model L-4C geophones perform well in the frequency range from 1 to 300 Hz, which offers crucial information in the deeper soil layers (from measurements in the 1- to 4-Hz range). In the tunnel sites, instead of geophones, accelerometers were used to monitor the surface waves. These accelerometers are Wilcoxon Model 736 accelerometers which have better performance than geophones in the high-frequency range (500 to 15000 Hz) that is required to profile rock within 0.5 to 2 ft of the exposed surface. The SASW tests conducted at the tunnel

sites were directly tested on tuff which can have shear wave velocities in the 2500 to 7500 fps range so that measurements of Rayleigh waves at high frequencies is important.

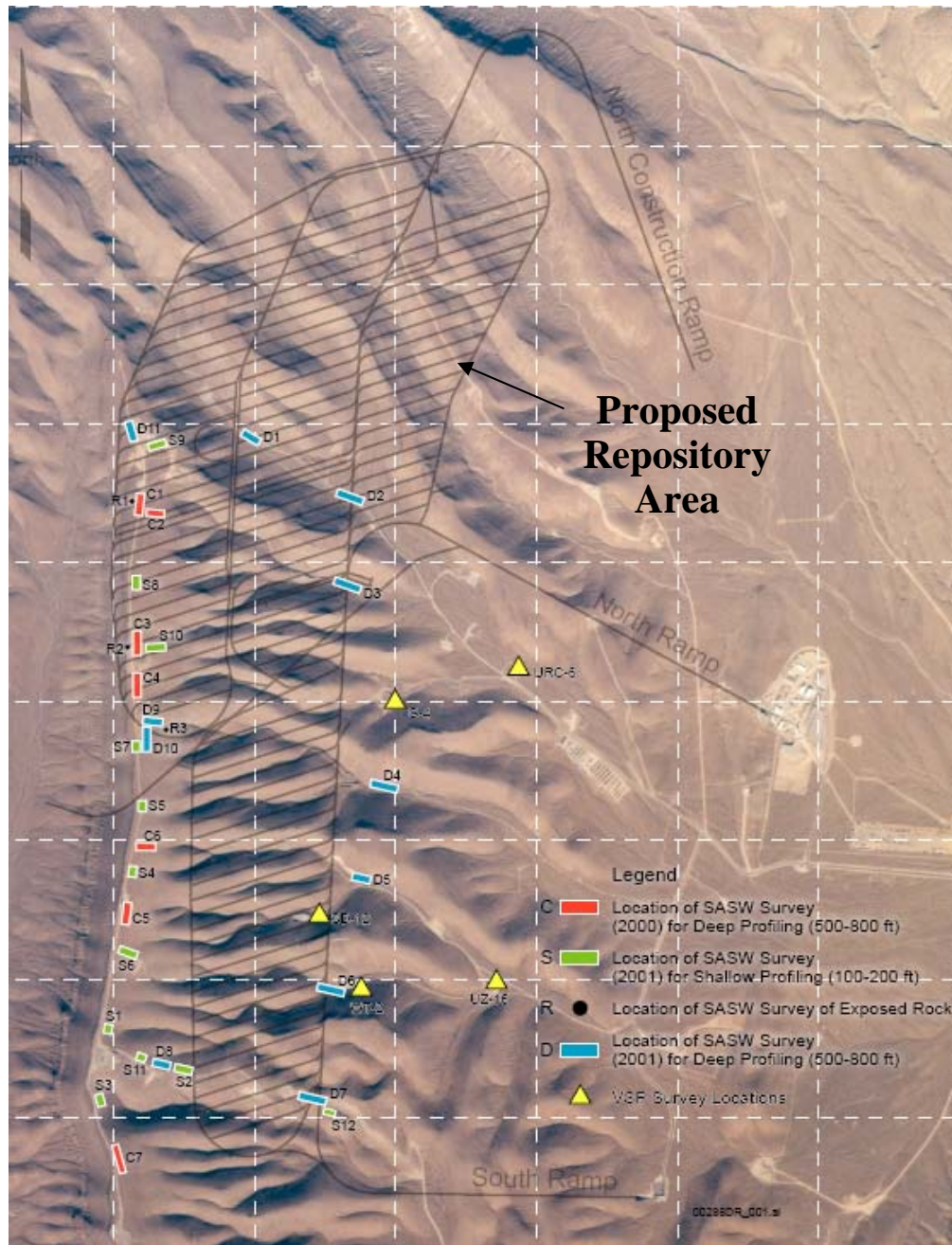


Figure 7.4 Approximate Locations of SASW Tests Performed on/near the Top of Yucca Mountain (from Schuhen, 2004)

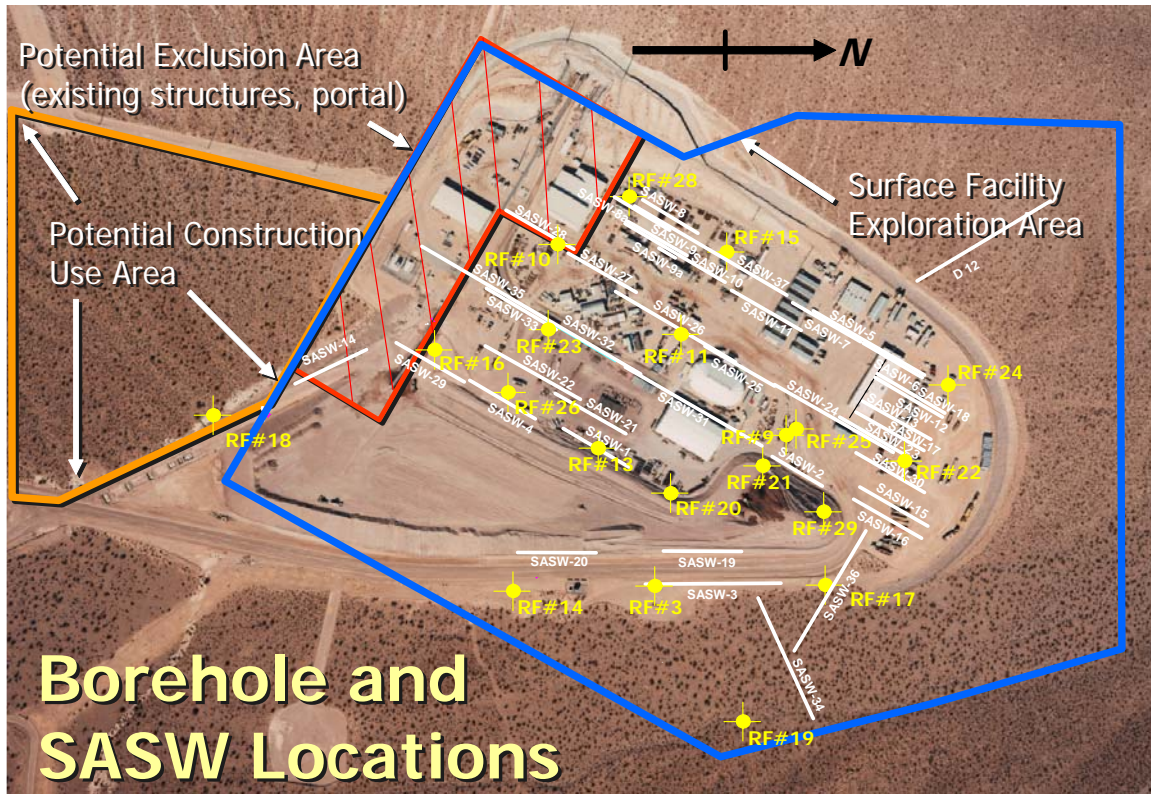


Figure 7.5 Approximate Locations of SASW Tests Performed at the WHB Area

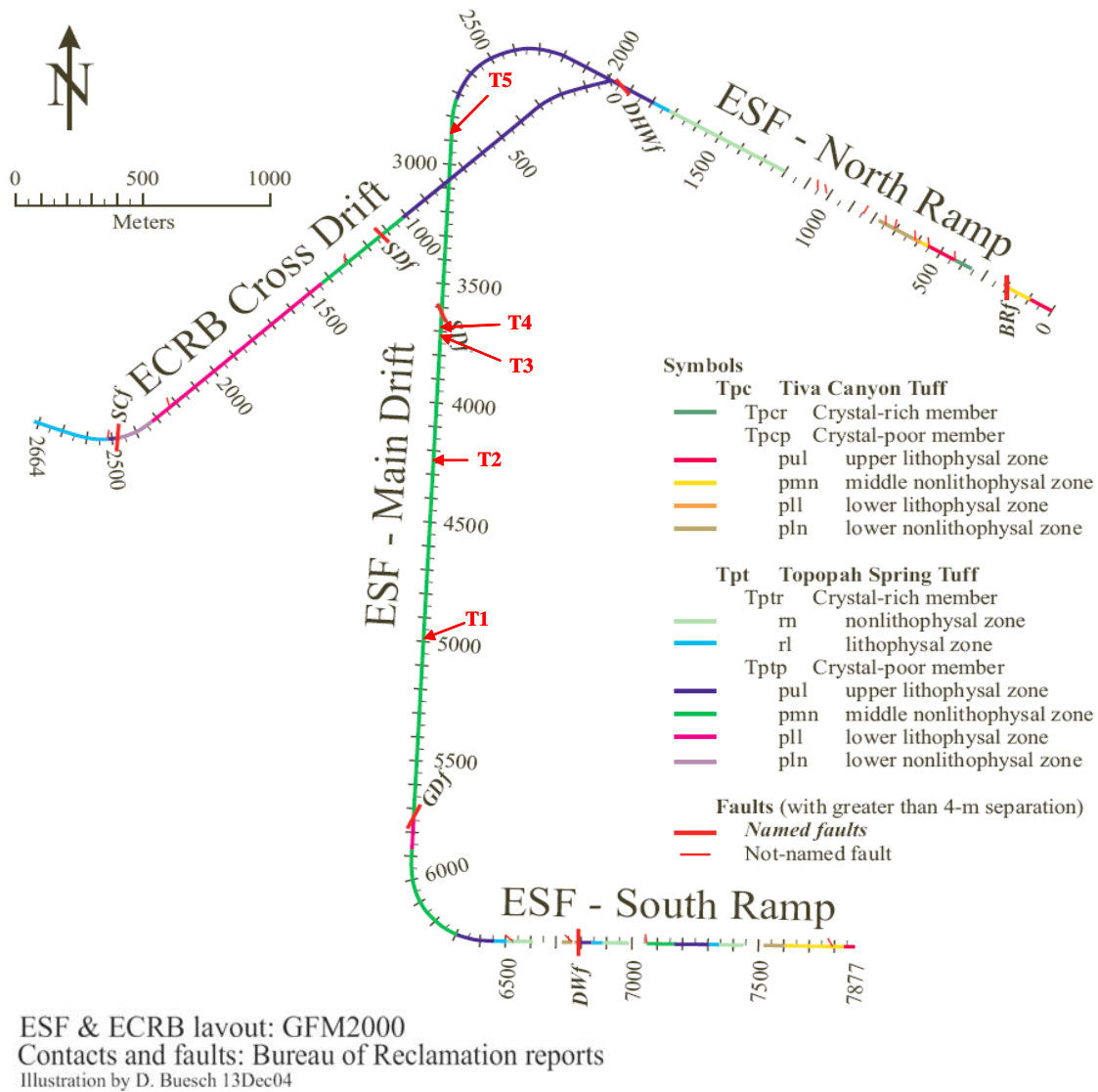


Figure 7.6 Approximate Locations of SASW Tests Performed in the ESF Tunnel (Modified from a Slide of Dr. David Buesch's Presentation at UT-Austin (Buesch, 2005a))

The SASW testing performed on the ground surface employed a vibroseis (Figure 2.11) at the C and D sites on/near the crest of Yucca Mountain and a bulldozer (Figure 2.8) at the WHB area and S sites in the mountain area as the active sources in most case

for test spacings larger than 25 ft. For the shorter-spacing tests and the testing conducted in the tunnels, a sledge hammer or a rock hammer was adapted to generate the surface waves. Typical spacings for the SASW test performed at the surface sites are 3, 6, 12, 25, 50, 100 and 200 ft. At some deep profiling sites (i.e. C and D sites at the crest of Yucca Mountain and SASW-35, 36 and 37 sites at WHB area), additional receiver spacings of 400, 600, (650) and 800 ft were used. The general deployment of the source and receivers for SASW testing at Yucca Mountain is illustrated in Figure 2.18. For shorter spacings (no more than 25 ft), both forward and reverse directions tests were conducted. For larger spacings, however, the SASW testing was only carried out in the forward direction because spacing limitations at the test locations. (The source was never allowed to move off the existing roads and into the deposit.) In the tunnel sites, the test spacing is much shorter than the ones on the surface sites. Test spacings of 6 in. and 1, 2, 4, 8, 16, 32 ft were typically used in the ESF tunnel and the tests were performed in both the forward and reverse directions.

7.2.2 SASW Testing Performed between 2004 and 2005

Because the lack of data between depths of 700 ft, the bottom of most SASW profiles from the tests carried out in 2000 and 2001 on top of Yucca Mountain, and 1000 ft (the approximate depth of the ESF tunnel where five SASW were performed in 2001), additional SASW tests were required. During 2004 and 2005, more SASW tests were performed by the University of Texas at Austin in several areas around Yucca Mountain region and in two different tunnel sections underground as shown in Figures 7.7 through 7.9. The surface areas included the mountain area (YM sites), the North Portal Facility area (NPF Sites), and the Aging Pad area (AP Sites) (see Figure 7.7). The two underground tunnel sections are the Exploratory Study Facility (ESF Sites) and the Enhanced Characterization of the Repository Block (ECRB Sites) tunnels. In total, 45

sites were tested in the two tunnels during this time. These SASW testing locations in the tunnels are marked on the map in Figures 7.8 and 7.9. The total number of sites on the surface was 49.

At the surface sites (YM, NPF and AP sites), especially at the mountain (YM) sites, V_s profiles over 1200 ft deep were desired because of the depth of the planned repository block and the lack of data at the depths between 700 and 1500 ft. Therefore, Liquidator, which can generate more vibratory energy than other vibration truck in low-frequency range, was used as the active SASW source. For shorter spacings or SASW tests in the ESF and ECRB tunnels, a sledge hammer and a rock hammer was adequate to generate the surface waves needed for SASW testing.

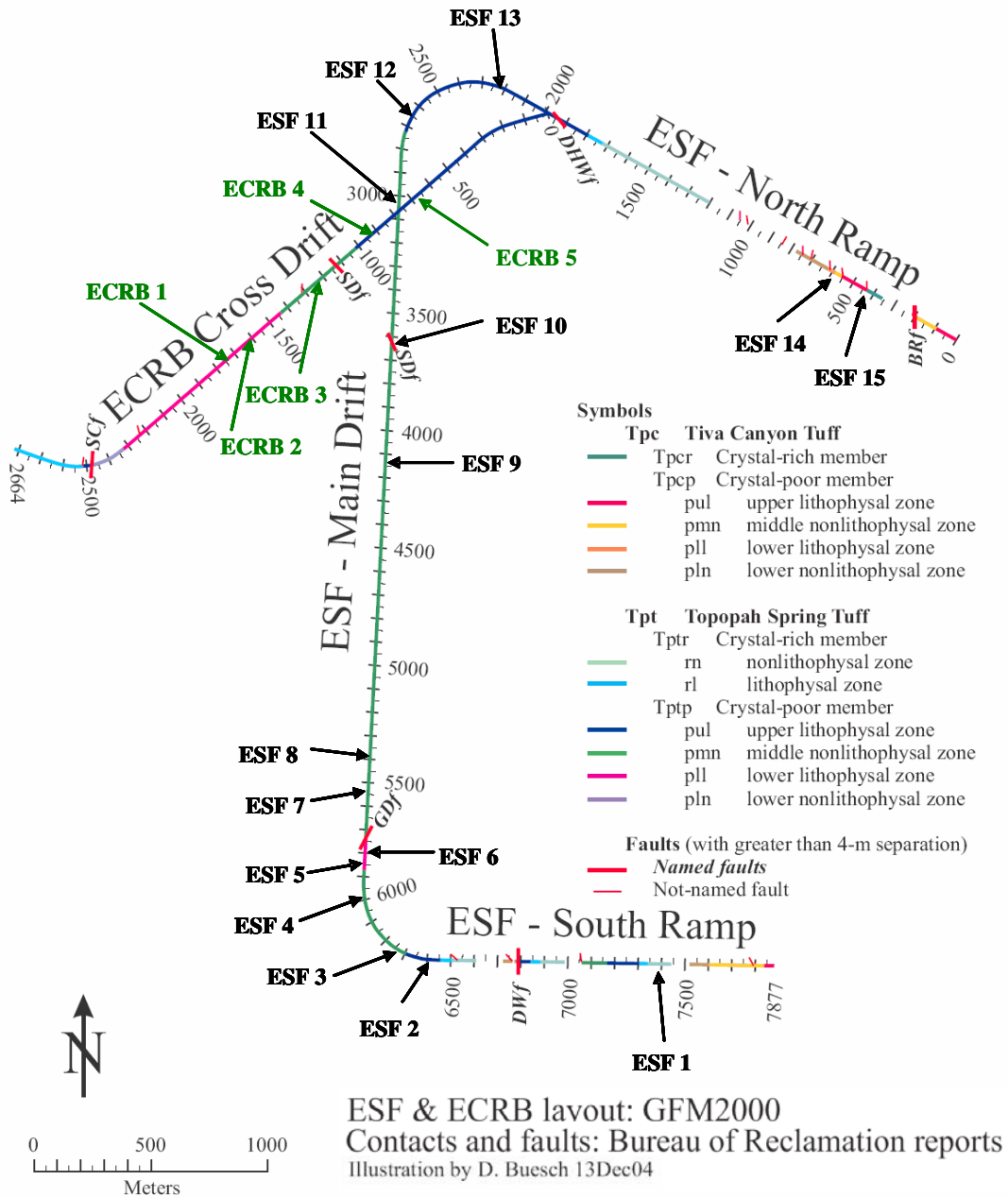


Figure 7.8 Approximate Locations of the SASW Tests Performed in the ESF and ECRB Tunnels Performed in 2004 (Modified from a Slide of Dr. David Buesch's Presentation at UT-Austin (Buesch, 2005a))

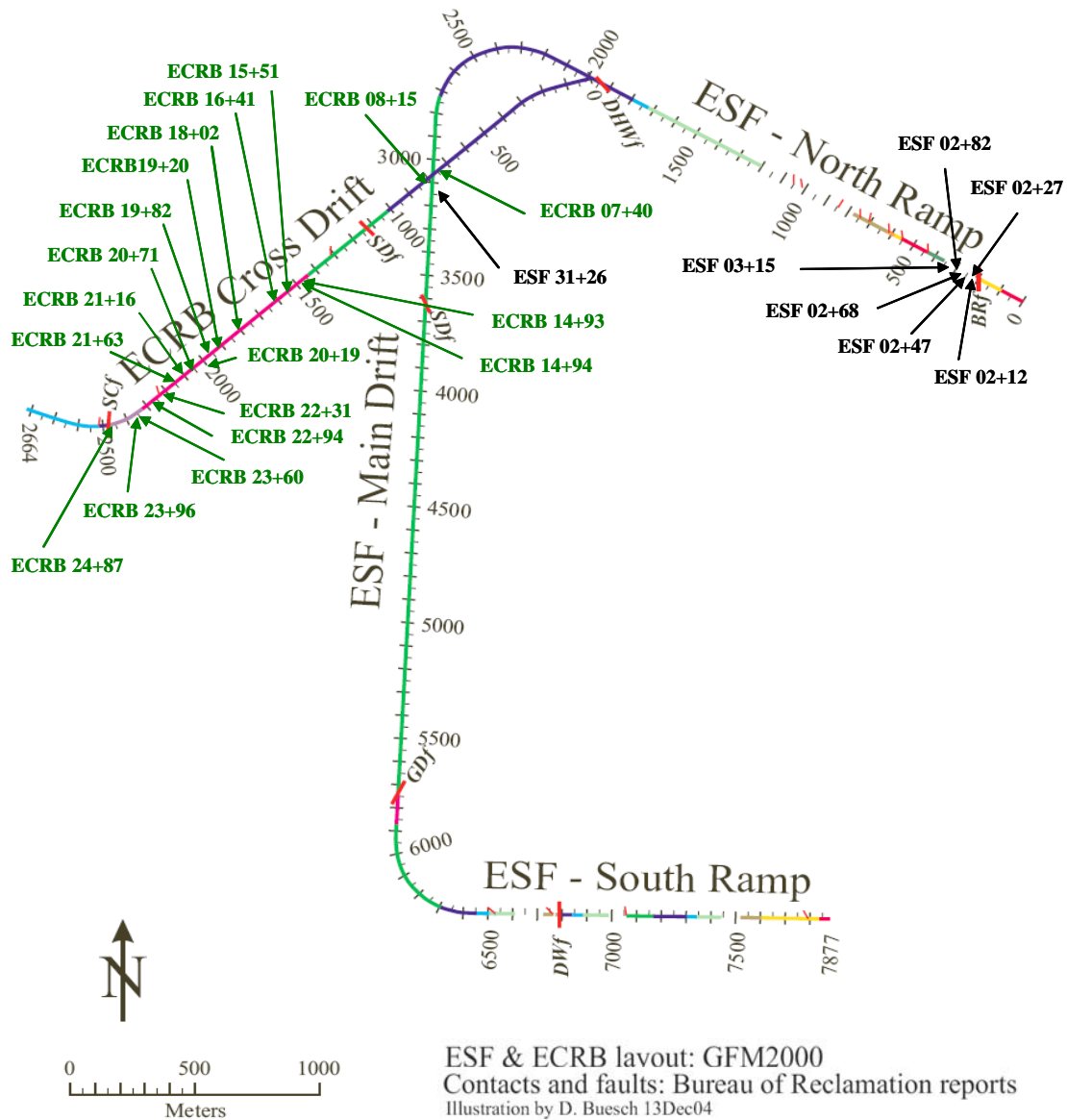


Figure 7.9 Approximate Locations of the SASW Tests Performed in the ESF and ECRB Tunnels Performed in 2005 (Modified from a Slide of Dr. David Buesch's Presentation at UT-Austin (Buesch, 2005a))

During 2004 and 2005, both a Hewlett-Packard (HP) and an Agilent 35670A Dynamic Signal Analyzers were used as the recording devices in the YMP for SASW

testing. Both of them are four-channel analyzers and they are almost identical but with different manufacturer names. These analyzers can record the signals detected by the sensors (geophones or accelerometers) and perform the FFT calculations to generate the phase plots of paired sensors. These phase plots allow the field test team to judge if the any further tests for specific spacings are needed. Because more channels were available, the SASW test arrangements were different from the tests conducted in 2000 and 2001. Instead of two receivers, three receivers were employed in each SASW setup. By doing so, data from two spacings were collected from one test array at a time. This saved about 50% of the testing time for the same number of test spacings compared to the setup using only two receivers.

The general test spacings at the surface and tunnel sites are similar to those used in 2000 and 2001 but the maximum spacings used at surface sites are larger due to the larger energy and lower operating frequency of Liquidator. The maximum spacings used were 750, 1000, 1200 or 1500 ft at different surface sites. At the surface sites, geophones were used to detect the Rayleigh waves generated by the active source. The same two types of geophones were employed in these SASW tests as in the 2000 and 2001 tests. Sometimes, the temperature at the surface sites was as high as 110 degree Fahrenheit. Therefore, some insulation materials and cooling wraps which did not interfere with the function of the geophones were used to assure the performance of the geophones was not affected by the high temperatures. In tunnel sites, the same accelerometers, Wilcoxon Model 736 accelerometers, were employed. As with the testing at the surface sites, three accelerometers were used to measure two receiver spacings at a time.

7.3 TESTING RESULTS IN TERMS OF V_s PROFILES IN TERMS OF V_s PROFILES

Because of the importance of the YMP, several different seismic profiling techniques were conducted at the Yucca mountain areas, but mainly at the WHB area. The types of tests are the SASW, downhole and suspension logging methods. The SASW tests were performed at the Yucca Mountain (YM, C, D and S sites), Waste Handling Building (WHB) area, North Portal Facility (NPF) sites, and Aging Pad (AP) sites and in the ESF and ECRB tunnels. The downhole profiles included in this study were obtained at mountain (8 profiles) and WHB areas (17 profiles from 16 boreholes). As to the available suspension logging profiles, all of them (16 profiles) were from the WHB area. In addition to the three profiling methods mentioned above, there were some other tests performed in the mountain area and tunnels. One of them was seismic tomography survey performed in the tunnels by NSA Engineering, Inc. Another one is also a seismic tomography survey but it was conducted in the area between the crest of Yucca Mountain and the ESF tunnel for the repository horizon. In addition, several vertical seismic profiling (VSP) were performed in the mountain area by Lawrence Berkeley National Laboratory. Some laboratory test results from free-free resonant column tests that were performed at UT-Austin are also discussed here.

7.3.1 SASW Testing

As discussed earlier, the SASW tests of Yucca Mountain Project were performed in two different phases. The first one was in 2000 and 2001 which used a traditional vibroseis to perform profiling to depths of about 700 ft. In addition, five SASW tests were conducted in the ESF tunnel. Because of lack of SASW data at the depths between 700 (bottom of SASW profiles) and 1000 ft (location of potential repository) at the crest of Yucca Mountain sites, the second phase of SASW testing was conducted to perform deeper profiling in the mountain area and at other location of interest.

Therefore, Liquidator, which is capable to generate more energy at low frequencies, was employed to conduct the SASW test in 2004 and 2005 at the surface sites. In addition, more SASW testing was conducted in the ESF and ECRB tunnels.

7.3.1.1 SASW Testing Performed in 2000 and 2001

During 2000 to 2001, in total, there were 30 sites tested on the crest of Yucca Mountain, 35 sites at the WHB area and five sites in the ESF tunnel. The information and V_S profiles of these SASW tests are discussed below.

● *Testing on/near Yucca Mountain Crest*

Information of the SASW tests performed on/near the crest on Yucca Mountain is given in Table 7.1. As seen, the shallowest SASW V_S profile is at Site S2 (a bulldozer was used as the seismic source) among the mountain sites. It is only 79 ft deep, the only profile not over 100 ft deep. The deepest SASW profile, in contrast, was obtained in Site C5 which is 750 ft long (a traditional vibroseis truck was used as the seismic source). The site classifications of the sites on the crest of Yucca Mountain fall into two groups, which are “B” and “C” sites. In total, there are 12 “B” sites and 18 “C” sites. Most of the “B” sites are distributed at the middle to southern portion of the crest. The range of $V_{S,30}$ of these sites is from 1621 to 3404 fps. The reason for the wide range in $V_{S,30}$ is explained by viewing Figure 7.10 which presents the 30 SASW V_S profiles and the statistical analysis. As observed, several sites have a velocity inversion in the profiles in the top 100 ft. These inversions may result from some weathering process on the tuff near the surface and/or changes in the rock types. The reason or reasons are not known. As to the COV profile, the COV values are generally smaller than 0.25, except within about 25 ft of the ground surface. This shows the variability caused by weathering near

the surface. In addition, because some of these sites overlapped with the SASW sites performed in 2004 and 2005, further comparisons are discussed in Section 7.3.1.2.

Table 7.1 Information of the 30 SASW Tests Performed on/near the Top of Yucca Mountain during 2000 and 2001

No.	Site Name	Profile Depth (ft)	$V_{s,30}$ (fps)	Site Class	Test Date	Test Performer
1	C1	503	2477	C	12-Sep-00	UTA
2	C2	200	2079	C	13-Sep-00	UTA
3	C3	700	2352	C	13-Sep-00	UTA
4	C4	705	3404	B	14-Sep-00	UTA
5	C5	750	3237	B	14-Sep-00	UTA
6	C6	299	2855	B	15-Sep-00	UTA
7	C7	601	3129	B	15-Sep-00	UTA
8	D1	500	1621	C	9-Jul-01	UTA
9	D2	500	1805	C	10-Jul-01	UTA
10	D3	350	2064	C	10-Jul-01	UTA
11	D4	200	2098	C	11-Jul-01	UTA
12	D5	350	2842	B	11-Jul-01	UTA
13	D6	304	1967	C	11-Jul-01	UTA
14	D7	200	2054	C	12-Jul-01	UTA
15	D8	400	2215	C	13-Jul-01	UTA
16	D9	200	2178	C	13-Jul-01	UTA
17	D10	350	2536	B	13-Jul-01	UTA
18	D11	500	2409	C	14-Jul-01	UTA
19	S1	150	3069	B	18-Jun-01	UTA
20	S2	79	2349	C*	19-Jun-01	UTA
21	S3	201	3102	B	19-Jun-01	UTA
22	S4	201	3056	B	19-Jun-01	UTA
23	S5	160	2838	B	19-Jun-01	UTA
24	S6	132	1972	C	20-Jun-01	UTA
25	S7	161	2648	B	20-Jun-01	UTA
26	S8	175	2575	B	20-Jun-01	UTA
27	S9	150	2156	C	20-Jun-01	UTA
28	S10	150	1936	C	21-Jun-01	UTA
29	S11	100	2495	C	21-Jun-01	UTA
30	S12	120	1942	C	21-Jun-01	UTA

*Based on extrapolated data

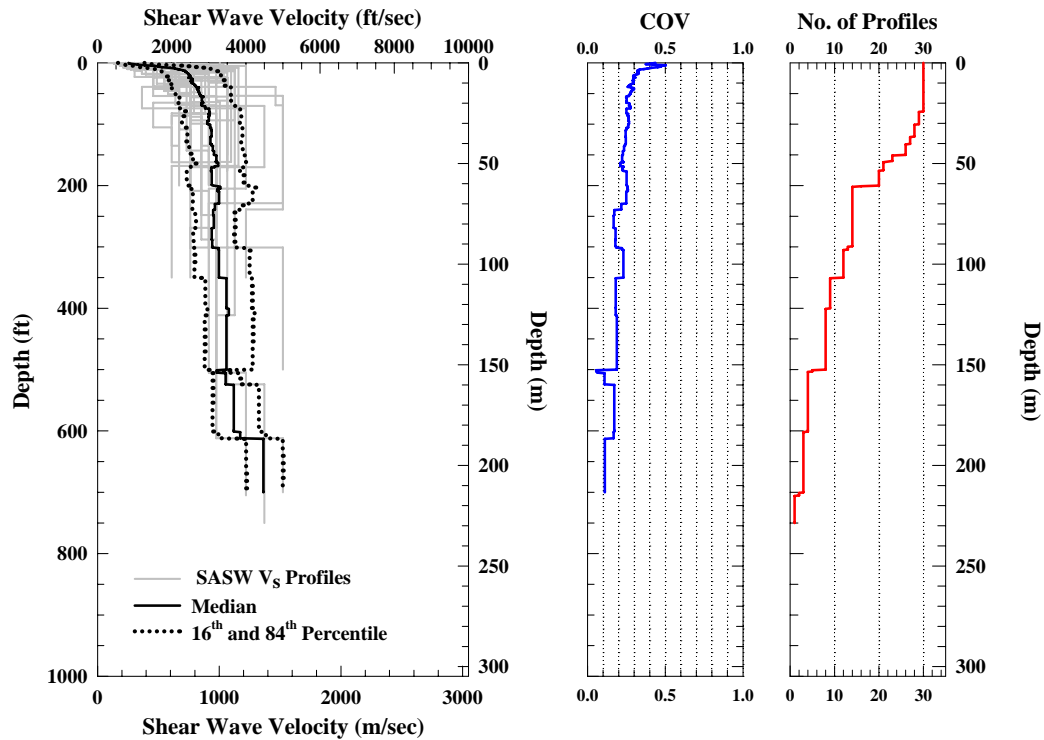


Figure 7.10 Individual Profiles and Statistical Analysis of 30 SASW Tests Performed on/near the Top of Yucca Mountain during 2000 and 2001

- **Testing in the WHB Area**

In the WHB area, most SASW profiles are over or close to 100 ft deep as shown in Table 7.2. The deepest one was obtained at Site SASW 32+35 which is 500 ft deep. At this site, a traditional vibroseis was used instead of a bulldozer. Based on this point, the vibroseis is a better source for deeper profiling than a bulldozer. In contrast, the shallowest SASW is 70 ft which were determined at Sites SASW 17, SASW 23 and SASW 30. These profiles were all determined with the test setup using a bulldozer source, except Sites SASW10+37, SASW 32+35 and SASW 34+36. The $V_{S,30}$ range, from 1419 to 2546 fps, is small compared to the mountain area and the $V_{S,30}$ of most sites is around 2000 fps. As to the site classifications in the WHB area, most sites

classify as “C” sites, with only two sites are classified as “B” sites. However, the $V_{S,30}$ of the two “B” sites are very close to the boundary of “B” and “C” sites which is 2500 fps. The two “B” sites are close to the north portal of the ESF tunnel where tuffs come to the ground surface. In general, the soil/rock deposits at the WHB area have a smaller variation than at the mountain area in the top 100 ft due to geology. In Figure 7.11, the COV profile has values larger than 0.20, except at depths from 30 to 150 ft. The higher COV values below 150 ft are due to the variation of the deeper tuff deposits in this area. This variation is attributed to the identified faulting (darker solid and dashed lines in Figure 7.12) in this area which causes stiffer soil layers to appear at shallower depths at some locations. This higher COV values in the top 25 ft of the profiles is typical of near surface variation.

Table 7.2 Information of 35 SASW Tests Performed at the WHB Area during 2000 and 2001

No.	Site Name	Profile Depth (ft)	V _{s,30} (fps)	Site Class	Test Date	Test Performer
1	SASW1	98	1781	C*	25-Jul-00	UTA
2	SASW2	96	2146	C*	25-Jul-00	UTA
3	SASW3	301	2195	C	25-Jul-00	UTA
4	SASW4	151	1419	C	25-Jul-00	UTA
5	SASW5	150	2050	C	26-Jul-00	UTA
6	SASW6	90	1814	C*	26-Jul-00	UTA
7	SASW7	175	2170	C	26-Jul-00	UTA
8	SASW8	150	2501	B	26-Jul-00	UTA
9	SASW9	90	2113	C*	2-Aug-00	UTA
10	SASW 10 + 37	250	2546	B	27-Jul-00	UTA
					16-Sep-00	
11	SASW11	280	1983	C	27-Jul-00	UTA
12	SASW12	150	2016	C	27-Jul-00	UTA
13	SASW13	150	2051	C	27-Jul-00	UTA
14	SASW14	120	1769	C	31-Jul-00	UTA
15	SASW15	170	2274	C	1-Aug-00	UTA
16	SASW16	127	2299	C	1-Aug-00	UTA
17	SASW17	70	2055	C*	1-Aug-00	UTA
18	SASW18	201	2154	C	1-Aug-00	UTA
19	SASW19	175	2235	C	2-Aug-00	UTA
20	SASW20	90	2063	C*	2-Aug-00	UTA
21	SASW21	85	1759	C*	2-Aug-00	UTA
22	SASW22	100	1466	C	2-Aug-00	UTA
23	SASW23	70	2012	C*	4-Aug-00	UTA
24	SASW24	320	2096	C	4-Aug-00	UTA
25	SASW25	175	1961	C	4-Aug-00	UTA
26	SASW26	301	2114	C	4-Aug-00	UTA
27	SASW27	149	2370	C	4-Aug-00	UTA
28	SASW28	150	2305	C	4-Aug-00	UTA
29	SASW29	141	1465	C	4-Aug-00	UTA
30	SASW30	70	2151	C*	5-Aug-00	UTA
31	SASW31	90	1945	C*	5-Aug-00	UTA
32	SASW 32 + 35	500	1910	C	5-Aug-00	UTA
					16-Sep-00	
33	SASW 33	175	1975	C	5-Aug-00	UTA
34	SASW 34 + 36	301	1801	C	5-Aug-00	UTA
35	D12	200	2394	C	14-Jul-01	UTA

*Based on extrapolated data

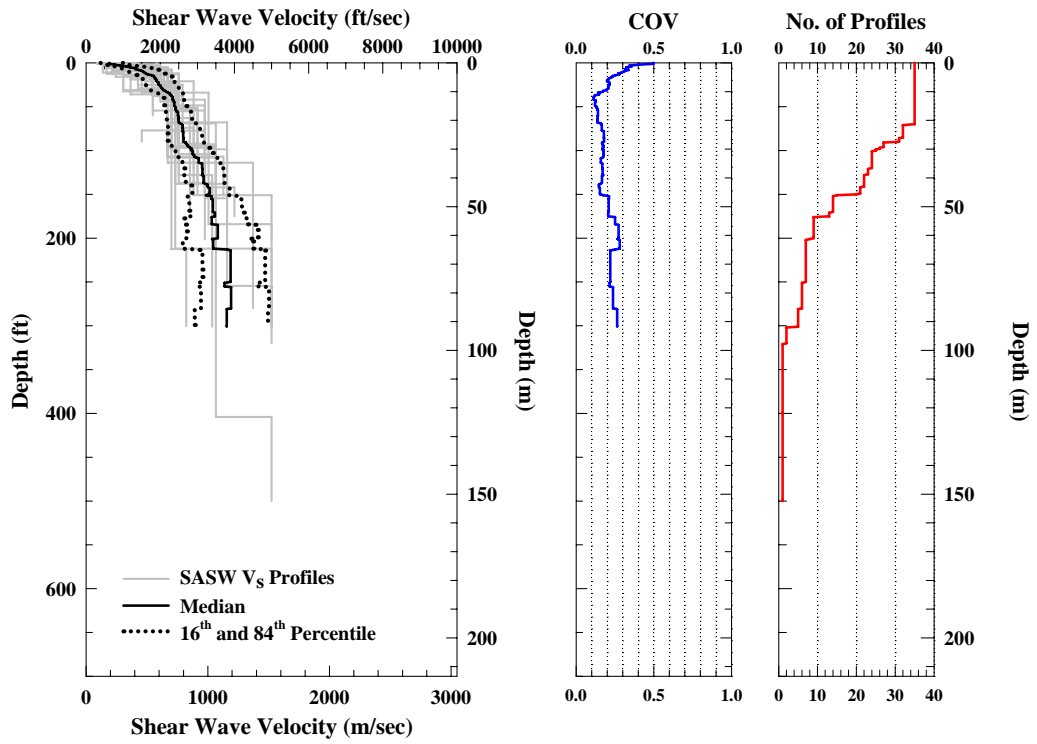


Figure 7.11 Individual Profiles and Statistical Analysis of 35 SASW Tests Performed at the WHB Area during 2000 and 2001

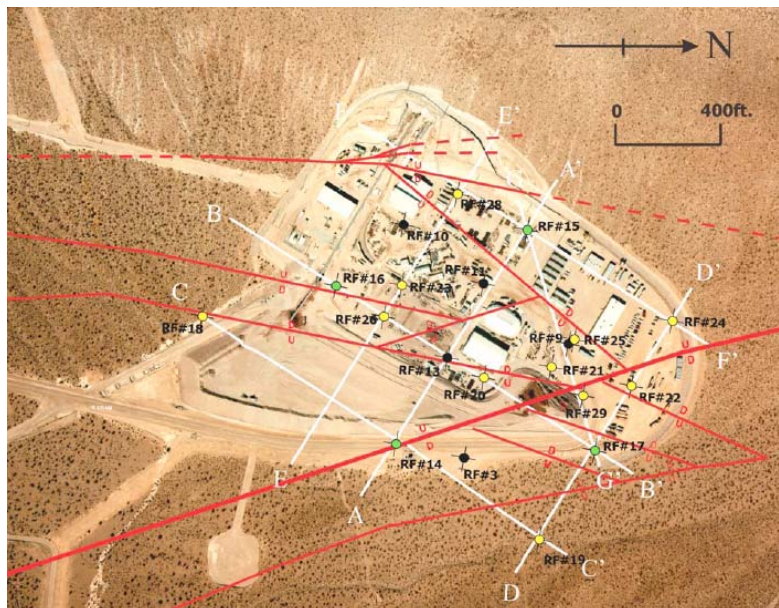


Figure 7.12 Locations of Faults or Possible Faults at the WHB area (BSC, 2004a)

- **Testing in the ESF Tunnel**

In 2001, only five SASW tests (Table 7.3) were conducted in ESF tunnel. According to the geologic map of the ESF and ECRB tunnels (Buesch, 2005a) in Figure 7.6, these five sites are all in the Tptpmn (Topopah Spring middle nonlithophysal) tuff. However, the possible V_S profiles of Site T1 (Figure 7.13) are obviously different from the other four sites. The possible reason for this difference is discussed in Section 7.3.1.2 with the other results of the SASW tunnel tests performed in 2004 and 2005. Because of the low-velocity V_S profile(s) at Site T1, the COV value is over 0.20 over the complete depths of the profiles.

Table 7.3 Information of the Five SASW Tests Performed in the ESF Tunnel in 2001

No.	Site Name	Tunnel	Location	Rock Type	Profile Depth (ft)	Test date	Test Performer
1	T1	ESF	49+92	Tptpmn	20	17-Jul-01	UTA
2	T2	ESF	42+31	Tptpmn	20	17-Jul-01	UTA
3	T3	ESF	37+06	Tptpmn	20	18-Jul-01	UTA
4	T4	ESF	36+75	Tptpmn	20	18-Jul-01	UTA
45	T5	ESF	28+95	Tptpmn	20.	18-Jul-01	UTA

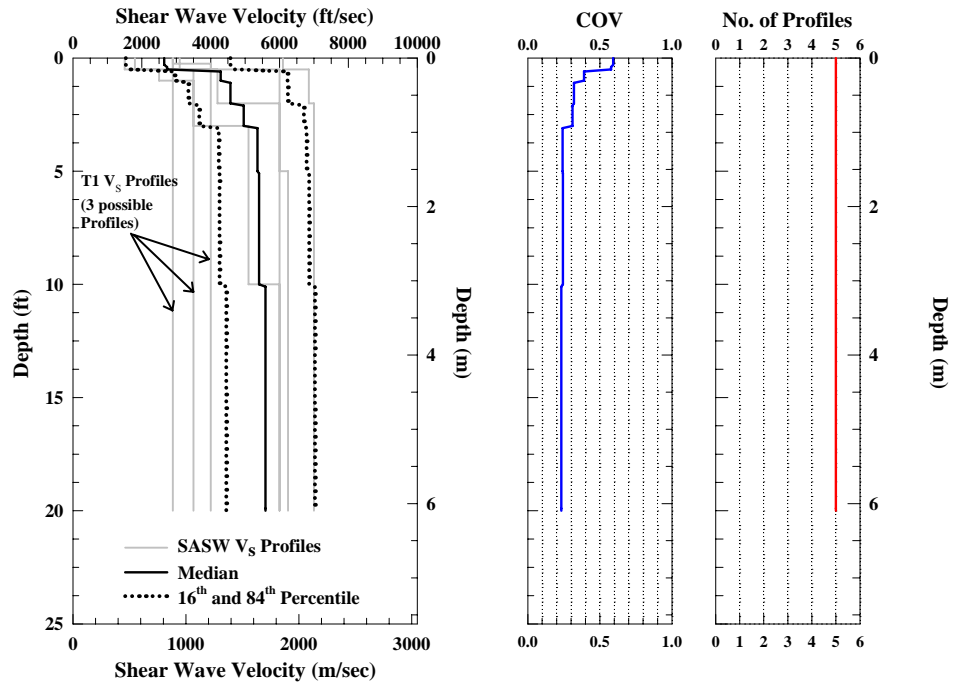


Figure 7.13 Individual Profiles and Statistical Analysis of Five SASW Tests Performed in the ESF Tunnel in 2001

7.3.1.2 SASW Testing Performed in 2004 and 2005

During 2004 and 2005, more SASW tests were conducted at the surface and tunnel sites. In total, 25 YM, 18 NPF and 6 AP sites were tested on the surface and 45 sites were tested in the ESF and ECRB tunnels.

- **Testing in the YM Sites**

The testing information of the 25 YM sites is listed in Tables 7.4. As observed, there is a wide range in the $V_{S,30}$ values from 1530 to 3364 fps. Figure 7.14 shows the V_S profiles of these 25 YM sites. There are some velocity inversions in these profiles, as was observed in Figure 7.10. These profiles show that there are some stiff materials near the surface of the mountain at shallow depths which cause a wide range in $V_{S,30}$. Regarding the site classes based on the SASW profiles, unlike previous SASW

measurements in 2000 and 2001 on/near the crest of Yucca Mountain, only a few (five) sites were determined as “B” sites and the remained 20 sites are “C” sites. The reason could be only three of these 25 sites are distributed along the middle to south portion of the crest of Yucca Mountain where most “B” sites in the 2000 and 2001 SASW surveys were found.

Table 7.4 Information about the 25 SASW Tests Performed in the Mountain Area during 2004 and 2005

No.	Site Name	Profile Depth (ft)	V _{s,30} (fps)	Site Class	Test Date	Test Performer
1	YM 1	1467	2259	C	13-Jul-04	UTA
					18-Aug-04	
2	YM 2	1314	3044	B	9-Jul-04	UTA
					17-Aug-04	
3	YM 3	1121	3364	B	10-Jul-04	UTA
					17-Aug-04	
4	YM 4	970	2990	B	9-Jul-04	UTA
5	YM 5	1496	2206	C	15-Jul-04	UTA
					19-Aug-04	
6	YM 6	456	1845	C	19-Jul-04	UTA
					19-Aug-04	
7	YM 8	833	1747	C	21-Jul-04	UTA
8	YM 10	976	1598	C	22-Jul-04	UTA
					20-Aug-04	
9	YM 12	743	1530	C	7-Jul-04	UTA
10	YM 13	734	1670	C	5-Jul-04	UTA
					14-Aug-04	
11	YM 14A	982	1742	C	2-Jul-04	UTA
					13-Aug-04	
12	YM 14B	982	1885	C	3-Jul-04	UTA
					13-Aug-04	
13	YM 15A	1276	2245	C	29-Jun-04	UTA
					30-Jun-04	
					9-Aug-04	
14	YM 15B	1139	2263	C	30-Jun-04	UTA
					16-Aug-04	
15	YM 16	1149	2311	C	1-Jul-04	UTA
					10-Aug-04	
					16-Aug-04	
16	YM 17	1492	2225	C	14-Jul-04	UTA
					19-Aug-04	
17	YM 18	492	2034	C	1-Jun-05	UTA
18	YM 19	678	3301	B	2-Jun-05	UTA
19	YM 20	965	2268	C	3-Jun-05	UTA
20	YM 21	995	2153	C	7-Jun-05	UTA
21	YM 22	945	1658	C	8-Jun-05	UTA
22	YM 23	1031	1695	C	10-Jun-05	UTA
23	YM 24	451	2525	B	10-Jun-05	UTA
24	YM 25	790	1657	C	11-Jun-05	UTA
25	YM 26	1243	2172	C	13-Jun-05	UTA

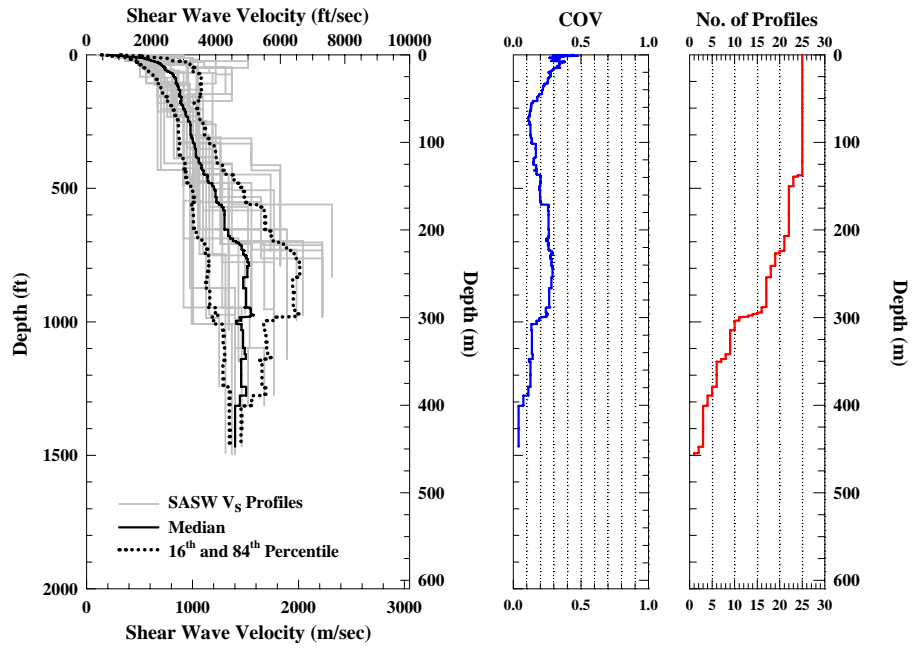


Figure 7.14 Individual Profiles and Statistical Analysis of 25 SASW Tests Performed at the Mountain Area during 2004 and 2005

Among the 25 YM sites, the shallowest SASW V_s profile is 451 ft at Site YM 24. In contrast, the deepest one, 1496 ft, is at Site YM 5. The maximum depth is almost twice the maximum profiling depth in the 2000 and 2001 SASW test at this area. Moreover, most of the 25 SASW V_s profiles are over 750 ft. Figure 7.14 shows the 25 V_s profiles of YM sites and their statistical analysis. Figure 7.15 presents only 19 of the 25 YM sites around the proposed repository area (see Figure 7.4 to locate the repository footprint). However, there is not much difference between the results in Figures 7.14 and 7.15. In addition, it seems that the velocity profiles can be separated into several velocity groups below 600 ft in Figure 7.14. This grouping is not observed in Figure 7.10 because the depths of the SASW profiles were not deep enough to see it. This point also highlights the fact that Liquidator is a better active source than a traditional vibroseis for deep profiling.

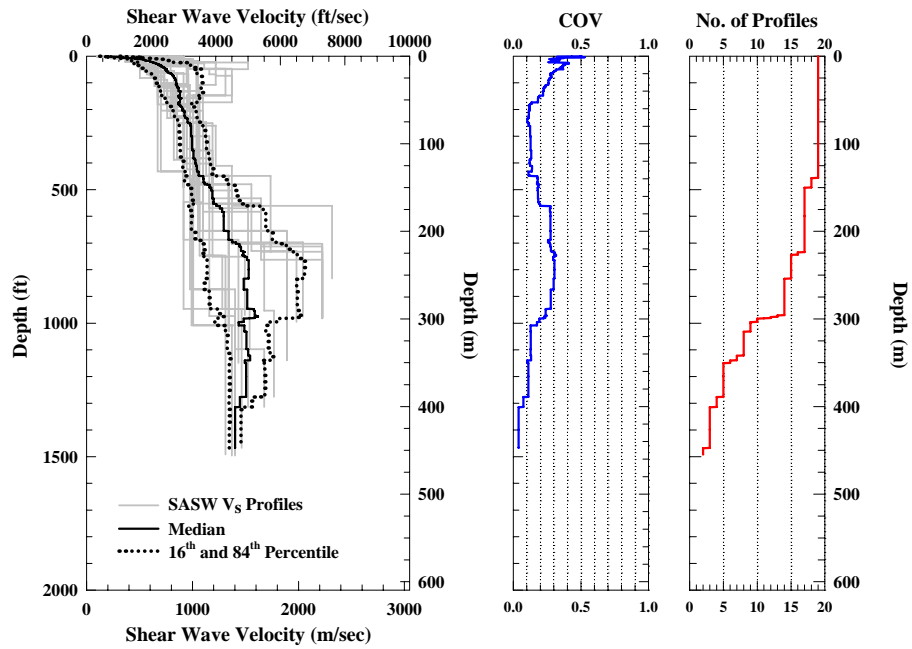


Figure 7.15 Individual Profiles and Statistical Analysis of 19 SASW Tests Performed at the Mountain Area during 2004 and 2005; These Sites are above Proposed Repository Area

Because of the large variation in the V_S profiles determined at the YM sites, the 25 sites are divided into three groups based on their V_S profiles. The first group is “stiffer” sites. This group exhibits V_S values larger than 5800 fps at the bottom of the profiles. The sites are YM 8, YM 10, YM 12, YM 13, YM 14A, YM 14B, YM 15B, YM 21 and YM 25. These nine sites are around the planned repository area, except for Site YM 25. The V_S profiles and corresponding statistical analysis of the stiffer sites are shown in Figure 7.16. The second group is “softer” sites. This group exhibits V_S values that never exceed 5800 fps in the profile. The sites are YM 1, YM 2, YM 3, YM 4, YM 5, YM 6, YM 16, YM 17, YM 23 and YM 26. Site YM 26 is the only site not around the planned repository area. The V_S profiles and statistical analysis of the softer sites are shown in Figure 7.17. The remaining six sites are “neutral” sites whose V_S

profiles are too short to group them into “stiffer” or “softer” categories or they have V_S profiles which are distributed between the first two groups. These “neutral” sites are shown in Figure 7.18.

If only the sites around the proposed repository area are considered, Figures 7.16 and 7.17 can be re-plotted as Figure 7.19 and 7.20 respectively. As seen, there is not much difference between Figures 7.16 and 7.19 and Figures 7.17 and 7.20 in terms of their median V_S profile, the 16th and 84th percentile boundaries and the COV profiles. This comparison is true even in Figures 7.14 or 7.15, where the COV values are larger in the top 180 ft and at the depths from 450 to 1000 ft. The reason for the larger variation in the top 180 ft is the velocity inversions in the shallow V_S profiles as mentioned earlier. The reason for the larger COV values at the depths from 450 to 1000 ft could be geologic variability and localized fracturing in some areas.

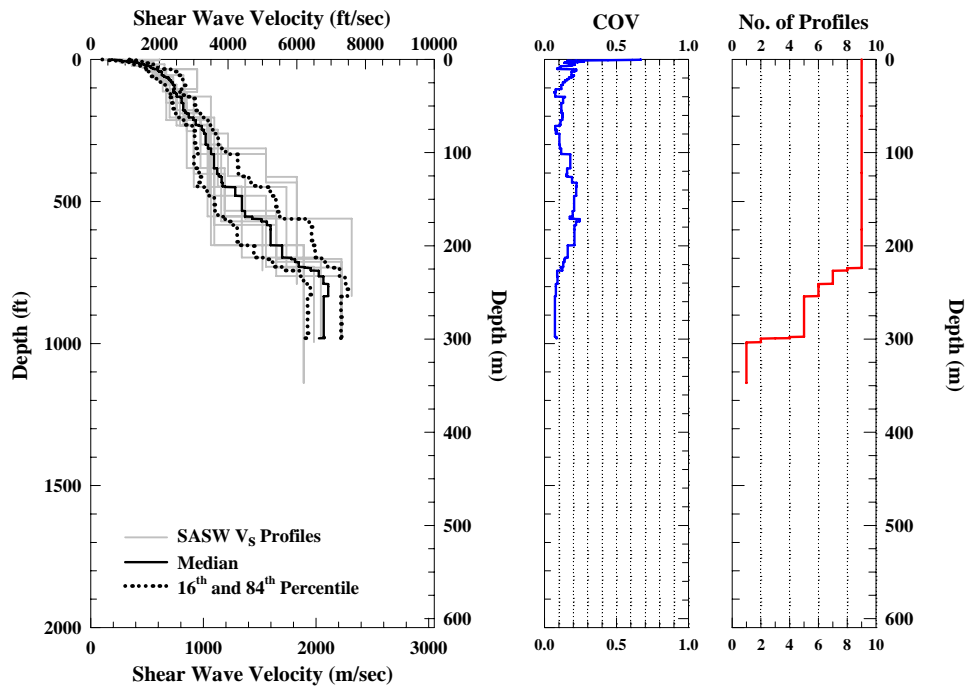


Figure 7.16 Individual Profiles and Statistical Analysis of the Nine “Stiffer” SASW V_S Profiles at the Mountain Area that were Measured during 2004 and 2005

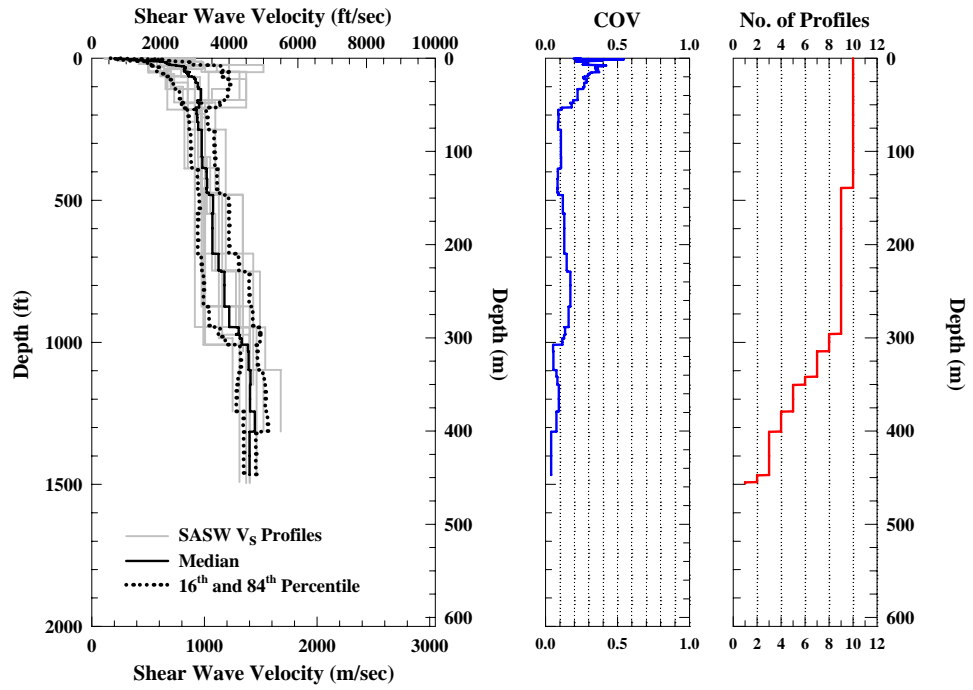


Figure 7.17 Individual Profiles and Statistical Analysis of the Ten “Softer” SASW V_S Profiles at the Mountain Area that were Measured during 2004 and 2005

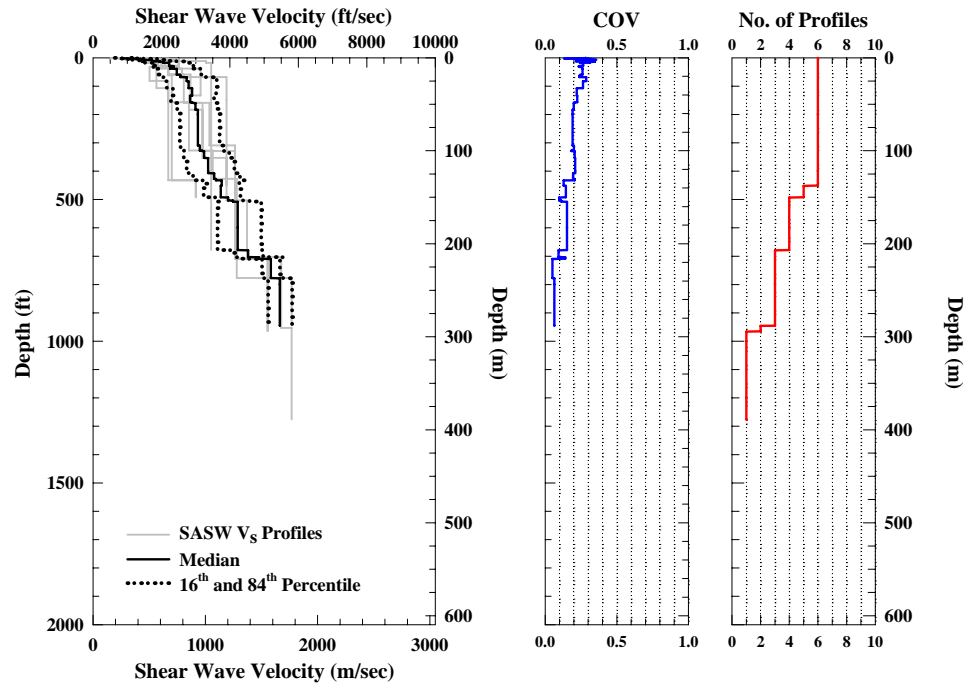


Figure 7.18 Individual Profiles and Statistical Analysis of the Six “Neutral” SASW V_S Profiles at the Mountain Area that were Measured during 2004 and 2005

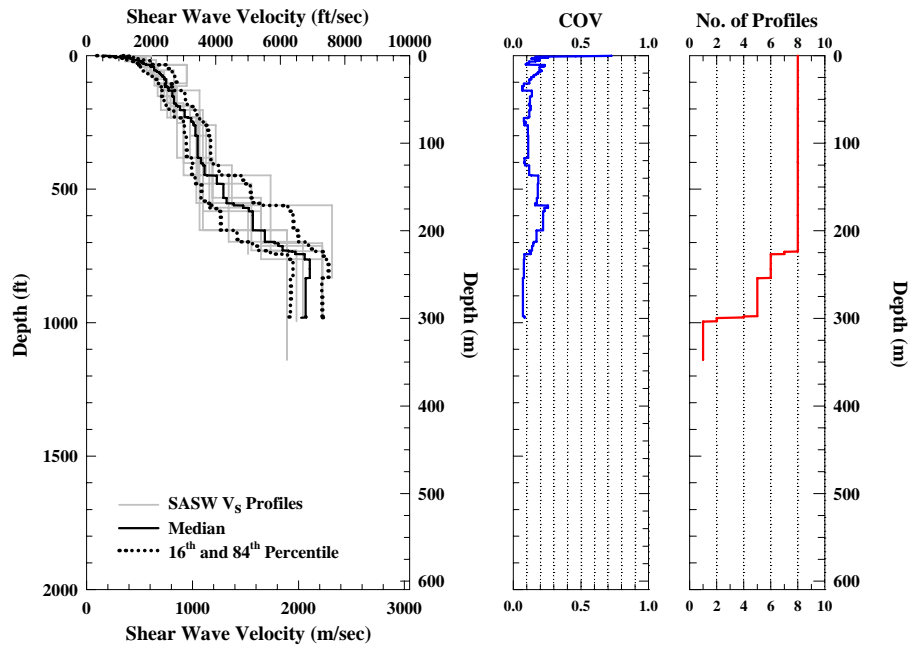


Figure 7.19 Individual Profiles and Statistical Analysis of the Eight “Stiffer” SASW V_s Profiles that were Measured at the Mountain Area and above the Proposed Repository Area during 2004 and 2005

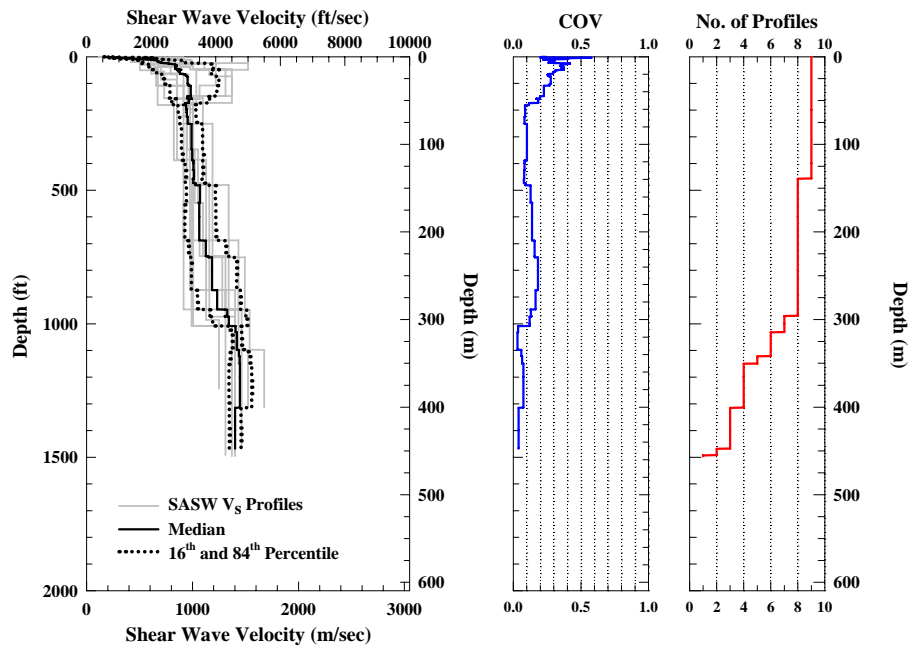


Figure 7.20 Individual Profiles and Statistical Analysis of the Nine “Softer” SASW V_s Profiles that were Measured at the Mountain Area and above the Proposed Repository Area during 2004 and 2005

- ***Testing in the NPF Area***

IN the North Portal Facility (NPF) area, 18 SASW tests were carried out in 2004 and 2005. Table 7.5 presents information about these 18 SASW test sites. Due to a large lateral variation at Site NPF 1, there are three possible profiles at this site. However, these three profiles are only consistent in the top 40 ft. Therefore, geologic variability at Site NPF 1 below 40 ft results in the top 40 ft being the only representative profile that can be used. Therefore, this depth is shown in Table 7.5 for Site NPF 1. The deepest SASW V_S profile in this area is 1472 ft at Site NPF 3 and 9. The site classification based on 17 profiles is “C” sites. Only Site NPF 1 is not classified due to the variability at this site. In addition, the $V_{S,30}$ of these 17 SASW sites is all around 1900 fps. Based on the information from site classification and $V_{S,30}$, a uniform soil deposit near the surface (top 30 m) is expected at the NPF sites. This happens because there is more than 100 ft of alluvium at most of these sites.

In Figure 7.21, the 18 NPF V_S profiles and the statistical analysis results are shown. As seen, the COV profile is quite constant (about 0.10) from 30 to 930 ft. However, below 930 ft the COV value becomes three times larger because of the high velocities in the lower parts of the V_S profiles from Sites NPF 2 and 14, and NPF 3 and 9. Many faults cross this area (as shown in Figure 7.12) so these two sites encounter stiffer layers at shallower depths than the other sites. In Figure 7.21, some “abnormal” profiles can be observed in the depth range of 280 to 430 ft. These profiles are from Site NPF 28 which is located within the WHB area, even though it was named as an NPF site by YMP personnel. Some comparisons between the WHB and NPF SASW sites are made later in this chapter to see possible causes of the V_S profiles at the NPF 28 site being stiffer than the other NPF sites at shallow depths. A new figure which excludes the “abnormal” V_S profiles at the bottom of Sites NPF 2 and 14, NPF 3 and 9, and NPF 28 is

presented in Figure 7.22. As seen, the COV profile has a constant value of 0.10 from about 30 to 1100 ft and has smaller values below 1100 ft as compared to Figure 7.21.

Table 7.5 Information of the 18 SASW Tests Performed at the NPF Area during 2004 and 2005

No.	Site Name	Profile Depth (ft)	V _{s,30} (fps)	Site Class	Test Date	Test Performer
1	NPF 1	40	N/A*	N/A*	16-Jul-04	UTA
					23-Jul-04	
2	NPF 2 and 14	1426	2000	C	16-Jul-04	UTA
3	NPF 3 and 9	1472	1832	C	17-Jul-04	UTA
					21-Aug-04	
4	NPF 10	1404	1830	C	23-Aug-04	UTA
5	NPF 12	1434	1727	C	24-Aug-04	UTA
					21-Aug-04	
6	NPF 16	533	1859	C	23-Jul-04	UTA
					24-Jul-04	
7	NPF 17	1409	2193	C	23-Jul-04	UTA
					24-Jul-04	
					10-Aug-04	
8	NPF 18	487	2002	C	24-May-05	UTA
9	NPF 19	751	1953	C	24-May-05	UTA
10	NPF 20	815	1907	C	25-May-05	UTA
11	NPF 21	743	1892	C	25-May-05	UTA
12	NPF 22	572	1930	C	26-May-05	UTA
13	NPF 23	1340	1822	C	26-May-05	UTA
14	NPF 24	949	1780	C	27-May-05	UTA
15	NPF 25	1345	1661	C	28-May-05	UTA
16	NPF 26	552	1769	C	28-May-05	UTA
17	NPF 27	635	1891	C	28-May-05	UTA
18	NPF 28	424	1787	C	11-Jun-05	UTA

* Site NPF 1 was not classified due to high lateral variability at this site

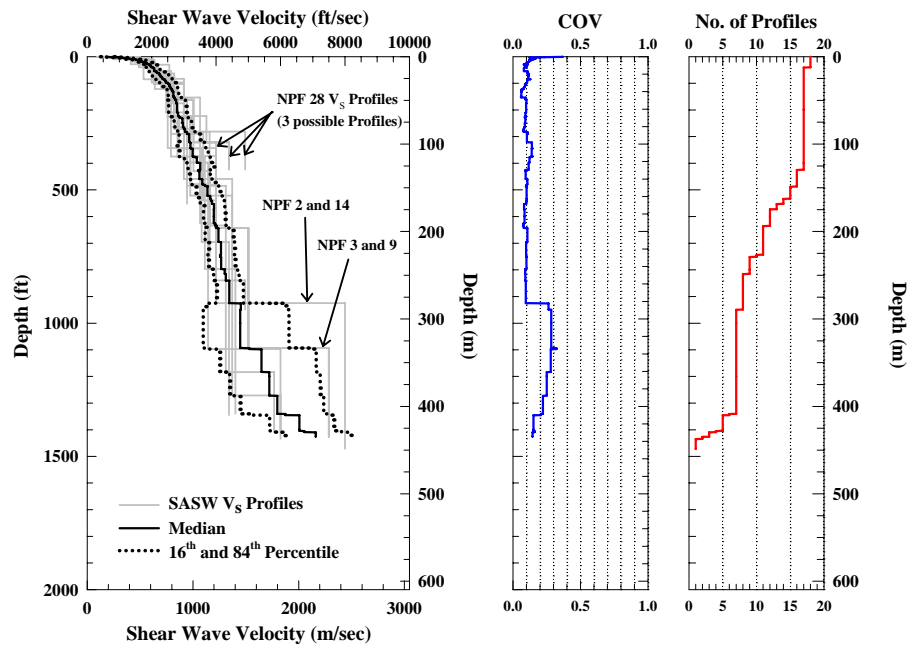


Figure 7.21 Individual Profiles and Statistical Analyses of 18 SASW Tests Performed at NPF Area during 2004 and 2005

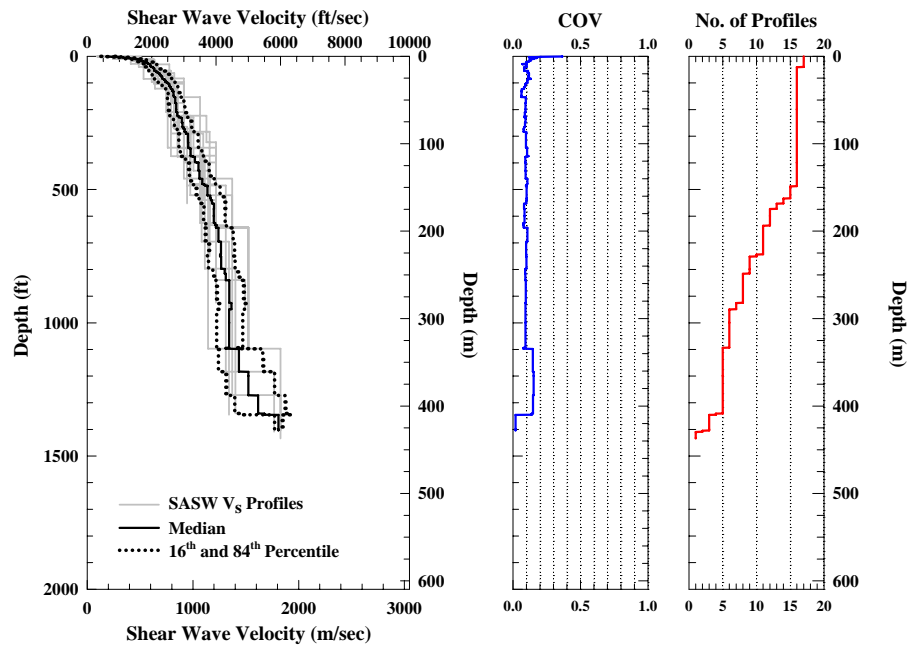


Figure 7.22 Individual Profiles and Statistical Analyses of 17 SASW Tests Performed at NPF Area without Site NPF 28 and Bottom V_s profiles of Sites NPF 2 and 14 and NPF 3 and 9 during 2004 and 2005

- **Testing in the AP Area**

At the Aging Pad area, six SASW tests were carried out in 2004 and 2005. The area (see Figure 7.7) that was covered by the SASW testing is about 800 ft by 1000 ft. Information about these six SASW testing is presented in Table 7.6. The required profiling depth was not as deep as the mountain or NPF areas so the deepest V_s profile is 949 ft at Site AP 8. The shortest one is about 490 ft at Site AP 5. Based on the $V_{s,30}$ calculated from the top 30 m in V_s profiles, all six sites are classified as “C” sites. The range of $V_{s,30}$ of these six profiles is from 1927 to 2231 fps, with an average value about 2100 fps. This information shows the top 100 ft (30 m) is very uniform compared to the other areas. This uniformity is attributed to the greater thickness of the alluvium and bedded tuffs. The six SASW V_s profiles are plotted in Figure 7.23 with their statistical information. As seen in the COV profile, in average, this area has a very low COV value, about 0.01, from surface to the depth of about 600 ft.

Table 7.6 Information about the Six SASW Tests Performed at the Aging Pad (AP) Area during 2004 and 2005

No.	Site Name	Profile Depth (ft)	$V_{s,30}$ (fps)	Site Class	Test Date	Test Performer
1	AP 1	587	2163	C	25-Aug-04	UTA
2	AP 3	564	2143	C	25-Aug-04	UTA
3	AP 5	491	2231	C	25-Aug-04	UTA
4	AP 6	670	2085	C	31-May-05	UTA
5	AP 7	796	2087	C	31-May-05	UTA
6	AP 8	949	1927	C	31-May-05	UTA

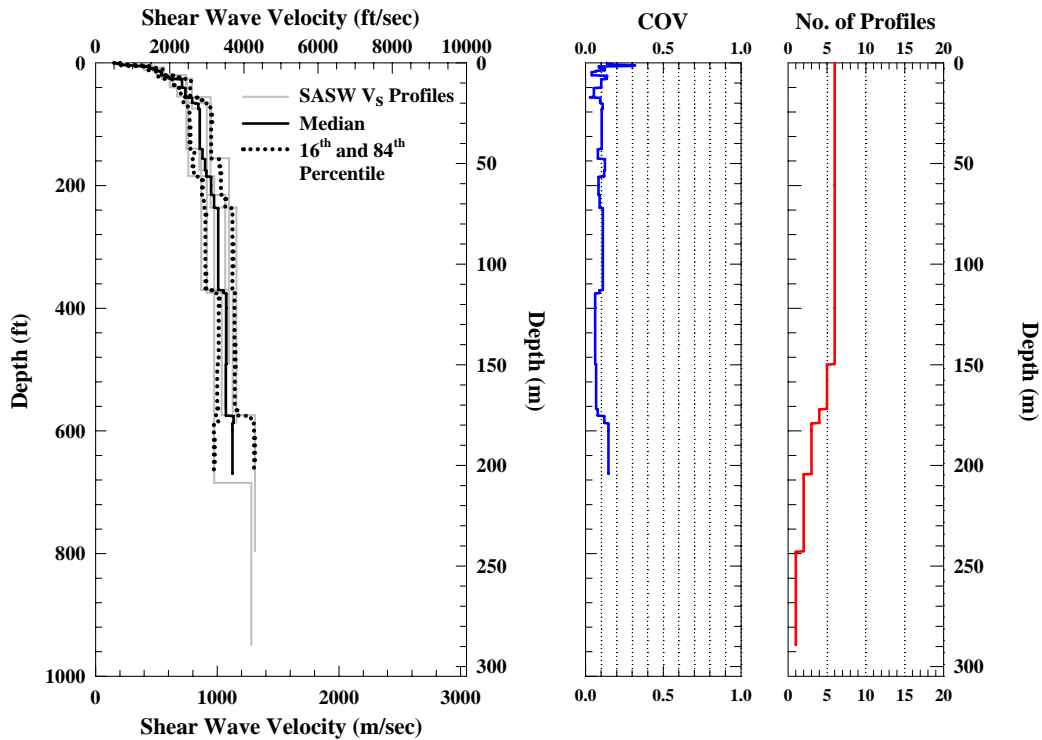


Figure 7.23 Individual Profiles and Statistical Analysis of the Six SASW V_S Profiles in the AP Area during 2004 and 2005

- **Testing in the ESF and ECRB Tunnels**

In the underground sites, there were 22 SASW tests conducted in the ESF tunnel and 23 tests in the ECRB tunnel in 2004 and 2005. The number is nine times as many tests as performed in the ESF tunnel in 2001. Based on the geologic information of the ESF and ECRB tunnels offered by Dr. David Buesch (Buesch 2005b), there are nine types of tuffs in the tunnel sites tested by the SASW method. The tuff types are listed in Table 7.7. The shear wave velocity at depths of 10 to 15 ft behind the tunnel face in each V_S profile should be adequate to represent the V_S of the tuff without the influence of stress release due to the tunnel excavation. Therefore, the median and 16th and 84th percentile boundaries are based on the bottom portion of the profiles for the SASW

measurements in each type of tuff. The SASW V_S profiles are divided into seven groups as discussed below.

First, there is only a single V_S profile obtained from the following types of tuffs: Tpcpmn-II (Tpcpmn (Tiva Canyon Tuff: middle nonlithophysal zone) or TpcplI (Tiva Canyon Tuff: lower lithophysal zone)), Tpcrn2 (Tiva Canyon Tuff: crystal-rich mixed-purric subzone) and Tptrn (Topopah Spring Tuff: crystal-rich nonlithophysal zone) Tuffs respectively (Figure 7.24(a)). Even they belong to three different types of tuffs, they have similar velocities, about 6200 fps, in the bottom of the shear wave velocity profiles.

For the Tmbt1 tuff (pre-Rainier Mesa Tuff bedded tuffs), all V_S profiles agree with each other except profile 1 of ESF 02+12 below 12 ft deep (Figure 7.24(b)). The ESF 02+12 site is close to the boundary between two different rock types, Tmbt1 and Tpcpmn, so this could be the reason for the difference. It makes more sense when comparing the V_S profiles of ESF 02+12 and ESF 14 (Tpcpmn-II).

As seen in Figure 7.24(c), the V_S profiles of the Tпки (Tuff unit “X”) tuff are consistent, except for Site ESF 03+15. Site ESF 03+15 is near the boundary between Tпки and Tpcr tuffs, with later seems stiffer than former based on the comparison of V_S profiles of Tпки and Tpcrn2 (ESF 15) tuffs. So, the “boundary effect” may be the reason for the inconsistency.

When comparing the Ttpul (Topopah Spring Tuff: crystal-poor upper lithophysal zone) tuff V_S profiles (Figure 7.24(d)), these profiles are inconsistent above the top 12 ft, but they reach similar V_S values below that depth. In general, they agree to each other.

Table 7.7 Information about the 45 SASW Tests Performed in the ESF and ECRB Tunnels during 2004 and 2005

No.	Site Name	No. of Sample	Tunnel	Location	Tuff Type*	Profile Depth (ft)	Test date	Test Performer
1	ESF 1	1	ESF	74+00	Tptrn	12.6	13-Dec-04	UTA
2	ESF 14	1	ESF	05+80	Tpcpmn-ll	7.6, 14.6	15-Dec-04	UTA
3	ESF 15	1	ESF	04+18	Tpcrn2	15.2	15-Dec-04	UTA
4	ESF 02+47	3	ESF	02+47	Tmbt1a	15.1	9-Jun-05	UTA
5	ESF 02+12		ESF	02+12	Tmbt1b	7.5, 14.5	9-Jun-05	UTA
6	ESF 02+27		ESF	02+27	Tmbt1b	14.7	9-Jun-05	UTA
7	ESF 02+68	3	ESF	02+68	Tpki	15.2	9-Jun-05	UTA
8	ESF 02+82		ESF	02+82	Tpki	13.9	9-Jun-05	UTA
9	ESF 03+15		ESF	03+15	Tpki	10.0	9-Jun-05	UTA
10	ESF 2	7	ESF	64+05	Tptpul	13.9	13-Dec-04	UTA
11	ESF 12		ESF	26+66	Tptpul	11.8	14-Dec-04	UTA
12	ESF 13		ESF	22+06	Tptpul	13.8	14-Dec-04	UTA
13	ECRB 4		ECRB	09+10	Tptpul	13.4	15-Dec-04	UTA
14	ECRB 5		ECRB	06+59	Tptpul	15.8	15-Dec-04	UTA
15	ECRB 07+40		ECRB	07+40	Tptpul	11.0	8-Jun-05	UTA
16	ECRB 08+15		ECRB	08+15	Tptpul	15.7	8-Jun-05	UTA
17	ESF 3	9	ESF	62+61	Tptpmn	15.5	13-Dec-04	UTA
18	ESF 4		ESF	59+80	Tptpmn	15.9	13-Dec-04	UTA
19	ESF 7		ESF	55+32	Tptpmn	15.2	14-Dec-04	UTA
20	ESF 8		ESF	53+81	Tptpmn	15.9	14-Dec-04	UTA
21	ESF 9		ESF	41+21	Tptpmn	15.3	14-Dec-04	UTA
22	ESF 10		ESF	36+22	Tptpmn	15.6	14-Dec-04	UTA
23	ESF 11		ESF	30+06	Tptpmn	15.8	14-Dec-04	UTA
24	ESF 31+26		ESF	31+26	Tptpmn	14.8	9-Jun-05	UTA
25	ECRB 3		ECRB	12+20	Tptpmn	15.5, 15	15-Dec-04	UTA
26	ESF 5	17	ESF	58+46	Tptpll	15	13-Dec-04	UTA
27	ESF 6		ESF	57+96	Tptpll	15.9	13-Dec-04	UTA
28	ECRB 1		ECRB	17+29	Tptpll	14.8	14-Dec-04	UTA
29	ECRB 2		ECRB	16+07	Tptpll	15.4	14-Dec-04	UTA
30	ECRB 14+93		ECRB	14+93	Tptpll	16.9	8-Jun-05	UTA
31	ECRB 14+94		ECRB	14+94	Tptpll	14.3	8-Jun-05	UTA
32	ECRB 15+51		ECRB	15+51	Tptpll	14.9	8-Jun-05	UTA
33	ECRB 16+41		ECRB	16+41	Tptpll	14.8	8-Jun-05	UTA
34	ECRB 18+02		ECRB	18+02	Tptpll	15.2	8-Jun-05	UTA
35	ECRB 19+20		ECRB	19+20	Tptpll	14.5	8-Jun-05	UTA
36	ECRB 19+82		ECRB	19+82	Tptpll	11.3, 12.3	7-Jun-05	UTA
37	ECRB 20+19		ECRB	20+19	Tptpll	15.7	7-Jun-05	UTA
38	ECRB 20+71		ECRB	20+71	Tptpll	13.8	7-Jun-05	UTA
39	ECRB 21+16		ECRB	21+16	Tptpll	10.1	7-Jun-05	UTA
40	ECRB 21+63		ECRB	21+63	Tptpll	15.0	7-Jun-05	UTA
41	ECRB 22+31		ECRB	22+31	Tptpll	15.6	7-Jun-05	UTA
42	ECRB 22+94		ECRB	22+94	Tptpll	14.9	7-Jun-05	UTA
43	ECRB 23+60	3	ECRB	23+60	Tptpln	15.9	6-Jun-05	UTA
44	ECRB 23+96		ECRB	23+96	Tptpln	14.7	6-Jun-05	UTA
45	ECRB 24+87		ECRB	24+87	Tptpln	12.7	6-Jun-05	UTA

* from Buesch 2005b

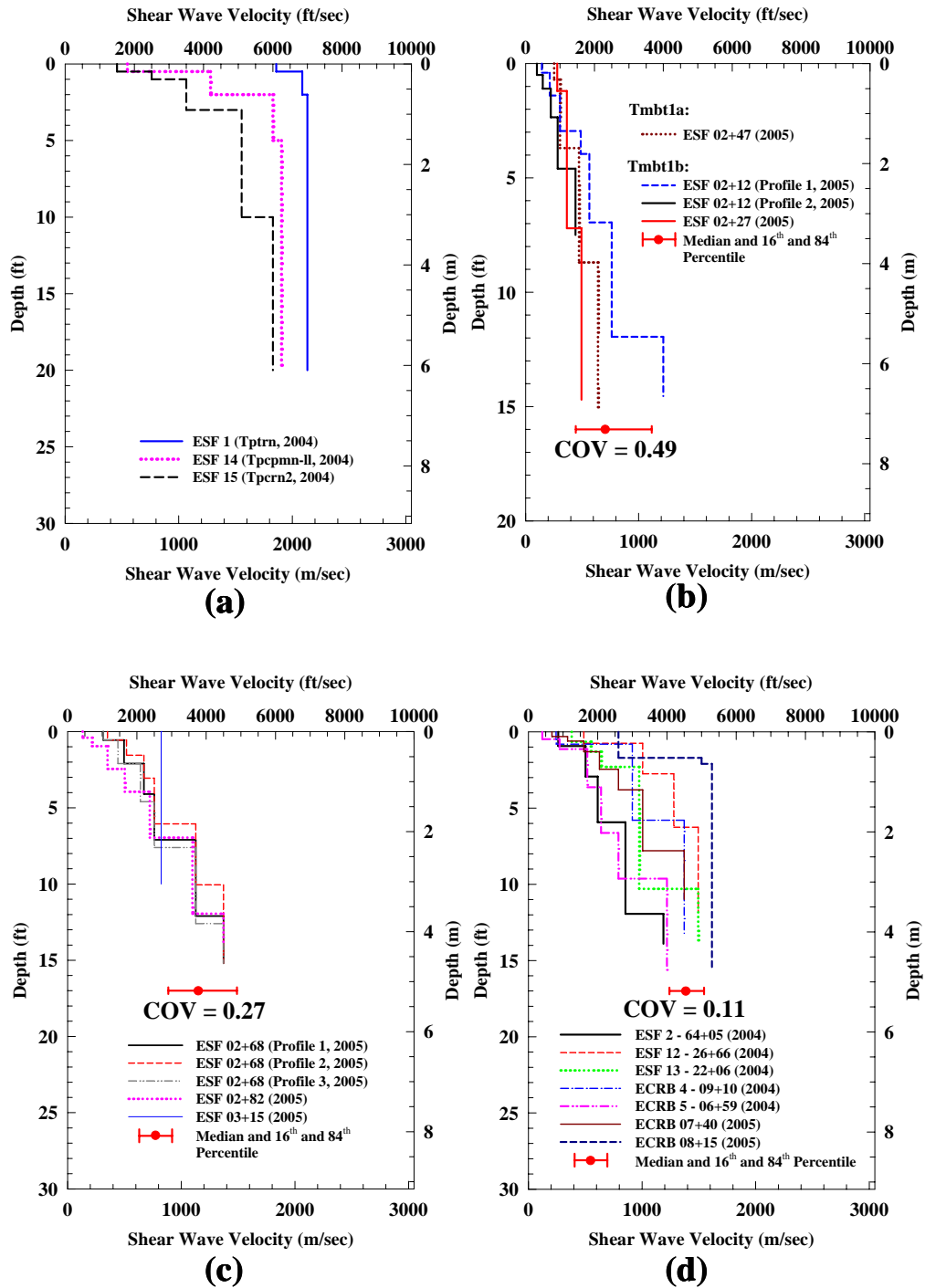


Figure 7.24 SASW V_S Profiles of (a) Single Sample, (b) Tmbt1, (c) Tpk1 and (d) Tptpul Tuffs Reduced from ESF and ECRB Tunnels in 2004 and 2005

In Figure 7.25, there is a large variation in the SASW V_S profiles of the Tptpmn (Topopah Spring Tuff: crystal-poor middle nonlithophysal zone) tuff. This same variability is as observed in Figure 7.13 for the 2001 SASW tunnel tests. By combining the SASW measurements on the Tptpmn tuff from 2001 and 2005, further studies were conducted. In total, there are 14 SASW profiles of the Tptpmn tuff (Figure 7.26) from 2001 to 2005. Based on the V_S values in the deepest parts of these 14 profiles, the general median and 16th and 84th percentile boundaries were obtained. Although there is a large variation in the 14 SASW profiles, it seems that they can be divided into two groups based on their deeper bottom V_S profiles. This division is a V_S value of 5800 fps which separates the “higher” and “lower” velocity groups in the mountain area. The two velocity groups as well as their median and 16th and 84th percentile boundaries are shown in Figures 7.27 and 7.28. These high and low velocity ranges are used to compare with the deep V_S profiles at the mountain area in Section 7.4.2.2.

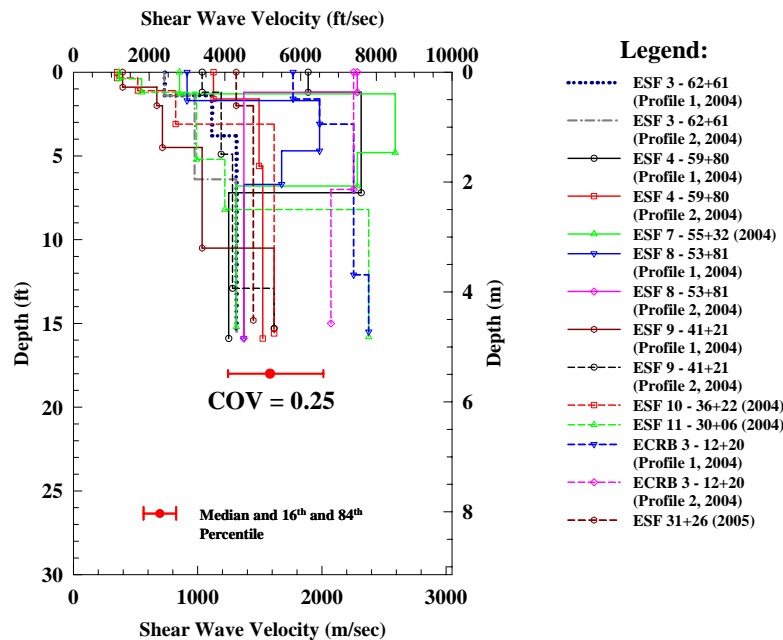


Figure 7.25 Nine SASW V_S Profiles of the Tptpmn Tuff in the ESF and ECRB Tunnels in 2004 and 2005

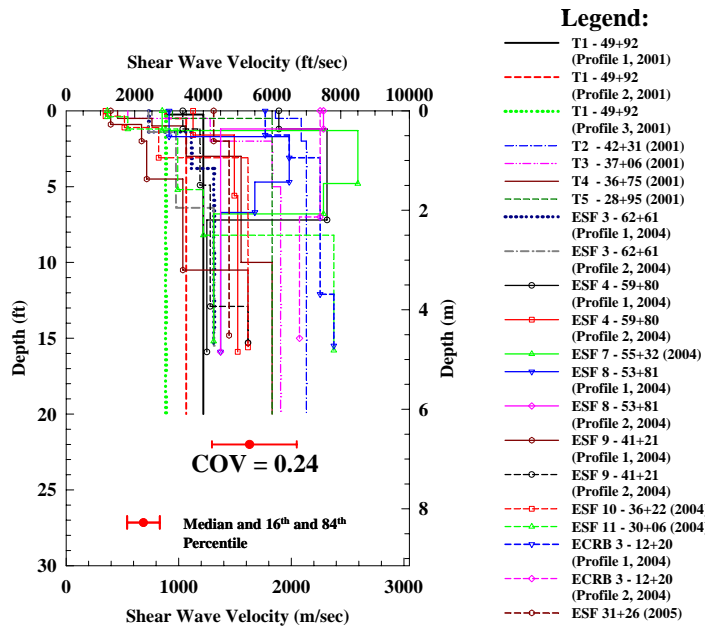


Figure 7.26 Fourteen SASW V_S Profiles of the Tptpmn Tuff in the ESF and ECRB Tunnels from 2001 and 2005

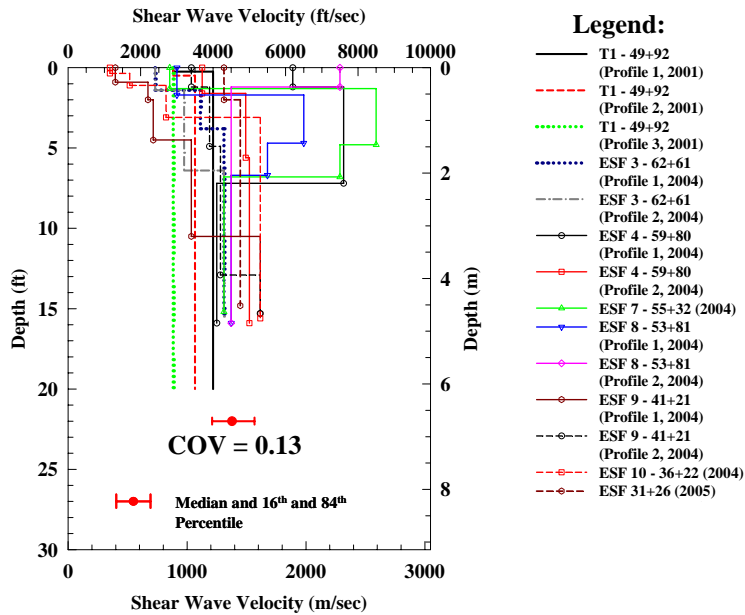


Figure 7.27 Eight Softer SASW V_S Profiles of the Tptpmn Tuff in the ESF and ECRB Tunnels from 2001 and 2005

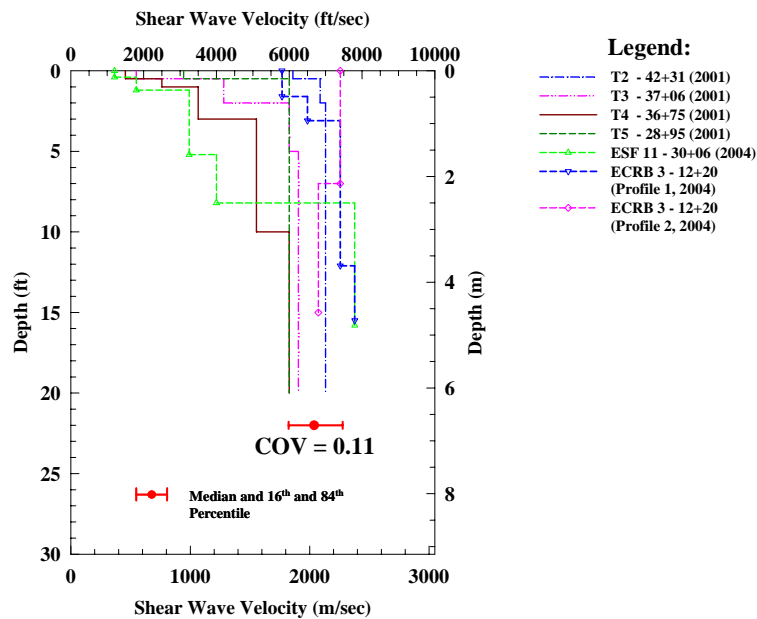


Figure 7.28 Six Stiffer SASW V_S Profiles of the Tptpmn Tuff in the ESF and ECRB Tunnels from 2001 and 2005

Regarding the Tptpll (Topopah Spring Tuff: crystal-poor lower lithophysal zone) tuff, the largest tuff group sampled, most V_S profiles come reasonably close together below 13 ft, except for Site ECRB 21+63 and ECRB 22+94 (Figure 7.29). The “boundary effect” may explain what happen to Site ECRB 22+94. However, the decrease in the V_S profile of Site ECRB 21+63 could result from the existence of more fractures caused by the nearby fault or the higher lithophysae content.

The last type of tuff compared is Tptpln (Topopah Spring Tuff: crystal-poor lower nonlithophysal zone) tuff and all V_S profiles converge to the range of 5000 to 6000 fps below about 10 ft as shown in Figure 7.30.

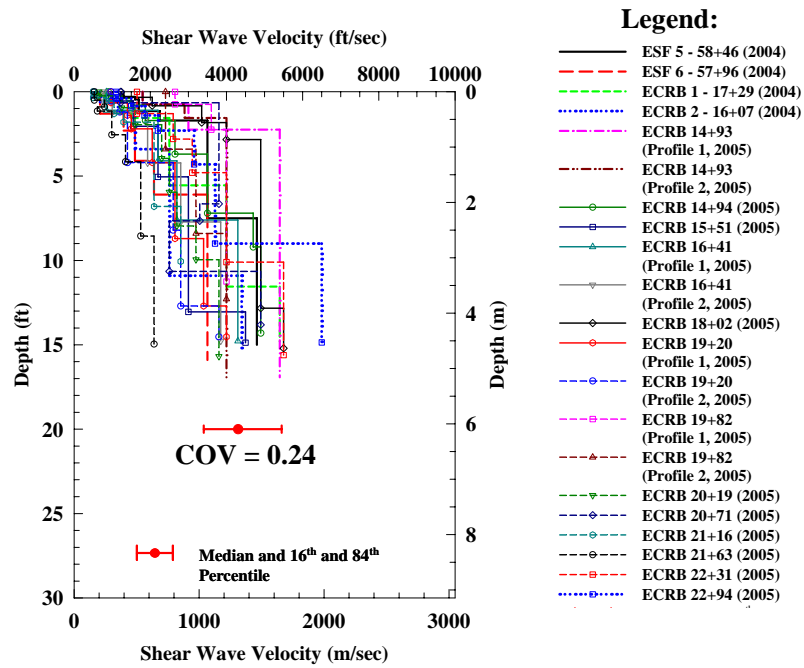


Figure 7.29 Seventeen SASW V_S Profiles of the Tptpll Tuff in the ESF and ECRB Tunnels in 2004 and 2005

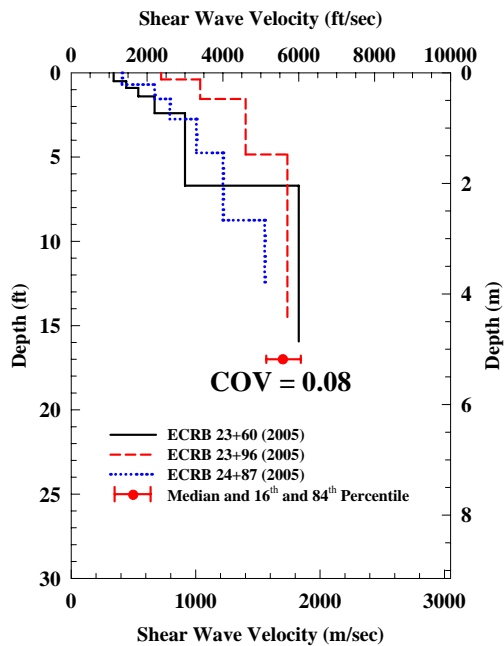


Figure 7.30 Three SASW V_S Profiles of the Tptpln Tuff in the ECRB Tunnel in 2005

7.3.2 Downhole Seismic Testing

Downhole measurements were performed in two areas around the Yucca Mountain. One area is the mountain area above the potential repository area. The other area is at the WHB area. The majority of the downhole measurements were performed in the WHB area.

7.3.2.1 Yucca Mountain Area

Eight downhole tests were conducted in the mountain area by Bruce Redpath of Redpath Geophysics in 2001. Information about these downhole tests is presented in Table 7.8 and Figure 7.31. In general these downhole profiles are no deeper than about 95 ft. The one exception, the deepest one was measured in borehole UZ-N27 to a depth of 179 ft deep. In contrast, the shallowest one was obtained in borehole UZ-N94 which is only 25 ft depth. Because the shortness of these downhole profiles, their $V_{S,30}$ values were calculated based on extrapolated data, except at borehole UZ-N27. The locations of the boreholes can be seen in Figure 7.31. As observed, most boreholes are located at the north or the south of the crest of Yucca Mountain, except UZ-N64. As observed in Figure 7.32, there is a large variation in the eight V_S profiles. The reasons could be the lack of profiles, the scatter in the borehole locations and/or the higher variability and velocity inversion seen in the SASW V_S profiles at the mountain area. These results are compared with the SASW results in the Section 7.4.

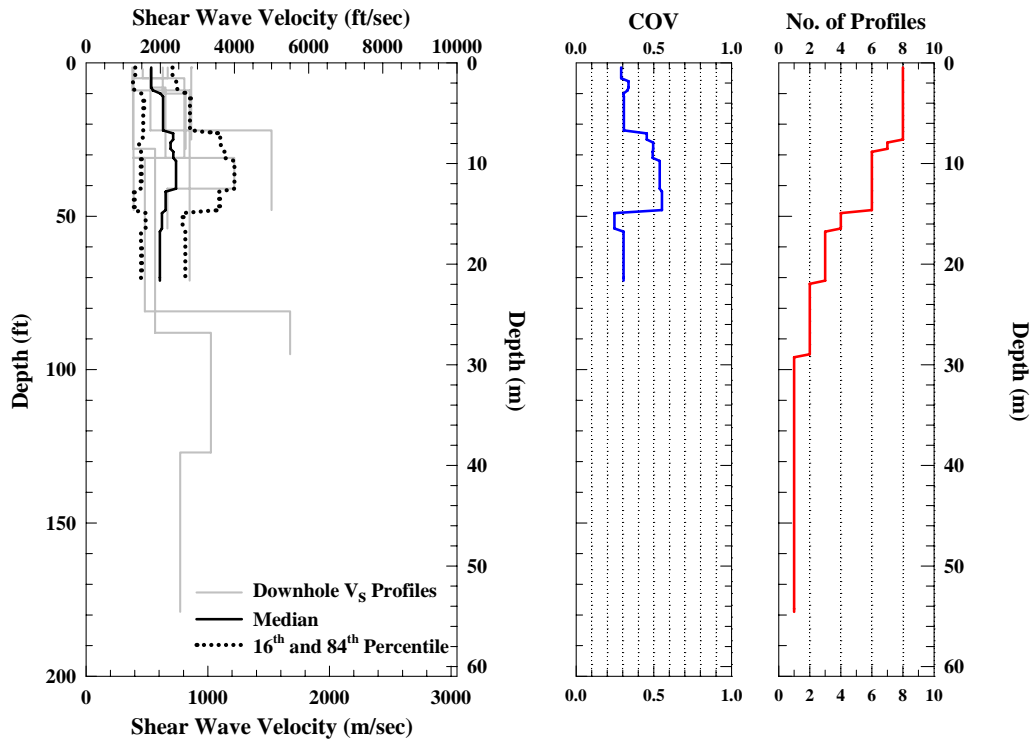


Figure 7.32 Individual Profiles and Statistical Analysis of the Eight Downhole Tests Performed in the Mountain Area in 2001

7.3.2.2 WHB Area

In addition to the downhole tests carried out in the mountain area, there were 17 downhole tests conducted at the WHB area. Fifteen out of the 17 downhole tests were performed by Bruce Redpath of Redpath Geophysics and the other two were performed by Rob Steller of GEOVision, Inc. All testing was done between October and December in 2000. Information about these downhole tests is listed in Table 7.9. The 17 downhole V_S profiles and their statistical analysis are shown in Figure 7.33. Because of the importance of these facilities, the borehole depth at the WHB area is deeper than those that were performed by Mr. Redpath in existing boreholes on the mountain (about

100 ft (30 m)). The average depth of the downhole tests at the WHB area is about 350 ft and the range is from 95 to 640 ft.

Table 7.9 Information about the 17 Downhole Tests Performed at the WHB Area in 2000

No.	Borehole ID	Profile Depth (ft)	$V_{s,30}$ (fps)	Site Class	Test Date	Test Performer
1	RF#13(RedPath)	345	1779	C	October to December, 2000	Bruce Redpath of Redpath Geophysics and Rob Steller of GEOVision, Inc.
2	RF#13(GEOVision)	345	1986	C		
3	RF#14	520	1972	C		
4	RF#15	320	2367	C		
5	RF#16	445	1627	C		
6	RF#17(GEOVision)	620	2057	C		
7	RF#18	480	2167	C		
8	RF#19	640	1969	C		
9	RF#20	155	1911	C		
10	RF#21	185	1853	C		
11	RF#22	500	2155	C		
12	RF#23	155	1933	C		
13	RF#24	260	1777	C		
14	RF#25	155	2203	C		
15	RF#26	260	1598	C		
16	RF#28	95	2528	B*		
17	RF#29	405	2061	C		

*Based on extrapolated data

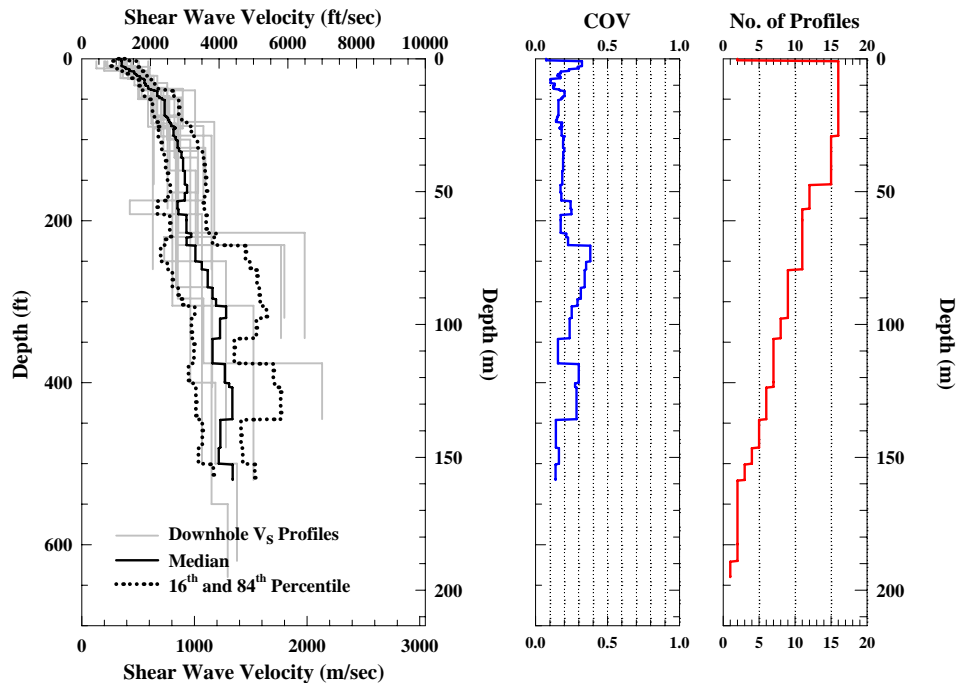


Figure 7.33 Individual Profiles and Statistical Analyses of the 17 Downhole Tests Performed at 16 Sites at the WHB Area in 2000

7.3.3 P-S Suspension Logging

Sixteen suspension logging tests were performed at the same boreholes where the 17 downhole tests were conducted in the WHB area. These P-S logging measurements were carried out by GEOVision, Inc during 2000. Table 7.10 presents information about 16 P-S logging tests. Generally, the profiling depths of the suspension logger are about the same as the downhole tests at each borehole because these depths should be close to the bottom of each borehole. The site classes at the test locations determined by P-S logging are two “B” sites and 8 “C” sites. The range of $V_{S,30}$ of these 16 sites is from 1423 to 2739 fps, which is larger than the SASW and downhole measurements performed at this area. Among the 16 WHB sites, six sites was not able to determine the site classes because of the lack of the V_S profile data in the top 34 to 235 ft. As seen in Figure 7.34, the COV values are larger in the top 150 ft of the profile than the other two methods. The larger COV values are expected because the P-S logger performs very localized measurements compared to the other methods. Below 150 ft, in general, the COV values increase with the depth. There is a wide range of the COV values which is from 0.10 to 0.60 at these depths. The reason which causes this large variation in the deeper COV profile seems to be the faults as stated in the SASW and downhole results observed in the WHB area.

Table 7.10 Information about the 16 P-S Suspension Logging Tests Performed in the WHB Area in 2000

No.	Borehole ID	Profile Start Depth (ft)	Profile Depth (ft)	$V_{s,30}$ (fps)	Site Class	Test Date	Test Performer
1	RF#13	18	343	1841	C	September 17-19 and December 5-12, 2000	GEOVision, Inc.
2	RF#14	51	543	N/A	N/A		
3	RF#15	26	310	2739	B		
4	RF#16	28	446	1423	C		
5	RF#17	54	648	N/A	N/A		
6	RF#18	34	484	N/A	N/A		
7	RF#19	34	638	N/A	N/A		
8	RF#20	21	151	1830	C		
9	RF#21	19	184	1753	C		
10	RF#22	235	394	N/A	N/A		
11	RF#23	11	151	1804	C		
12	RF#24	30	262	2357	C		
13	RF#25	84	151	N/A	N/A		
14	RF#26	20	256	1492	C		
15	RF#28	30	94	2663	B*		
16	RF#29	26	402	1983	C		

*Based on extrapolated data

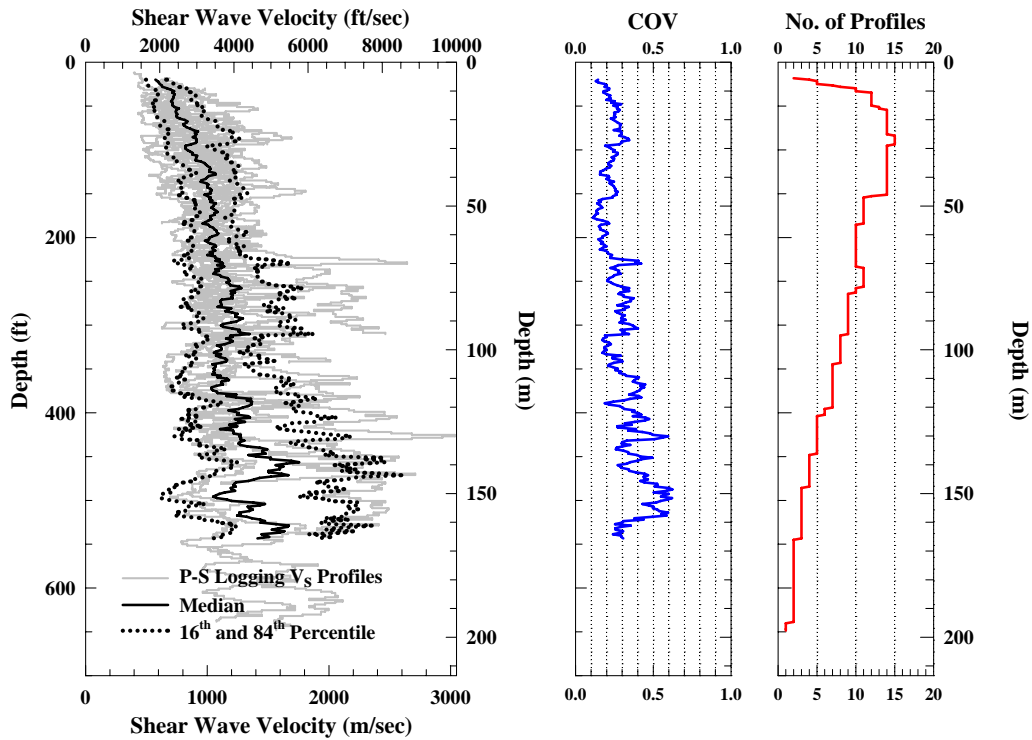


Figure 7.34 Individual Profiles and Statistical Analysis of the 16 P-S Suspension Logging Tests Performed at the WHB Area in 2000

7.3.4 Laboratory Testing

In addition to the field tests discussed above, laboratory tests were also conducted at the Soil Dynamic Laboratory (SDL) in University of Texas at Austin. This work was also part of the Yucca Mountain Site Characterization Project. This laboratory tests include testing of eight types of tuffs. These results are used to compare with the measurements from the surface and tunnel field SASW tests. The types of tuffs tested in the laboratory are Tmbt1 (pre-Rainier Mesa Tuff bedded tuffs), Tpki (Tuff unit “X”), Pah (or Tpp) (Pah Canyon tuff), Tptrn, Tptpul (Topopah Spring Tuff: crystal-poor upper lithophysal zone), Tptpmn (Topopah Spring Tuff: crystal-poor middle nonlithophysal zone), Tptpll (Topopah Spring Tuff: crystal-poor lower lithophysal zone) and Tptpln (Topopah Spring Tuff: crystal-poor lower nonlithophysal zone). Two types of laboratory test methods were used to dynamically test the specimens. One is a free-free resonant column (RC) test; the other is a fixed-free resonant column test. In this study, only results from the free-free resonant column tests were compared with the field results because many more samples were tested in the free-free resonant column test. It is important to note that the specimens in the free-free RC test are larger than fixed-free test and may better reflect the actual field conditions than the smaller specimens. Statistical results of the free-free RC test are presented in Table 7.11.

Table 7.11 Free-Free Resonant Column Results of Different Tuff Specimens from YMP

Tuff Type	Number of Specimen	V _s			COV
		Median	16 th Percentile	84 th Percentile	
Tpki	6	3079	2421	3915	0.25
Pah (Tpp)	2	3493	2790	4373	0.23
Tptrn	6	6491	6033	6983	0.07
Tptpul	7	5834	4682	7269	0.22
Tptpmn	8	8779	8659	8901	0.01
Tptpll	7	6657	6171	7181	0.08
Tptpln	8	8633	8007	9308	0.08

Note: Updated to July 14, 2006

7.3.5 Vertical Seismic Profiling (VSP)

In 1995, VSP surveys were conducted in six boreholes in the Yucca Mountain area by LBNL (Lawrence Berkeley National Laboratory). These boreholes are G-2, G-4, NRG-6, SD-12, UZ-16 and WT-2 (see Figure 7.35). Among the six VSP measurements, only four of them have reliable V_P and/or V_S profiles. They were measured at boreholes G-2, NRG-6, UZ-16 and WT-2 near SASW Sites YM 17, YM 14A, YM 15A and YM 16 respectively. The V_S profiles of these VSP measurements are shown in Figure 7.36.

Based on the SASW (2000 and 2001), downhole (2001) and VSP (1995) V_S profiles performed in the mountain area, two base case profiles were developed. These two profiles are presented in Figure 7.37. The base case #1 profile was developed based on the smoothed SASW and downhole data to a depth of 700 ft (BSC, 2004a). Because the data from a depth of 700 ft to the depth of the potential repository at about 1000 ft was not available at the time, a linear interpolation was made in V_S from 3800 fps at a depth of 700 ft to 6000 fps at a depth of 1100 ft where five SASW measurements were performed in the ESF tunnel in 2001.

Based on a smoothed V_S profile calculated from four VSP profiles, the base case #2 profile was developed by increasing the value of V_S by 600 fps on the smoothed VSP profile (BSC, 2004a). These profiles are compared with the SASW tests performed in the mountain area in 2004 and 2005 in Section 7.4.1.1.

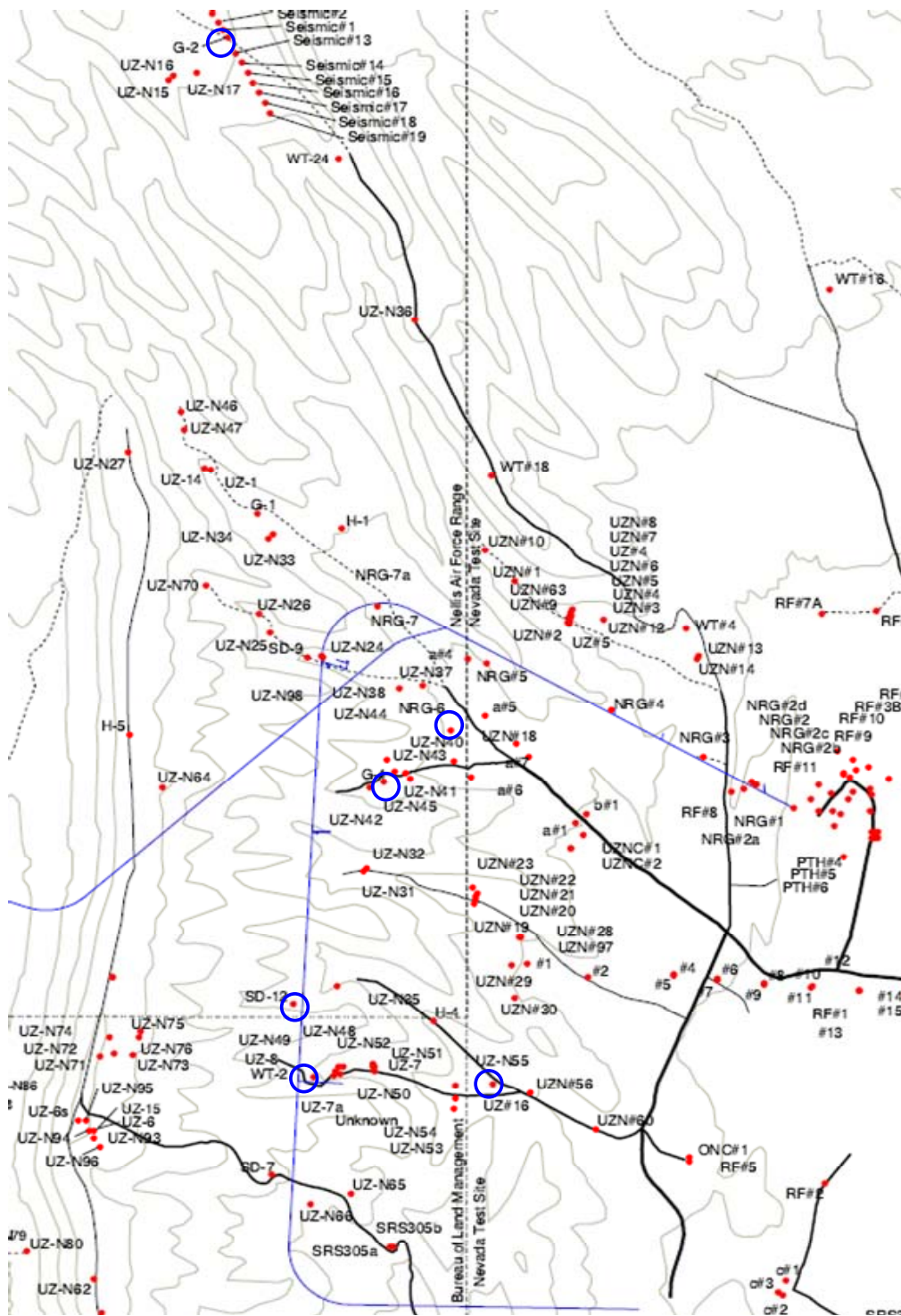


Figure 7.35 Locations of Boreholes where the Vertical Seismic Profiling (VSP) were Performed

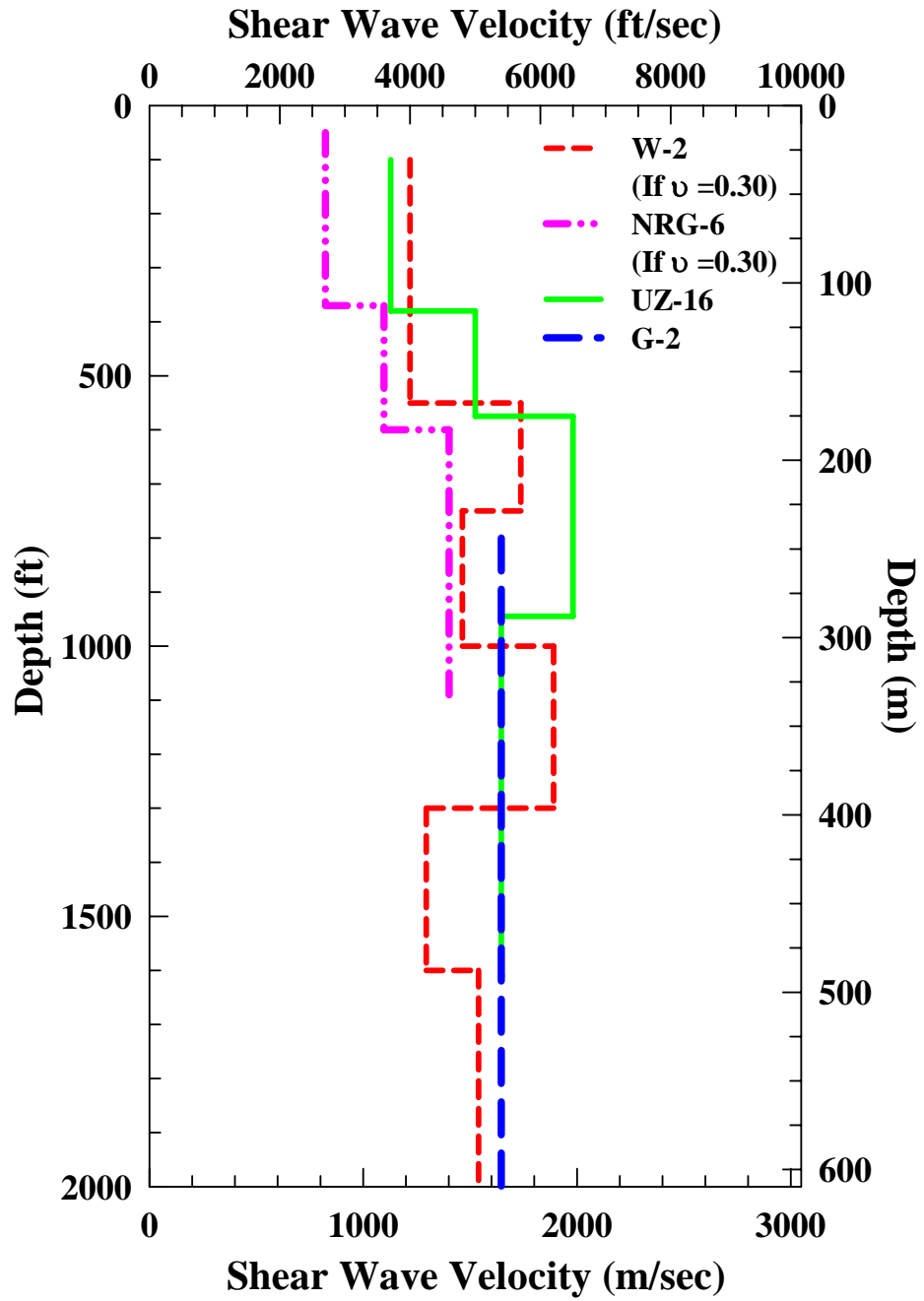


Figure 7.36 Four VSP V_s Profile Performed in Borehole W-2, NRG-6, UZ-16 and G-2 in Yucca Mountain (Re-plotted based on BSC, 2004a)

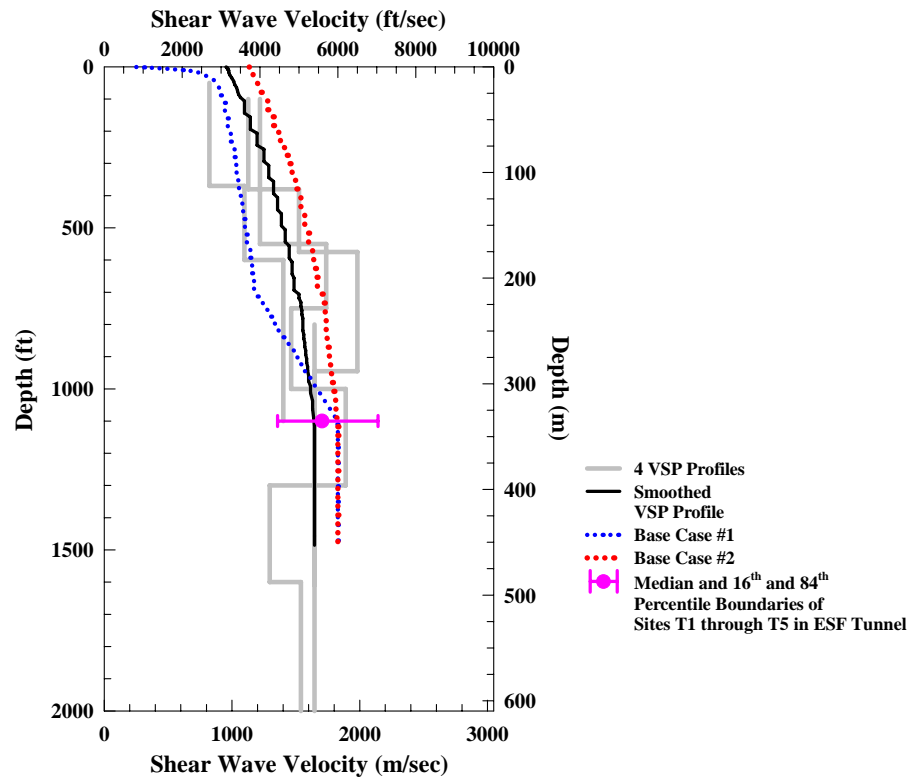


Figure 7.37 Four VSP V_S Profile Performed in Borehole W-2, NRG-6, UZ-16 and G-2 in Yucca Mountain (Re-plotted based on BSC, 2004a)

7.3.6 Seismic Tomography Testing

In 2004, Gritto et al. performed seismic tomography studies at the area from the Yucca Mountain crest to the ESF tunnel. This study was to estimate fracture intensity and distribution in the potential high-level radioactive waste repository area at Yucca Mountain, NV. Two vibroseis trucks were employed as the seismic source on the crest of Yucca Mountain which is about 5 km long. With a 30-m source spacing, this survey had 161 source locations along the source line. The receiver line was in the ESF tunnel with 224, 2-D (vertical and horizontal) geophones. These geophones were deployed along about 3 km of the ESF tunnel with a 15-m receiver spacing. The image of the shear wave estimates of the repository horizon is shown in Figure 7.38. As observed, in

general, the velocity is highest in the middle portion of the surveyed area and the north area is stiffer than south area. With an assumed Poisson's ratio of 0.30, the V_S range along the ESF tunnel is about from 6400 to 7190 fps (1951 to 2192 m/s) which is converted from the range of V_P from 11,975 to 13,459 fps (3650 to 4100 m/s). With the assumed Poisson's ratio, the average V_S of the whole survey area ranges from 6226 to 7278 fps (1898 to 2218 m/s) which is calculated from the range of V_P from 11,647 to 13,615 fps (3550 to 4150 m/s). These V_S values are compared with the SASW measurements on surface of the Yucca Mountain area or in the ESF tunnel in the next section.

There was another seismic tomography survey performed between the ESF (Niche #3) and ECRB (Alcove #8) tunnels by NSA Engineering, Inc. in 2000 (Descour et al., 2001). This location is denoted in Figure 7.39 (a) and the survey configuration is illustrated in Figure 7.39 (b). In the upper lithophysal zone (Ttptul) (near Alcove #8), the average shear wave velocity is about 5463 fps and the range is between 5052 and 5840 fps. In the middle non-lithophysal zone (Ttptmn) (near Niche #3), the shear wave velocity is in the range between 6234 to 6562 fps which is higher than the upper lithophysal zone. These results are also compared with the SASW tunnel tests.

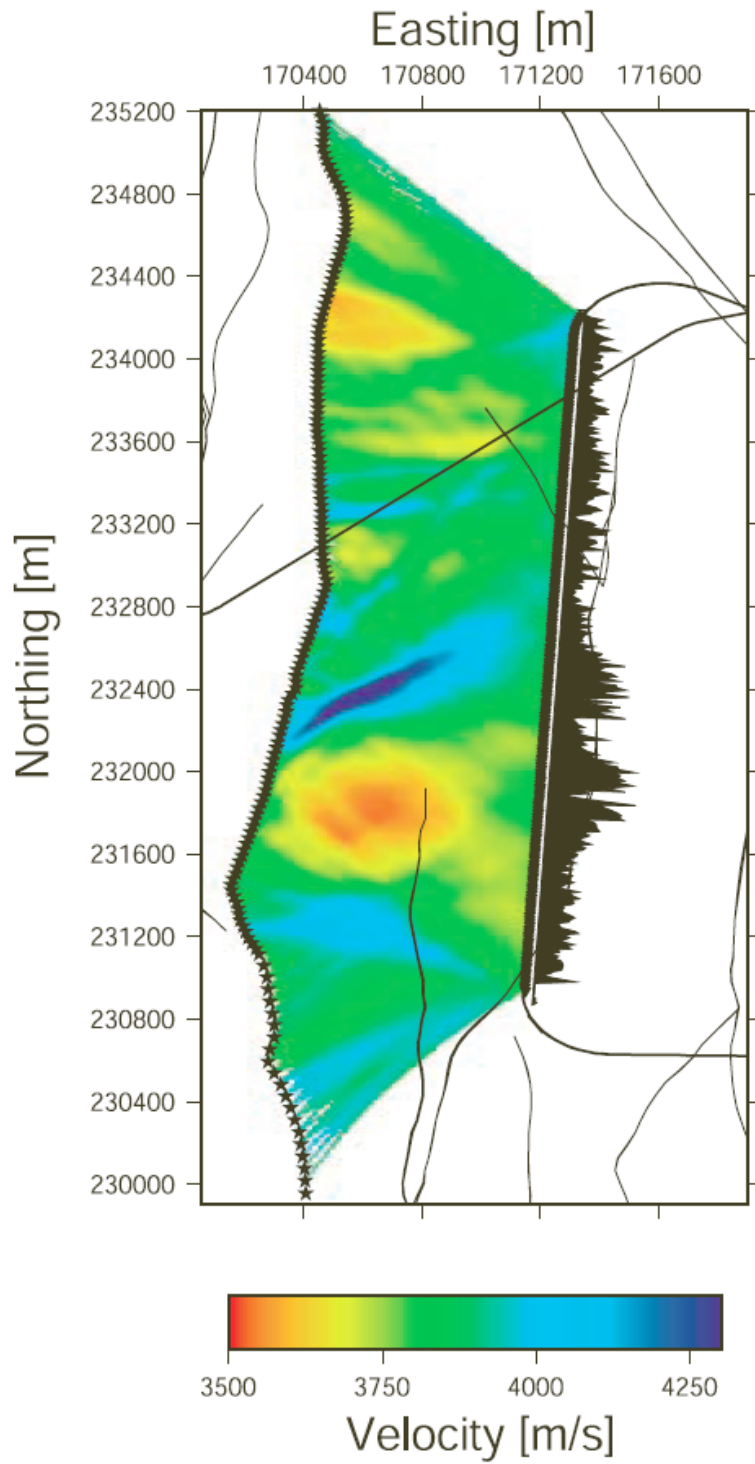


Figure 7.38 P-Wave Velocity Estimates at the Repository Horizon Based on Curved-Ray-Travel-Time Inversion (Gritto et al., 2004)

7.4 STATISTICAL ANALYSES AND COMPARISONS

In this section, several different comparisons are made based on different profiling techniques performed in the same area, profiles from different active sources used in the SASW tests, different geologic formation and so on.

7.4.1 Comparisons between Different Profiling Methods in the Same Area

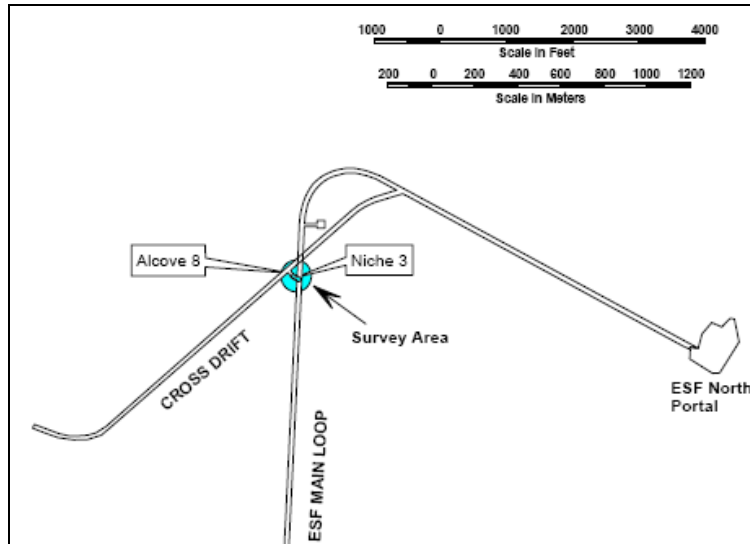
Because of the distribution of downhole and suspension logging surveys, the general (apples-to-oranges), common site (green-apples-to-red-apples) and identical-site-and-depth comparisons (green-apples-to-green-apples) can only be made at the mountain and WHB areas at this time. Additional testing is planned for the summer of 2007 but the results will not be available until Fall 2007 or Spring 2008.

7.4.1.1 Yucca Mountain Area

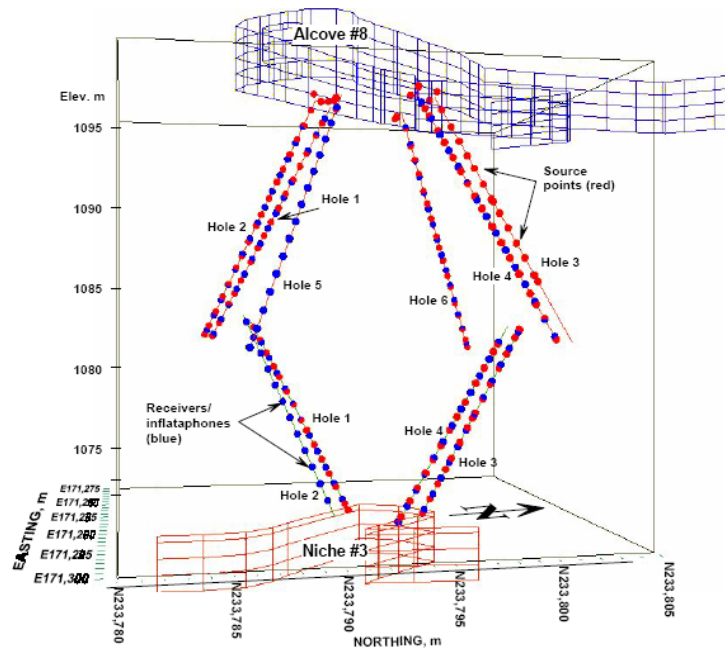
- **SASW and Downhole Measurements**

As discussed above, eight downhole tests were conducted in the mountain area in 2001. To do a general (apples-to-oranges) comparison between SASW and downhole V_S profiles, the statistical analyses of 55 SASW measurements (2000 to 2005) was performed to compare with the downhole results. This comparison is shown in Figure 7.40. Because most downhole profiles are quite shallow, the comparison can only be made in the top 70 ft of the mountain area. In the top 10 ft, the downhole median profile is higher than the SASW median profile as usually found. Between 10 and 40 ft, the two measurements agree well. Below 40 ft, however, the downhole median V_S profile is lower than the SASW median V_S profile by about 25% in average. The COV profiles from both methods are close to or larger than 0.30 at most depths. These large values of COV show large variation in their V_S profiles from site to site. The reason for the difference in the median V_S profiles below 40 ft could be a bias in the V_S profiles due

to borehole locations. As seen, the SASW measurements outnumber the downhole profiles, with a ratio of about 7 to 1.



(a)



(b)

Figure 7.39 Illustrations of: (a) the Seismic Tomography Test Location and (b) the Survey Configuration (Descour et al., 2001)

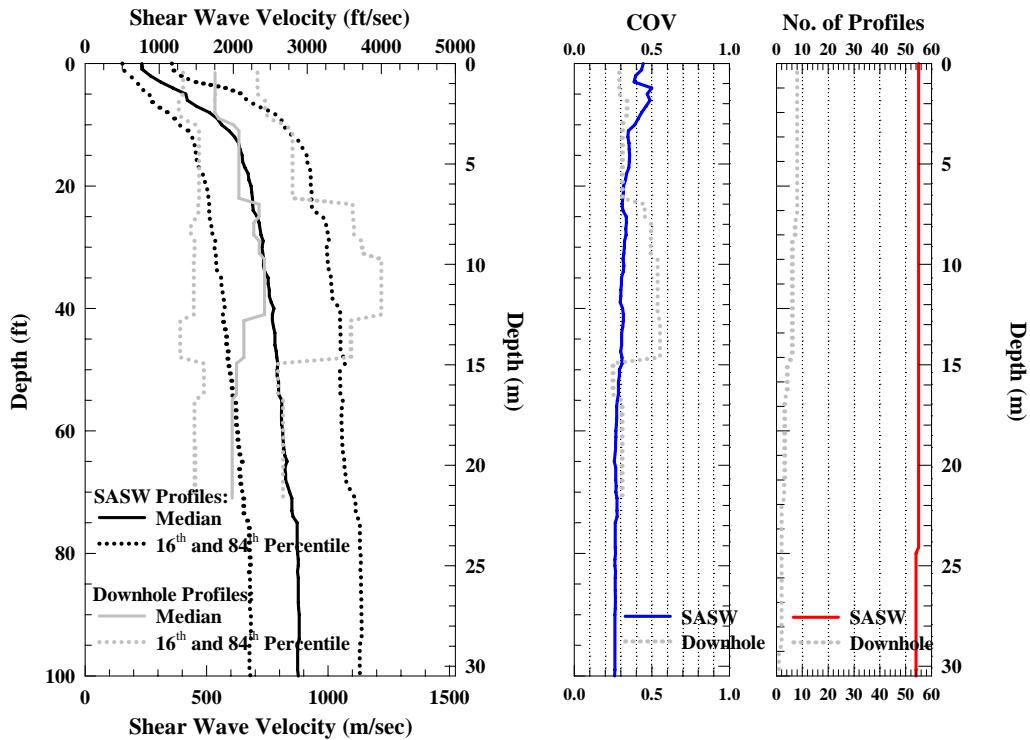


Figure 7.40 General Comparison between SASW and Downhole Measurements Performed in the Mountain Area during 2000 and 2005

To compare these two measurements more objectively (“green-apples-to-red-apples”), only the SASW V_s profiles near the downhole measurements locations were used in the comparison. The SASW tests near the eight downhole tests are listed in Table 7.12 with the corresponding borehole ID. In total, 13 SASW profiles were chosen. The SASW and downhole comparison is presented in Figure 7.41. The median V_s profile of the SASW measurements is slightly lower than the one in Figure 7.40 in the 15- to 75-ft depth range but it is still consistent with the downhole measurements at the depths from 10 to 40 ft. The difference between the median values of these two methods below 40 ft is smaller compared to the previous figure but the difference is still about 20%. However, the COV profile of these two measurements is

similar after excluding the other SASW profiles that were not around the eight boreholes where the downhole tests were conducted.

Table 7.12 Table of the Boreholes where the Downhole Tests were Performed and the Nearby SASW Test Locations

Borehole ID	Corresponding SASW Sites
UZ-N27	D 11
UZ-N33	D 2 nad YM 13
UZ-N46	D1 and YM 12
UZ-N64	D 9 and D 10
UZ-N66	S 12
UZ-N71	S1 and YM 4
UZ-N75	S 6
UZ-N94	S 3 and S 11

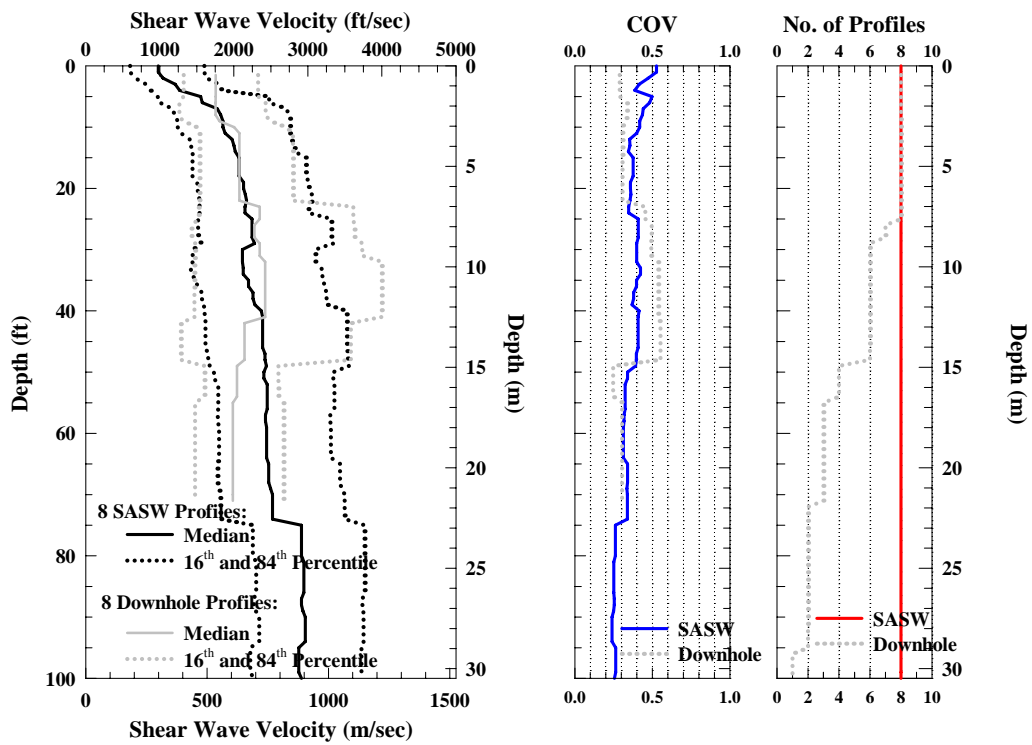


Figure 7.41 Comparison between the SASW and Downhole Measurements Performed at Common Borehole Locations in the Mountain Area during 2000 and 2005

To remove the bias from the profiling length difference at each borehole site between the two techniques, either one or both of SASW and downhole V_S profiles were trimmed to be identical in terms of the profiling depth before the comparison was made (a “green-apples-to-green-apples” comparison). Figure 7.42 shows the Identical-site-and-depth comparison between these two measurements. On average, the two median V_S profiles are slightly more similar in Figure 7.41. The inconsistency is slightly larger at the depth from 25 to 42 ft but it is smaller at depths between 42 and 70 ft. The consistency between the COV profiles is better than the previous two figures, except at depths below 55 ft. This difference could be caused by the appearance of stiffer and/or softer layers that are not laterally significant so that borehole locations sample somewhat different layers at some depths than the global SASW measurement.

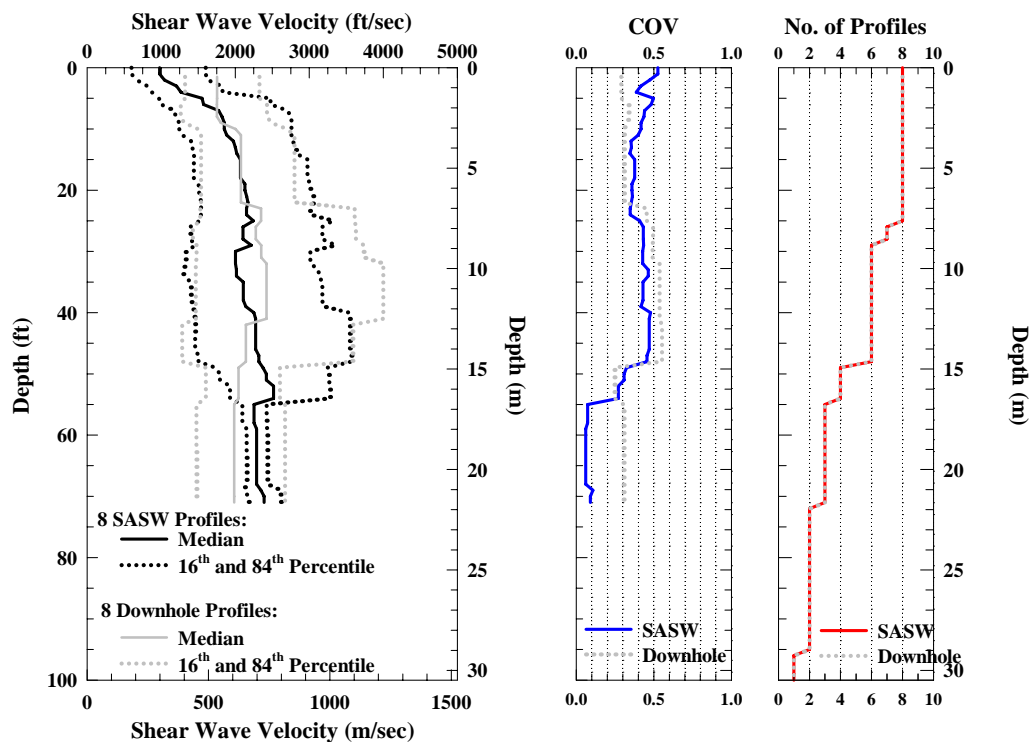


Figure 7.42 Identical-site-and-depth comparison between the SASW and Downhole Measurements Performed at Common Borehole Locations in the Mountain Area during 2000 and 2005

- **SASW and VSP Measurements**

The four VSP profiles are distributed around the mountain area, so only 19 SASW V_S profiles from around the mountain area are compared. The locations of these 19 SASW tests site are shown on the map in Figure 7.7. This comparison is made in Figure 7.43. Based on the individual V_S profiles in Figure 7.43 (a), the VSP profiles and SASW measurements are consistent, although the VSP profiles seem to be slightly higher in the mid-depth range. In Figure 7.43 (b), the smoothed VSP profile and the base case #2 are all higher than the median V_S profiles of the SASW results from 19 YM sites. From the surface to about 1000 ft, base case #1 is close to the SASW median profile. However, the 16th and 84th percentile ranges of the 19 YM sites cover (or agree with) the smoothed VSP profile, base case #1 and base case #2 at the depths from about 600 to 1000 ft. The data in this range are crucial to the potential repository level.

7.4.1.2 WHB Area

- **SASW, Downhole and Suspension Logging Measurements**

There were 35 SASW, 17 downhole and 16 suspension logging measurements performed at the WHB area in 2000 and 2001. The locations of these measurements are shown in Figure 7.5. Because of large number of V_S profiles from each profiling technique at this small (800 ft by 1200) ft area, this offers an excellent opportunity to do comparisons between the SASW, downhole and suspension survey methods.

First, as usual, general comparisons (“apples-to-oranges” comparisons) were made by using all the V_S profiles obtained from the different methods. The comparison between the SASW and downhole, the SASW and P-S logging, and the downhole and P-S logging methods are presented in Figures 7.44 through 7.46 respectively. As seen in these three figures, the median V_S profiles of SASW and P-S logging show the best

agreement among the tree comparisons, except the top 20 ft where there are no P-S logging measurements. The inconsistency at the depths from about 150 to 250 ft between the downhole and the other two methods could be somewhat attributed to the downhole profile measured at borehole RF#22 which has a large inversion at the depths from 175 to 192 ft. This inversion is not observed in the SASW and P-S logging profiles near/in Borehole RF#22 because the SASW profiles (SASW 23 and SASW 30) nearby are too short to measure it and the P-S logging profile was missing data in the top 235 ft of Borehole RF#22.. The COV profile of the SASW measurements, in general, shows smaller values than the downhole and P-S logging methods at WHB area. In addition, as the COV profile goes deeper, the COV values associated with the SASW, downhole and P-S logging measurements tend to become larger.

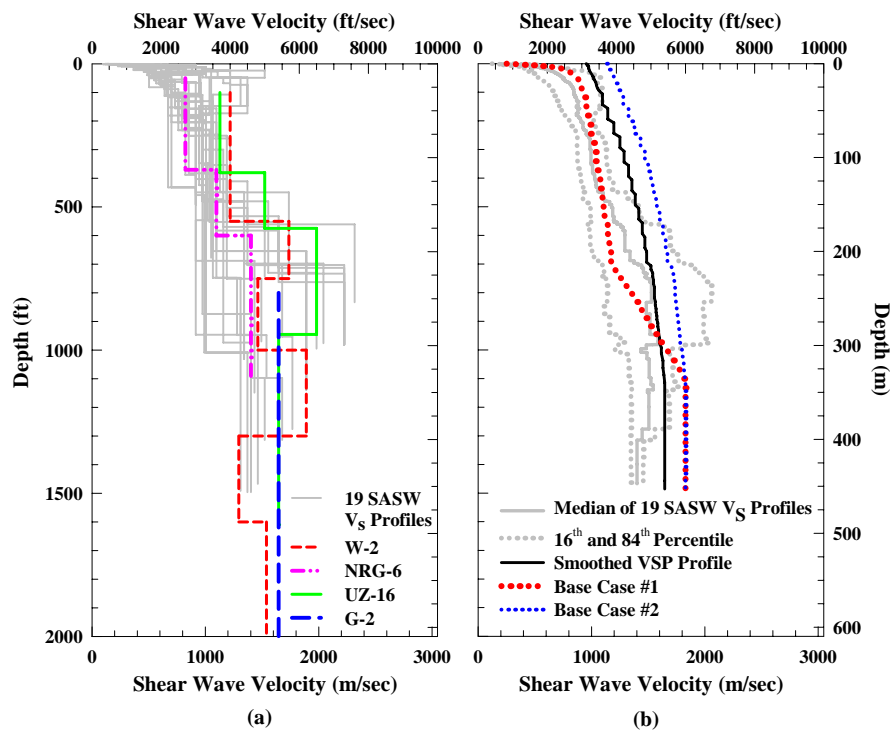


Figure 7.43 Comparisons of: (a) 19 SASW V_S Profiles and Four VSP Profiles and (b) Median and 16th and 84th Percentile Boundaries of 19 SASW V_S Profiles, the Smoothed VSP Profile, and Base Cases #1 and #2 at the Mountain Area

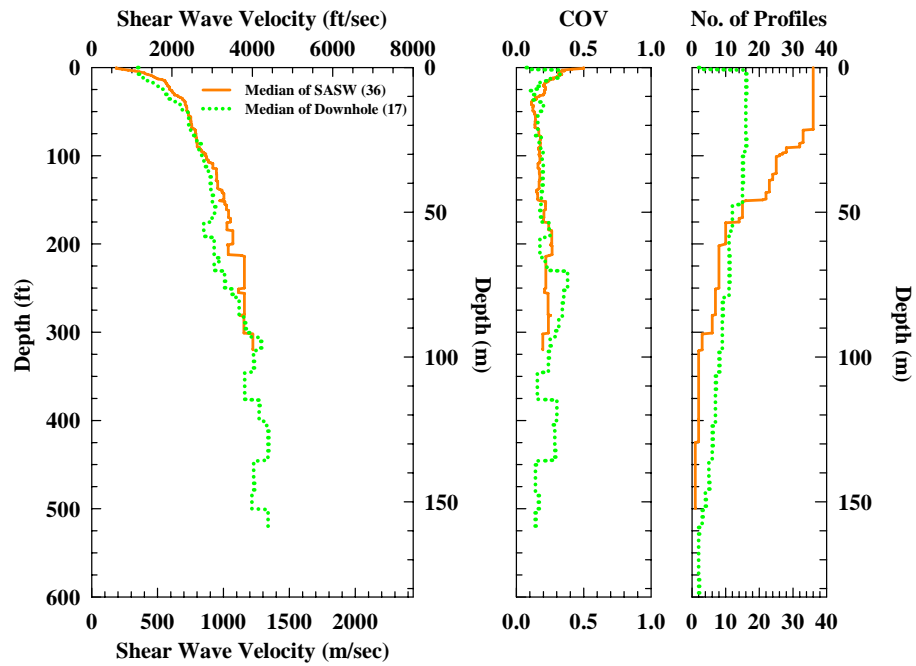


Figure 7.44 General Comparison of SASW and Downhole Measurements at the WHB Area

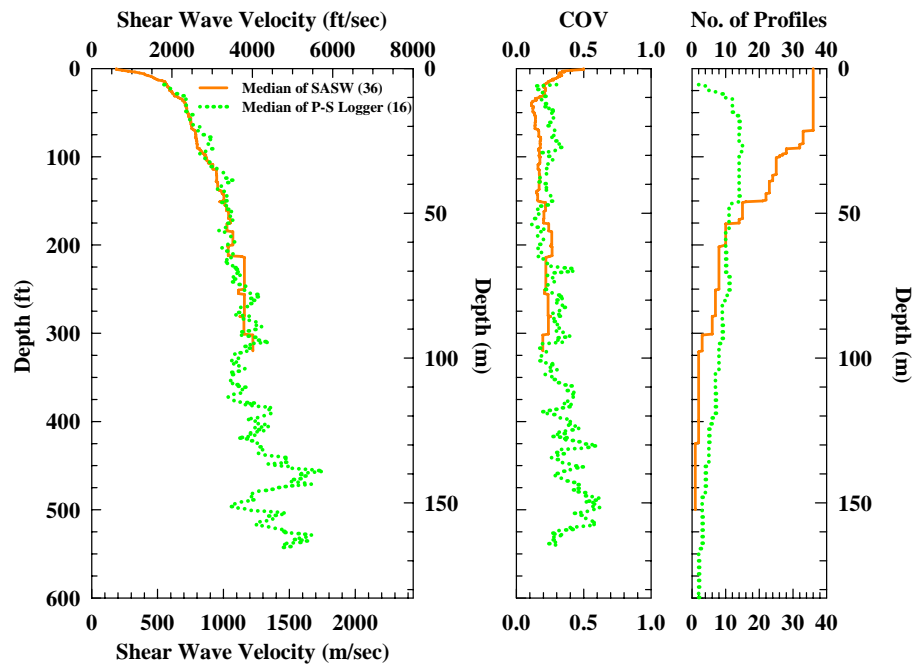


Figure 7.45 General Comparison of SASW and P-S Logging Measurements at the WHB Area

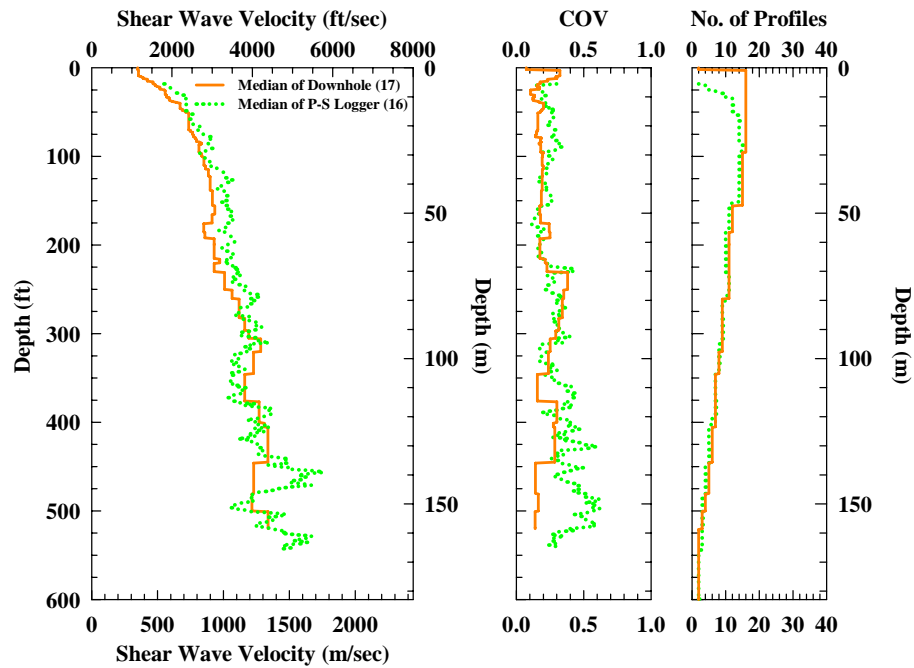


Figure 7.46 General Comparison of Downhole and P-S Logging Measurements at the WHB Area

Second, because not every borehole has the SASW measurements nearby, only data from 12 of the 16 borehole locations were chosen to compare. The common site comparisons (“green-apples-to-red-apples”) made between the SASW and downhole, the SASW and P-S logging, and the downhole and P-S logging methods at the 12 common borehole sites which is tabulated in Table 7.13. Figures 7.47 through 7.49 show that the median V_S profiles are very consistent between the SASW and downhole method in the top 170 ft. Below 170 ft, the number of SASW profiles is rather small and is likely a key reason for the difference. Although the difference between the SASW and P-S logging methods is larger, the difference is less than 15% on average. However, it is clear that the V_S values from P-S logging are consistently higher in the top 200 ft. In general, the P-S logging measurements are also higher than downhole measurements in the 240 ft.

Table 7.13 Common Sites in the WHB area Used to Compare V_s profiles from SASW, Downhole and P-S Logging Measurements

No.	Borehole ID	Corresponding SASW Arrays
1	RF#13	SASW 1 and SASW 21
2	RF#14	SASW 20
3	RF#15	SASW 10 + 37
4	RF#16	SASW 29
5	RF#17	SASW 34+ 36
6	RF#18	SASW 14
7	RF#22	SASW 23 and SASW 30
8	RF#23	SASW 32 +35
9	RF#24	SASW 5, SASW 6, SASW 12 and SASW 18
10	RF#25	SASW 24
11	RF#26	SASW 4
12	RF#28	SASW 8 and SASW 9

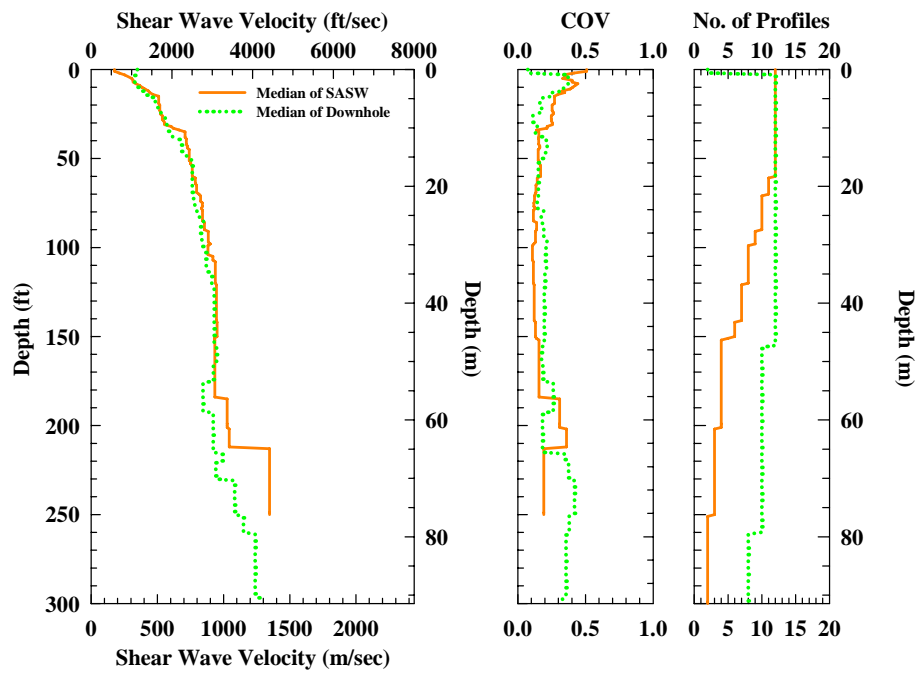


Figure 7.47 Comparison of SASW and Downhole Measurements at Common Sites in the WHB Area

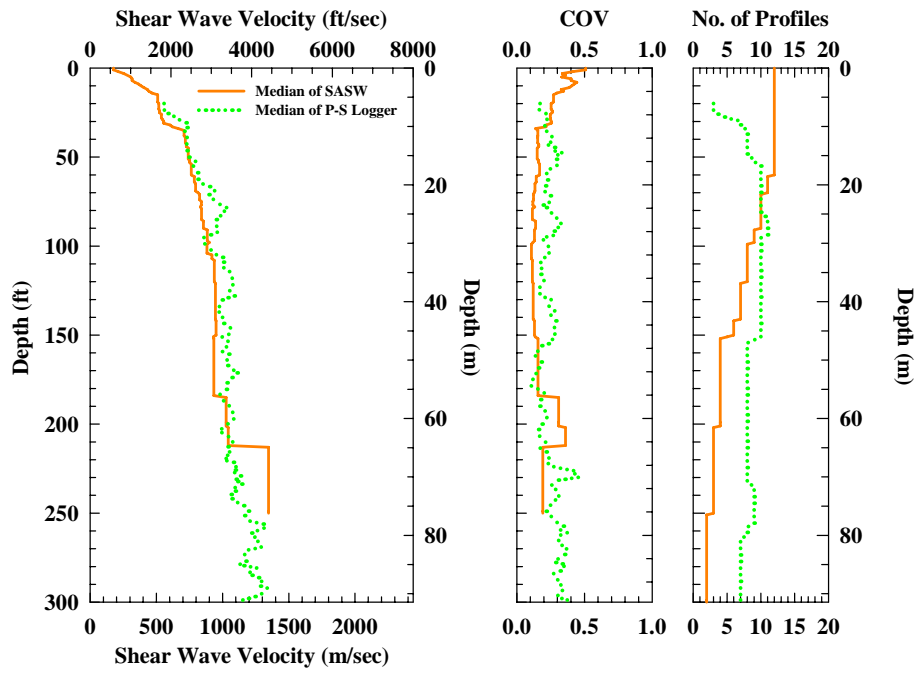


Figure 7.48 Comparison of SASW and P-S Logging Measurements at Common Sites in the WHB Area

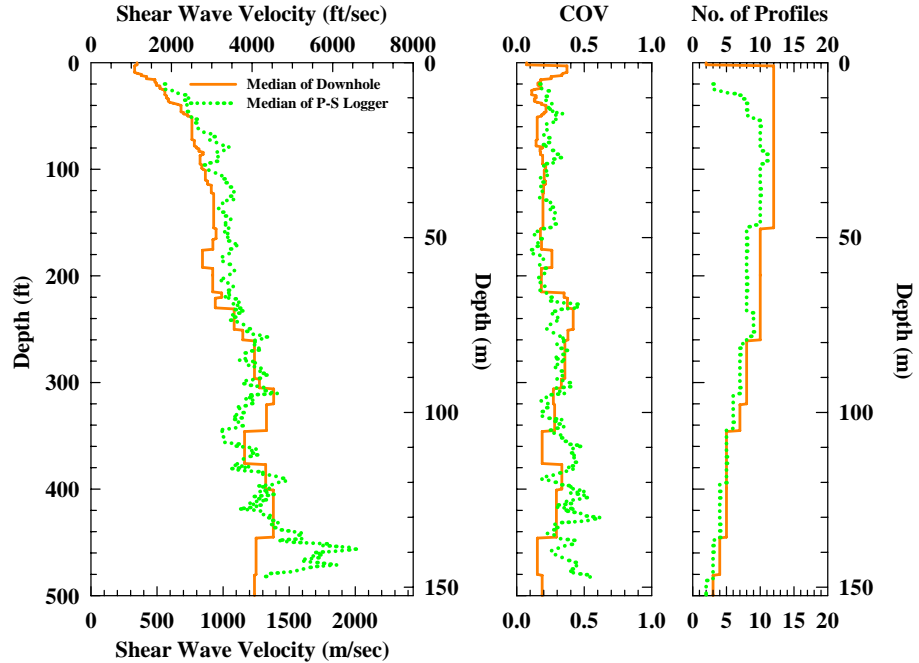


Figure 7.49 Comparison of Downhole and P-S Logging Measurements in the Common Sites at WHB Area

Lastly, the identical-site-and-depth (“green-apples-to-red-apples”) comparisons are made between the SASW and downhole, SASW and P-S logging, and downhole and P-S logging measurements in terms of their profiling depths at each borehole. The results are shown in Figures 7.50 through 7.55. The common profiling depths associated with each borehole are shown in Figures 7.51, 7.53 and 7.55. These figures help give a better idea about which depth at the different locations enter the analyses. Good agreement between the median SASW and downhole measurements is clearly seen in Figure 7.50. The COV profiles of the two measurements are similar in the top 180ft. From seen in Figures 7.52 and 7.54, the P-S logging measurements are slightly higher than the other two techniques. However, the COV profiles of downhole and P-S logging measurements are very similar (see Figure 7.54). Both COV profiles show larger variations than the COV profile from the SASW measurements. On average, the SASW and downhole measurements are consistent and the suspension logging measurements are slightly higher in the top 200 ft. This difference is affected, in some points, by the very localized measurements performed by in P-S suspension logging.

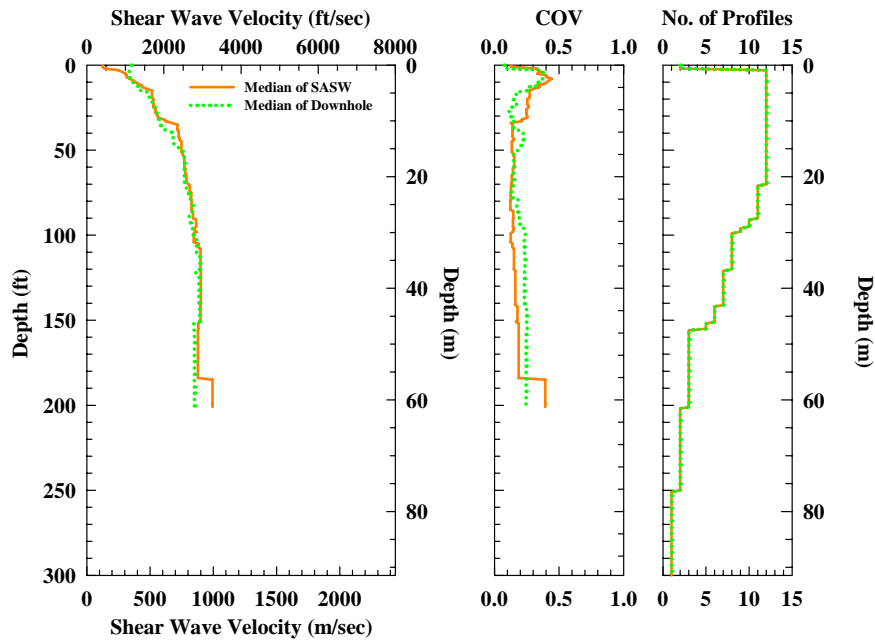


Figure 7.50 Identical-site-and-depth comparisons of SASW and Downhole Measurements at Common Sites and the Same Profiling Depths in the WHB Area

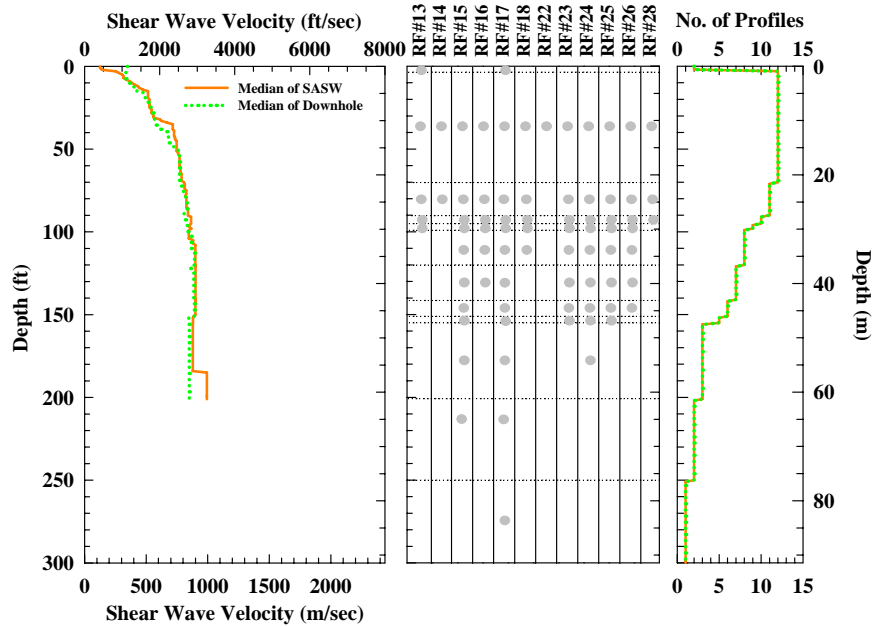


Figure 7.51 Identical-site-and-depth comparisons of SASW and Downhole Measurements at Common Sites and the Same Profiling Depths in the WHB Area with Borehole Information

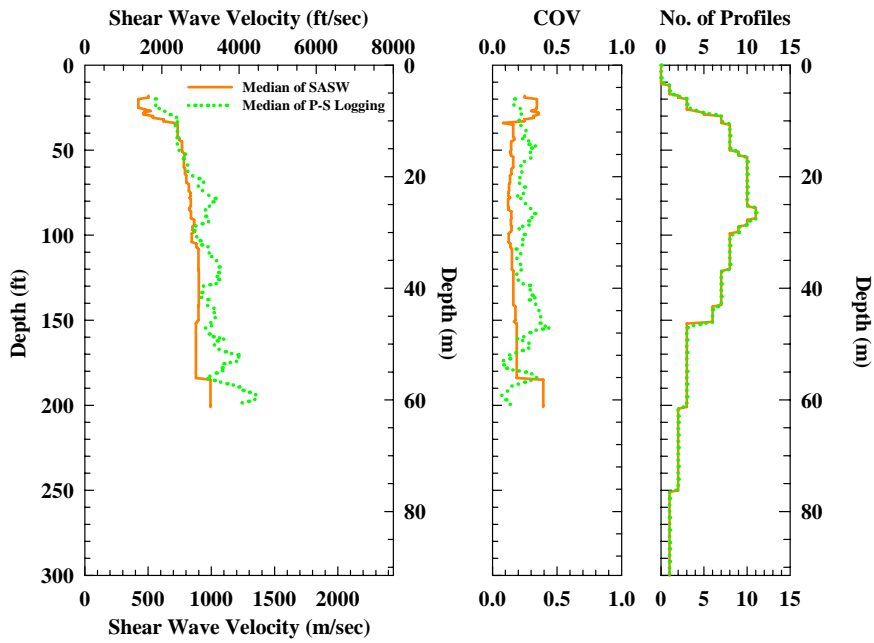


Figure 7.52 Identical-site-and-depth comparisons of SASW and P-S Logging Measurements at Common Sites and the Same Profiling Depths in the WHB Area

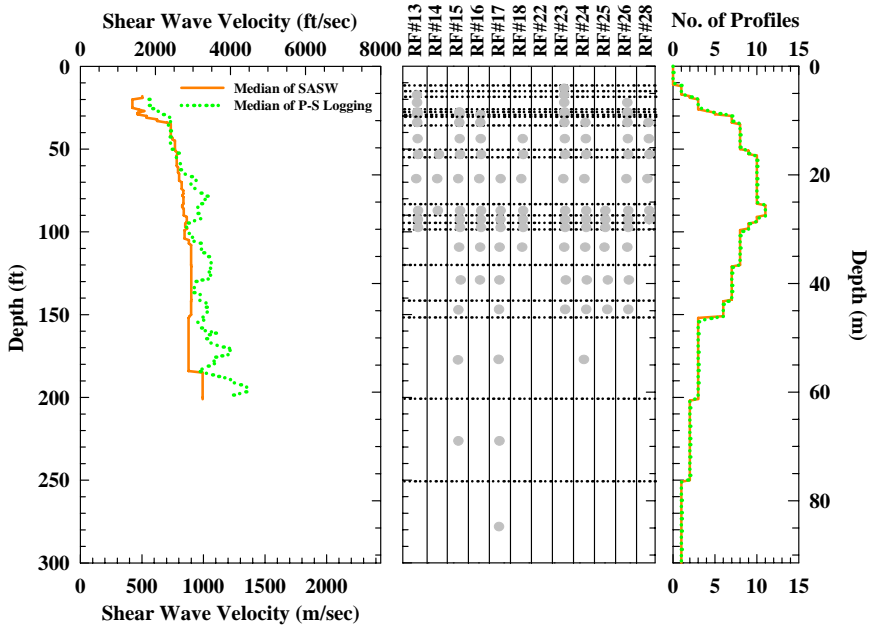


Figure 7.53 Identical-site-and-depth comparisons of SASW and P-S Logging Measurements at Common Sites and the Same Profiling Depths in the WHB Area with Borehole Information

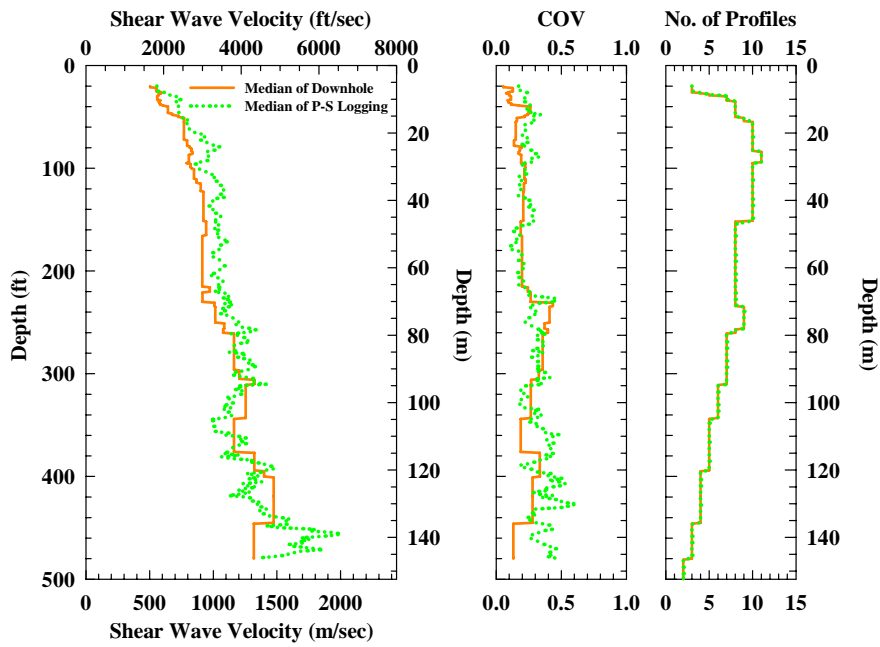


Figure 7.54 Identical-site-and-depth comparisons of Downhole and P-S Logging Measurements at Common Sites and the Same Profiling Depths in the WHB Area

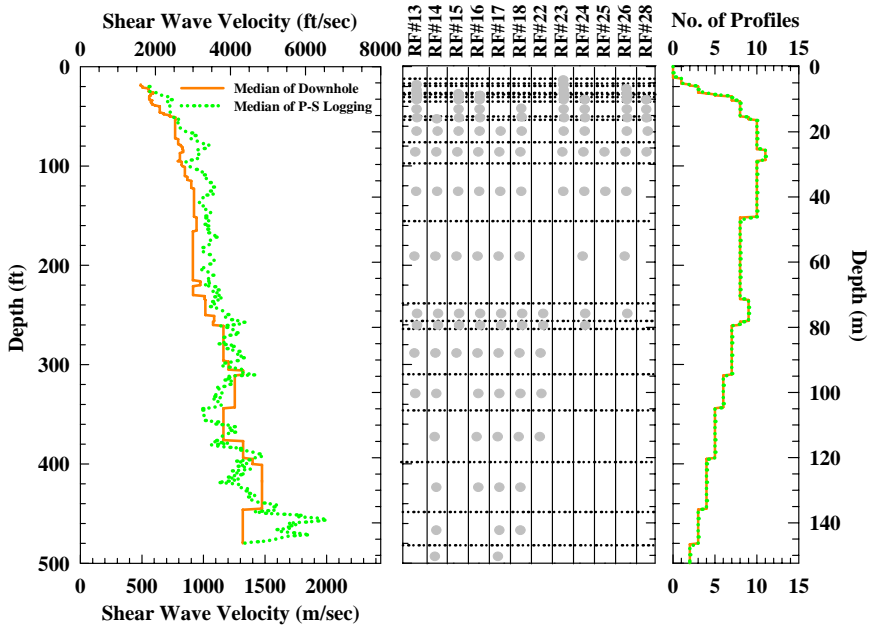


Figure 7.55 Identical-site-and-depth comparisons of Downhole and P-S Logging Measurements at Common Sites and the Same Profiling Depths in the WHB Area with Borehole Information

7.4.2 Comparisons between Different Test Areas

7.4.2.1 Surface SASW Testing Sites

The SASW tests performed on the ground surface at four different areas are compared in Figure 7.56. These four areas are the mountain (YM, C, D and S sites), WHB, NPF and AP areas. One thing that needs to be mentioned is the statistical data of the NPF sites are from Figure 7.22 instead of Figure 7.21 because Site NPF 28 has different properties than the other NPF sites and is actually located in the WHB area. As seen, the number of SASW profiles in the mountain area exceeds the other areas. In contrast, the AP area only has six SASW profiles. Based on their median V_S profiles, in general, the mountain area is stiffer than the other three areas in the top 100 ft. This difference is expected because little to no alluvium exists on the mountain but it does exist in the other areas. In the depth range of 100 to 300 ft, the WHB area exhibits higher V_S values than the other areas, likely due to the shallow Tiva Canyon tuffs. The mountain and AP areas have very similar properties in the top 450 ft. The NPF area is the softest one in the depth range from 20 to 500 ft, due to thick alluvium in this area. In addition, the WHB area is stiffer than the NPF area, even though they are next to each other. There is major faulting between these areas.

According to the COV profiles, the soil and rock deposits at the NPF and AP sites are more uniform than the mountain and WHB areas. One of the reasons for this difference is that the area covered by the SASW tests at the mountain sites is much larger than the other areas and hence covers more differences in geology; that is the V_S values of the tuff formations have larger variations. As to the WHB area, faults cross this area which explains the large COV values.

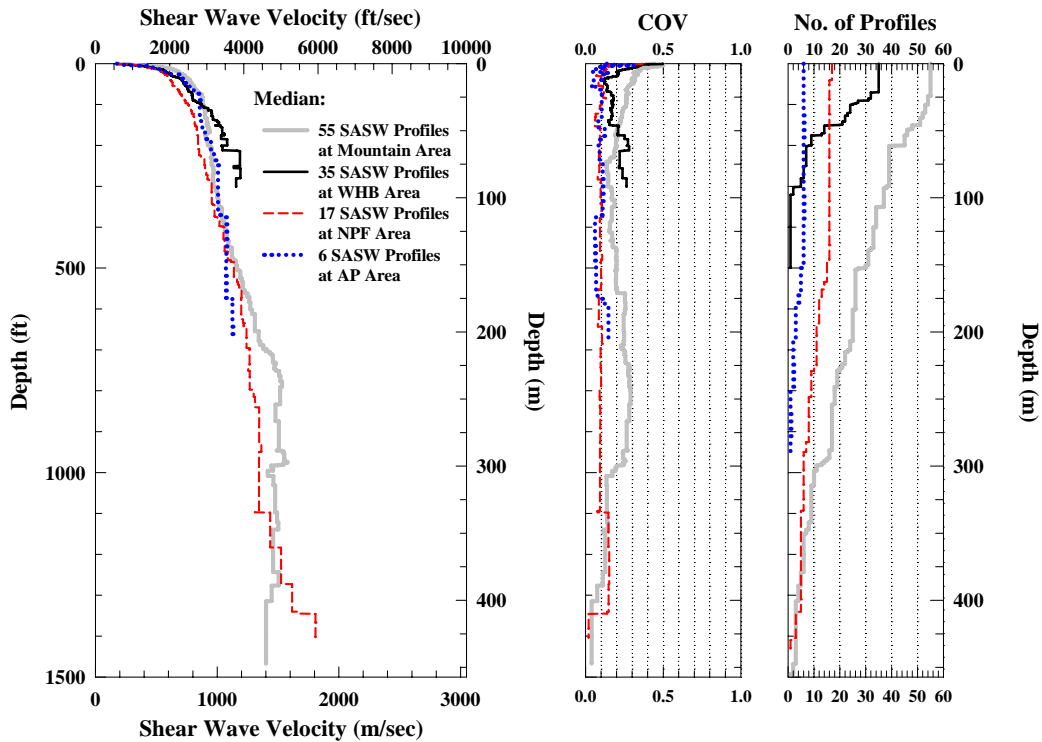


Figure 7.56 Comparisons of SASW Measurements Obtained from Different Areas in the YMP from 2000 to 2005

7.4.2.2 Mountain and Tunnel Testing Sites

Because SASW tests that were carried out in the mountain area in 2004 and 2005 profiled to depths over 1000 ft, a comparison can be made between the SASW V_S profiles from the mountain area at about 1000 ft deep with V_S values measured in the tunnel by SASW testing as discussed in Section 7.3.1.2. The SASW V_S profiles of 19 YM sites in Figure 7.15 were chosen for comparison with the tunnel SASW results. In addition, both of the seismic tomography surveys conducted by NSA Engineering, Inc. between ESF (Niche #3) and ECRB (Alcove #8) tunnels, and performed by Gritto et al. are also included in this comparison. Comparison between these different tests is presented in Figure 7.57 which shows very good consistency between these

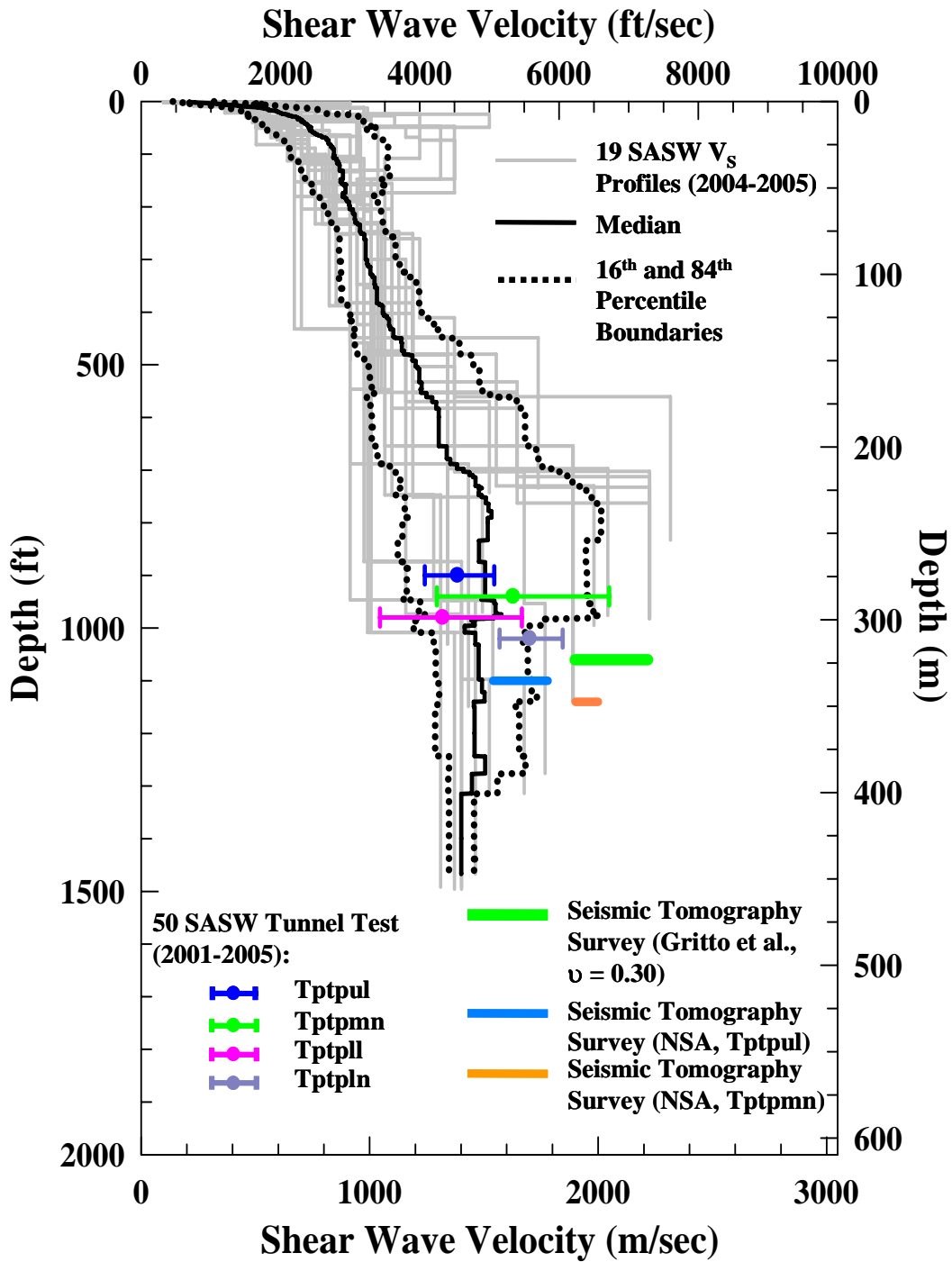


Figure 7.57 Comparisons of: (1) SASW Measurements in the Mountain Area above the Proposed Repository Area, (2) SASW Measurements in the ESF and ECRB Tunnels, (3) Seismic Tomography Surveys Performed by Gritto et al., and (4) Seismic Tomography Surveys Performed by NSA Engineering, Inc.

measurements. Furthermore, if the V_S ranges of the high and low velocity groups of the Tptpmn tuff are used instead of their overall V_S range, it can be seen that the high and low velocity groups at the mountain area match the high and low velocity groups of the Tptpmn tuff. This comparison is shown in Figure 7.58. This comparison shows same type of tuff may have large variations in the stiffness due to fracturing (and/or voids) in the tuff.

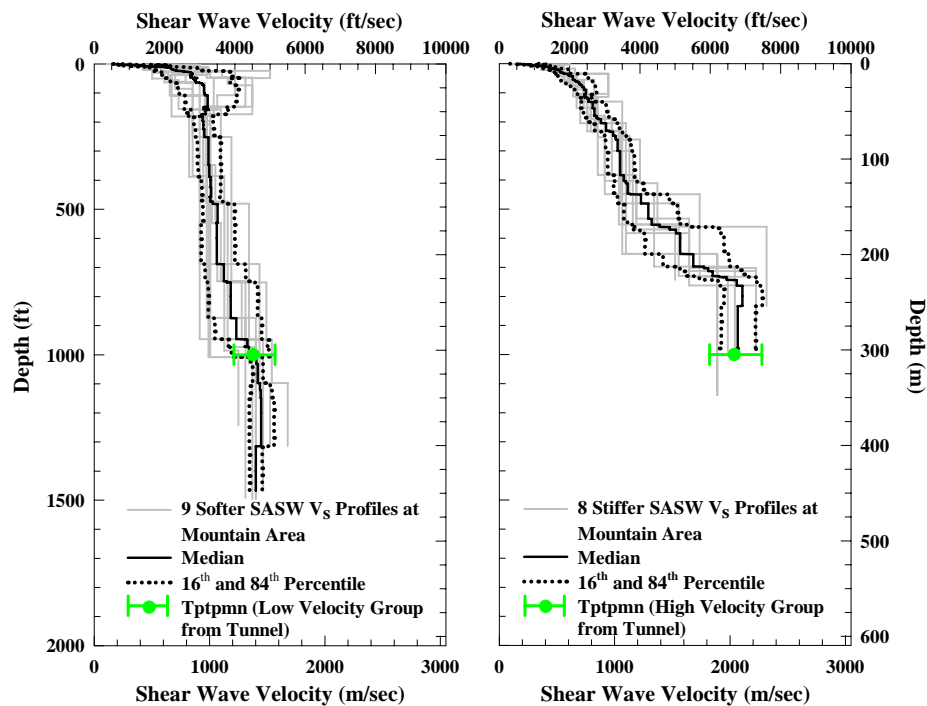


Figure 7.58 Comparisons of the High-and-Low Velocity Groups of the SASW Measurements at Mountain Area above the Proposed Repository Area and V_S Values of the Tptpmn Tuff Measured in the ESF and ECRB Tunnels

7.4.3 Comparisons Based on Geologic Information

Based on some geologic profile information offered by Mr. Michael Schuhen (Schuhen, 2005), more studies were conducted. The comparison of shear wave

velocities from surface SASW measurements with respect to different alluvium or tuff formations can be made based on the available geologic profiles. Also, the shear wave velocity of different tuffs obtained from SASW tests in the tunnels and other tests can also be compared with the surface SASW test results. Because the depths and thicknesses of layers varying, the same materials are compared regardless of their depths and thicknesses.

The geologic profiles include all SASW tests performed at the surface sites (16 YM, seven NPF and three AP sites) in 2004 and seven SASW test sites (D 1, D2, D 3, D5, D 8, D 9 and D 10) performed in 2001. These comparisons are made between the SASW surface and tunnel sites, free-free resonant column test results, VSP measurements, results from NSA Engineering, Inc. tunnel tests, and seismic tomography studies made by Gritto et al. The comparisons are presented in Figure 7.59. As seen, in most cases, the median laboratory results give the highest V_S values compared to the other measurements for the same type of tuff. In contrast, the median V_S values from the surface SASW measurements are the lowest. This difference is because the laboratory tests are always performed on “high quality” specimens; that is, less fractures or voids in the laboratory samples. For the field SASW tests, even the small spacing tests in the tunnels, the tested samples are much larger than the laboratory specimens. The same logic can be applied to the SASW tests performed on surface and in tunnel. SASW tests conducted at the surface site sample a larger amount of tuff than the tunnel SASW tests so that the SASW measurements obtained in the tunnels are higher. This difference is further amplified by the fact that SASW tests in the tunnel could not be performed on tuffs that were highly fractured or have numerous large voids.

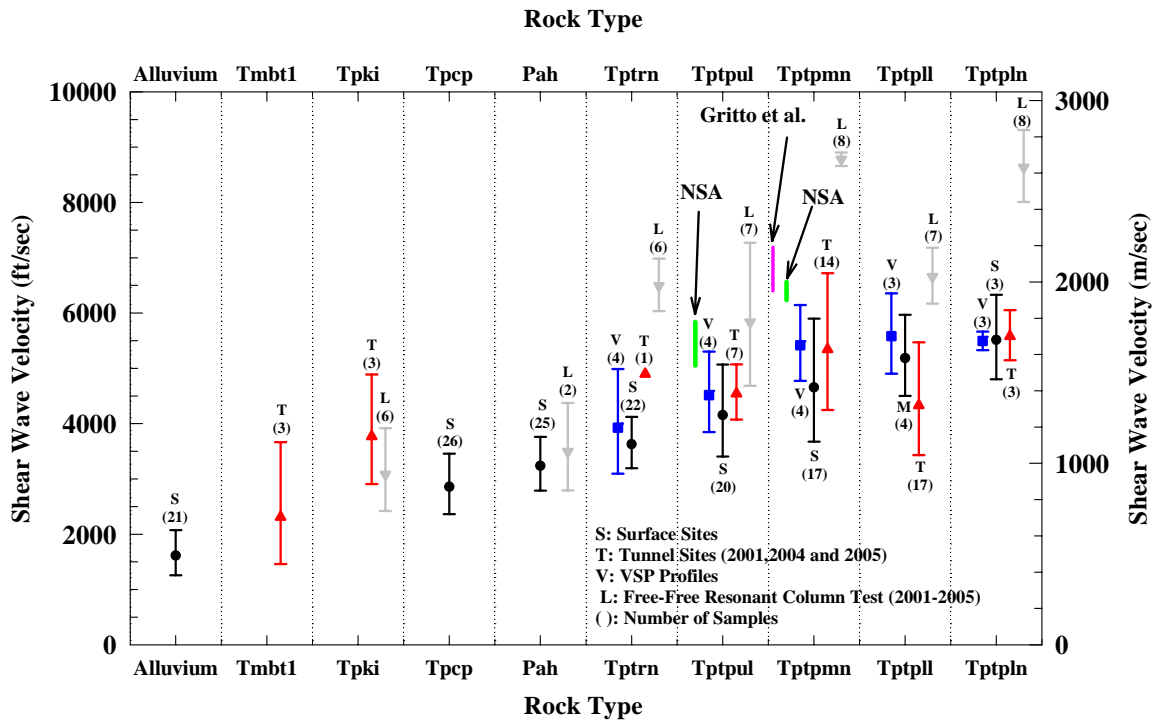


Figure 7.59 Comparisons of V_S Measurements from Different Techniques with Respect to the Alluvium and Different Tuffs

7.5 SUMMARY

In this chapter, SASW tests are presented that were performed for the Yucca Mountain Site Characterization Project from 2000 to 2005. The purpose of the Yucca Mountain Project is to use the SASW method to survey the rock (tuff) stiffness at the proposed repository depth and at associated facility locations around the site. Other seismic tests were also conducted at many of the same areas and the V_S profiles from these tests are compared with the SASW measurements. In general, V_S profiles from the SASW tests are consistent with the downhole and suspension logging methods, especially in the “green-apples-to-green-apples” comparisons. However, the SASW and downhole measurements exhibit slightly better consistency than the suspension logging

data at the WHB test sites where the most data are available. One problem that occurred in making these comparisons is missing V_S data in some of the profiles. Because the tuffs are fractured and porous, it was difficult to keep water in the boreholes for the P-S suspension logging. Therefore, the suspension logging profiles had zones where data was missing as well as no data near the surface (within about 20 to 30 ft). Also, the downhole profiles often had no data in the top 3 ft and tended to exhibit higher velocity within the top 3 to 15 ft. These differences made comparing $V_{S,30}$ and site classifications more difficult at times. In general, the site classifications were in agreement. However, the downhole measurements seem to overestimate the $V_{S,30}$ and hence determine the next higher site classification, if the actual $V_{S,30}$ of the test site was very close to the upper boundary of a site class.

Other than the downhole and P-S logging surveys, other seismic tests results were also compared with the SASW measurement. In general, these measurements are consistent with SASW test results, except for the free-free resonant column tests. However, this difference was expected because the specimens tested in laboratory were biased to the better quality (less fractures or voids) due to their small sizes. In contrast, the SASW tests usually resulted in the lowest values of V_S due to the global nature of the SASW test. As observed in Figure 7.59, the contrast of V_S velocities between the tuffs is not large enough to identify the different tuffs from the V_S measurements. Therefore, it was not possible to use the measured shear wave velocities to determine the depth or locations of the different tuff formations.

Chapter 8 Sensitivity Studies

8.1 INTRODUCTION

In this dissertation, the SASW method was used to obtain shear wave velocity profiles of the subsurface at several different locations in the United States and in Taiwan. Based on these V_S profiles and the IBC-2006 provisions, a site can be classified using the V_S profiles in the top 30 m (100 ft) ($V_{S,30}$) for the site characterization. As discussed/observed in the preceding chapters, in general, the SASW measurements agree well with the results from other techniques, such as downhole and suspension logging methods, in terms of shear wave velocity profiles and site classes as long as the comparisons are made on a “green-apples-to-green-apples” base. However, the impact of changing some assumed parameters used to determine the field V_S profiles in the WinSASW program was not investigated. Therefore one sensitivity study was conducted to evaluate the impact of the assumed parameters used in forward modeling with WinSASW on the V_S profiles. In some cases, the V_S profiles from the suspension logging method shows a relatively softer layer between stiffer ones which is not observed in the SASW profile at the same site. To study if the SASW method is sensitive enough to detect this kind of geotechnical structure, another sensitivity study was performed. Again, the WinSASW program was employed to do the analysis. Both of these sensitivity studies are discussed in the following sections.

8.2 STUDIES OF ASSUMED PARAMETERS USED IN FORWARD MODELING WITH WINSASW

In the forward modeling process used in WinSASW, some parameters need to be assumed in order to develop the V_S profile. These parameters include layer thickness, unit weight (γ) and two of the following three parameters, V_P , V_S and Poisson’s ratio (ν)

of each layer. To study the impact of changing these parameters on the resulting V_S profile, forward modeling was performed with the WinSASW program to generate dispersion curves for corresponding V_S profiles, and to see how well or poorly the fit between the dispersion curves before and after the parameter were changed.

8.2.1 Poisson's Ratio

Actually, one of the three parameters, V_P , V_S and ν , of each layer can be calculated from the other two by:

$$\frac{V_P}{V_S} = \sqrt{\frac{2(1-\nu)}{1-2\nu}} \quad (8.1)$$

The relationship between V_S and V_R can be obtained from Equation 2.1 or Figure 2.4 with respect to different Poisson's ratios. As seen, all the equations mentioned here are related to the Poisson's ratio. Therefore, ν is an important parameter in the SASW data analysis as long as the soil is unsaturated; hence, V_P is less than 5000 fps for the soil skeleton. To investigate the impact of changing Poisson's ratio on the resulting V_S profiles, a sensitivity study was performed with the real data from the NPF 20 site in Yucca Mountain, NV. The field dispersion curve and the matched theoretical dispersion curve (Figure 8.1), shear wave velocity profile (Figure 8.2) and tabulated parameters (Table 8.1) used in the forward modeling to generate the matched theoretical dispersion curve are shown below.

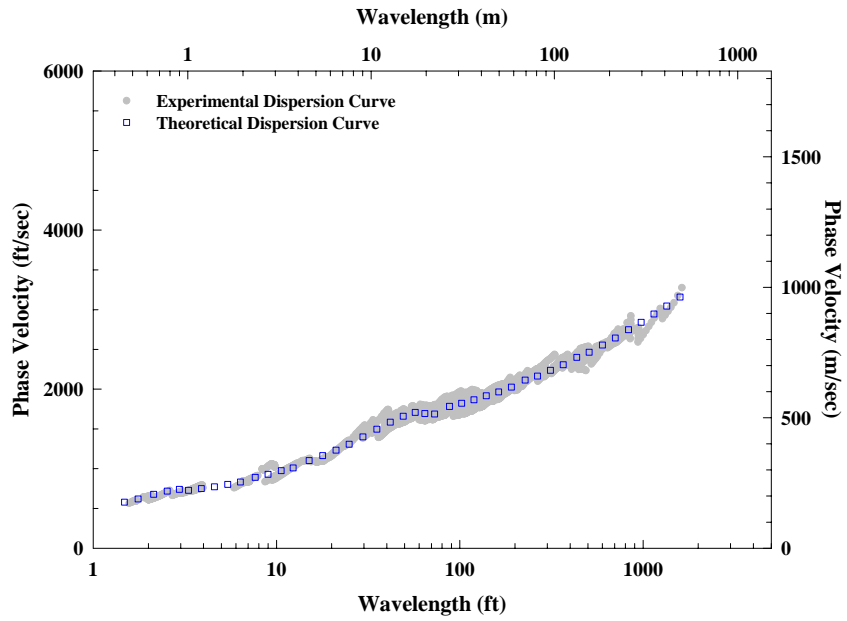


Figure 8.1 Original Experimental and Theoretical Dispersion Curves from a SASW Test Site (Site NPF 20 in Yucca Mountain, NV)

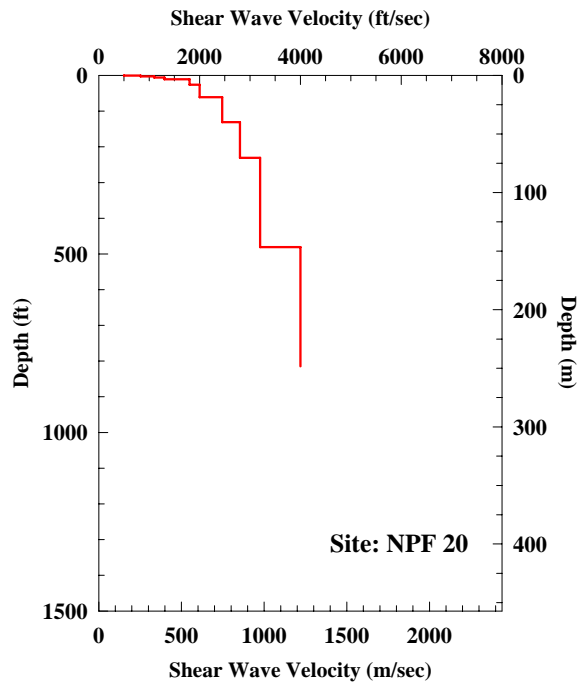


Figure 8.2 Original Shear Wave Velocity Profile Determined from the Forward-Model Match Shown in Figure 8.1

Table 8.1 Original Profile Parameters Used to Develop the Theoretical Dispersion in Figure 8.1

Layer No.	Thickness, ft	Depth to Top of Layer, ft	S-Wave Velocity, ft/s	Assumed Poisson's Ratio	P-Wave Velocity, ft/s	Assumed Mass Density, pcf
1	0.6	0	500	0.33	993	120
2	2.2	0.6	830	0.33	1648	120
3	3	2.8	1100	0.33	2184	120
4	5	5.8	1300	0.33	2581	120
5	15	10.8	1800	0.33	3573	120
6	35	25.8	2000	0.25	3464	130
7	70	61	2450	0.25	4244	130
8	100	131	2800	0.25	4850	130
9	250	231	3200	0.25	5543	130
10	334	481	4000	0.25	6928	130
11*	Half Space	815	4000	0.25	6928	130

* Layer below maximum depth of the V_S Profile

For general soil or rock material, the range of Poisson's ratio is between 0.20 and 0.40 as mentioned in Chapter 2. To study the effect of the Poisson's ratio on the resulting V_S profile, the minimum and maximum values of the range of common Poisson's ratio (i.e. 0.20 and 0.40) are used to replace the all original values of Poisson's ratio in Table 8.1. For each study, the initial V_S profile is the same as the Table 8.1 but with modified Poisson's ratios which are equal to either 0.20 or 0.40 in each case. The corresponding theoretical dispersion curves of each case are shown in Figure 8.3. As seen, there are obvious differences between the three theoretical dispersion curves. After performing the forward modeling as illustrated in Chapter 2 from Figures 2.51 to 2.55, the final V_S profiles reduced from each case can be obtained by matching theoretical dispersion curve to the original field dispersion curve. The original and two new theoretical dispersion curves, and the field dispersion curve are shown in Figure 8.4. As seen, the three theoretical dispersion curves generated by forward modeling are almost "identical" as shown by their corresponding V_S profiles presented in Figure 8.5. As observed, the V_S profile with $\nu = 0.20$ does not differ much from the original V_S profile (averages less than 3%). In addition, the difference at the deeper depths is less

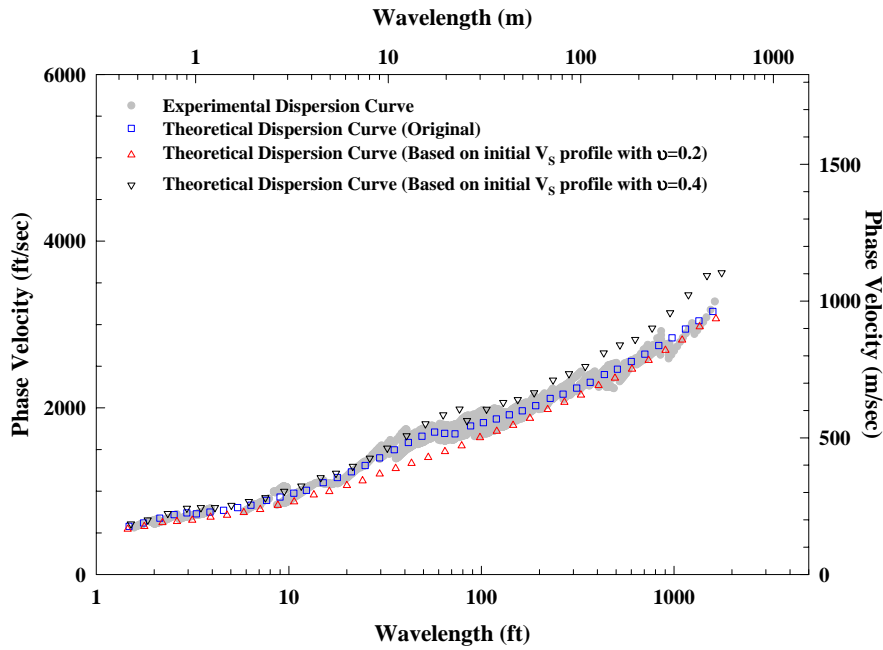


Figure 8.3 Comparison of Original Experimental and Theoretical Dispersion curves in Figure 8.1, and Two New Theoretical Dispersion Curves of Original V_S Profile with Modified Poisson's Ratios ($\nu=0.20$ and $\nu=0.40$)

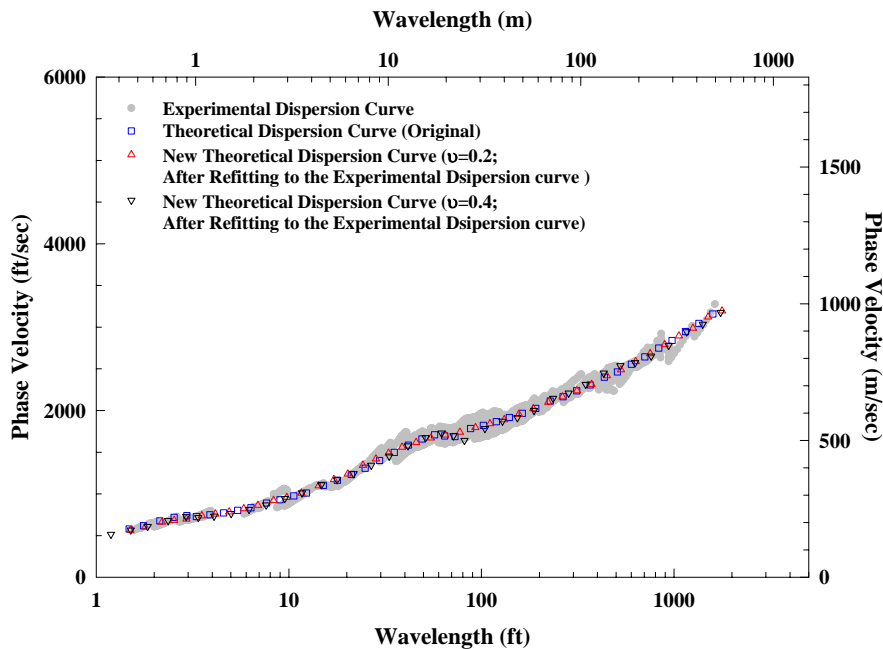


Figure 8.4 Comparison of Original Experimental and Theoretical Dispersion curves in Figure 8.1, and Two New Best-Matched Theoretical Dispersion Curves

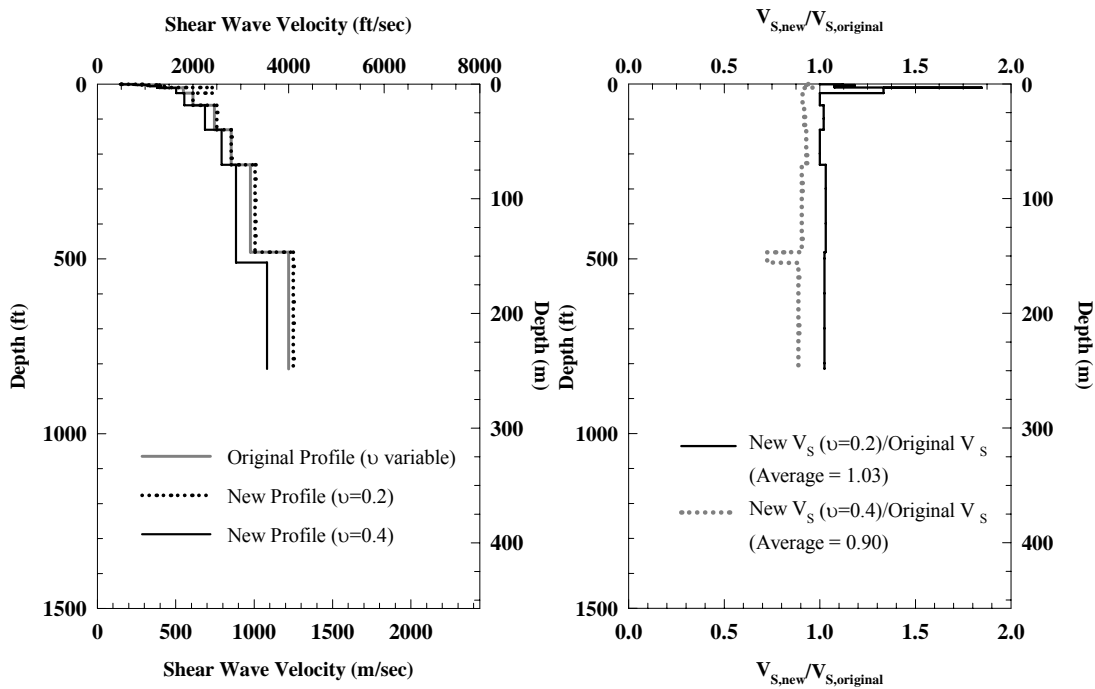


Figure 8.5 Comparison of Original and New Shear Wave Velocity Profiles Determined for the Same Site with Different Assumed Values of Poisson's Ratios

than at the shallower depths between the two V_S profiles. This difference is expected because the assumed Poisson's ratio of the original V_S profile is larger (closer to 0.40) at the shallow depths and becomes smaller (closer to 0.20) at the deeper depths. The same logic can be applied to the V_S profile with $\nu = 0.40$. The difference is larger at the bottom of the original V_S profile. However, the average difference is 10 %. The parameters of the two new V_S profiles used to generate the matching theoretical dispersion curves with the field one are tabulated in Tables 8.2 and 8.3. The differences in the V_S profiles compared to the original one are also shown in the tables. In general, the difference is no more than 10% in both cases. This variance, however, is somehow larger than the value discussed in Chapter 2. This is because the difference compared in

Chapter 2 is based on 2-D solution, i.e. it is according to the plane Rayleigh waves. In contrast, the inconsistency obtained here is based on the 3-D solution. That means it take higher modes and the effects of body waves into account. Even the V_S profile difference is bigger here compared to the same range of Poisson's ratio studied in Chapter 2 based on Rayleigh wave 2-D solution but, in general, the total difference is less than 13% from the range of $\nu = 0.20$ to 0.40 in this case. This difference is still within an acceptable "error" range in V_S profile for engineering practice. Moreover, it is rare to use the Poisson's ratio at 0.20 or 0.40 so this difference compared here should be smaller in the real world. Of course, the way to handle this problem if one has no information about the site would be to use a range in Poisson's ratios and present a range in the V_S profile.

The study above is only for unsaturated soil layers or rock. The impact of saturation (or water table) is discussed in the Brown (2002).

8.2.2 Unit Weight

Based on some theoretical studies (Stokoe et al., 1994), the accuracy of the assumption of unit weight (γ) used in the SASW analysis is small; that is, changes in the assumed unit weight have little effect on the V_S profile. To investigate further the impact of the change in unit weight on the resulting V_S profile, the example used in the previous section is again used here.

First, the range of unit weight of normal geotechnical materials needs to be decided. Generally, the range of the unit weight from 90 to 165 pcf should cover most soil and rock materials. The upper and lower boundaries of this range (90 and 165 pcf) are used to study the how different unit weights affect the final V_S profile reduced from the SASW method.

Table 8.2 New Profile Parameters Used to Develop the Theoretical Dispersion Curve in Figure 8.4 for a Constant Value of Poisson's Ratio of 0.20

Layer No.	Thickness, ft	Depth to Top of Layer, ft	S-Wave Velocity, ft/s	Assumed Poisson's Ratio	P-Wave Velocity, ft/s	Assumed Mass Density, pcf	$\frac{V_{s, New}}{V_{s, Original}}$
1	0.6	0	500	0.2	817	120	1.00
2	2.2	0.6	930	0.2	1519	120	1.12
3	3	2.8	1300	0.2	2123	120	1.18
4	4	5.8	1400	0.2	2286	120	1.08
5	1	9.8	2400	0.2	3919	120	1.85
6	15	10.8	2400	0.2	3919	120	1.33
7	35	26	2000	0.2	3266	130	1.00
8	70	61	2500	0.2	4083	130	1.02
9	100	131	2800	0.2	4572	130	1.00
10	250	231	3300	0.2	5389	130	1.03
11	334	481	4100	0.2	6695	130	1.03
12*	Half Space	815	4100	0.2	6695	130	1.03

* Layer below maximum depth of the V_s Profile

Weighted^Δ Average = 1.03

Δ Based on layer thickness and neglecting the half space

Table 8.3 New Profile Parameters Used to Develop the Theoretical Dispersion Curve in Figure 8.4 for a Constant Value of Poisson's Ratio of 0.40

Layer No.	Thickness, ft	Depth to Top of Layer, ft	S-Wave Velocity, ft/s	Assumed Poisson's Ratio	P-Wave Velocity, ft/s	Assumed Mass Density, pcf	$\frac{V_{s, New}}{V_{s, Original}}$
1	0.6	0	470	0.4	1151	120	0.94
2	2.2	0.6	760	0.4	1862	120	0.92
3	3	2.8	1050	0.4	2572	120	0.95
4	5	5.8	1250	0.4	3062	120	0.96
5	15	10.8	1650	0.4	4042	120	0.92
6	35	26	1820	0.4	4458	130	0.91
7	70	61	2250	0.4	5511	130	0.92
8	100	131	2600	0.4	6369	130	0.93
9	250	231	2900	0.4	7104	130	0.91
10	30	481	2900	0.4	7104	130	0.73
11	304	511	3550	0.4	8696	130	0.89
12*	Half Space	815	3550	0.4	8696	130	0.89

* Layer below maximum depth of the V_s Profile

Weighted^Δ Average = 0.90

Δ Based on layer thickness and neglecting the half space

Second, the methodology used to conduct this study should be clarified. Actually, the way to carry out the study is very straight forward. The original field and theoretical dispersion curves can be used as the comparison reference. Then use the original V_s

profile with the changed unit weights (all 90 or 165 pcf) can be used to calculate the corresponding theoretical dispersion curves. By comparing the two new theoretical dispersion curves with the original field or theoretical dispersion curve, the impact of the modified unit weight can be studied. Figure 8.6 shows the comparison of dispersion curves generated from the same V_S profile with different unit weights. As seen, there is no obvious difference between these dispersion curves. Actually, the three theoretical dispersion curves are almost identical. Therefore, the impact of the wrongly assumed unit weight in the analysis of the SASW method is very minor or it has almost no effect.

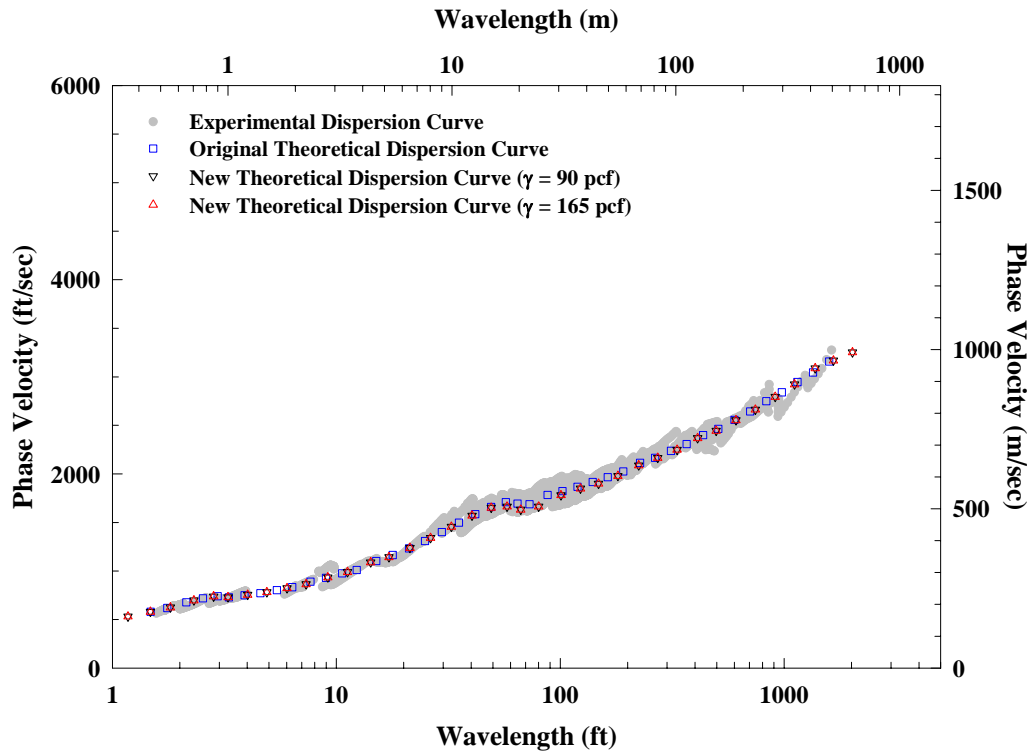


Figure 8.6 Comparison of the Original Field and Theoretical Dispersion Curves with Two New Theoretical Dispersion Curves Generated using from Modified Unit Weights and the Original V_S Profile

8.2.3 Layer Thickness

To study the impact of changing layer thickness on the original theoretical dispersion curve, the thickness of Layer #9 (see Table 8.1) in the original V_S profile was changed ($\pm 10\%$, $\pm 20\%$ and $\pm 30\%$ with respect to original thickness (250 ft)) to generate new theoretical dispersion curves. These theoretical dispersion curves were compared with the original theoretical (or experimental) dispersion curve in Figure 8.7. As seen, the differences are very minor. The same study was performed on Layer #8. As seen in Figure 8.8, the differences between the new theoretical dispersion curves and original theoretical dispersion curve are very small. Therefore, the change of layer thickness has very minor effect in the analysis of the SASW method.

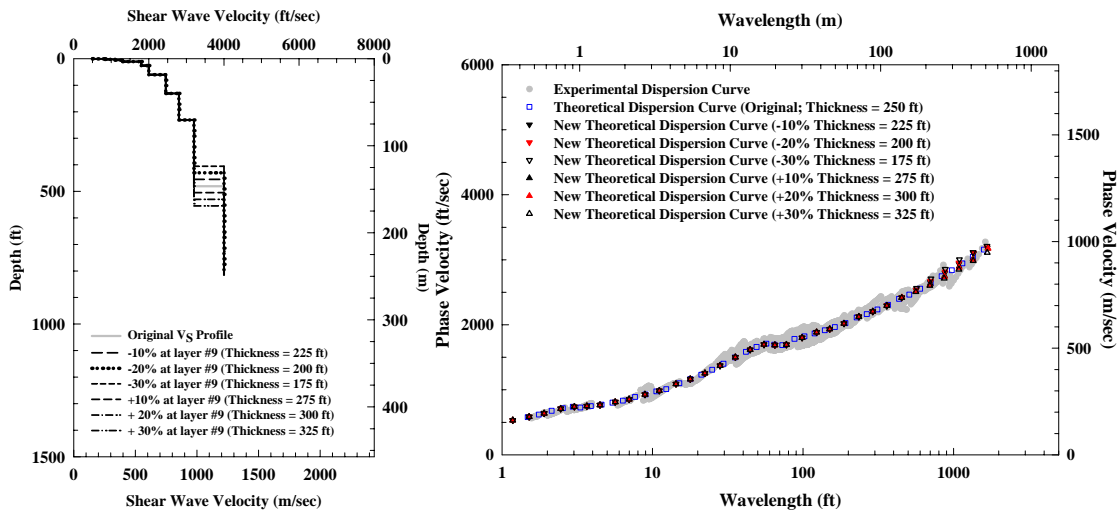


Figure 8.7 V_S Profiles with Various Thickness of Layer #9 (in Table 8.1) and Corresponding Theoretical Dispersion Curves

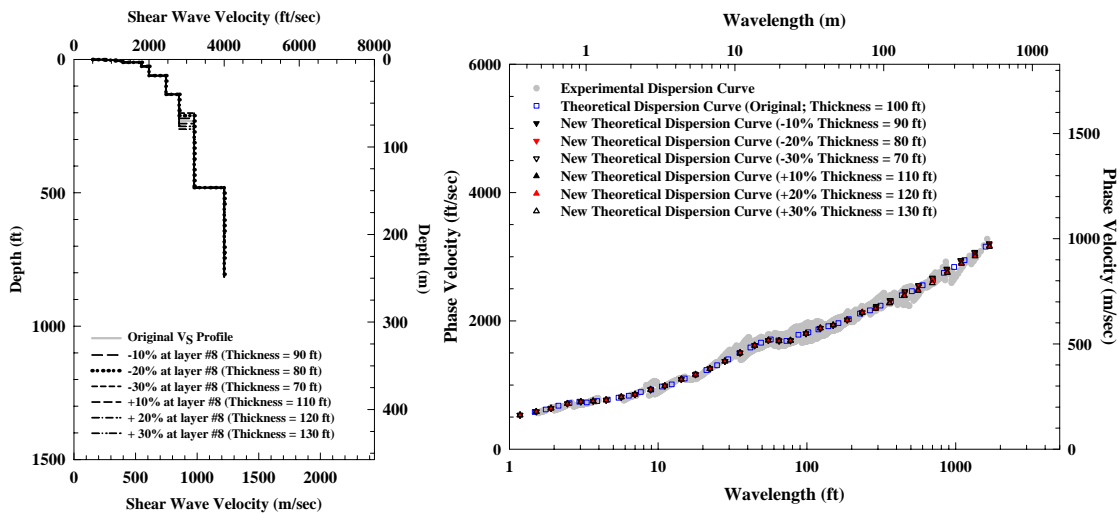


Figure 8.8 V_S Profiles with Various Thickness of Layer #8 (in Table 8.1) and Corresponding Theoretical Dispersion Curves

8.3 STUDIES OF THE CAPABILITY OF THE SASW METHOD TO DETECT SOFT LAYERS AT DEPTH

It is usually important to know if there is a soft layer at depth that is located between stiffer layers, especially for locations with important structures where large (differential) settlements due to the loading of the structures or large ground motions due to earthquakes may occur. If the soft layer is very deep or very thin, it may not cause a problem to the structure above it. However, if the soft layer is thick and/or shallow enough, it may damage the structure.

A sensitivity study was conducted to investigate what kind of the soft layer, in terms of thickness, depth and V_S contrast between the soft and stiffer layers, can be detected by the SASW method using the WinSASW program.

Some parameters have to be assumed before the study is started. First, the V_S of normal/stiffer layer is assumed to be 2000 fps adjacent to the soft layer. The value of 0.30 and 130 pcf are assumed for Poisson's ratio and unit weight (γ), respectively.

In this study, three thicknesses and three different V_S contrasts of a soft layer are investigated in the depth range from 2.5 to 500 ft. The studied thicknesses are 5, 10 and 20 ft and the assumed V_S contrasts are 20%, 35% and 50%. A velocity contrast of less than 20% typically has a minor effect on the engineering properties of a site. In contrast, a velocity contrast larger than 50% seems too large for the common geotechnical sites. This is why 20% and the 50% velocity contrasts were chosen as the upper and lower boundaries in this study. As to the thicknesses of the soft layers, they might be any number because they can be a value relative to the depth of the soft layer. By performing the study with the assumed parameters above, the relationships between the thickness, depth and V_S contrast of a softer layer can be determined within some ranges. Also, the criterion used to determine if the softer layer is detectable or not has to be defined. The "detectable" criterion adopted here is based on the difference (δ) between the minimum V_R value in the theoretical dispersion curves generated from each case with different depths, thicknesses and velocity contrasts, and the Rayleigh wave velocity (V_R) corresponding to the V_S of 2000 fps (normal/stiffer layers). If the difference (δ) is equal or less than 3%, the soft layer is considered as not detectable by the SASW method.

To understand the methodology used here, the procedure is illustrated in the Figure 8.9. The reference profile has: $V_S = 2000$ fps, $\gamma = 130$ pcf and the velocity is constant over the entire depths. Three difference cases (Cases A, B and C) with the same parameters but with the soft layer at different depths are presented. The soft layer has: $V_S = 1000$ fps, $\gamma = 100$ pcf and thickness = 10 ft. As seen, as the soft layer goes

deeper, the “dip” of the corresponding dispersion curve becomes smaller. If the δ is less than or equal to 3%, it is determined as “not detectable” by the SASW method.

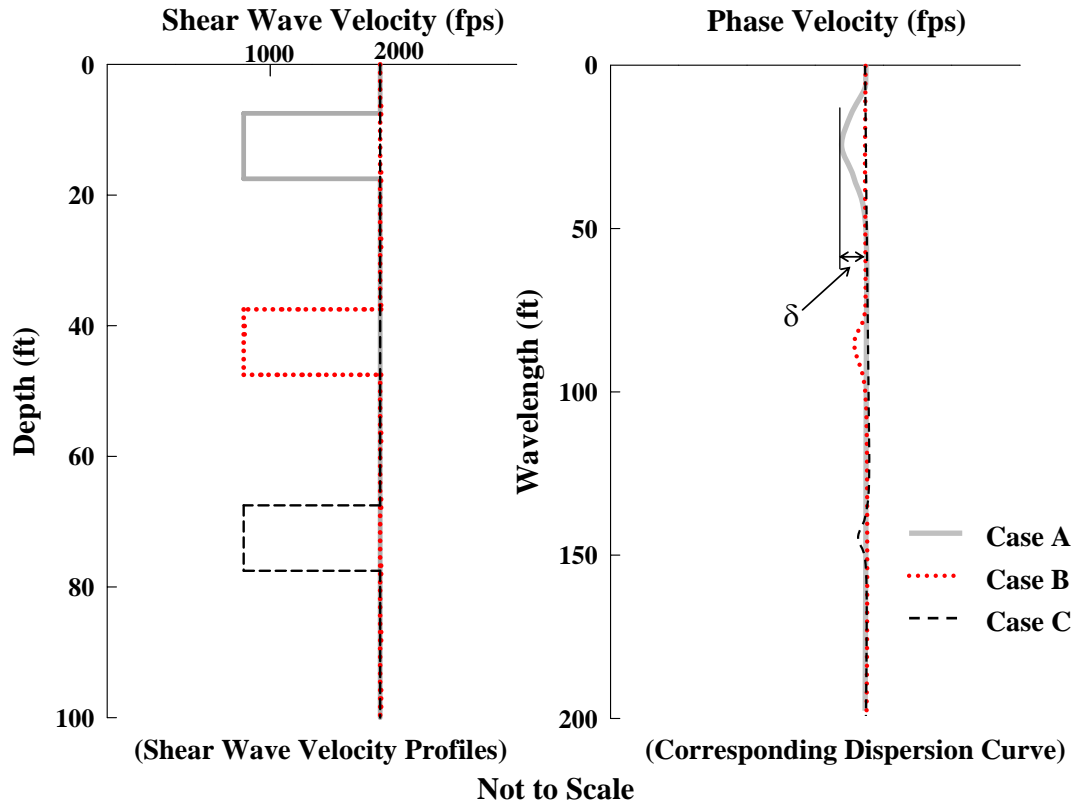


Figure 8.9 Illustration of the Methodology to Study the Sensitivity of the SASW Method in Detecting a Soft Layer

Based on the assumptions and methodology discussed above, the results are plotted with respect to the velocity contrast and depth of the soft layer with different thicknesses in Figure 8.10 and tabulated in Table 8.4. The area above each curve means the specific soft layer can be detected by the SASW method. For example, a 5-ft thick softer layer with 40% velocity contrast can be detected at the depth of 50 ft (point A). However, the same soft layer cannot be recognized with a 30% velocity contrast (point B). In addition, the curves from three soft layers with different thicknesses have a

similar shape. If the maximum detectable depths are normalized by the thickness of the corresponding soft layer, the three curves seem to be nearly the same as shown in Figure 8.11 and Table 8.5. If the average numbers in Table 8.5 are used, the three curves can be represented by the one curve as shown in Figure 8.12. Furthermore, if a log scale is used for the ordinate, the curve in Figure 8.12 becomes a straight line in Figure 8.13.

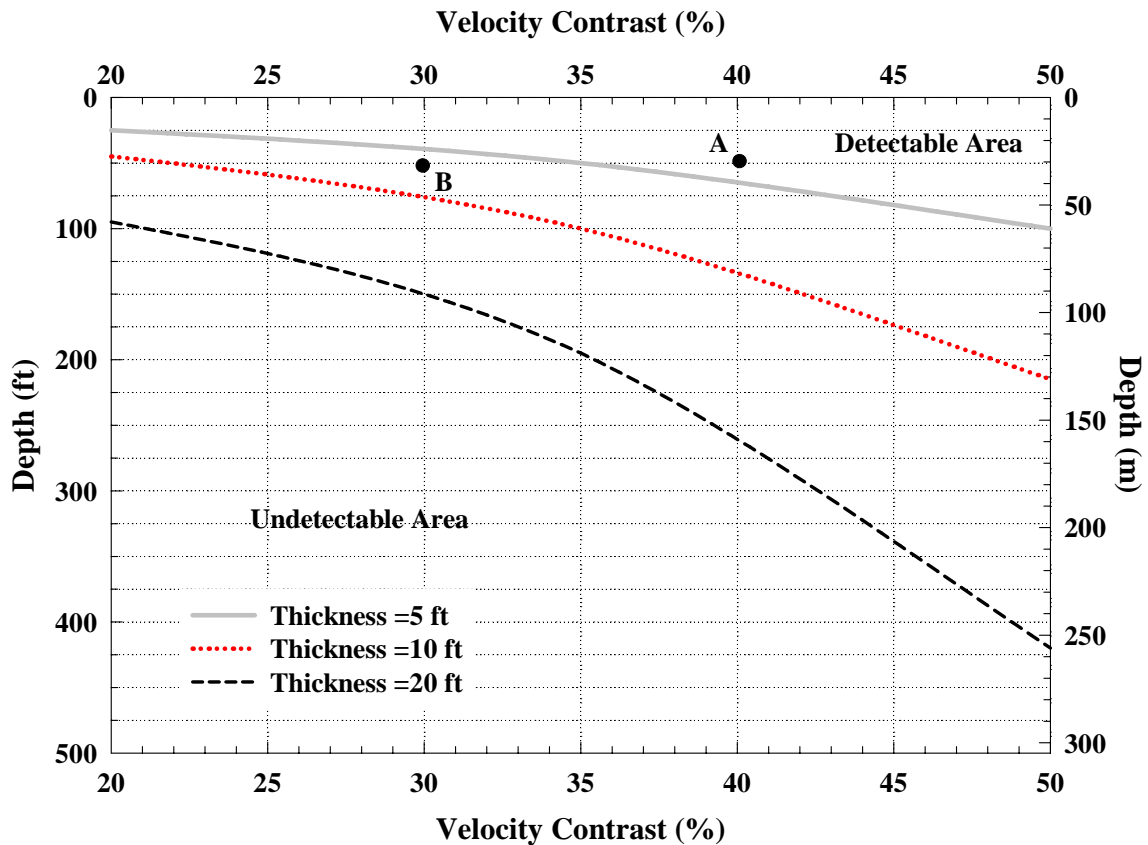


Figure 8.10 Relationships of Maximum Detectable Depth of Soft Layers with Respect to Different Velocity Contrast and Their Thickness

Table 8.4 Maximum Detectable Depth with Respect to Different Thicknesses and Velocity Contrasts of the Soft Layers

Velocity Contrast \ Thickness (ft)	20% (1600 fps)	35% (1300 fps)	50% (1000 fps)
5	25	50	100
10	45	100	215
20	95	195	420

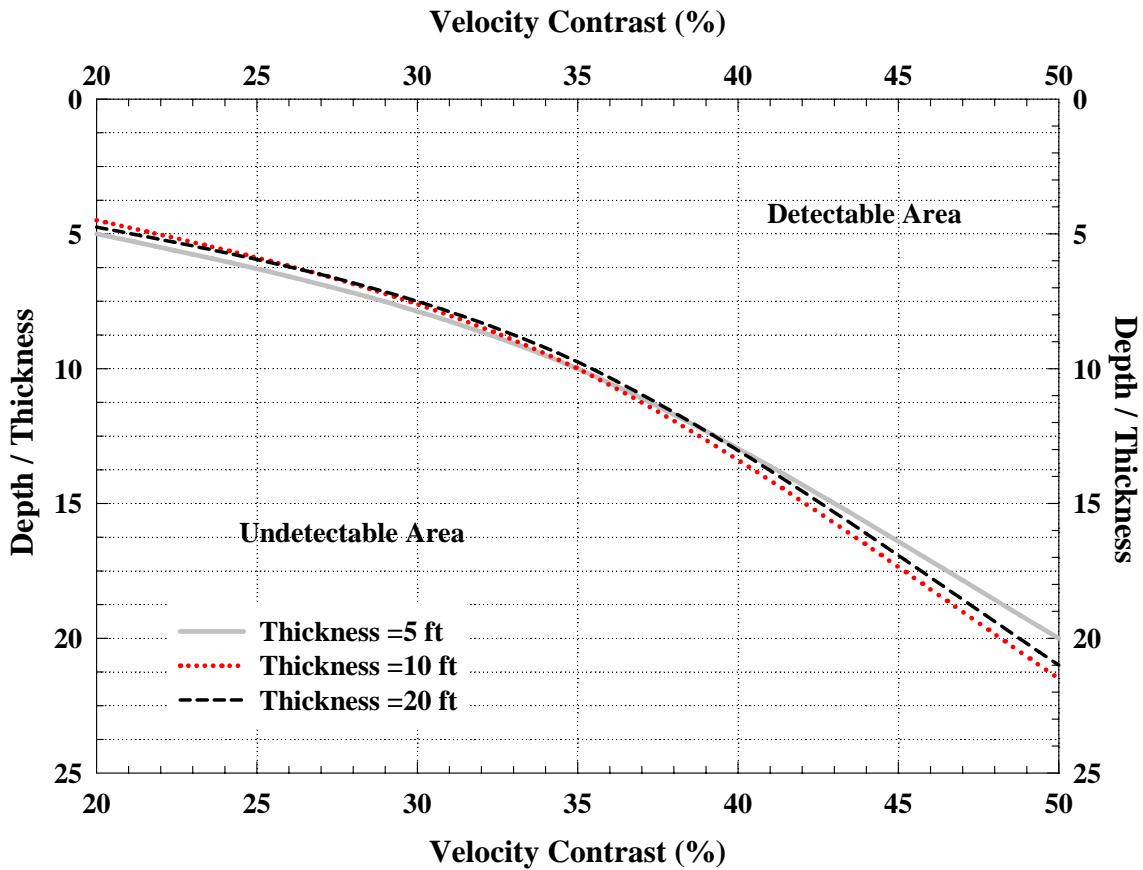


Figure 8.11 Normalized Relationships of Maximum Detectable Depth of Soft Layers with Respect to Different Velocity Contrast and the Ratio of Depth to Thickness

Table 8.5 Normalized Maximum Detectable Depth with Respect to Different Thicknesses and Velocity Contrasts of the Soft Layer

Velocity Contrast \ Thickness (ft)	20% (1600 fps)	35% (1300 fps)	50% (1000 fps)
5	5	10	20
10	5	10	22
20	5	10	21
Average	5	10	21

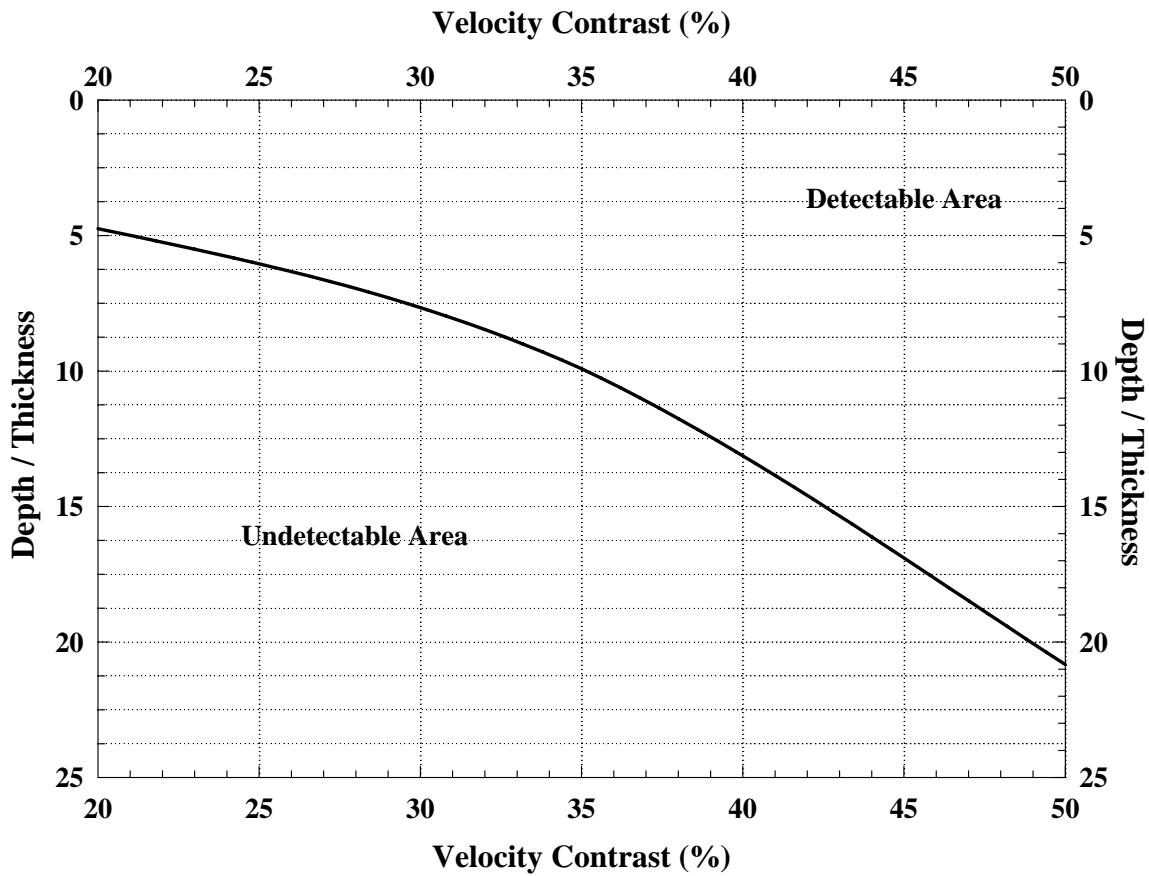


Figure 8.12 Representative Curve of Normalized Relationships of Maximum Detectable Depth of Soft Layers with Respect to Different Velocity Contrast and the Ratio of Depth to Thickness

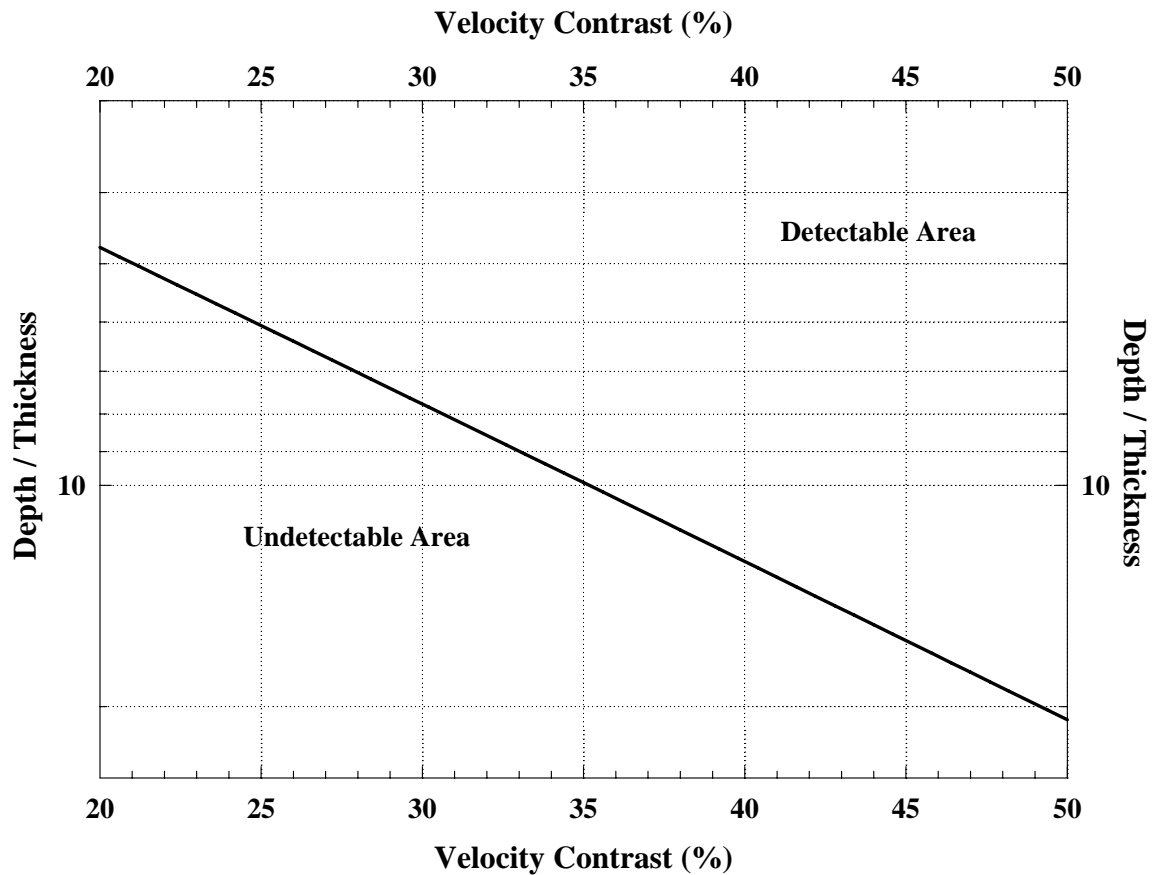


Figure 8.13 Representative Curve of Normalized Relationships of Maximum Detectable Depth of Soft Layers with Respect to Different Velocity Contrast and the Ratio of Depth to Thickness in Log Scale

Either Figure 8.12 or Figure 8.13 can be applied to various cases regardless of the thickness and depth of a soft layer. Even the V_s for the normal/stiffer soil layer in this study is 2000 fps, it could be change to any numbers because the velocity contrast was used here instead of shear wave velocity difference. Based on Figure 8.13, the minimum thickness to depth ratio of a detectable soft layer is from 5 to 20 with respect to the velocity contrast of the adjacent layer(s) to the soft layer for velocity contrast of 20% to 50%, respectively. That means the thickness of a soft layer should be at least 5% to 20% of its depth to be detected by SASW method within the range of velocity contrast

from 20% to 50% between the soft layer and its adjacent layers. However, if the “detectable” criteria were changed, the curve might become somehow different. The studies of using 5% and 10% as the “detectable” criteria are also conducted and the results are shown in the Figure 8.14.

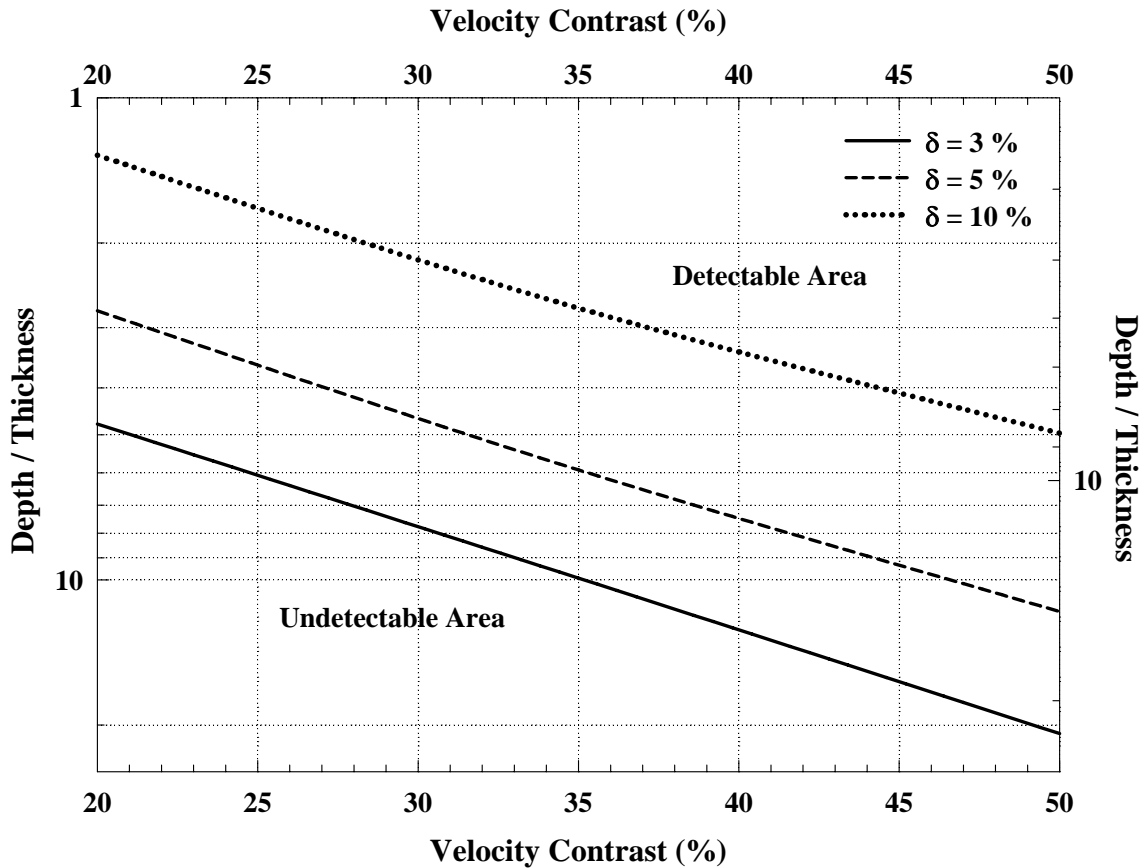


Figure 8.14 Representative Curves of Normalized Relationships of Maximum Detectable Depth of Soft Layers with Different “Detectable” Criteria with Respect to Different Velocity Contrast and the Ratio of Depth to Thickness in Log Scale

8.4 SUMMARY

In this chapter, two sensitivity studies were conducted. One considers the parameters used in the forward modeling with WinSASW and the other investigates the

capability of the SASW method to detect relatively softer layers. In the first study, three parameters, Poisson's ratio, unit weight and layer thickness were investigated. The other parameters, such as V_P or V_S , were not studied because they are all related to the Poisson's ratio. Based on this study, it shows the change of Poisson's ratio has more impact on the resulting final shear wave velocity profile than unit weight and layer thickness and the difference, on average, should be no more than 13% which is an acceptable range to the engineering practice. However, if an average Poisson's ratio (i.e. 0.30) is chosen to generate the original theoretical dispersion curve, the difference between this curve and the theoretical curves with Poisson's ratio 0.20 or 0.40 should be no more than 10%. In addition, the difference observed in this study is bigger than what was discussed in Chapter 2 because in Chapter 2, the 2-D solution (Plane Rayleigh waves) was used instead of 3-D solution in this chapter.

The other sensitivity study investigated the ability of the SASW method to detect relatively softer layers at depth. In this study, a reference profile was assumed with a soft layer having various thicknesses, depths and velocity contrasts in the reference profile. By means of the WinSASW program, the relationships between the thickness, depth and velocity contrast to the adjacent layer of a soft layer was developed. The generalized relationships or models with different "detectable" criteria are shown in Figure 8.14. This simple model can also be applied to other cases that are different than what was studied because most of the parameters used in the model are relative values, such as thickness to depth ratio and velocity contrast to the adjacent layer(s) of a soft layer. As to changing Poisson's ratio to this model, based on the first study, the difference caused by that should be no more than 10%.

Chapter 9 Summary, Conclusions and Recommendations

9.1 SUMMARY

The shear wave velocity (V_S) profiles of geotechnical sites offer important information used to characterize geotechnical sites and to the design of structures and facilities that may be subjected to earthquake shaking at these sites. The Spectral-Analysis-of-Surface-Waves (SASW) method is an excellent seismic profiling technique that can be used to evaluate V_S profiles. First, the SASW method is a non-intrusive method that requires no boreholes to survey the subsurface so the cost is lower than borehole seismic tests, such as the downhole and suspension logging tests. For the same reason, the SASW test can be performed at any location even though boreholes are not available or may not even be allowed. Also, the profiling depth of the SASW method is not limited by the borehole depth. Instead, it is mainly limited by the seismic source and the site conditions. The maximum survey depth by SASW testing until now is about 2000 ft in Hanford, WA. Second, V_S profiles determined by SASW testing can have more resolution and accuracy at shallow depths (in the top 30 ft) than downhole and P-S logging measurements as observed in the data presented in this dissertation. The reason the V_S profile was missed or overestimated at the shallow depth may be relative to casing or poor coupling in P-S logging and refraction combined with relatively large V_S increases in the top 5 to 15 ft in downhole testing. The velocity measured by the two borehole methods may propagate along the ground surface and along the casing or borehole wall instead of the shortest path between the source and receiver(s). Poor coupling between the borehole wall and receiver(s) near the surface or other depths may result in data hard to be interpreted as well.

Also, the downhole and suspension logging tests were performed by separate organizations and the profiles were submitted to a third party before any comparisons were made so it was a “blind” study.

WinSASW, used to conduct many studies in this work, is a comprehensive software package with which forward modeling, both global- and array-based, and inversion can be performed. Forward modeling incorporated in WinSASW is based on the dynamic stiffness matrix method presented by Kausel and Roesset (1981) and Kausel and Peek (1982). In this study, WinSASW was used to perform forward modeling. For the vast majority of the analyses, global forward modeling was done. In some cases, array forward modeling was used to investigate the field dispersion curve at largest receiver spacings.

Conclusions from SASW tests performed in four different regions and from sensitivity studies of the SASW method are presented below.

9.2 CONCLUSIONS

9.2.1 Tests Performed in Imperial Valley, CA

In Imperial Valley, in addition to 31 SASW tests performed in 2005 and 2006, there are 21 downhole and three P-S logging measurements available in the same area. Based on the median and 16th and 84th percentile boundaries of the V_s profiles obtained from these three different methods, different comparisons were made with respect to three criteria. These criteria are: (1) general (apples-to-oranges), (2) common site (green-apples-to-red-apples) and (3) identical-site-and-depth (green-apples-to-green-apples) comparisons.

These comparisons show that V_s profiles from the SASW method are more consistent with the downhole and P-S logging methods or vice versa in the “green-

apples-to-green-apples” comparison than the other two comparisons. The “green-apples-to-green-apples” comparisons have the best consistency between the SASW and downhole measurements, especially when the V_S profiles obtained in mountain area and at the perimeter area of the valley were excluded. The value of COV (value of one standard deviation divided by mean) profile of the SASW measurements becomes smaller when the included sites have similar site classes or are at similar geologic locations. For the SASW measurement in the central valley area where the soil deposit is quite uniform, the COV profile is close to 0.10 at many depths, with an average value around 0.15 or lower. When the V_S profiles from the other locations whose soil properties are not similar to the central valley area are added to the comparison, the SASW COV profiles jump up to a value over 0.18 or much higher in most depths. Based on this point, if the value of the (average) COV profile of the SASW V_S profiles obtained from a area is no more than 0.15, this area can be considered quite uniform.

Regarding the site class based on the IBC-2006 provisions, among the 22 common test sites (including all downhole and P-S logging sites) only four sites have site classes that differ, depending on seismic method. However, the $V_{S,30}$ (average V_S in the top 30 m or 100 ft) of these four sites are all close to the boundary of the “D” and “E” sites which is 600 fps. Since they are close to the $V_{S,30}$ boundary, these four site actually have similar V_S profiles or engineering properties in the top 100 ft. So, it would be proper to show the site class with the corresponding $V_{S,30}$ value to avoid the data being misinterpreted.

A G_{max} profile was generated for the central valley area where most population is located. As observed, the G_{max} value increases with depth until 30 ft deep. Then the profile seems to remain nearly constant from 30 to 70 ft with a value of 12 ksi. After

that depth, the COV value enlarges until it reaches 100 ft deep. Below 100 ft, there is another uniform layer which has a G_{\max} value of about 20 ksi.

9.2.2 Tests Performed in Taiwan

Based on the 26 SASW V_S profiles measured in Taiwan, there were two velocity groups observed. Coincidentally, the higher velocity group consists of “C” sites only and the lower velocity group contains “D” sites only. The same fact was noticed from ten available suspension logging V_S profiles from the area covered by the 26 SASW tests. From this point, in general, the SASW and P-S logging measurements are consistent with each other. When comparing the median and 16th and 84th percentile boundaries of the V_S profiles of these two methods, it shows the SASW and suspension measurements have very consistency in the range of depths from 25 to 70 ft, especially in the “green-apples-to-green-apples” comparisons. However, it always shows there is an inconsistency between them in the top 25 ft and below 70 ft. The explanation for the difference in the top 25 ft could be the casing effect or some other reason(s). Regarding the inconsistency below 70 ft, the cause could be the different wavelength (or frequency) range used in the SASW and suspension logging methods to perform the soil profiling. As to the COV value, the COV profile of the SASW measurements becomes smaller as the included sites become similar or closer. This change simply means that tests performed within a smaller area typically have a smaller COV value. For the common eight “C” sites of the SASW and P-S logging tests which are distributed in an area about 30 mi by 20 mi, the SASW COV profile is close to 0.15. For the four “D” sites determined by SASW in Taiwan, the COV value of their V_S profiles is even close to 0.10.

The comparison of site classes between the SASW and P-S logging measurements has 100% agreement. Also, the G_{\max} values reduced from the SASW “filtered”

measurements of “C” sites are consistent to the downhole and cyclic triaxial tests performed by other researchers (Lin et al., 2000).

9.2.3 Tests Performed in Hanford, WA

Ten SASW tests were performed around the Waste Treatment Plant (WTP) near the 200 East Area at Hanford, WA. Nine of these ten SASW tests are located around the WHP within about a 6000 ft by 8000 ft area. Six downhole measurements were also conducted in five boreholes at the same area. Although somewhat higher velocities in the downhole measurements were observed in the shallow depth compared to the SASW measurements, this difference only in the top 10 ft of the downhole profiles. In this study, most comparisons were made between the nine SASW and six downhole measurements that were performed in alluvium. In general, the “green-apples-to-green-apples” comparisons have best agreement between the SASW and downhole median V_S profiles. In addition, some other comparisons based on the geologic profiles were also studied. No matter in what kind of comparisons, the median V_S profiles and the 16th and 84th percentile boundaries are very consistent between these two methods in the top 200 ft. In addition, the COV profiles of the SASW tests in these comparisons are always lower than 0.15, on average, within these depths. In some cases, the COV values are even close to 0.10. The low COV values mean the soil deposit is quite uniform over this area. As to the site classifications, the site classes determined by the SASW and downhole measurements completely agree.

The G_{\max} values reduced from the SASW measurements were studied based on different formations. Most formations have a wide range of G_{\max} value, except the Saddle Mountain basalt which has a constant G_{\max} value about 600 ksi.

9.2.4 Tests Performed at the Yucca Mountain Project, NV

The most of the SASW tests studied in this dissertation were performed as part of the Yucca Mountain Project (YMP), NV. At the Waste Handling Building (WHB) area, there were 35 SASW, 17 downhole and 16 P-S logging measurements conducted so this is an ideal test area to study the consistency between the SASW, downhole and P-S logging methods. Based on the comparisons, especially the “green-apples-to-green-apples” comparisons, the results show that the SASW and downhole V_S profiles are very consistent and this consistency is not as strong with the suspension logging method in the top 180 ft in terms of their median V_S profiles. The median V_S profile of the suspension logging is usually slightly higher than the other seismic measurements. The higher velocity and lack of data at shallow depth were observed again in the downhole profiles. However, they are minor at these sites. As to the P-S logging measurements, the higher velocity at shallow depths was absent due to the lack of data in the top 20 to 30 ft of the V_S profiles.

Some comparisons based on the geologic profiles were also studied. Several measurements from different techniques with respect to the same geologic material were compared. These techniques include SASW tests (performed on surface and tunnel sites), free-free resonant column tests, Vertical Seismic Profiling (VSP) tests and seismic tomography tests (Descour et al., 2001 and Gritto et al., 2004). The comparisons always show the resonant column measurements have the highest V_S values and the results from the SASW surface tests are lowest. This difference is expected because of the difference in sample size. However, due to the low velocity contrast between the different geologic materials, it seems impossible to determine, throughout the YMP area, the location of different soil deposits or rock formations by means of the shear wave velocities in the profile.

9.2.5 Sensitivity Study of Assumed Parameters Used in Forward Modeling

Three parameters were investigated in this study. They are Poisson's ratio and unit weight and layer Thickness. The other parameters, i.e. V_p and V_s , were not studied because they are related by the Poisson's ratio. Based on this study with real SASW test results (for rock or unsaturated soil), it shows the maximum difference in the final SASW V_s profiles are no more than 10% when reasonable range for Poisson's ratio is selected and are no more than 20% when a wide range (0.20 to 0.40) of Poisson's ratio is selected. These differences in V_s profiles are acceptable in engineering practice. As to the unit weight and layer thickness, the study shows it has almost no impact on the final SASW V_s profile because the change in the unit weight or layer thickness has very a minor effect to the theoretical dispersion curve.

9.2.6 Sensitivity Study of Detecting Relative Soft Layer in the Subsurface

A simple case was modeled to perform this study. By properly assuming and defining some parameters, a representative curve of maximum detectable depth of a soft layer by means of the SASW method can be obtained. Based on this simple model and using 3% as the "detectable" criterion, the minimum-thickness-to-depth ratio of a detectable soft layer is from 5 to 20 with respect to the velocity contrast of the adjacent layer(s) for the soft layer from 20% to 50%, respectively. These results mean that the thickness of a soft layer should be at least 5% to 20% of its depth to be detected by SASW method within the range of velocity contrast from 20% to 50% between the soft layer and its adjacent layers. The results of using different criteria ($\delta = 5\%$ and 10%) are also shown in Figure 8.14.

9.2.7 Summation of the Study

To sum up, the identical-site-and-depth (“green-apples-to-green-apples”) comparison is a very objective comparing criterion using to study the consistency between different seismic profiling methods. Based on the studies above, SASW measurements are comparable to downhole or suspension logging results or vice versa under many conditions. These conditions include small to medium velocity contrasts, reasonable lateral continuity compared with the investigation depth, and profiling depths generally less than 1000 ft. Moreover, the SASW method is less costly and more time efficient compared to the downhole and suspension logging methods as discussed before.

Also, the COV (Coefficient of Variation) associated with the V_S profiles is shown to be an index of the uniformity of the test area. Smaller COV values indicate a more uniform geotechnical test area. The COV values for the SASW measurements to judge a site as uniform are about 0.15 or less in this study according to the SASW tests performed in different regions.

Based on the $V_{S,30}$ of a site, its site class can be determined by the IBC-2006 provisions. However, in some cases, sites which have very similar $V_{S,30}$ values and these values are close to the classification boundaries can sometimes fall into two different classes. In order to avoid misinterpreting the site characterization information, it would be beneficial to show also the site class along with the calculated $V_{S,30}$ value.

Last, if a geotechnical site has big velocity contrast between the different layers, such as the interbedded basalt layer at the Hanford site, it is possible to determine the depth of the top of the basalt layer from the resulting SASW V_S profile. However, if the shear wave velocity increase smoothly with depth, it may not be able to locate the different geologic materials by means of the SASW V_S profile as discussed in Chapter 7.

9.3 RECOMMENDATIONS FOR FUTURE WORK

There are many advantages of surface-wave methods, including the SASW method, compared to other seismic profiling techniques (such as borehole methods) as mentioned earlier. However, the SASW method has some disadvantages, too. Based on the experience of the writer with to the SASW method, post-field-test analysis takes much of the time associate with the SASW method. This time is spent on masking phase plots to generate field dispersion curves and performing forward modeling to match the theoretical dispersion curve and field dispersion curve to obtain a shear wave velocity profile that can represent the test site. If some filters can be developed to remove the noise or interference in the measured data obtained from SASW method and they do not distort the real field information, the phase plot masking process could be much easier. Furthermore, if a more user-friendly and stable inversion analysis algorithm can be developed, it will contribute to fully automating the SASW method and make it more robust. Then the SASW method will be more widely adopted by engineers to profiling the subsurface.

References

- Aki, K. and Richards, P. G., (1980), "Quantitative Seismology : Theory and Methods," San Francisco : W. H. Freeman, 2 vols. 932 pp.
- Andrus, R. D., Fairbanks, C. D., Zhang, J., Camp, W. M. III, Casey, T. J., Cleary, T. J., and Wright, W. B. (2006), "Shear-wave Velocity and Seismic Response of Near-Surface Sediments in Charleston, South Carolina," *Bulletin of the Seismological Society of America*, 96(5), 1897-1914.
- BSC (Bechtel SAIC Company), (2002), "Geotechnical data for a Potential Waste Handling Building and for Ground Motion Analyses for the Yucca Mountain Site Characterization Project," ANL-MGR-GE-000003 REV 00d, Las Vegas, Nevada: Bechtel SAIC Company.
- BSC (Bechtel SAIC Company), (2004a), "Development of Earthquake Ground Motion Input for Preclosure Seismic Design and Postclosure Performance Assessment of a Geologic Repository at Yucca Mountain, NV," MDL-MGR-GS-000003 REV 01, Las Vegas, Nevada: Bechtel SAIC Company. ACC: DOC.20041111.0006.
- BSC (Bechtel SAIC Company), (2004b),"Geologic Framework Model (GFM2000)," MDL-NBS-GS-000002 REV 02, Las Vegas, Nevada: Bechtel SAIC Company. ACC: DOC.20040827.0008.
- BSC (Bechtel SAIC Company), (2004c), "Yucca Mountain Site Description" Volume I: Sections 1 – 5, TDR-CRW-GS-000001 REV 02 ICN 01, Las Vegas, Nevada: Bechtel SAIC Company. ACC: DOC.20040504.0008.
- Ballard, R. F., Jr., (1964), "Determination of Soil Shear Moduli at Depth by in-situ Vibratory Techniques" U.S. Army Engineer Waterways Experiment Station, Corps of Engineers, Miscellaneous Paper no. 4-691, Vicksburg, MS.
- Brown, L. T., Boore, D. M. and Stokoe, K. H., II, (2002), "Comparison of Shear-Wave Slowness Profiles at 10 Strong-Motion Sites from Noninvasive SASW Measurements and Measurements Made in Boreholes," *Bulletin of the Seismological Society of America*, Vol. 92, No. 8, pp. 3116–3133.
- Buesch, D., USGS, (2005a), "Properties of volcanic rocks at Yucca Mountain: The connection of geology and engineering," and "Geologic investigations at the cross roads: Examples of multidisciplinary studies at Yucca Mountain," Presentations at University of Texas at Austin on April 05, 2005.
- Buesch, D., USGS, (2005b), "Re: Rock type information at some locations in the ESF tunnel," E-mail, Received on October 12, 2005.

- Chang, F. K. and Ballard, R. F., Jr, (1973), "Rayleigh-Wave Dispersion Technique for Rapid Subsurface Exploration" U.S. Army Engineer Waterways Experiment Station, Soil and Pavements Laboratory, Vicksburg, MS.
- Davis, J. L., (1988), "Wave Propagation in Solids and Fluids," New York: Springer-Verlag, 386 pp.
- Descour, J. M., Hanna K., Conover D. and Hoekstra B., (2001), "Seismic Tomography Technology for the Water Infiltration Experiment," TDR-EBS-MD-000017 REV 00, Las Vegas, Nevada: Bechtel SAIC Company.
- Ernst, W. G., Ho, C. S. and Liou, J. G., (1985), "Rifting, Drifting and Crustal Accretion in the Taiwan Sector of the Asian Continental Margin in Tectonostratigraphic Terranes of the Circum-Pacific Region," ed. David Howell, Circum Pacific Energy & Mineral Resource, Earth Sci. Series, no.1, p. 375-390.
- Ewing, W. M., Jardetzky, W. S., and Press, F., (1957), "Elastic Waves in Layered Media," New York, McGraw-Hill, 380 pp.
- Fry, Z. B., (1963), "A Procedure for Determining Elastic Moduli of Soils by Field Vibratory Techniques," U.S. Army Engineer Waterways Experiment Station, Corps of Engineers, Miscellaneous Paper no. 4-577, Vicksburg, MS.
- GEOVision, Inc., <http://www.geovision.com/>, Webpage, Retrieved April 19, 2007
- Gritto R., Korneev, V. A., Daley, T. M., Feighner, M. A., Majer, E. L. and John E. Peterson, (2004), "Surface-to-tunnel seismic tomography studies at Yucca Mountain, Nevada," 27 March 2004
- Gucunski, N., and Woods, R. D., (1992), "Numerical Simulation of the SASW Test," Soil Dynamics and Earthquake Engineering, Vol. 11, pp. 213-227
- Haskell, N. A., (1953), "The Dispersion of Surface Waves on Multilayered Media," Bulletin of the Seismological Society of America, Vol. 43, pp. 17-34.
- Haskell, N. A., (1964), "Total Energy and Energy Spectral Density of Elastic Wave Radiation from Propagating Faults," Bulletin of the Seismological Society of America, Vol.54, 1811-1841.
- Heisey, J. S., (1981), "Determination of in situ shear wave velocities from spectral analysis of surface waves," Thesis, The University of Texas at Austin, 265 pp.
- Heukelom, W., and Foster, C.R., (1960), "Dynamic Testing of Pavements," Journal of Soil Mechanics and Foundation, Proceedings ASCE, 86 (SM1), 1, 1- 28

- Hiltunen, D. R., Woods, R. D., (1989), "Influence of Source and Receiver Geometry on the Testing of Pavements by the Surface Waves Method," *Nondestructive Testing of Pavements and Backcalculation of Moduli*, ASTM STP 1026, A. J. Bush III and G. Y. Baladi, Eds., American Society of Testing and Materials, Philadelphia, pp. 138-154.
- Hiltunen, D. R., Woods, R. D., (1990), "Variables Affecting the Testing of Pavements by the Surface Waves Method," *Transportation Research Record No. 1260*, Transportation Research Board, Washington, D.C., pp. 42-52
- Hoar, R. J., (1982), "Field measurement of seismic wave velocity and attenuation for dynamic analyses," Ph.D. Dissertation, The University of Texas at Austin, 478 pp.
- International Code Council, Building Officials and Code Administrators International, International Conference of Building Officials and Southern Building Code Congress International, (2006), "International building code," Falls Church, Va.
- Joh, S.-H., (1992), "User's Guide to WinSASW, a Program for Data Reduction and Analysis of SASW Measurements" The University of Texas at Austin.
- Joh, S.-H., (1996), "Advances in the Data Interpretation Technique for Spectral-Analysis-of-Surface-Waves (SASW) Measurements," Ph.D. Dissertation, The University of Texas at Austin, 240 pp.
- Jones, R., (1958), "In Situ Measurement of the Dynamic Properties of Soil by Vibration Methods" *Géotechnique*, vol.8, no.1, pp.1-21.
- Kausel, E. and Roesset, J. M., (1981), "Stiffness Matrices for Layered Soils," *Bulletin of the Seismological Society of America*, Vol. 71, pp. 1743-1761.
- Kausel, E. and Peek, R., (1982), "Dynamic Loads in the Interior of a Layered Stratum: an Explicit Solution," *Bulletin of the Seismological Society of America*, Vol. 72, pp. 1459-1508.
- Lin, S. Y., Lin, P. S., Luo, H. S. and Juang, C. H., (2000), Shear modulus and damping ratio characteristics of gravelly deposits, *Can. Geotech. J.* 37, 638–651.
- Loh, C.-H., Lee, Z. -K., Wu, T. -C. and Peng, S.-Y., (2000), "Ground motion characteristics of the Chi-Chi earthquake of 21 September 1999," *Earthquake Engineering and structural Dynamics*, 29, pp867-897
- Nazarian, S., and Stokoe K. H., II, (1983), "Evaluation of moduli and thicknesses of pavement systems by spectral- analysis-of-surface-waves method," University of Texas at Austin. Center for Transportation Research, no. 256-4,

- Nazarian, S., (1984), "In situ determination of elastic moduli of soil deposits and pavement systems by spectral-analysis-of-surface-waves method," Ph.D. Dissertation, The University of Texas at Austin, 453 pp.
- Nazarian, S., and Stokoe K. H., II, (1984), "In situ shear wave velocities from spectral analysis of surface waves," Proceedings of the World Conference on Earthquake Engineering, 8, San Francisco, Calif., July 21-28
- Nevada State Government, <http://www.state.nv.us/nucwaste/yucca/seismo01.htm>, webpage, Retrieved April 19, 2007
- Newland, D. E., (1993), "An introduction to random vibrations, spectral and wavelet analysis," 3rd ed., Harlow, Essex, Engla, 477 pp.
- Park, C. B., Miller, R. D., and Xia, J., (1999), "Multichannel analysis of surface waves (MASW)," Geophysics, 64, 800-808.
- Porcella, R. L., (1984), "Geotechnical Investigations at strong-motion stations in the imperial valley, California," Open-File Report 84-562, USGS, Menlo Park, California, August
- Rayleigh, L., (1885), "On Waves Propagating Along the Plane Surface of an Elastic Solid," Proceedings, London Mathematical Society, Vol 17, pp. 4-11.
- Richart, F. E., Jr., Woods, R. D., and Hall, J. R. Jr. (1970), "Vibrations of Soils and Foundations," Prentice Hall, Englewood Cliffs, New Jersey, 414 pp.
- Rodriguez-Ordonez, J. A., (1994), "A new method for interpretation of surface wave measurements in soils," Ph.D. Dissertation, North Carolina State Univ., Raleigh, North Carolina
- Roesset, J.M., Chang, D.-W., Stokoe, K.H., II and Aouad, M., (1990), "Modulus and Thickness of the Pavement Surface Layer from SASW Tests," Transportation Research Record 1260, pp. 53-63.
- Roesset, J. M., Chang D.-W., and Stokoe, K. H., II, (1991), "Comparison of 2D and 3D Models for Analysis of Surface Wave Tests," Proceedings of the 5th International Conference on Soil Dynamics and Earthquake Engineering, pp. 111-126.
- Rouhani, S., ASTM Committee D-18 on Soil and Rock, (1996), "Geostatistics for environmental and geotechnical applications," West Conshohocken, Pa.: ASTM, 280 pp.

- Satoh, T., Yamagata, K., Poran C. J. and Rodrlguez, J. A., (1991), "Soil Profiling by Spectral Analysis of Surface Waves," Second International Conference on Recent Advances in Geotechnical Earthquake Engineering and Soil Dynamics Proceedings: March 11 - 15
- Schuhen, M., BSC (Bechtel SAIC Company, LLC), (2004), "SASW_002.pdf," PDF File, January 26, 2004.
- Schuhen, M., BSC (Bechtel SAIC Company, LLC), (2005), "Re: SASW V_S Profiles of YMP," E-mail, Received on May 06, 2005.
- Simmons, A. M., (2004), "Yucca Mountain Site Description," TDR-CRW-GS-000001 REV 02. Two volumes. Las Vegas, Nevada: Bechtel SAIC Company. ACC: DOC.20040120.0004.
- Stokoe, K. and Nazarian, S., (1985), "Use of Rayleigh Waves in liquefaction Studies," in, R.D. Woods, ed., "Measurement and use of Shear Wave Velocity for Evaluating Dynamic Soil Properties," ASCE, New York, 1-17
- Stokoe, K. H., II, Roesset, J. M., Bierschwale, J. G. and Aouad M., (1988), "Liquefaction Potential of Sands from Shear Wave Velocity," Proceedings, Ninth World Conference on Earthquake Engineering, Tokyo, Vol. III, pp. 213-218.
- Stokoe, K. H., II, Wright, S. G., Bay, J. A. and J. M. Roesset, (1994), "Characterization of Geotechnical Sites by SASW Method," ISSMFE Technical Committee 10 for XIII ICSMFE, Geophysical Characteristics of Sites, A.A. Balkema Publishers/Rotterdam & Brookfield, Netherlands, pp. 785-816.
- Stokoe, K. H., II, Rosenblad, B. L., Bay, J. A., Redpath, B., Diehl, J. G., and Steller, R. A. (2003). "Comparison of V_S profiles from three seismic methods at Yucca Mountain." Proc., Soil and Rock America 2003, ed. P. J. Culligan, H. H. Einstein, and A. J. Whittle. Verlag Glückauf GMBH, Essen, (1), 299-306.
- Stokoe, K. H. II, Rosenblad, B. L., Wong, I. G. Bay, J. A. Thomas, P. A. and Silva, W. J., (2004), "Deep V_S Profiling Along the Top of Yucca Mountain Using a Vibroseis Source and Surface Waves," 13th World Conference on Earthquake Engineering Paper No. 538.
- Stokoe, K. H., II, Lin, Y.-C., Cox, B. R., Kurtulus, A. and Jung, M. J., (2005a), "Shear Wave Profiling at the Waste Treatment Plant Site, Hanford, WA," Geotechnical Engineering Report GR05-1 Geotechnical Engineering Center Civil Engineering Department The University of Texas at Austin.

- Stokoe, K. H., II, Lin, Y.-C., Menq, F.-Y. and Rosenblad, B. L., (2005b), "SASW Measurements in Taiwan at 26 Strong-Motion Recording Stations: Summary Report of the Shear Wave Velocity Profiles," Geotechnical Engineering Report GR05-2 Geotechnical Engineering Center Civil Engineering Department The University of Texas at Austin.
- Stokoe, K. H., II, Cox, B. R., Lin, Y.-C., Jung, M. J., Menq, F.-Y., Bay, J. A., Rosenblad, B., and Wong, I. (2006), "Use of Intermediate to large vibrators as surface wave sources to evaluate V_S profiles for earthquake studies", Proc. Symposium on the Application of Geophysics to Engineering and Environmental Problems, Seattle, WA, pp.1241-1258.
- Thompson, W. T., (1950), "Transmission of Elastic Waves through a Stratified Solid Medium," Journal of Applied Physics, Vol. 21, pp. 89-93.
- Tokimatsu, K., Kuwayama, S., and Tamura, S., (1991), "Liquefaction Potential Evaluation Based on Rayleigh Wave Investigation and Its Comparison with Field Behavior," Proceedings, Second International Conference on Recent Advances in Geotechnical Earthquake Engineering and Soil Dynamics, held in St. Louis, Missouri, S. Prakash, Ed., University of Missouri-Rolla, Vol. I, pp. 1649-1654.
- Williams, O., (1981), "Rayleigh Wave Velocity Measurements Using Broad Band Frequency Sources: Final Report," U.S. Army Engineer Waterways Experiment Station, Environmental Laboratory, Vicksburg, MS.

Vita

Yin-Cheng Lin, the son of A-Chun Lin Yao and King-Fu Lin, was born in Taipei, Taiwan in 1972. He graduated from Chung Cheng High School in 1990 and received his B.S. and M.S. degrees from National Cheng Kung University in 1994 and 1996, respectively. Between 1996 and 1998, he performed the compulsory military service in Matsu. In 1998, he started to work as a geotechnical engineer in an engineering consulting firm in Taipei. In 2001 fall, he enrolled in the Graduate School of the University of Texas at Austin to pursue a doctoral degree.

Permanent address: 2F 258 Wenchang St., Taipei 106, Taiwan

This dissertation was typed by Yin-Cheng Lin.